JPLCA$_T$

Vol. 9, Part A-1, No. 7, July 1971

Journal of Polymer Science

Part A-1: Polymer Chemistry

Contents

(*continued inside*)

Published by INTERSCIENCE PUBLISHERS a division of John Wiley & Sons, Inc.

Journal of Polymer Science **Part A-1: Polymer Chemistry**

Contents (continued)

(continued on inside back cover)

The Journal of Polymer Science is published in four sections as follows: Part A-1, Polymer Chemistry, monthly; Part A-2, Polymer Physics, monthly; Part B, Polymer Letters, monthly; Part C, Polymer Symposia, irregular.

Published monthly by Interscience Publishers, a Division of John Wiley & Sons, Inc., covering one volume annually. Publication Office at 20th and Northampton Sts., Easton, Pa. 18042. Executive, Editorial, and Circulation Offices at 605 Third Avenue, New York, N. Y. 10016. Second-class postage paid at Easton, Pa. Subscription price, $325.00 per volume (including Parts A-2, B, and C). Foreign postage $15.00 per volume (including Parts A-2, B, and C).

JOURNAL OF POLYMER SCIENCE: PART A-1 VOL. 9, 1789–1798 (1971)

Electroinitiated Polymerization of Vinylic Monomers in Polar Systems. II. Polymerization of Ethyl Methacrylate in Methanol Solutions

MICHAEL ALBECK and JOSEPH RELIS, *Department of Chemistry, Bar Ilan University, Ramat-Gan, Israel*

Synopsis

Ethyl methacrylate is polymerized by electroinitiation in methanol–electrolyte mixtures in which the monomer is soluble whereas the polymer obtained is insoluble. A technique of changing the polarity of the electrodes is used. With this technique a polymer of high molecular weight can be obtained. The relationships between molecular weight and monomer concentration, current densities, and time of the reaction as well as the yield as a function of current density, time of the reaction and initial monomer concentration are given. A free-radical mechanism is proposed for the reaction.

The electroinitiated polymerization of vinyl monomers in homogeneous systems was investigated by several workers[1–7] but relatively few studies of electroinitiated reactions were carried out in heterogeneous systems in which the polymer was insoluble.[8–19] Studies in heterogeneous medium reported low yields of polymer and low molecular weight due to the deposition of the polymer produced on the electrodes.

The importance of a suitable solvent and its influence on the yield and molecular weight of the polymer obtained was investigated by Funt et al.[1,6] Methanol was found[4,6] to inhibit the electropolymerization of methylmethacrylate in solutions of dimethylformamide containing tetramethylammonium chloride. In this paper we describe the electroinitiated polymerization of ethyl methacrylate in solutions of methanol.

Experimental

Ethyl methacrylate (Fluka, Switzerland, analytical grade) was freed from inhibitor by washing twice with a 5% NaOH solution followed by 5% H_3PO_4 solution and then saturated NaCl solution, dried over Na_2SO_4 or $CaSO_4$ for 24 hr and finally fractionally distilled under reduced pressure (1 mm Hg). The middle fraction was collected and stored at −30°C.

Methanol (Frutarom, Israel, analytical grade) was dried over Mg turnings for 24 hr and fractionally distilled. The middle fraction, bp 65°C, was collected.

Lithium acetate (Schuchardt, Munich, Germany, analytical grade), magnesium chloride (Frutarom, Israel, analytical grade) and lithium nitrate (Baker, U.S.A., analytical grade) were anhydrous.

The vessel in which the polymerization was carried out was constructed from a glass cell 20 × 35 × 85 mm sealed with a glass cap through which electric wires were sealed and provided with an opening for bubbling with an inert gas. Two "special material very hard" graphite electrodes (Bode, W. Germany), were fitted to the cell. The electrodes had an area of 24.3 cm^2 each, and were separated from each other by 5 mm Teflon spacers. A constant current supply was obtained by modification of a voltage supply (Kepco, U.S.A. Model HB 525M), to control current in the range 5–100 mA with a constancy of 0.1%. The polarity of the electrodes was changed every 5 min in order to prevent the coating of the electrodes by a polymer film deposited on them during the polymerization process.

Molecular weights were determined by the viscosity method. Intrinsic viscosities were measured in methyl ethyl ketone at 23°C in Ubbelohde viscometers and the molecular weights determined from the Staudinger equation. Values for K of 2.83×10^{-5} and α of 0.79 were used.[20]

In a typical experiment, 15 ml of monomer, 15 ml of methanol, and 1 g of lithium acetate were placed in the electrolytic cell kept at a constant temperature of 40°C (thermostatted water bath).

Polymerization was conducted at a constant current of 50 mA at the cell. After 18 hr the polymerization procedure was stopped and additional methanol was added to the polymer–solution mixture. The polymer obtained was collected, dissolved in acetone, reprecipitated with methanol, dried at 50°C under reduced pressure (1–2 mm Hg) to constant weight, weighed, and its molecular weight determined. Repeated experiments gave results which were reproducible within ±3%.

Control experiments showed that under these conditions nonelectroinitiated polymerization did not take place.

Results and Discussion

The solvent used for the polymerization was methanol since it has a high dielectric constant and in this solvent the monomer is soluble whereas the polymer formed is insoluble. In an 18-hr polymerization at 40°C with a current of 50 mA, a 9.8% conversion was obtained with lithium acetate, whereas with magnesium chloride and lithium nitrate conversions of 4.8% and 0.5%, respectively, were obtained. Because of these results, lithium acetate was used in subsequent experiments. These results are in agreement with the mechanism proposed, since the initiating species are metal atoms[21] and since it was found polarographically that in the case of $LiNO_3$ oxygen is liberated by the electrolyte during the electrolysis which results in the low conversions. This point will be elaborated below.

It was found that in experiments in which the polarity of the electrodes was not changed during the course of the polymerization, the cathode was coated with a film of polymer shortly after the start of the experiment.

During this process the resistance between the electrodes gradually increased, as was evident from the increasing cell voltage at constant amperage. At a point where the current requirements of the coated electrodes could no longer be met, the current density decreases. Reproducible results could not be obtained under these conditions. These results are in accordance with the results obtained by other investigators for similar

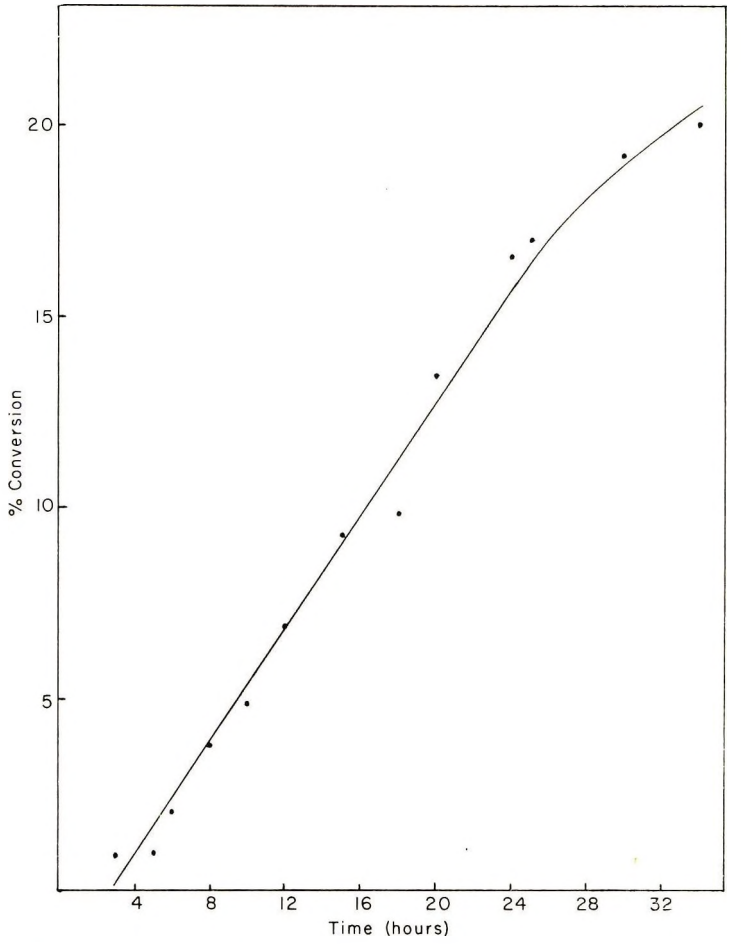

Fig. 1. Yield of poly(ethyl methacrylate) as function of the reaction time. Volume ratios of monomer to methanol 1:1; polymerization carried out at 50 mA and 40°C.

experiments.[8–13] The change of the polarity of the electrodes prevent the coating of the cathode by the polymer produced, and as a result the current density and the resistance between the electrodes were kept constant during the whole course of the reaction and reproducible results were obtained. It was found that best results were obtained when the polarity was changed every 5 min. Resistance measurements of the electrodes before and after the polymerization process in which the polarity was

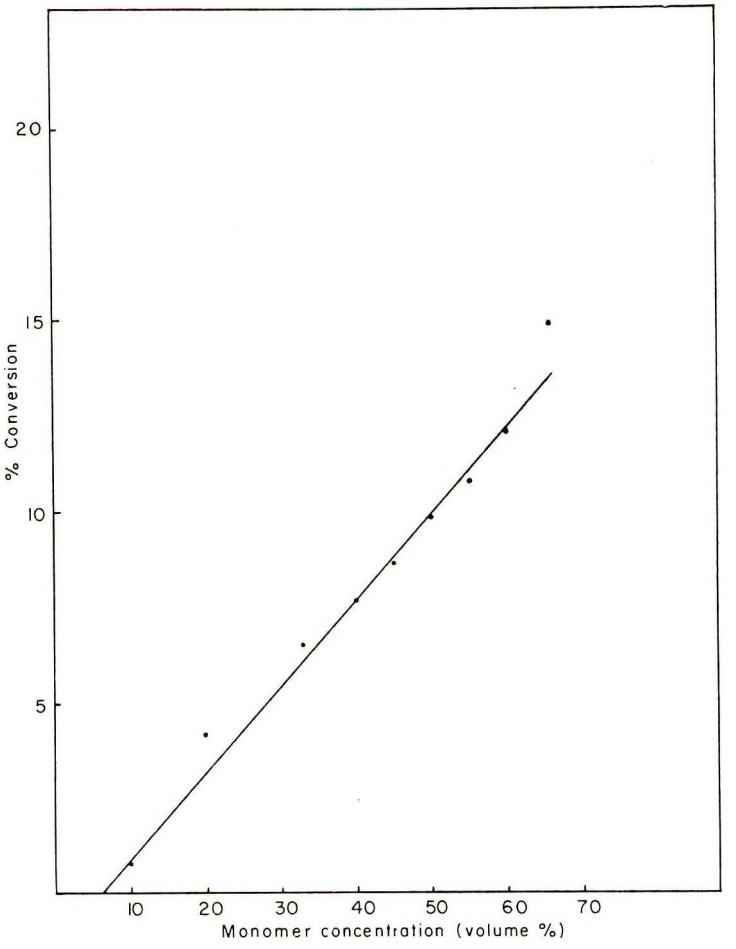

Fig. 2. Yield of poly(ethyl methacrylate) as function of initial monomer concentration (volume %). Polymerization carried out at 50 mA, 40°C, 18 hr.

changed every five minutes indicated that the electrodes were not coated during the polymerization.

Kinetic experiments were conducted with ethyl methacrylate in methanol (1:1 v/v, monomer to solvent) with a constant current of 50 mA at 40°C. Results are given in Figure 1. After an inhibition period of 2 hr, the yield of the polymer increased linearly with time up to 17% yield.* The inhibition time at the beginning of the polymerization is due to impurities which are known[1] to inhibit this kind of polymerization and to oxygen dissolved in the solution. It was found polarographically[21] that oxygen remains in the solution, even after flushing for 15 min with oxygen-free nitrogen. This oxygen is reduced during the first period of the electrolysis.

* Percentage yields (or conversions) are based on initials monomer weight.

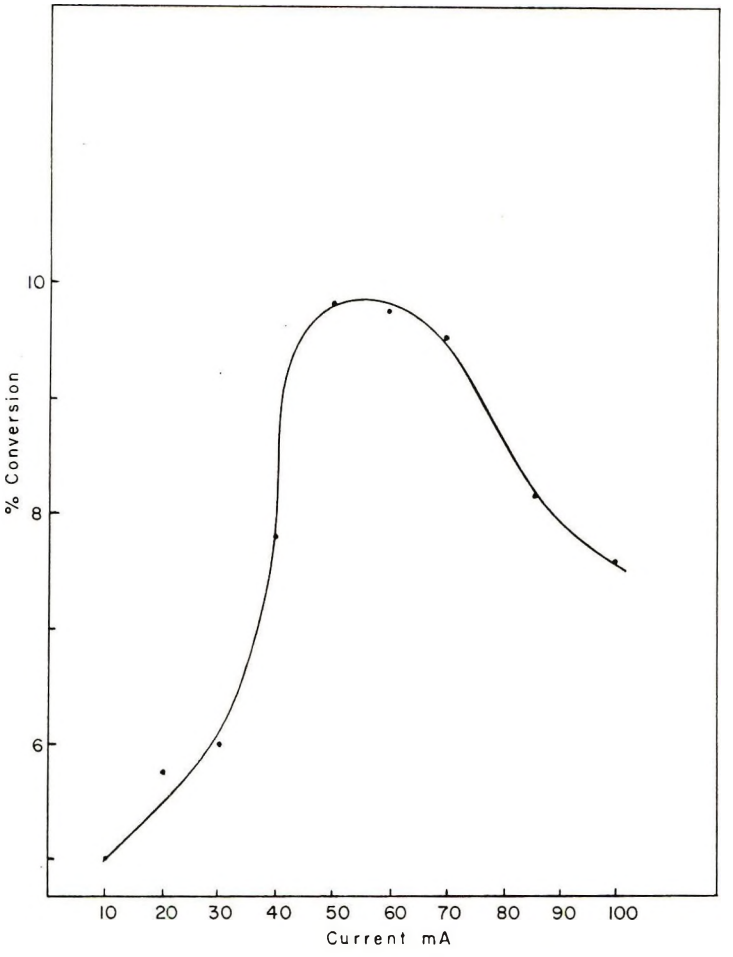

Fig. 3. Yield of polymer as function of the current. Polymerization carried out at 40°C for 18 hr; volume ratios of monomer to methanol 1:1.

The linear dependence of the yield to time is consistent with a free-radical mechanism for the polymerization (see below). The leveling off in the curve of the yield of the polymer after 17% conversion is due to the dilution effect caused by the consumption of the monomer as the reaction proceeds. This effect is also shown in Figure 2 where the polymer yield is given as a function of monomer concentration. It was found that the yield increases from 1.8% at 10 vol-% concentration to 15% at 66% concentration.

In this range no inflection point in the conversion was obtained, and the direct proportionality of yield to concentration indicates that no appreciable decrease in the concentration of the ions available for conversion to metal atoms (see below) is obtained in solutions of high dielectric constant such as methanol. The fact that the polymer is not appreciably dissolved

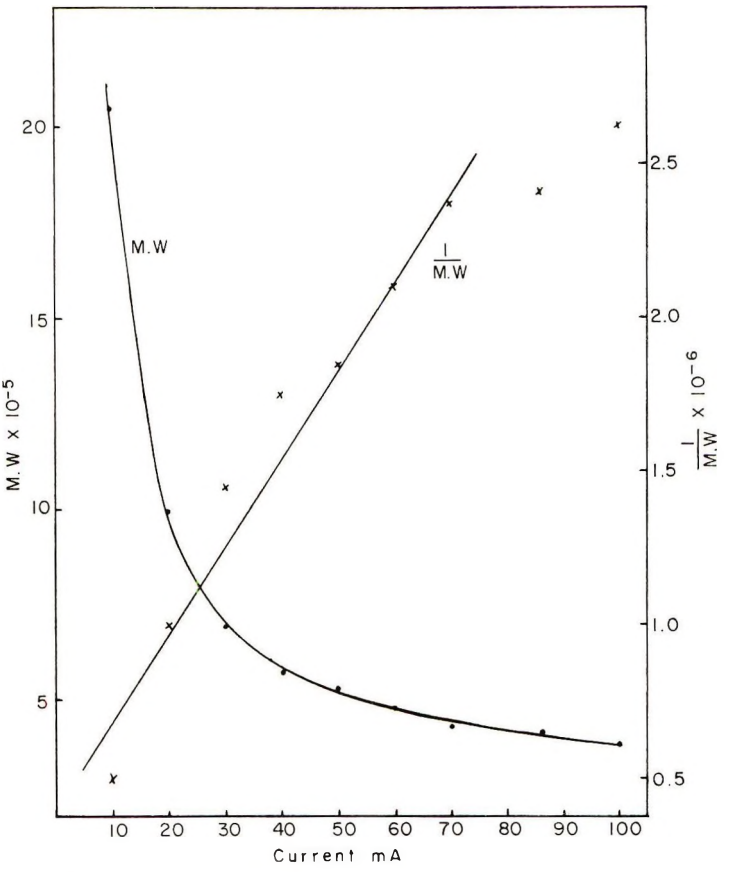

Fig. 4. Molecular weight as function of the current for experiments at 40°C, 18 hr and volume ratios of monomer to solvent 1:1.

in the methanol solution maintains the viscosity of the polymerization solution practically unchanged, and so no change in the ion mobility occurs. For these reasons initial zero-order kinetics up to 17% conversion are obtained as long as the current is maintained constant. The overall kinetics are first-order in monomer over the whole course of the reaction (Fig. 2).

The yield of the polymer as a function of the current is given in Figure 3 and Table I. The yield of the polymer reaches a maximum at 50 mA and then a decrease in the yield of the polymer is obtained. Polarographic evidence[21] indicated that in the ascending section of the graph the current reduces the lithium ions to metal atoms which initiate the polymerization. In the decending section of the graph, the higher current densities cause an increase in hydrogen ions and atoms formed in the vicinity of the anode and cathode respectively. The hydrogen ions so formed react with part of the lithium atoms to give metal cations and hydrogen atoms. This reaction is much faster than the free radical reaction between lithium atoms and the monomer at high concentration of H^+. Most of the

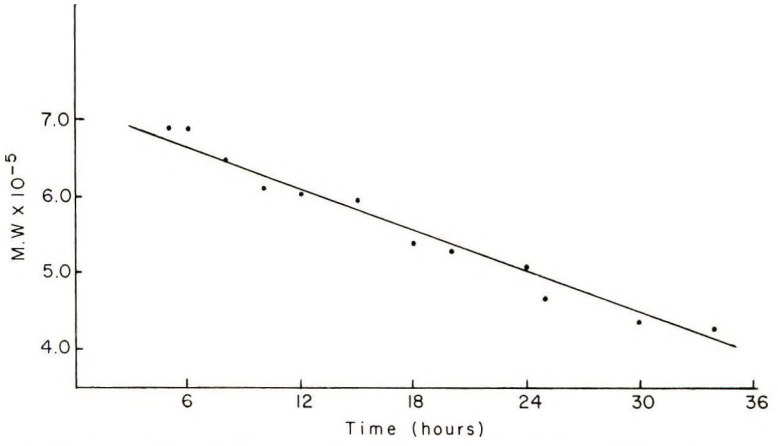

Fig. 5. Variation of molecular weight with time of reaction; 40°C, volume ratios of monomer to solvent 1:1; current of 50 mA.

lithium free radicals are oxidized at currents above 50 mA, and a lowering in the conversion results. H^+ and H· are present only at low concentrations at low currents and does not quench the polymerization to an appreciable degree.

The relationship between molecular weight and current density is given in Figure 4 and Table I. The molecular weight decreases with increase in current density up to 40–50 mA and then levels off. The inversion point in the decrease of the molecular weight is in good agreement with the results obtained for the relationship between the yield and the current density. At relatively low current densities the increase in the current yields an increase in the concentration of the initiating species and thus a decrease in the molecular weight is obtained. The linearity of the plot of the reciprocal of the molecular weight versus current density up to a current of 40–50 mA is another confirmation to the free-radical mechanism proposed for the reaction. In the range above 50 mA, large amounts of hydrogen

TABLE I
Molecular Weight and Conversion of Polymer as Functions of the Current Density[a]

Current density, mA/cm²	Conversion of polymer, %	Intrinsic viscosity, dl/g	MW × 10^{-5}	(1/MW × 10^6)
0.41	5.00	2.18	20.51	0.49
0.82	5.74	1.55	9.96	1.00
1.24	5.96	1.17	6.97	1.47
1.65	7.79	1.00	5.72	1.75
2.06	9.78	0.95	5.36	1.87
2.47	9.70	0.87	4.79	2.09
2.88	9.56	0.79	4.24	2.36
3.54	8.16	0.78	4.17	2.40
4.12	7.57	0.73	3.84	2.60

[a] Polymerization conducted at 40°C; ratio of monomer to solvent, 1:1 (V/V), time of reaction, 18 hr; Salt concentration, 0.067 g/ml.

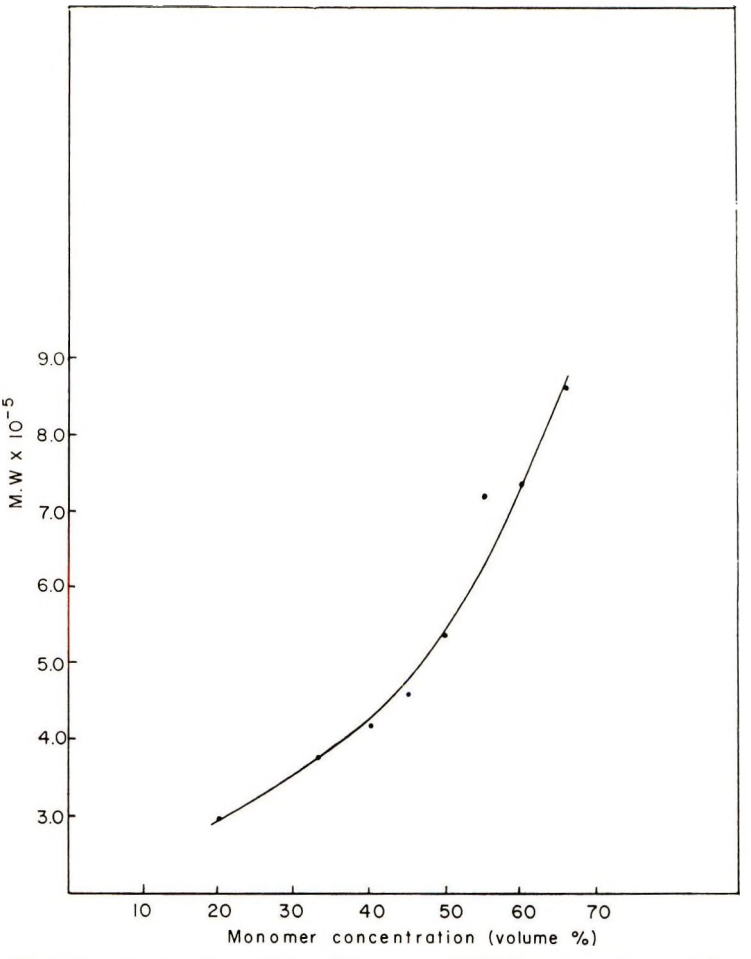

Fig. 6. Variation of molecular weight with monomer initial concentration. Polymerization conducted at 50 mA for 18 hr at 40°C.

ions are formed which react with the lithium radicals and thus decrease the relative concentration of the initiator, and so no linear relationship can exist between the reciprocal of the molecular weight and the current density, as can be seen in Figure 4. Figure 5 gives a plot of molecular weight versus time. The dilution effect on the average molecular weight as the reaction proceeds is seen by a decrease in the average molecular weight. This effect can also be seen in Figure 6, where the molecular weight is given as a function of the initial monomer concentration.

That the polymerization proceeds by a free-radical mechanism was shown by the addition of 0.4% of *p*-benzoquinone to the reaction mixture. The yield of the polymer was decreased by 90%. The same decrease in the yield, i.e., by 90%, was obtained when oxygen was bubbled during the reaction or when $LiNO_3$ was used as an electrolyte.

A mechanism for electroinitiation of polymerization of methyl meth-

acrylate in which the anionic species of the electrolyte is oxidized to a radical at the anode and the radical so formed is the initiator for the polymerization was proposed by Funt et al.[1] The polymerization in their case occurred at the anode compartment and the termination was by combination of the growing radical chain and the radical initiator. This mechanism does not apply to our system. It was shown by polarography[21] that in the electroinitiated polymerization of acrylates and methacrylates in methanolic solutions in the presence of lithium acetate, the lithium cation has the lowest reduction potential. It was also shown[21] that at above a certain current density (for the methacrylate systems 50–60 mA at 8–10 ohms) hydrogen ions are formed in appreciable amounts at the anode compartment and as a result a decrease in the yield of the polymerization is obtained (Fig. 3). According to the above and due to the fact that in the system described the polymerization and deposition took place at the cathode in experiments where the polarity was not changed, the following scheme is proposed:

$$Me^+ + e^- \xrightarrow{k_e} Me\cdot \tag{1}$$

$$Me\cdot + M \xrightarrow{k_i} M\cdot \tag{2}$$

$$M\cdot + xM \xrightarrow{k_p} M\cdot_{x+1} \tag{3}$$

$$M_x\cdot + H\cdot \xrightarrow{k_t} P \tag{4}$$

$$M_x\cdot + Me\cdot \xrightarrow{k'_t} P \tag{5}$$

where Me^+, $Me\cdot$, M, $M\cdot$, $H\cdot$ and P are metal cations, metal atoms, monomer, monomer radicals, hydrogen atoms, and polymer respectively.

At currents above 50 mA the reactions (6) and (7) are appreciable:

$$CH_3OH \rightarrow HCHO + 2H^+ + 2e \tag{6}$$

$$CH_3OH + e \rightarrow CHO_3^{\ominus} + N\cdot \tag{7}$$

The hydrogen ions which are formed according to eq. (6) at the anode migrate to the cathode and can react in three ways: (a) reaction of H^+ with metal atoms to give $Me^+ + H\cdot$ according to eqs. (8) and (9);

$$Me\cdot + H^+ \rightarrow Me^+ + H\cdot \tag{8}$$

$$2H\cdot \rightarrow H_2 \tag{9}$$

(b) reaction of H^+ at the cathode with the formation of hydrogen atoms; (c) reaction between the hydrogen cations and the methoxide anions formed by the reaction between the lithium atoms and the methanol.[21]

At low current densities where the amount of the hydrogen ions formed according to eq. (6) and (7) is low, the reactions (4) and (8) do not take place in appreciable amounts, and thus a direct proportionality between current density (up to 50 mA) is obtained. At current densities above 50 mA, where the hydrogen cation and atom formation according to eq. (6) and (7) becomes significant, a decrease in the polymerization is obtained (Fig. 3). Since reactions (8) and (9) are much faster than reac-

tion (2), reactions (6), (7), and (8) inhibit the formation of the polymer obtained at currents above 50 mA.

Other reactions which might take place during the electrolysis and are not contributing to the polymerization are described elsewhere (21).

The high molecular weight and conversions obtained in this system are in contrast to results reported by others[8–17] for electropolymerization in a similar system. There are several advantages in the polymerization system where the polymer obtained precipitates over the homogeneous one.

The fact that the polymer formed is precipitated as soon as it is formed enables one to work with large amounts without appreciably effecting the viscosity of the medium and the mobility of monomer and ions in the vicinity of the electrodes. The use of different solvents in which the polymer formed precipitates at different degrees of polymerization can be a tool for obtaining polymers of given molecular weights. The direct inverse proportionality between molecular weight, current density, and monomer concentration indicates the possibility of desired molecular weight distribution in the range determined by the solvent used.

We wish to thank Dr. M. Königsbuch for useful discussions.
This work is taken in part from the Ph.D. thesis of J. Relis.

References

1. B. L. Funt and K. C. Yu, *J. Polym. Sci.*, **62**, 359 (1962).
2. B. L. Funt and S. W. Laurent, *Can. J. Chem.*, **42**, 2728 (1964).
3. B. L. Funt and F. D. Williams, *J. Polym. Sci. B*, **1**, 181 (1963).
4. B. L. Funt and S. N. Bhadani, *Can. J. Chem.*, **42**, 2733 (1964).
5. B. L. Funt and F. D. Williams, *J. Polym. Sci. A*, **2**, 865 (1964).
6. B. L. Funt and S. N. Bhadani, *J. Polym. Sci. A*, **3**, 4191 (1965).
7. B. L. Funt and S. N. Bhadini, in *Macromolecular Chemistry, Tokyo-Kyoto* **1966** (*J. Polym. Sci. C*, **23**), I. Sakurada and S. Okamura, Eds., Interscience, New York, 1968, p. 1.
8. W. B. Smith and H. G. Gilde, *J. Amer. Chem. Soc.*, **81**, 5325 (1959).
9. W. B. Smith and H. G. Gilde, *J. Amer. Chem. Soc.*, **82**, 659 (1960).
10. W. B. Smith and H. G. Gilde, *J. Amer. Chem. Soc.*, **83**, 1355 (1961).
11. W. Kern and H. Quast, *Makromol. Chem.*, **10**, 202 (1953).
12. G. Parravano, *J. Amer. Chem. Soc.*, **73**, 628 (1951).
13. E. Dineers, T. C. Schwan, and C. L. Wilson, *J. Electrochem. Soc.*, **96**, 226 (1949).
14. U. Y. Yang, W. E. McEwen, and J. Kleinberg, *J. Amer. Chem. Soc.*, **79**, 5833 (1957).
15. R. V. Lindsey, Jr., and M. L. Peterson, *J. Amer. Chem. Soc.*, **81**, 2073 (1959).
16. J. W. Breitenbach, Ch. Srna, and O. F. Olay, *Makromol. Chem.*, **42**, 171 (1960).
17. J. W. Breitenbach and H. Gabler, *Monatsh.*, **91**, 202 (1960).
18. D. Laurin, and G. Parravano, in *Macromolecular Chemistry Brussels-Louvain 1967* (*J. Polym. Sci. C*, **22**), G. Smets, Ed., Interscience, New York, 1968, p. 103.
19. B. L. Funt and F. D. Williams, *J. Polym. Sci. B*, **1**, 181 (1963).
20. S. N. Chinai and R. J. Samuels, *J. Polym. Sci.*, **19**, 463 (1956).
21. M. Albeck, M. Königsbuch, and J. Relis, *J. Polym. Sci. A-1*, 00, 000 (1971) (Part I).

Received August 31, 1970
Revised January 11, 1971

JOURNAL OF POLYMER SCIENCE: PART A-1 VOL. 9, 1799–1806 (1971)

Polybenzopinacolones. Acid-Catalyzed Rearrangement of Aromatic Polybenzopinacols

D. A. McCOMBS, C. S. MENON, and JERRY HIGGINS,* *Department of Chemistry, Illinois State University, Normal, Illinois 61761*

Synopsis

Polybenzopinacols resulting from the photocondensations of *p,p'*-dibenzoyldiphenyl ether, *p,p'*-dibenzoyldiphenylmethane, and *p,p'*-dibenzoyl-1,2-diphenylethane were rearranged in sulfuric acid–dioxane solutions. The inherent viscosities of the polybenzopinacolones did not differ significantly from the inherent viscosities of the polybenzopinacols after rearrangement. A model compound study by NMR and infrared methods indicated that the polymer chain was probably the main migrating group for each of the polymer rearrangements.

INTRODUCTION

In previous papers[1,2] we reported the synthesis of polybenzopinacols (Ia–Ic) by the photocondensation of the corresponding aromatic diketones in benzene–isopropanol solution. The structures of these polymers were confirmed by comparison of infrared and nuclear magnetic resonance (NMR) spectra of the polymers with those of the corresponding model compounds (IIa–IIc).

In this paper we would like to report the rearrangements of the polymers Ia–Ic and the model compounds IIa–IIc to the corresponding polybenzopinacolones IIIa–IIIc and benzopinacolones IVa–IVc.

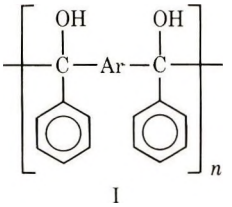

I

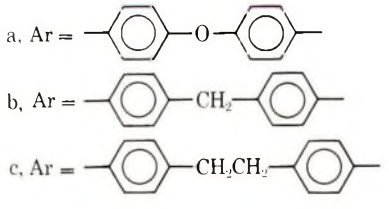

* To whom correspondence should be addressed.

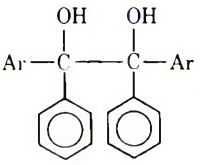

II

a, Ar = 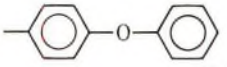

b, Ar = 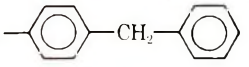

c, Ar = 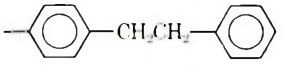

RESULTS AND DISCUSSION

Polymers

The rearrangements of polymers Ia–Ic were effected by stirring dioxane solutions of the polymers in the presence of sulfuric acid. Reaction times

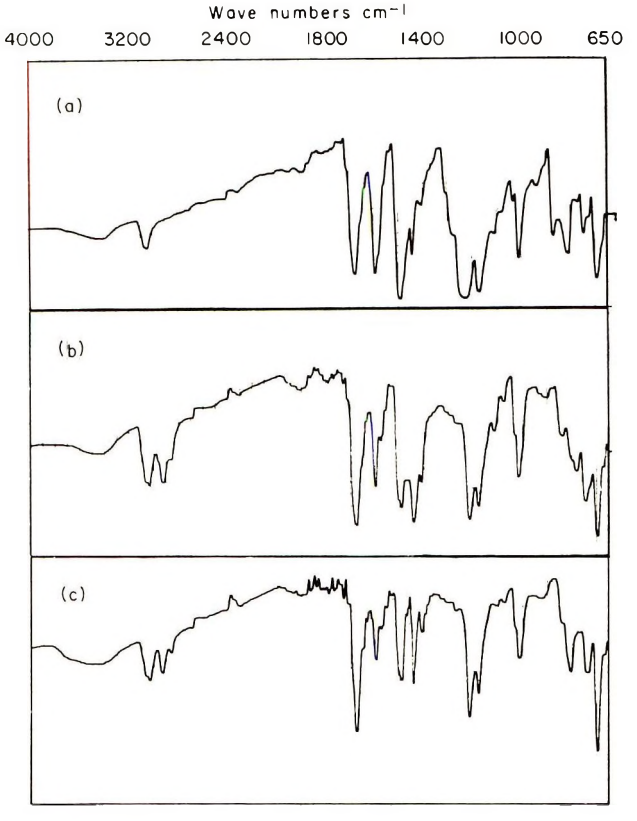

Fig. 1. Infrared spectra of pinacolone polymers (KBr): (*a*) IIIa; (*b*) IIIb; (*c*) IIIc.

TABLE I

Polypinacol	Polypinacol η_{inh}[a]	Reaction time, hr	Polypinacolone	Polypinacolone η_{inh}[a]
Ia	0.28	3	IIIa	0.28
Ib	0.13	3	IIIb	0.12
Ic	0.20	4	IIIc	0.18

[a] Viscosities taken in dioxane (0.5 g/100 ml).

ranged from 3 to 4 hr at room temperature (Table I). Refluxing of these polymer solutions generally led to a decrease in viscosities which was probably due to decomposition under these more vigorous reaction conditions.

When the rearrangements were carried out in glacial acetic acid with iodine catalyst, considerable decomposition occurred, particularly with polymers Ib and Ic. Some decomposition also occurred when the model pinacol compounds were rearranged under these reaction conditions as determined by infrared and NMR studies.

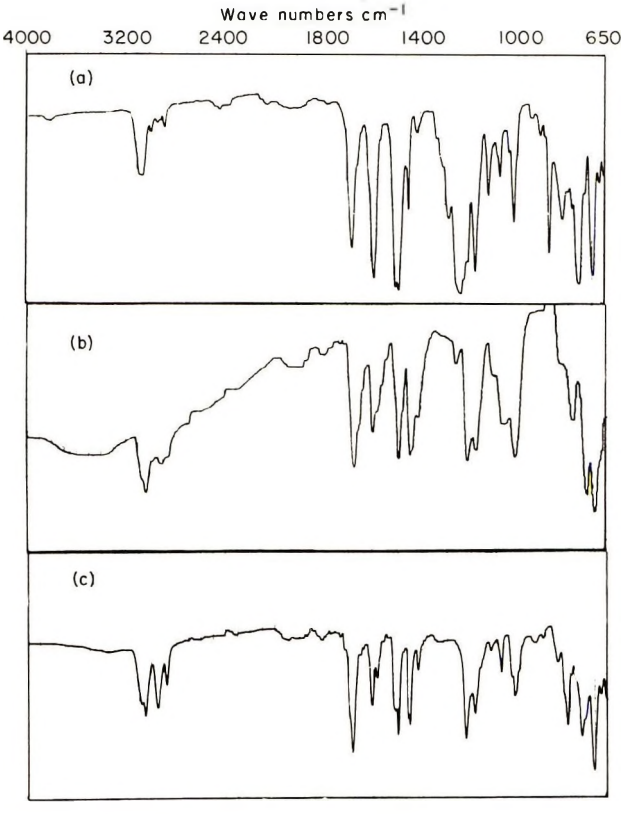

Fig. 2. Infrared spectra of model pinacolones (KBr): (*a*) IVa; (*b*) IVb; (*c*) IVc.

Infrared spectra of polymers IIIa–IIIc showed strong absorption bands around 1680 cm^{-1} (Fig. 1). Also, a small absorption band was present around 3500 cm^{-1} which was probably due to a small amount of unre-

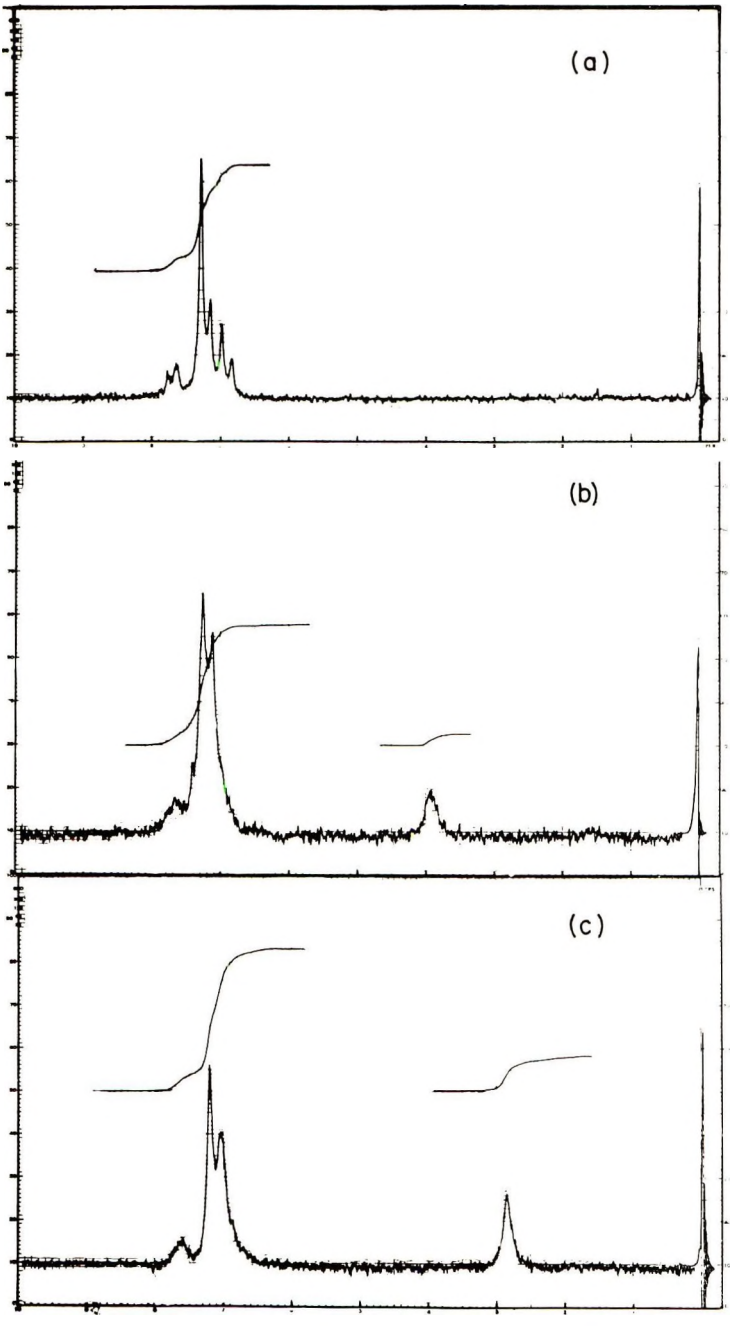

Fig. 3. NMR spectra of pinacolone polymers: (*a*) IIIa; (*b*) IIIb; (*c*) IIIc.

arranged pinacol segments in the polymer chains. This suggestion was also substantiated by elemental analysis, in which the oxygen content of each of the rearranged polymers was slightly greater than theory. The NMR

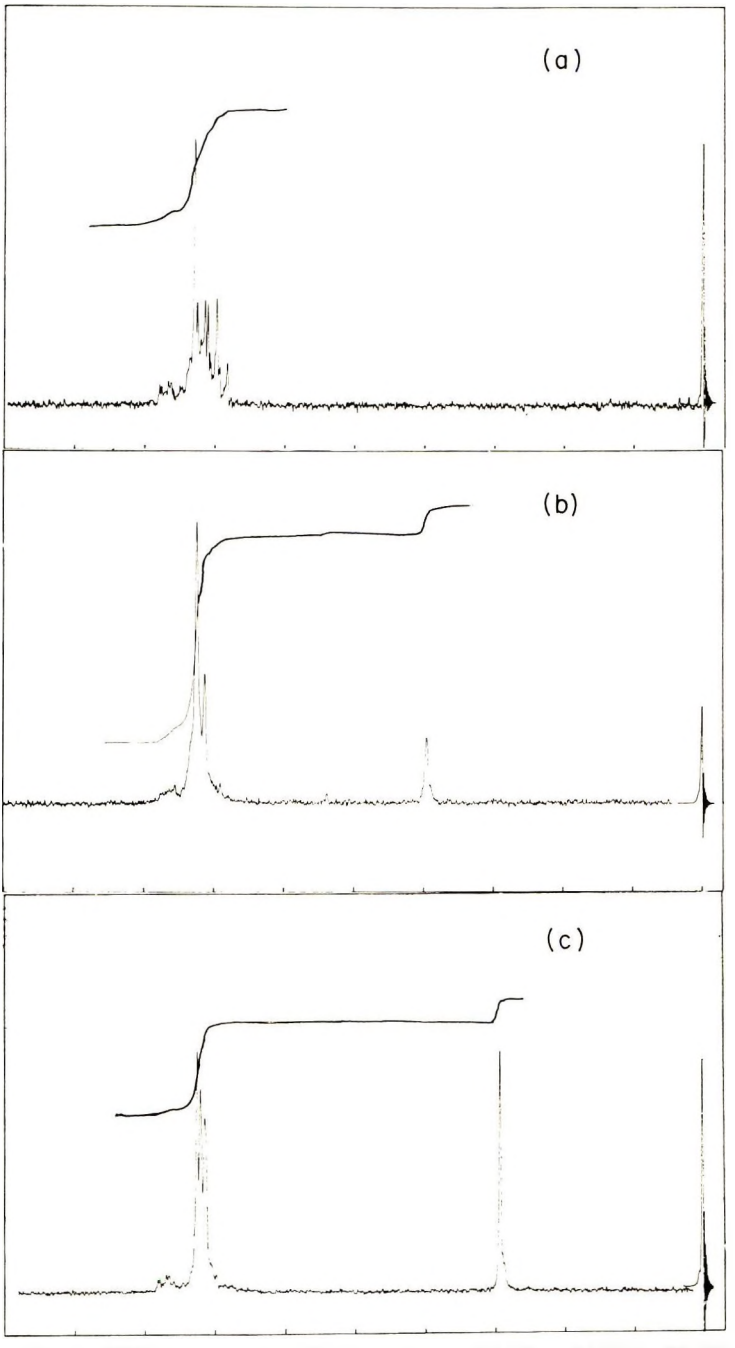

Fig. 4. NMR spectra of model pinacolones: (*a*) IVa; (*b*) IVb; (*c*) IVc.

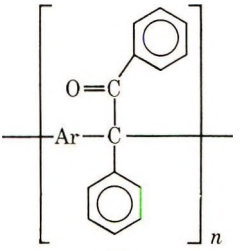

III

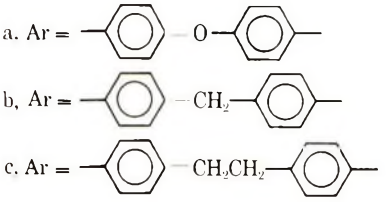

spectra of polymers IIIa–IIIc indicated only the presence of methylene and aromatic hydrogens (Fig. 3). Since the NMR peaks were broad bands for the polymers, no conclusive evidence could be obtained from these spectra except for comparison purposes with those spectra of the model compound rearrangements (Fig. 4). However, comparison of NMR and infrared spectra of the polymers together with those infrared spectra of the model compounds (Figs. 2–4) seems to be quite conclusive for the suggested structures for the rearranged polymers.

Model Compounds

Model pinacolones IVa–IVc were prepared in order to aid in the characterization of polymers IIIa–IIIc. The infrared spectra of the model pinacolones are quite similar to those of the corresponding polymers (Figs. 1 and 2). However, since there are two different groups, the phenyl and *p*-substituted phenyl, which can migrate during the rearrangement reactions, it was necessary to use NMR for predicting which, if not both, groups migrate (Figs. 3 and 4). In the NMR spectra of the model compounds the appearance of the small quartets at 7.7 ppm with coupling constants of 7 H_z (*ortho* splitting) and 2 H_z (*meta* splitting) indicates that the *p*-substituted phenyl groups were favored over the unsubstituted phenyl groups in the acid catalyzed migrations. Thus, compounds IVa–IVc are apparently the favored products of these rearrangements.

These results are in agreement with those of Bachmann and Ferguson,[3] in which the migrating aptitudes of various *p*- and *o*-substituted phenyl groups were studied in the pinacol rearrangement. These workers found that the ratio of *p*-methoxyphenyl migration to unsubstituted phenyl migration was approximately 500:1 and that the ratio of *p*-methylphenyl to unsubstituted phenyl migration was 16:1.

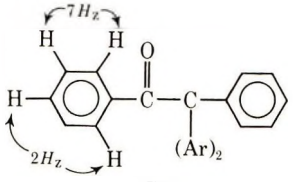

IV

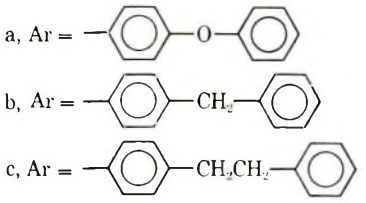

In the cases of the polymers IIIa–IIIc the NMR spectra showed only broad absorption bands around 7.7 ppm. Although spin-spin coupling is not evident, these absorption bands do correspond to the same chemical shifts as for those of the model pinacolones at 7.7 ppm. Although this is not conclusive evidence for only polymer chain migration in the polymer rearrangements, it does suggest, however, that polymer chain migration is favored over phenyl migration.

EXPERIMENTAL

Instruments

Infrared spectra were taken on Beckman IR-8 and Perkin-Elmer Model 700 instruments. Nuclear magnetic resonance spectra were obtained with a Hitachi Perkin-Elmer R-20 instrument. All melting points are uncorrected.

Polymer Rearrangements

Rearrangement of Polymer Ia. A solution of 1 g of polymer Ia in 30 ml of *p*-dioxane and 5 ml of concentrated sulfuric acid was stirred at room temperature for 3 hr. The solution was then poured into ice water. The precipitate was filtered, redissolved in tetrahydrofuran (THF), the solution filtered, and then poured into water and filtered. The resulting white precipitate was washed with 10% aqueous sodium bicarbonate, with water, and finally with 95% ethanol. The rearranged polymer was dried *in vacuo* at 80°C to give 0.8 g (80%), mp 230–250°C; η_{inh} 0.28 (dioxane).

ANAL. Calcd for $(C_{26}H_{18}O_2)_n$: C, 86.18%; H, 5.01%; O, 8.81%. Found: C, 84.69%; H, 5.05%; O, 9.94%.

Rearrangement of Polymer Ib. The same procedure as that for the rearrangement of polymer Ia was used for polymer Ib. After drying *in vacuo* there was obtained a quantitative yield of rearranged polymer; mp 225–235°C; η_{inh} 0.12 (dioxane).

ANAL. Calcd for $(C_{27}H_{20}O)_n$: C, 89.97%; H, 5.59%; O, 4.44%. Found: C, 88.82%; H, 5.58%; O, 5.43%.

Rearrangement of Polymer Ic. The same procedure as above was used for the rearrangement of polymer Ic. A quantitative yield of polymer IIIc was obtained; mp 165–180°C; η_{inh} 0.18 (dioxane).

ANAL. Calcd for $(C_{28}H_{22}O)_n$: C, 89.80%; H, 5.93%; O, 4.27%. Found: C, 88.88%; H, 5.73%; O, 5.17%.

Model Compounds

Rearrangement of Pinacol IIa. A solution of 1 g of pinacol IIa in 30 ml of *p*-dioxane and 5 ml of concentrated sulfuric acid was stirred at room temperature for 3 hr and then poured into ice water. The white precipitate was washed with 10% aqueous sodium bicarbonate solution, with water, and finally with 95% ethanol. The product IVa was dried *in vacuo* and then reprecipitated from pentane to give 0.5 g of product melting at 50–60°C.

ANAL. Calcd for $C_{38}H_{28}O_3$: C, 85.70%; H, 5.30%. Found: C, 85.99%; H, 5.46%.

Rearrangement of Pinacol IIb. The same procedure as that for pinacol IIa was used. The corresponding product, pinacolone IVb, would not crystallize at room temperature and was used as the thick oil. The yield of product IVb was 0.5 g.

ANAL. Calcd for $C_{40}H_{32}O$: C, 90.86%; H, 6.10%. Found: C, 90.57%; H, 6.04%.

Rearrangement of Pinacol IIc. The same procedure as above was used for the rearrangement of pinacol IIc. The yield of product IVc was 0.5 g melting at 85–95°C.

ANAL. Calcd for $C_{42}H_{36}O$: C, 90.59%; H, 6.54%. Found: C, 90.35%; H, 6.39%.

This work was supported by the Army Research Office-Durham, Durham, North Carolina.

References

1. J. Higgins, A. H. Johannes, J. F. Jones, R. Schultz, D. A. McCombs, and C. S. Menon, *J. Polym. Sci. A-1*, **8**, 1987 (1970).
2. D. A. McCombs, C. S. Menon, and Jerry Higgins, *J. Polym. Sci. A-1*, in press.
3. W. E. Bachmann and J. W. Ferguson, *J. Amer. Chem. Soc.*, **56**, 2081 (1934).

Received January 13, 1971

JOURNAL OF POLYMER SCIENCE: PART A-1 VOL. 9, 1807–1822 (1971)

Thermal Degradation of Nylon 66

L. H. PEEBLES, JR.,* and M. W. HUFFMAN, *Chemstrand Research Center, Inc., Durham, North Carolina 27702*

Synopsis

The rate of gel formation and color formation in poly(hexamethylene adipamide), nylon 66, is found to be dependent upon the rate of removal of the volatile products of degradation. If a sample of nylon is heated above its melting point in a sealed tube, the material will remain soluble for extended periods of time as the intrinsic viscosity first passes through a maximum, then a minimum, followed by the abrupt formation of insoluble material. The color remains reasonably white. On the other hand, if the volatile material is permitted to escape, rapid gelation and color formation will occur, even in the complete absence of oxygen. Intermediate rates of gelation and color formation can be obtained by control of the rate of volatile material distillation. The decrease in molecular weight evidenced in the sealed tubes is probably due to hydrolysis and ammonolysis of the amide groups which occur simultaneously with the formation of multifunctional crosslinking agents. The volatile material contains an intense absorption in the 290 mμ region. Analysis of the volatile material shows that it contains *inter alia*, water, carbon dioxide, ammonia, cyclic monomer, hexylamine, hexamethyleneimine, hexamethylenediamine, cyclopentanone, 2-cyclopentylcyclopentanone, 2-cyclopentylidinecyclopentanone, and 1,2,3,5,6,7-hexahydrodicyclopenta[b,e]pyridine,, which has an intense absorption at 287 mμ, $\epsilon = 8.87 \times 10^4$ l./mole-cm, (methanol).

INTRODUCTION

Thermal Degradation of Nylon 66

When nylon is heated above its melting point for extended periods of time, it gradually darkens and changes occur in the average molecular weight as determined by viscometry. Korshak et al.[1] showed that heating nylon 66 of various molecular weights at 270°C under a gentle stream of nitrogen caused no changes in molecular weight, whereas at 300°C polymers with 18,000, 35,000, and 55,000 molecular weight all decreased to approximately 9,000 within 2 hr and remained constant at this level for at least 8 hr. On the other hand, if the polymer is heated at 330°C, gelation-type reactions occur. Kroes[2,3] indicated that part of the gelation occurs from dimerization of the hexamethylenediamine portion followed by amide formation [eq. (1)].

* Present address: Office of Naval Research, 495 Summer St., Boston Mass. 02210, to whom all communications should be addressed.

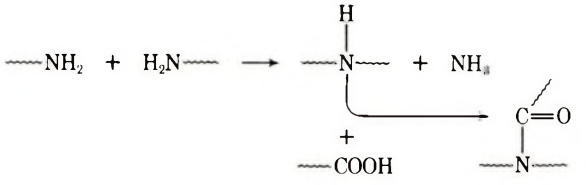

(1)

Addition of 6,6′-diaminodihexylamine to the polymerizate caused gelation but the polymer remained white. The dihexylamine has been identified in gelled nylon.[3] In addition to NH_3, CO_2, and H_2O, less volatile materials such as cyclopentanone, hexamethyleneimine, and hexylamine have been identified in the off gases, along with minor components of other cracking products.

Goodman[4] studied the thermal degradation of a number of model compounds of nylon, among them the diamides of diamines and dicarboxylic acids. He found that the diamine derivatives were all reasonably stable at 350°C, whereas the diacid derivatives degraded in varying amounts, the degradation reaching completeness in the case of the adipic acid derivative, dibutyl adipamide. Analysis of the degradation products of this compound showed the presence of butylamine, butane, butene, hydrogen, along with CO, CO_2, and NH_3, but no traces of cyclopentanone. Goodman did, however, isolate various substituted cyclopentanone derivatives, such as I and II.

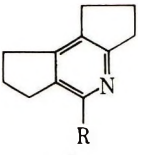

I

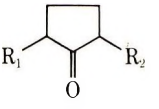

II

Further, he found that the thermal degradation products of nylon 66 and dibutyl adipamide gave a positive Ehrlich reaction (reddish-purple coloration with *p*-dimethylaminobenzaldehyde hydrochloride in HCl) which is indicative of pyrroles, but the Ehrlich-positive material was present in very small amounts. A detailed examination of the reactions of cyclopentanone with various amines by Edgar and Johnson[5] also showed the presence of small quantities of Ehrlich-positive materials, but they were not able to obtain enough for identification. Goodman was also able to show that the Ehrlich-positive material was not responsible for the adsorption at 290 mμ which appears when nylon 66 is thermally degraded. Liquori et al.[6] showed that an intense absorption occurred at 290 mμ when nylon was heated for several hours at 275°C and which remained after the sample was hydrolyzed, indicating that it did not arise from the amide bond. Goodman as well as Edgar and Johnson[5] showed that the bicyclopentapyridine derivatives (I) (R = propyl or butyl) absorb at 275–284 mμ. One possible mechanism for the formation of the butyl derivative (I, R =

Bu) is based on the condensation of two cyclopentanone moieties and ring opening of a third cyclopentanone (CPO), followed by cyclization with ammonia [eq. (2)].

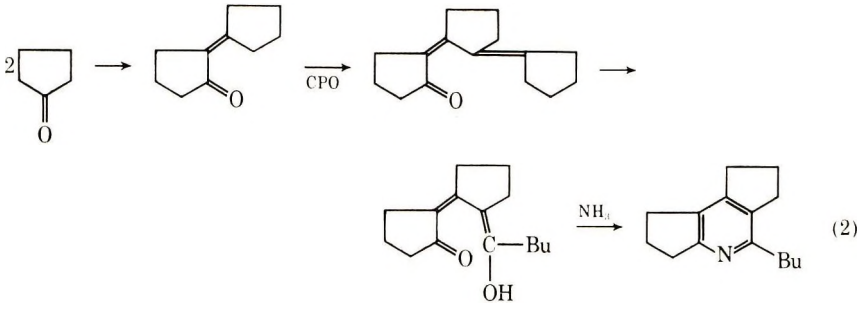

(2)

In addition to the dimerization of hexamethylenediamine, the formation of cyclopentanone from the adipic acid residue, the possible presence of small amounts of Ehrlich-positive materials and the presence pyridine compounds in model systems, evidence also exists for the presence of nitrile and isocyanate groups in the polymer and the formation of amino acids from hexamethylenediamine adipamide. Beyond these points, little quantitative chemical analysis of the degraded material has been published, mainly because of the inherent difficulties of analyzing trace quantities of materials. More detailed reviews can be found in the literature.[2,3,7,8]

Photochemical Degradation of Nylon 66

A great many articles exist showing that nylon degrades in sunlight and that the degradation is enhanced by the presence of the titanium dioxide pigment. Taylor et al.[9] have shown that the phototendering effect of TiO_2 proceeds by a chemical rather than an energy transfer mechanism. The prime observable quantities of photodegradation are the loss of mechanical properties and a lowering of the molecular weight. Beyond this, little exists concerning the presence of chemical entities which enhance degradation and the chemical entities which result from photochemical degradation, aisde from a general impression of a correlation between the amount of 290 mμ absorption and the rate of photodegradation. Again, the primary reason is the extreme difficulty of isolating and identifying compounds which occur only in trace amounts. Details of the photodegradative processes have been reported.[10–15]

None of the enumerated products of photochemical degradation absorb in the 290 mμ region. To obtain more definitive information on this system, we began a study of the phenomenon of gel and color formation with the aim of identifying in greater detail the products of thermal degradation with emphasis on materials which absorb in the 290 mμ region. This report summarizes our progress to date.

RESULTS AND DISCUSSION

Phenomenological Studies

When nylon 66 is heated at 285–305°C and a stream of inert gas is passed through the melt, the material rapidly becomes colored, volatile material is given off, and the residue becomes insoluble. Independent work in these laboratories on the thermodynamics of nylon polymerization[16] indicated that if nylon salt is heated at these temperatures for extended periods of time in a sealed tube, polymerization occurs, but the polymer remains white and soluble. To check this effect further, samples of a nylon polymer were placed in an I-tube and one leg of a U-tube; both

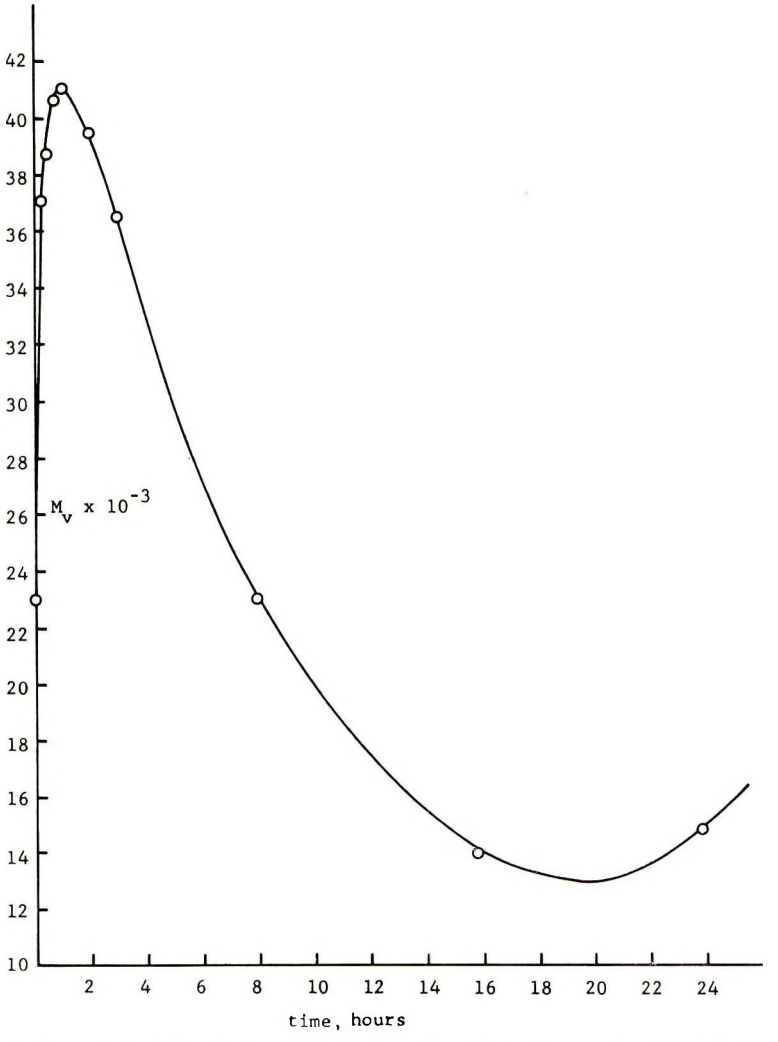

Fig. 1. Change in molecular weight as a function of time for a nylon 66 at 282°C contained in a sealed tube such that the volatile materials were maintained over the melt.

tubes were repeatedly flushed with argon and evacuated to remove oxygen and volatile water. After sealing under hard vacuum (10^{-5} torr), the I-tube was completely submerged in a vapor bath at 305°C, whereas the U-tube had the polymer leg in the 305°C bath and the empty leg chilled with liquid nitrogen. The samples were heated for 6 hr. The I-tube sample

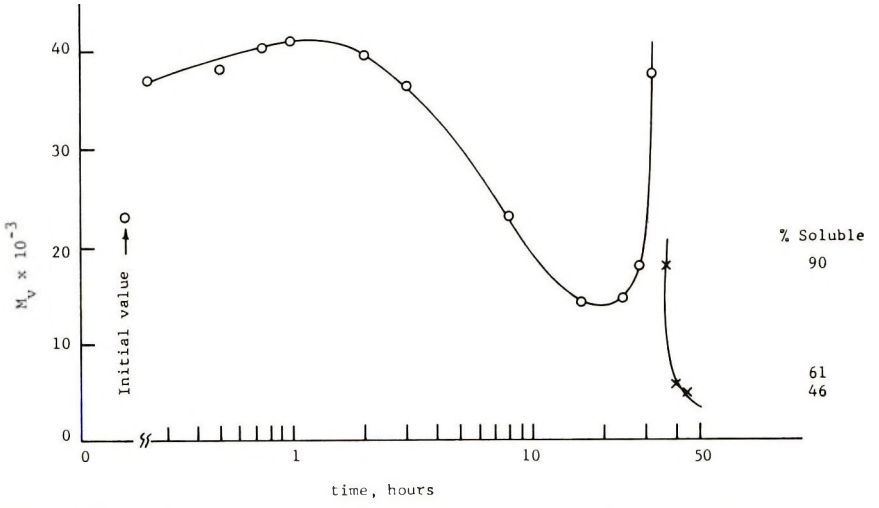

Fig. 2. Molecular weight as a function of log time, same conditions as in Fig. 1. O, M_v determined on total sample; x, on soluble portion only.

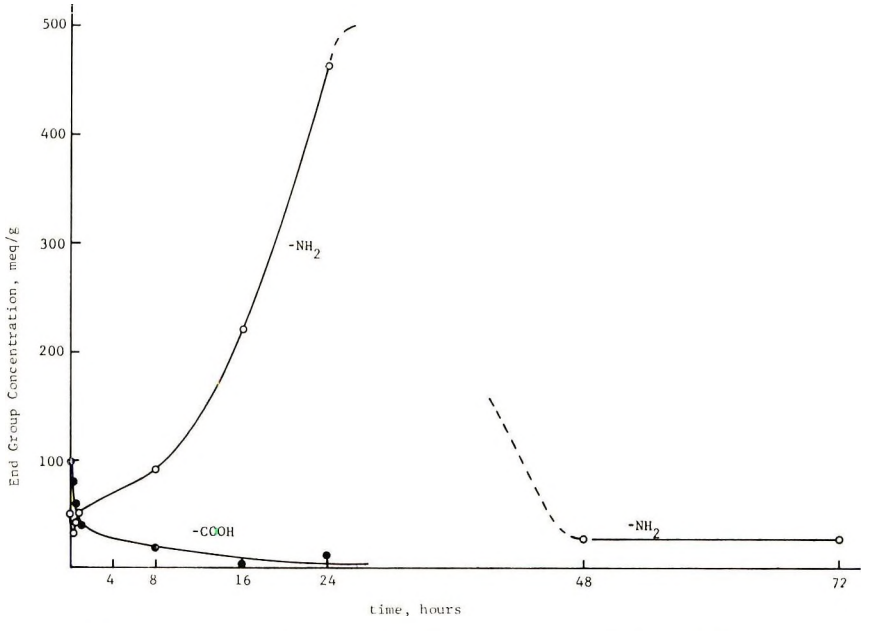

Fig. 3. Endgroup concentrations (in μeq/g) as a function of time. Same conditions as in Fig. 1.

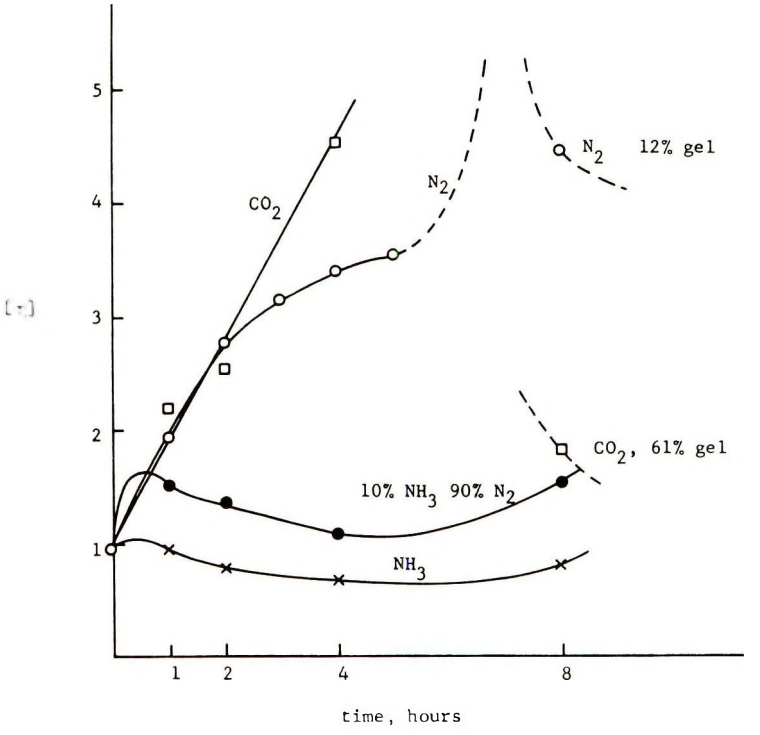

Fig. 4. Influence of gas flowing at 1 ft^3/hr through molten nylon 66 as a function of time at 282°C.

remained white and soluble, and a small amount of material crystallized out away from the polymeric mass. The U-tube sample became black almost instantly, was insoluble and nonswellable, and it gave off copious quantities of distillate. This experiment demonstrated two items: (1) the rate of gelation depends upon the rate of distillation of volatile material; (2) the color change occurs in the ostensible absence of oxygen (perhaps chemisorbed oxygen was not removed by outgassing). The I-tube experiments indicated that by preventing distillation, or alternately by retaining an atmosphere of volatile products over the melt, the rate of gelation and the rate of color formation are reduced. To check this aspect, a series of I-tubes were prepared with a commercial polymer and reacted at 282° for a variety of times. The viscosity of the soluble portion, the gel content, and the content of acid and basic groups were determined. Figures 1–3 give the results. Initially, the material tends to polymerize, reaching a maximum value in about 1 hr. The polymer is known to be a "nonequilibrium" product, as the molecular weight tends to increase upon spinning. Following the maximum, the molecular weight drops to a minimum value, then climbs steeply towards an infinite molecular weight. The concentration of amine endgroups initially decreases, as it should because of polymerization, then increases markedly, becoming very large at about the

point of incipient gelation, then it returns to a small value in the gelled material. The carboxyl content of the material gradually decreases during the course of reaction. Throughout the reaction, the color remained reasonably white. These results are at variance with those reported by Korshak,[1] who maintained a nitrogen flow at 300°C; in his experiments he found the molecular weight to fall to a minimum and remain there for several hours. We repeated these experiments with nitrogen, carbon dioxide, ammonia, and a 10% ammonia–90% nitrogen mixture. The gases were passed through molten nylon at 282°C at 1 ft³/hr. The results are presented in Figure 4. Nitrogen causes a rapid increase in molecular weight, the material becoming gelled between 5 and 8 hr. Carbon dioxide caused gelation to occur even more rapidly. Ammonia and mixed ammonia–nitrogen caused the molecular weight to remain sensibly constant over the course of the experiment. Comparison of these results with those of Figure 2 indicates that the initial climb in molecular weight in Figure 2 is due to polymerization of the unreacted ends, but deamination also is occurring. The vapors over the polymerizing system (less than 1 hr reaction) will give a positive test for base. The depolymerization observed is probably due to ammonolysis reactions of the form of eq. (3)

$$R_1\overset{\displaystyle OH}{\overset{\|}{C}}NR_2 + NH_3 \rightarrow R_1\overset{\displaystyle O}{\overset{\|}{C}}NH_2 + H_2NR_2 \qquad (3)$$

as well as the usual hydrolysis reactions, but at the same time cross-linking reaction(s) are also occurring. If we assume dimerization of amine ends as given in eq. (1), then we can speculate that the reaction (4) occurs.

$$R_1\overset{\displaystyle O}{\overset{\|}{C}}NH_2 + R_2\overset{\displaystyle H}{\overset{|}{N}}R_3 \rightarrow R_2N\overset{\displaystyle R_1}{\overset{|}{C}}{=}O - R_3 + NH_3 \qquad (4)$$

Thus chain scission and crosslinking are occurring simultaneously. Eventually sufficient crosslinking sites are created so that molecular weight can rise again and it does so abruptly.

Nylon will darken rapidly when it is heated in the presence of small amounts of oxygen. The outgassing experiments described earlier indicated that nylon will darken even in the absence of oxygen. A number of experiments were conducted using a flow of nitrogen or helium through the melt, using various techniques to ensure absence of oxygen from the flow gases and almost complete desorption of oxygen from the nylon flake. The nylons darkened even under the most stringent of conditions if the volatile degradation products were permitted to escape. Thus, color formation is an inherent property of the nylon molecule itself.

Analysis of the Products of Thermal Degradation

The products of thermal degradation fall into three broad classes: (a) highly volatile small molecules, (b) less volatile higher molecular weight

material which condenses just outside the hot zone, and (3) the polymeric residuum. The highly volatile material has been examined earlier by Kamerbeek et al.[3] and Achhammer et al.[17] In general, water is always given off, even from extensively dried material. One major source is thermal cracking followed by dehydration:[3]

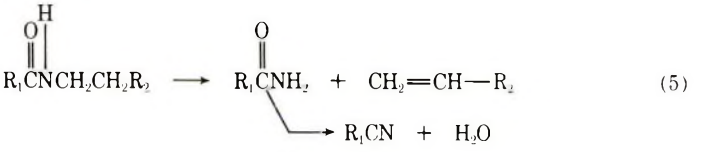

(5)

Nitrile groups are detectable in the volatile fraction and in the residuum by infrared spectroscopy. Ammonia and carbon dioxide result from decarboxylation and the deamination as a result of hydrolysis of amide bonds. Some CO_2 probably arises from the same reaction path that produces cyclopentanone, the exact mechanism of which is still obscure. Condensation of the cyclopentanone [eq. (6)] produces even more water.[18]

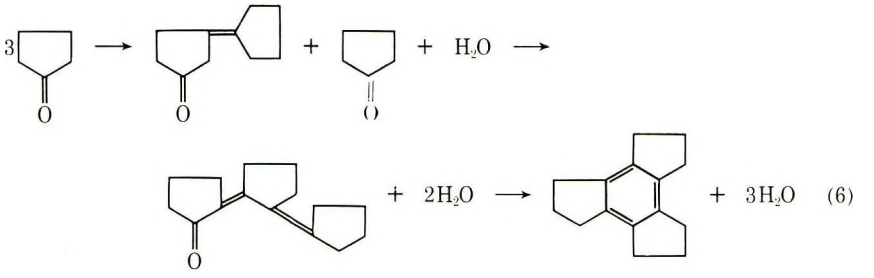

(6)

Cyclopentanone dimers have been identified in the volatile fraction.

The brown-black, bubbly polymeric residuum, containing fragments of the glass reactor, was cut into pieces and refluxed in 50:50 HCl–water for 24 hr. If the polymer was just slightly swellable in formic acid, hydrolysis in the HCl solution was complete. Portions of nonswellable gel would resist hydrolysis for extended periods of time. On cooling the hydrolyzate to 0°C, a portion of the adipic acid would crystallize. This was recrystallized from water and the liquors combined. The acid and neutral species were removed from the hydrolyzate by continuous extraction with ether. The acid fraction generally had far less color than the remaining basic fraction. The neutral species was isolated from the acid species by extraction. The HCl solution was evaporated to concentrate the remaining liquor, and neutralized, whereupon a brown-black oil appeared in the heavily degraded samples. Undegraded nylon was colorless throughout the hydrolysis operation. The oil was soluble in methanol, but not in water-immiscible solvents. It could be removed from the aqueous phase, along with other basic organic species by continuous extraction of the aqueous phase with methanol-chloroform. The oil could not be charac-

TABLE I
Degradation Products of Nylon 66 at 305°C

	Product
Highly volatile materials	CO_2
	NH_3
	H_2O
Less volatile materials	
Neutral fraction	Cyclic monomer
	Cyclopentanone
	Cyclopentylidinecyclopentanone
	Cyclopentylcyclopentanone
Basic fraction	Hexylamine
	Hexamethyleneimine
	Hexamethylenediamine
	[b,e]-Pyridine
	Several unknown materials
Polymeric residuum after hydrolysis (black)	
Neutral fraction	3-Pentanone[a]
	Cyclopentylcyclopentanone,
	Cyclopentylcyclopentanol
	Cyclopentylidinecyclopentanone
	Other unknowns, three in high concentration
Acid fraction (straw-colored)	Succinic acid
	Glutaric acid
	Adipic acid
	Pimelic acid[a]
	Suberic acid[a]
	Many other unknowns, some in high concentration
Basic fraction (black oil)	Hexylamine
	Hexamethyleneimine
	Hexamethylenediamine
	6,6′-Diaminodihexylamine
	Nonvolatile black oil

[a] Identification based on retention time only.

terized further either by gas or thin-layer chromatography. The identified components of the residuum are listed in Table I.

The volatile fraction contains a strong adsorption at approximately 290 mμ. Because so much emphasis has been placed on this adsorption peak in photodegradation studies, we decided to determine the major components in order to isolate and characterize the adsorbing species. One of the major components of the volatile fraction is the cyclic monomer of nylon 66 (III):

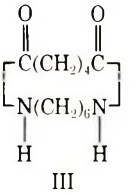

III

This could be separated easily from the other components by rinsing the volatile condensate with water, the intense ultraviolet-adsorbing species appeared to dissolve in the water, leaving the cyclic monomer behind. The remaining material was soluble in methanol when degradation was performed under flowing nitrogen at 1 ft^3/hr. Under vacuum, a water- and methanol-insoluble material appeared in the volatile fraction, presumably a low molecular weight nylon. Both the water and methanol fractions tended to turn yellow when exposed to air and light. The methanol fraction was not examined further.

The water fraction of the volatile material was basic. Distillation of the basic solution produced a foreshort of white solid, ammonium carbamates, followed by a water fraction with a very intense ultraviolet spectrum. Again the products darkened rapidly with time. If the water fraction was made acid with H_2SO_4 (nonvolatile) and distilled, CO_2 and materials absorbing at 260 mμ were separated. Distillation was continued until an ultraviolet clean distillate was obtained. The separation into acid volatile and acid nonvolatile fractions rendered them more stable. Both fractions would darken with time, but at a far slower rate than prior to fractionation. The acid volatile material was extracted with ether, dried, concentrated, and subjected to gas chromatography (see Table I for the compounds identified). The acid nonvolatile material was made basic with KOH and distilled until an ultraviolet-clean distillate was obtained. Extraction of the distillate with ether caused the chromophores to pass into the ether phase which were then dried, concentrated, and subjected to gas chromatography (see Table I). Some of the gas chromatographic experiments were performed such that 90% of the eluant stream could be trapped, the remaining 10% passed through the flame ionization detector. Examination of the major components of the basic fraction indicated the presence of a single component with an intense absorption at 287 mμ. Sufficient quantities were obtained for mass, IR and NMR spectroscopy. The material was identified as 1,2,3,5,6,7-hexahydrodicyclopenta-[b,e]-pyridine (IV) and not the [b,d] derivative (V).

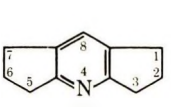

IV

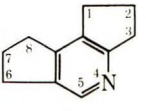

V

Structure V is structure I with R = H. The ultraviolet, infrared, mass, and NMR, spectra as well as results of melting point and elemental analysis of IV agreed with those of the material obtained by direct synthesis

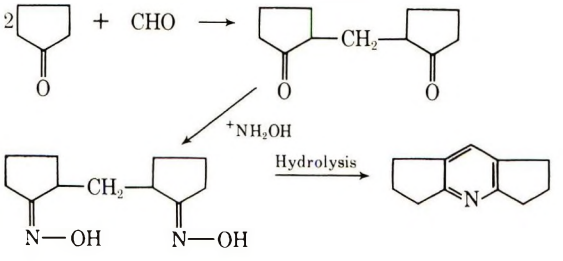

(8)

which involved condensation of cyclopentanone with formaldehyde, formation of the dioxime, and ring closure to the pyridine [eq. (7)].

NMR spectroscopy shows that the single pyridine hydrogen is located at the 8-position as in IV and not at the 5-position as in V. Thus the [b,e]-pyridine is a newly identified product of nylon degradation; it must be formed by a different route than the [b,d]-pyridines found in the pyrolysis of dibutyladipamide and cyclopentanone with ammonia. The [b,e]-pyridine arises from the adipic acid portion of the molecule because the pyridine could not be detected in the volatile portion from nylon 6 and nylon 6,10 (polyhexamethylene sebacamide) degradation, but it was present in the volatile fraction in nylon 66 and nylon 10,6 (polydecamethylene adipamide) both prepared by interfacial polymerization. The mechanism of eqs. (9)–(11) is suggested.[19]

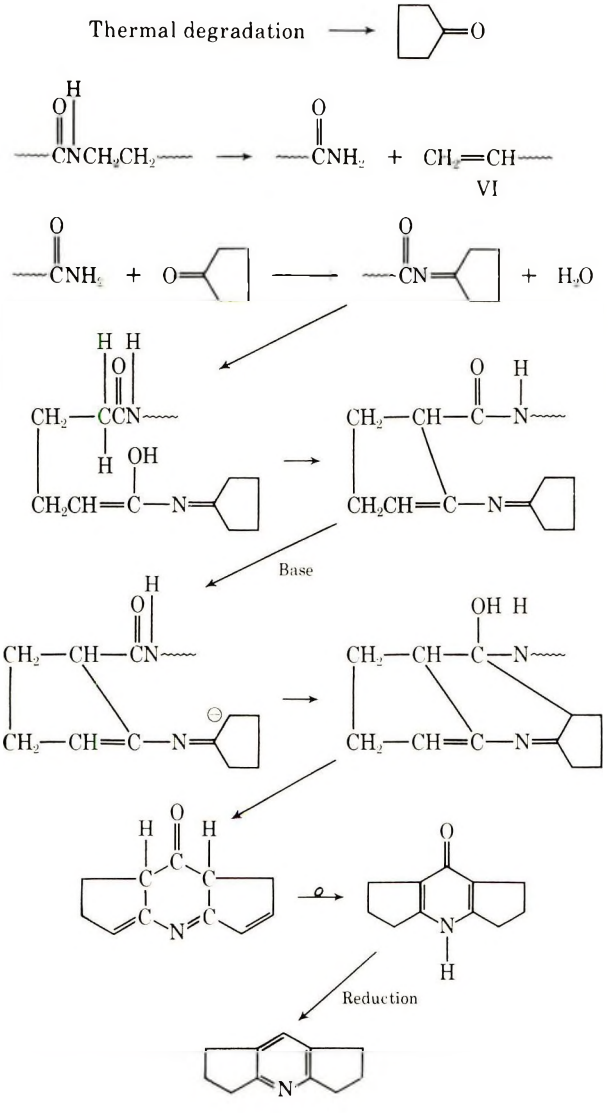

The hexamine VI in eq. (10) has not been isolated, nor is it described in the literature, but the isomeric hexamethyleneimine is a product of thermal degradation. The final reduction step in the scheme [eq. (11)] is not unreasonable, because reduction apparently occurs in the acid volatile fraction. Comparison of the cyclopentanone condensation products gave the following relative concentrations: cyclopentanone, 1.0; cyclopentylcyclopentanone, 0.20; cyclopentylidinecyclopentanone, 0.03. Since the cyclopentyl derivative is probably formed from the cyclopentylidine derivative, other species in the system must be losing hydrogen, perhaps in the color formation step where conjugated moieties are required.

Gas and thin-layer chromatography of the various fractions listed in Table I showed that whereas some of the degradation products of nylon 66 have been identified, there exist a number of other components, some in rather high concentration which have not yet been characterized. It is intertesting to note that none of the assorted fractions gave positive Ehrlich tests. Perhaps this is due to the low temperature of degradation which did not produce volatile Ehrlich positive products, whereas the dark color of the hydrolyzed basic fraction obscured the test.

EXPERIMENTAL

Nylon Degradation Reactors

To obtain reasonable quantities of the volatile fraction, approximately a 10-g portion of nylon chips was degraded under a flow of nitrogen at 1 ft^3/hr, 305°C, for 24 hr. The amount of volatile material obtained by this procedure was only a few milligrams, but it was sufficient for all of the separation and characterization procedures used. Further, it could be worked up rapidly without significant changes in color. Temperature was maintained by a benzophenone vapor bath (305°C) or dimethyl phthalate (283°C) similar to that described by Sorenson and Campbell.[20] A U-tube was constructed, with one leg of 8 mm od tubing joined by a small ring seal to a 25 mm od tube so that gases passing down the smaller tube would be heated to operating temperature before contacting the flake in the larger tube. The U-tube was inserted into a rubber stopper to maintain the vapors in the boiler. From the large tube, an air condenser led to a liquid nitrogen condenser, then to a water bubbler. When nitrogen was used as flow gas, it was first passed through a liquid nitrogen bath to remove condensable material. Polyethylene or glass tubing was used throughout.

Determination of Gel Content

The content of gel in a sample was determined by grinding the sample to 20 mesh, placing a weighed quantity (ca. 0.25 g) in a tared, extracted alundum crucible, extracting with 100% formic acid for 48 hr, freeze-drying the remains, then reweighing, hydrolyzing the remains with 50% HCl/H_2O for 24 hrs, and reweighing to correct for glass which contaminated

the sample originally. The per cent gel is ratio of insoluble nylon to the original nylon, multiplied by 100. The correction for glass must be applied because gelled nylon will pull glass off of the container walls as it cools. The gelled nylon plugs containing the glass coating were chilled in liquid nitrogen, ground in a Wiley mill maintained cool with Dry Ice outside the grinding chamber, and dried. The extractor consisted of an especially constructed Soxhlet extractor in which the formic acid entering extraction chamber was at room temperature; this procedure prevented formolysis reactions between nylon and formic acid which would have occurred had hot formic acid been in contact with the nylon for extended periods of time. Vacuum freeze-drying was accomplished by maintaining the samples below $-60°C$ to ensure that the gel–formic acid–water system remained solid at all times. The system worked quite well except at the point of incipient gelation where very large molecules of nylon tended to clog the pores of the crucible. No difficulties were experienced either with nongelled or material containing more than 3% gel. Reproducibility was generally within $\pm 2\%$.

Preparation of the [b,e]-Pyridine

2,2′-Methylenedicyclopentanone. This was prepared in low yield (17%) by the procedure of Colonge et al.[21] from cyclopentanone, paraformaldehyde, and sodium methylate.

ANAL. Calcd for $C_{11}H_{16}O_2$: C, 73.30%; H, 8.95%; O, 17.75%. Found: C, 73.45% H, 9.23%; O, 17.42%.

Dioxime of 2,2′-Methylenedicyclopentanone. A 1-g portion of the above ketone was added to 2.5 g hydroxylamine hydrochloride, 15 cc water, 10 cc 10% NaOH, and just enough alcohol until the ketone started to dissolve and a crystalline ppt simultaneously started to form. The mixture did not become clear. It was stirred overnight on a magnetic stirrer, washed with water, and dried. The product melted at 214°C (reported mp, 193 and 216°C[21]).

ANAL. Calcd for $C_{11}H_{18}N_2O_2$: C, 63.82%; H, 8.63%; N, 13.33%; O, 15.22%. Found: C, 63.15%; H, 8.71%; N, 13.29%; O, 14.95%.

1,2,3,5,6,7-Hexahydrodicyclopenta[b,e]pyridine. Product from above put in a flash with 3 ml concentrated HCl and refluxed for 30 min following the procedure of Colonge et al.[22] Upon addition of base a white precipitate formed which darkened rapidly. This was extracted with ether, dried, evaporated to dryness, and recrystallized from petroleum ether, mp 90°C (reported mp 87°C). NMR Spectra showed 1 proton at the 4 position, 8 protons at the almost equivalent 1, 3, 5 and 7 positions, and 4 protons for the equivalent 2 and 6 positions (Fig. 5). The molecular weight by high-resolution mass spectroscopy was 159.10467; calculated for $C_{11}H_{13}N$, 159.10473.

ANAL. Calcd for $C_{11}H_{13}N$: C, 82.97%; H, 8.23%; N, 8.80%. Found: C, 82.32%; H, 8.53%; N, 8.70%.

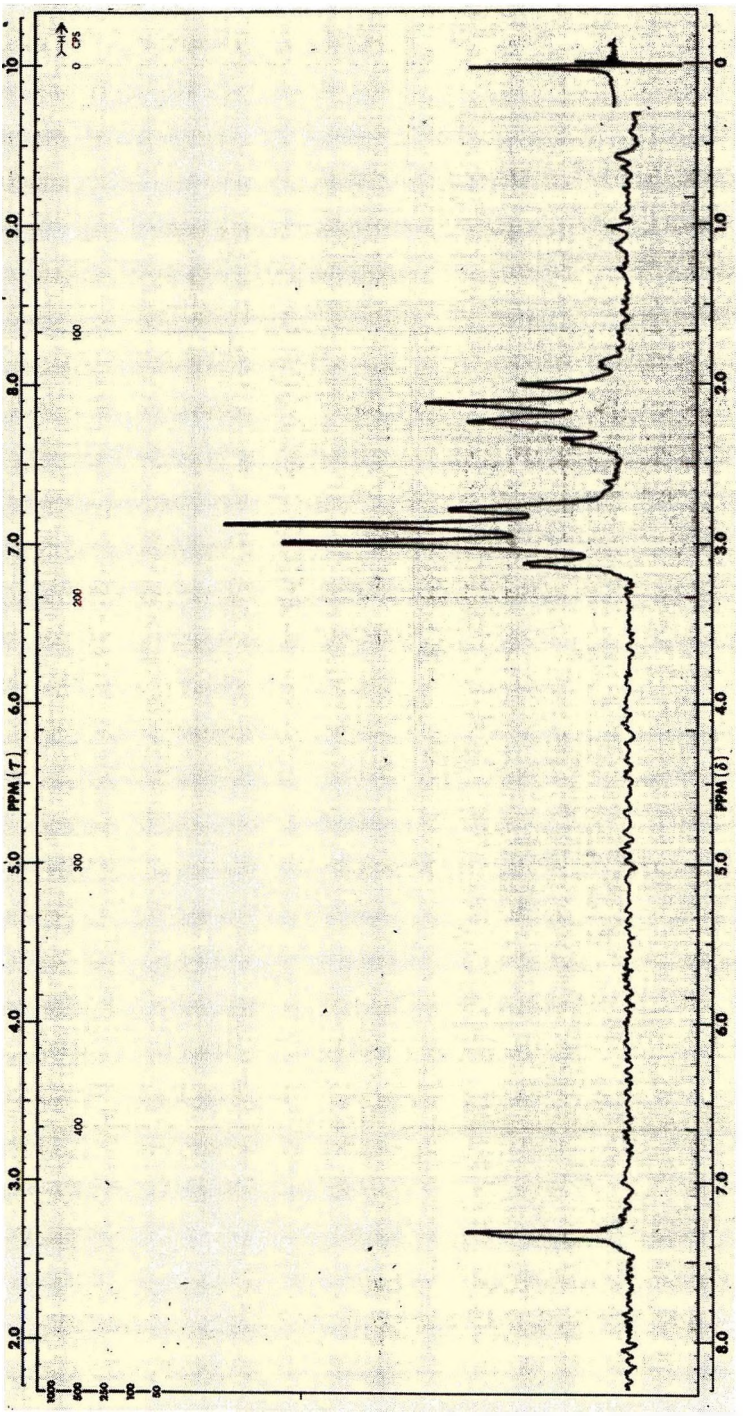

Fig. 5. NMR spectrum of 1,2,3,5,6,7-hexahydrodicyclopenta[b,e]-pyridine in $CDCl_3$.

The ultraviolet spectrum λ_{max} 287 mμ, $\epsilon = 8.87 \times 10^3$ l/mole cm in methanol; $\lambda_{max} = 298$ mμ, $\epsilon = 1.4 \times 10^4$ l/mole cm in formic acid.

Condensation of Cyclopentanone

Cyclopentanone was refluxed over KOH, and the aqueous product was collected in a Dean-Stark trap following the procedure of Edgar and Johnson.[5] After workup, two fractions were obtained, the dimer, cyclopentylidine-cyclopentanone, bp 136–141°/21 mm (VII) and the trimer, cyclopentylidine(2′-cyclopentylidine)cyclopentanone, (VIII), mp 71–72°C.

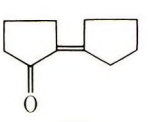

VII

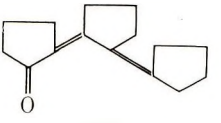

VIII

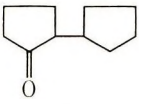

IX

Gas chromatic analysis of the dimer showed that it contained ca. 10% of the hydrogenated dimer, cyclopentylcyclopentanone (IX).

Ultraviolet analysis showed cyclopentanone, (single maximum at 288 mμ, ϵ = 17.7 l/mole-cm in methanol), dimer VII (single maximum at 258 mμ, $\epsilon = 1.075 \times 10^4$ l./mole-cm in methanol, log ϵ = 4.03, reported log ϵ = 4.10 in ethanol); trimer VIII (two maxima, located at 302 and 363 mμ, $\epsilon_{302} = 2.31 \times 10^4$ l./mole-cm, log ϵ = 4.36 (methanol), reported 4.46 (ethanol), and $\epsilon_{363} = 2.35 \times 10^2$ l./mole cm, log ϵ = 2.37. The tricyclopentenobenzene is reported to have the following spectra:[23] λ_{max} 267 mμ, log ϵ = 2.55 (cyclohexane); λ_{min} 245 mμ, log ϵ = 2.25 (cyclohexane).

Cyclopentylcyclopentanone was easily prepared by hydrogenation of VII over Adam's catalyst at 60 psi. It contained approximately 10% cyclopentylcyclopentanol.

Cyclopentylcyclopentanol was easily prepared by reduction of VII in ethanol with metallic sodium.

Gas Chromatography

The neutral volatile materials and the methylated acids were chromatographed on 30% Carbowax 20M-terephthalate on Chromosorb G, AW-DMCS 60–100 mesh.

The basic volatile materials where chromatographed on 10% Carbowax 20M + 2% KOH on Anakrom u.

The acid materials were methylated by using the BF_3–methanol procedure of Metcalfe et al.[24]

Thin-Layer Chromatography

The basic materials were chromatographed on silica gel GF with 77% ethanol–23% ammonium hydroxide and visualized with ninhydrin. The pyridine and secondary amines required about 30 min at 100°C for color to be developed.

To obtain positive identification of the [b,e]-pyridine from the small amounts available required the combined talents of R. B. Coffey (IR), M. R. Jackson (MS), W. W Lanier (GLC), and J. C. Randall (NMR) to whom we wish to express our appreciation.

References

1. V. V. Korshak, G. L. Slonimskii, and E. S. Krongauz, *Izvest. Akad. Nauk SSSR, Otdel. Khim. Nauk*, **1958**, 221.

2. G. H. Kroes, *Degradation of Synthetic Polyamides*, Thesis, Delft, 1963.

3. B. Kamerbeek, G. H. Kroes, and W. Grolle, *Thermal Degradation of Some Polyamides*, (Soc. Chem. Ind. Monographs, Vol. 13) Society of Chemical Industry, London, 1961, p. 357.

4. I. Goodman, *J. Polym. Sci.*, **13**, 175 (1954); *ibid.*, **17**, 587 (1955).

5. O. B. Edgar and D. H. Johnson, *J. Chem. Soc.*, **1958**, 3925.

6. A. M. Liquori, A. Mele, and V. Carelli, *J. Polym. Sci.*, **10**, 510 (1953).

7. V. V. Korshak and T. M. Frunze, *Synthetic Heterochain Polyamides* (Translation), Israel Program for Scientific Translation, Jerusalem, 1964.

8. M. B. Nieman, *Ageing and Stabilization of Polymers*, Consultants Bureau, New York, 1965.

9. H. A. Taylor, W. C. Tincher, and W. F. Hamner, *J. Appl. Polym. Sci.*, **14**, 141 (1970).

10. R. A. Ford, *J. Colloid Sci.*, **12**, 271 (1957).

11. W. H. Sharkey and W. E. Mochel, *J. Amer. Chem. Soc.*, **81**, 3000 (1959).

12. E. H. Boasson, B. Kamerbeek, and G. H. Kroes, *Rec. Trav. Chem.*, **81**, 624 (1962).

13. F. R. Moore, *Polymer*, **4**, 493 (1963).

14. M. V. Lock and F. B. Sagar, *Proc. Chem. Soc.*, **1960**, 358.

15. G. M. Burnett and K. M. Riches, *J. Chem. Soc. B*, **1966**, 1229.

16. R. A. McKinney and T. A. Orofino, private communication.

17. B. G. Achhammer, F. W., Reinhart, and G. M. Kline, *Polymer Degradation Mechanisms*, (Nat. Bur. Stand. Circ. No. 525); *J. Res. Nat. Bur. Stand.*, **46**, 391 (1951).

18. S. R. Rafikov, G. N. Chelnokova, and R. A. Sorokina, *Vysokomol. Soedin.*, **4**, 1639 (1962).

19. W. R. Urry, private communication.

20. W. R. Sorenson and T. W. Campbell, *Preparative Methods of Polymer Chemistry*, Interscience, New York, 1961.

21. J. Colonge, J. Dreux, and H. Delplace, *Bull. Soc. Chim. France* **1956**, 1635.

22. J. Colonge, J. Dreux, and H. Delplace, *Bull. Soc. Chim. France*, **1957**, 447.

23. F. Petru and V. Galik, *Chem. Listy*, **51**, 2371 (1957); *Chem. Abst.*, **52**, 6299e (1958).

24. L. D. Metcalfe, A. A. Schmitz, and J. R. Pelka, *Anal. Chem.*, **38**, 514 (1966).

Received December 29, 1970
Revised February 5, 1971

JOURNAL OF POLYMER SCIENCE: PART A-1 VOL. 9, 1823–1833 (1971)

Thermal Decomposition of Poly(vinyl Chloride) and Chlorinated Poly(Vinyl Chloride). I. ESR and TGA Studies

S. A. LIEBMAN, J. F. REUWER, Jr., K. A. GOLLATZ, and C. D. NAUMAN, *Armstrong Cork Company, Lancaster, Pennsylvania 17604*

Synopsis

Significant effort has been made in the past by many workers to investigate the mechanism of thermal decomposition of poly(vinyl chloride) (PVC). The presence and role of free radicals has been controversial in this regard. Our data on PVC and chlorinated PVC systems demonstrate the existence of macroradicals in the early stage of thermal decomposition under inert and oxidative atmospheres. Data from conventional thermogravimetric experiments are used in conjunction with the electron spin resonance findings.

Some workers[1,2] have concluded that under low extent of thermal dehydrochlorination, poly(vinyl chloride) (PVC) did not show any evidence of the presence of radicals. Accordingly, evidence cited for a radical mechanism in this polymer based on electron spin resonance (ESR) measurements of a recorded singlet signal had little justification. Our investigation of carefully purified PVC and systems related to PVC gives evidence which contradicts the above conclusion.

Powdered samples of PVC prepared by different methods, a chlorinated PVC series with varying chloride content, and a reference sample of poly(vinylidene chloride) ($PVCl_2$) were examined by ESR and thermogravimetric analysis (TGA). The temperature of the initially detected ESR signal, its generation and decay rates under certain conditions, and the corresponding temperature for initial weight loss and maximum dehydrochlorination rate from derivative TGA data were recorded for these samples. In addition, apparent activation energies and frequency factors were calculated and dependence of the former on conversion are described.

EXPERIMENTAL

PVC Diamond 450 was obtained from Diamond Shamrock Chemical Company, Cleveland, Ohio. Purification was accomplished by repeated H_2O washing and precipitations with MeOH. Low-temperature PVC ($-70°C$) was prepared by a free-radical method by using tributylboron–H_2O_2 initiator. Chlorinated PVC samples were obtained by suspending

PVC in CCl_4 and irradiating with a low-pressure, 3660-Å ultraviolet source at 77°C during chlorination with Cl_2. Chloride content of polymers was determined by the Schöniger combustion method. A reference sample of $PVCl_2$ was donated by Dr. E. J. Quinn, Armstrong Cork Company. A sample of Tyrin QX (chlorinated polyethylene), obtained from the Dow Chemical Co., Midland, Michigan, contained 48% Cl by the above analysis.

ESR spectra were obtained as first derivatives on a Varian 4500-10A, X-band spectrometer with a 12-in. rotating magnet, 100-kHz field modulation, variable temperature accessory, V-4540 controller, and a V-4533 cylindrical cavity. Instrumental parameters were identical for the comparative series: receiver gain 2000, modulation amplitude 2.4 gauss, and 15-db attenuation from 400-mW klystron output. Samples (~100 mg) were examined in sealed quartz ESR tubes (unless otherwise noted) placed in the variable temperature cavity to allow highly sensitive signal detection. 1,1-Diphenyl-2-picrylhydrazyl (DPPH) was used as the reference for the estimation of the g value. TGA data were obtained by using an Aminco thermogravimetric analyzer (American Instrument Company, Inc., Silver Spring, Maryland) on 100-mg samples in either air or N_2 atmosphere, as indicated. (A test with a 25-mg sample gave the same determined parameters as were obtained with the larger sample.)

Computer programs were written for use on the IBM System/360, Model 44 computer following the differential method of Friedman.[3] Derivative calculations were smoothed by second-order Lagrangian interpolation techniques and compared to first-order calculations to determine the significance of small variations. Slopes were determined by using a least-squares treatment. Alternative calculations of the apparent activation energy were made using dual heat rates (3 and 10°C/min) and slope determinations in a computer program written by A. Mitchell and C. Nauman, and the maximum-point method.[4,5] Full duplicate runs were made on certain samples for the Friedman calculations and the dual heat rate program in the temperature ranges needed for comparison (at ~30% isoconversion points) and to insure reproducibility. A model calculation was used with incremental 1-mg weight losses, which demonstrated that the detection level in the derivative thermogravimetric (dTGA) presentation was ca. 1% (dw/dT). Temperature determinations are estimated to be reproducible to better than 10%. The experimental conditions and data handling were identical for all samples and provided direct, internally consistent data.

RESULTS AND DISCUSSION

ESR Studies

The data obtained are shown in Table I and Figures 1–4 for the specific polymer systems. Initial ("threshold") temperatures, T_t, for the first ESR signal are listed for the denoted systems for identical thermal his-

TABLE I[a]

Sample	T_t (ESR, threshold temp), °C	$T_{5\%}$ (temp at 5% wt loss, dehydrochlorination), °C	T_b (TGA breakpoint temp) °C	T_d, (dTGA, max-rate temp, $-dw/dT_{max}$), °C
Dia 450 PVC				
N_2	240	282	278	298
Air	220	278	276	292
64.1% Cl-PVC				
N_2	200	307	312	341
Air	—	297	305	329
67.4% Cl-PVC				
N_2	200	285	295	320
Air	220	292	290	311
70.2% Cl-PVC				
N_2	—	322	327	340
Air	—	321	320	336
72.2% Cl-PVC				
N_2	240	332	335	353
Air	—	327	330	353
74.2% Cl-PVC				
N_2	240		335	355
Air	—	—	—	—
75.2% Cl-PVC				
N_2	—	330	338	352
Air	—	325	328	344
$PVCl_2$ (72.8% Cl)				
N_2	180	240	238	257
Air	180	235	236	258
Low temp. PVC (−70°C)	240	307	303	335
48% Cl-PE	220	300	311	355

[a] Heating rate = 10°C/min.

tories and instrument parameters. The comparative slopes of ESR signal-generation curves are shown in Figure 1 for a sample maintained at ca. 220°C in a sealed N_2 atmosphere. The prior heating rate to the final 220°C level was 10°C/min for each sample. Figure 2 allows comparison of slopes of the ESR signal-generation curves for PVC Diamond 450 and for 67.4% Cl-PVC in an oxygen and in a nitrogen atmosphere, respectively, all other parameters were held constant. The decay slopes are shown in Figure 3 and were obtained by recording a change of the ESR signal intensity at 40°C. Various workers[6-12] have analyzed macroradical recombination and decay phenomena in PVC and other systems and found, generally, that radical decay follows bimolecular kinetics and has relatively high activation energies. In addition, the use of the duPont Curve Resolver with derivative channels[13] allowed insight into the number

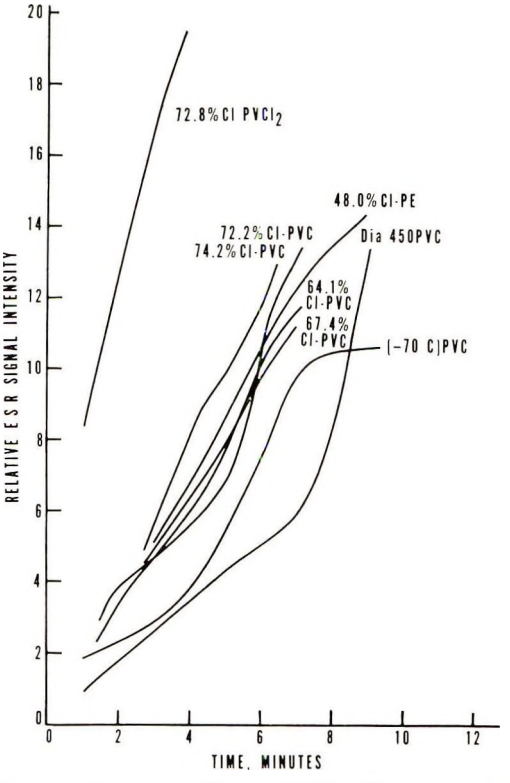

Fig. 1. Free-radical generation under N_2 at 220°C. Curves are displaced along the vertical axis in arbitrary units for ease of comparison.

and possible types of radical species that were responsible for the ESR signal generated in PVC Diamond 450. The curves seen in Figure 4 could be simulated by the composite presentation of three Gaussian derivative curves. The change in curve shape at 220, 100, and 40°C was followed by the curve resolver utilizing varying proportions of the three component curves, adding skew to the function generators, and by offsetting the position of one component. This would be indicative of a radical signal occurring at a different g value than the other component signals. Since, generally, hydrocarbon radicals have closely similar g values ($g = 2.00$) and peroxy radicals have g values significantly higher ($g = 2.01$),[11,12] the inference as to the possible presence of the latter species is direct. The change in proportions would likewise be a result of differing rates of radical decay at those temperatures and conditions. Further studies under varied experimental conditions will be attempted to establish the identity of the macroradicals.

TGA Studies

Data obtained from thermal analysis on these identical source samples were processed to provide further insight into the initial dehydrochlorina-

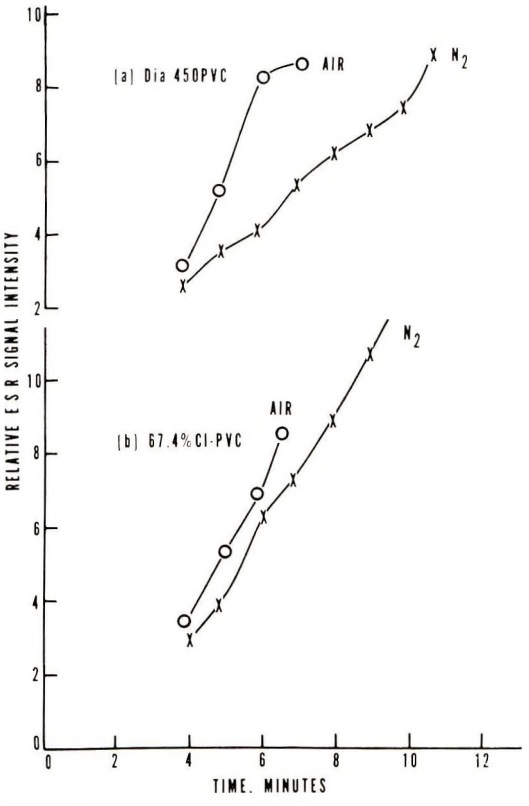

Fig. 2. Free-radical generation at 220°C: (*a*) Diamond 450 PVC, air or N_2 atmospheres; (b) 67.4% Cl-PVC, air or N_2 atmospheres.

tion stage.[14–17,45] The "breakpoint" temperature T_b from the TGA curve is shown in Table I for comparison with the "threshold" temperature T_t by ESR of a detectable signal. Also, the temperature for the initial 5% weight loss is recorded as $T_{5\%}$. The derivative presentation of the loss of HCl and subsequent calculation of the activation energies[18–21] (see Experimental) for that degradative step provided a means to detect minor changes in the kinetics[4,5,22–31] and substantiate the trends noted in breakpoint temperatures. ESR signals, dTGA data, and activation energies could, therefore, be compared in these temperature regions with a reasonable reliability. The threshold temperature for the initial detection of a free-radical signal at $g = 2$ in the carefully heated PVC in all cases is significantly lower than the breakpoint temperature from TGA for the dehydrochlorination process. Use of conservative limits of accuracy for such temperature determinations (± 10°C) still results in a definitive ESR signal well below the weight-loss TGA indication, T_b or $T_{5\%}$ (Table I). Examination of $T_{1\%}$ (the temperature of initial 1% weight loss), although approaching limiting TGA detection and unrecorded, allows the same conclusion. It is conclusive experimental evidence that free radicals

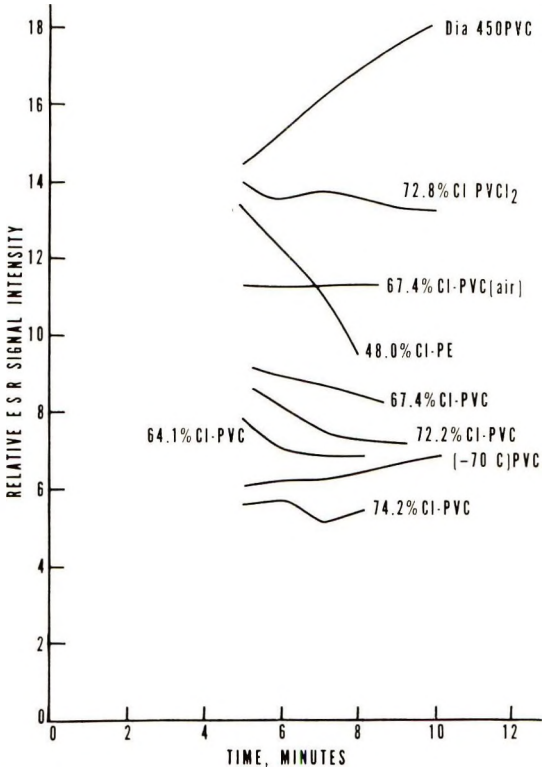

Fig. 3. Free-radical decay under N_2 at 40°C. Curves are displaced along the vertical axis in arbitrary units for ease of comparison.

are present during the early stages of dehydrochlorination. Also, the temperature at maximum rate of dehydrochlorination $(-dw/dT)_{max}$ displays an increasing trend as the degree of chlorination increases in this series.

In addition, kinetic treatment of TGA data allowed comparable apparent Arrhenius activation energies E_a and pre-exponential factors A to be calculated for a systematic study of the influence of chloride content in PVC, Cl-PVC, and $PVCl_2$. Literature values for a control PVC using varied methods of calculation throughout the dehydrochlorination range are recorded from 25 to 70 kcal/mole for the activation energy and reaction orders from 0.8 to 2.9.[29]

Our values for these polymer systems are based on calculations from the Friedman differential method[3,32,33] by use of the basic relationship, $\log(-\rho dw/dT) = -E_a/2.3RT + \log[Af(W)]$, where $f(W)$ is an uncommitted concentration function (mg), T is absolute temperature, E_a is activation energy (kcal/mole), ρ is the heating rate (°C/min), A is the pre-exponential factor, and R is the gas constant (2 cal/mole-deg). The use of alternative methods gave supportive evidence to the above calculations. Apparent activation energies were obtained by the Friedman

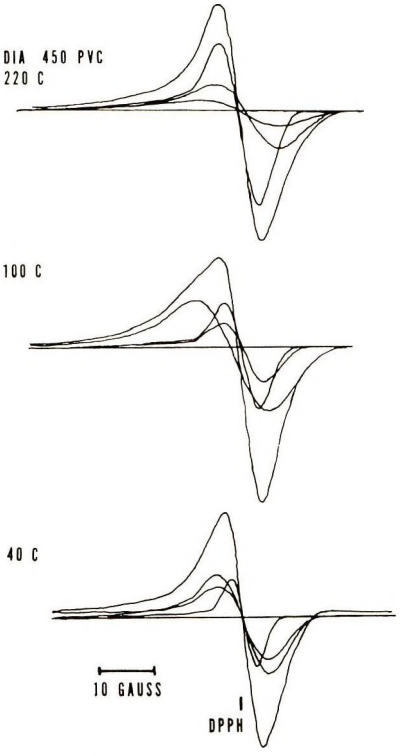

Fig. 4. First-derivative ESR signals analyzed with the duPont Curve Resolver.[13] Diamond 450 PVC at 220, 100, 40°C. The g value indicated by reference to the DPPH position, with H_0 increasing left to right.

method for 10, 20, 30, and 40% conversion levels during the dehydrochlorination process at a minimum of three different heating rates. Also, an average value for E_a was obtained in this limited region for the family of conversions. The use of 3 and 10°C/min heating rates was made in E_a calculations by a separate computer program written by Mitchell and Nauman (see Experimental) in the necessary temperature range. A "maximum-point" method[4,5] involving use of dTGA data from a single thermogram at 10°C/min heating rate (Table II), was useful for still further comparison of the E_a, A, and n (reaction order) values obtained by the Friedman multiple heating-rate calculations. Certain of these results are included in Table II for the denoted polymers.

Importantly, the E_a values from 10 to 40% dehydrochlorination tend toward decreasing numbers in both air and nitrogen atmospheres, as the extent of conversion increases for PVC dehydrochlorination, while for Cl-PVC, the opposite trend is observed; i.e., it becomes progressively easier energetically for the PVC dehydrochlorination process to proceed as the per cent dehydrochlorination increases, while it is progressively more difficult for the Cl-PVC. For the respective samples studied, essentially parallel families of lines were obtained for the activation energy calculations

TABLE II

Sample	Friedman Differential Method						Maximum point method (10°C/min)			Dual heat-rate program (3, 10°C/min), E_a, kcal/mole
	E_a, kcal/mole						E_a, kcal/mole	log A	Reaction order, n	
	10%	20%	30%	40%	Avg	log A				
PVC Dia 450										
Air	26.7	23.0	21.6	21.3	23.1	10.4	20.8	9.0	1.5	32.7
N_2	26.3	23.2	23.1	21.7	23.6	10.1	26.0	9.1	2.0	31.5
64.5% Cl-PVC										
Air	32.4	35.6	36.4	47.4	38.0	8.1	33.6	9.0	2.5	37.9
Air	27.2	26.5	28.7	33.8	29.1	7.4	28.1	9.4	2.0	31.8
67.4% Cl-PVC										
Air	38.3	40.8	44.3	52.6	44.0	10.3	43.6	7.3	3.0	49.2
N_2	28.0	28.7	32.5	40.9	32.5	6.1	29.3	9.4	2.0	38.0
70.2% Cl-PVC										
Air	35.8	38.0	41.4	46.2	40.3	9.9	38.7	9.0	1.5	45.7
N_2	37.4	40.7	41.1	43.8	40.8	11.8	33.1	9.6	1.5	48.1
72.2% Cl-PVC										
Air	37.3	40.4	42.2	47.7	41.9	10.4	41.6	9.1	1.5	56.0
N_2	40.7	42.9	45.8	50.2	44.9	11.6	39.7	9.4	2.0	56.2
74.2% Cl-PVC										
Air	—	—	—	—	—	—	—	—	—	—
N_2	37.9	43.4	45.3	48.5	43.8	11.2	44.7	8.7	2.0	50.6
75.2% Cl-PVC										
Air	32.6	40.0	45.4	47.9	41.5	8.6	45.8	8.2	2.0	46.6
N_2	36.0	42.2	47.3	46.8	43.1	10.8	39.5	9.4	2.0	53.7
72.8% Cl-$PVCl_2$										
Air	31.1	30.0	26.3	14.0	29.1	15.2	28.6	8.0	3.0	28.3
N_2	42.9	45.1	43.6	32.0	40.9	22.6	30.8	7.6	4.0	40.1
48% Cl-PE										
Air	—	—	—	—	—	—	—	—	—	—
N_2	37.5	42.4	45.2	47.6	43.1	11.2	43.3	8.9	2.0	50.6
−70°C PVC										
Air	—	—	—	—	—	—	—	—	—	—
N_2	32.0	31.2	27.4	29.2	29.9	11.5	30.9	9.6	3.0	40.3

by using log $\rho f(A)$ versus $1/T$ plots, indicative of similar basic mechanistic steps occurring within the chosen temperature regions.[3,32,33] This different dependence of E_a on conversion and heat rate is included elsewhere in a more comprehensive study for these polymers.[29–31,34]

It is noted that the effect of an oxidative atmosphere was to slightly decrease the activation energy (except for samples 64.5 and 67.4% Cl-PVC), and to provide a slightly steeper slope in the E_a versus per cent conversion plots. Arrhenius frequency factors are considered in the "normal range" with values approximately $10^{14.5}$ to $10^{11.5}$. Values lower than these indicate large negative entropies of activation.[18] Thus, oxidative degradation appears energetically more favorable than degradation occurring in an inert atmosphere,[35,36] as determined by TGA data. This is supported by the ESR data to some extent by the increase in macroradical signal-generation slope for PVC heated in air, although not readily apparent by the ESR signal-detection temperature, T_t. Control PVC samples showed only slight lowering of T_b in an oxidative environment, while for the 67.4% Cl-PVC sample T_t appeared at slightly higher temperature than that obtained in an inert atmosphere. A high sensitivity to overall thermal degradation[1] was shown by the $PVCl_2$ polymer, which gave identical T_t (180°C) and T_b (~240°C) values in both air and N_2. Higher thermal lability for the 1,1-dichloro unit relative to the 1,2-dichloro units seen in Cl-PVC systems may be inferred.[34]

The evidence in Table I gives similar "threshold" temperatures T_t for chlorinated and nonchlorinated systems; this supports a common initial process for radical production, but the different TGA breakpoint temperatures T_b reflect a different rate for the systems to achieve detectable dehydrochlorination weight loss. Since the only common "defect" structures to both systems would be tertiary Cl atoms at branch sites, oxidized structures, and/or initiator end groups, these would be possible initiators for the dehydrochlorination in the 220°C range.[36] The chlorination procedure is likely to have removed any low amount of unsaturation, and —C=C— content is thus assumed to be negligible for both systems. However, significantly larger amounts of 1,2- and 1,1-dichloro units were introduced on chlorination relative to the control PVC. Therefore, these latter sites, i.e., $(-CHCl-)_n$, $-CCl_2-$, do not appear to be dominant influences in the initial free-radical production in this series.

Although similar generation temperatures and slopes for macroradical production are observed (Fig. 2), the decay plot (Fig. 3) demonstrates a significant difference between the PVC homopolymers (Diamond 450 and low-temperature −70°C PVC) and the Cl-PVC compounds. The former two samples exhibit a positive slope; the latter, as well as $PVCl_2$ and Cl-polyethylene (Cl-PE, 48% Cl), exhibit negative slopes. The number of radicals at 40°C in the control polymers was, therefore, increasing by subsequent homolytic scission and/or electron-transfer mechanisms. The Cl-PVC samples demonstrated ESR signal decay and therefore were undergoing radical recombinations, disproportionation, cyclizations, and

any other process whereby macroradicals terminate under these experimental conditions. It is evident that macroradicals produced in the PVC system differ from those produced in the Cl-PVC or $PVCl_2$ systems based on the above ESR spectral parameters and differing TGA breakpoint temperatures.

CONCLUSIONS

The above carefully treated experimental series of PVC, Cl-PVC, and $PVCl_2$ systems has allowed reasonable conclusions to be made regarding the participation of free radicals during the initial dehydrochlorination process. Effects of an oxidative atmosphere compared to an inert atmosphere show macroradicals have only a slightly changed threshold temperature, but a more rapid radical-generation rate in the control PVC polymer. An oxidative atmosphere generally produced a lowering of E_a, A, T_b, and T_d values by varying amounts for the observed polymer samples in this series. Computer shape analysis of the derivative ESR signals for PVC Diamond 450 indicated changing proportions of at least three macroradicals present from the initial generation temperature at 220°C to the final monitoring at 40°C. These were different from the ESR curve shapes given by Cl-PVC systems, and detailed organic analysis will be reported.[34]

It must be concluded that a free-radical mechanism is, in fact, occurring within the control PVC and chlorinated-PVC systems at low initial reaction conditions of dehydrochlorination.* This would substantiate results of previous investigations by chemical, spectroscopic, and tracer methods under varied experimental conditions.[36–44]

We gratefully acknowledge the donation of chlorinated PVC samples by Dr. E. J. Quinn and J. D. Helm and the aid in computer analysis by J. T. Meluskey and A. Mitchell. Technical assistance in the ESR experiments by G. B. Kemmerer, Jr., Physics Department, Temple University, Philadelphia, is appreciated, as well as helpful comments by Dr. L. Goldfarb and Dr. T. Garrett, Armstrong Cork Company.

References

1. J. N. Hay, *J. Polym. Sci. A-1*, **8**, 1201 (1970).
2. W. C. Geddes, *Rubber Chem. Technol.*, **40**, 177, (1967) and references therein.
3. H. L. Friedman, in *Thermal Analysis of High Polymers* (*J. Polym. Sci. C*, **6**), B. Ke, Ed., Interscience, New York, 1964, p. 183.
4. J. H. Flynn and L. A. Wall, *J. Res. Nat. Bur. Stand.*, **70A**, 487 (1966).
5. R. W. Mickelson and I. N. Einhorn, paper presented at Polymer Conference Series, Univ. of Utah, Salt Lake City, Utah, July 1970.
6. Z. Kuri, H. Ueda, and S. Schida, *J. Chem. Phys.*, **32**, 371 (1960).
7. Z. S. Egonova, Yu. M. Malinsky, V. L. Karpov, A. E. Kalmanson, and L. A. Blumenfeld, *Vysokomol. Soedin.*, **4**, 64 (1962).
8. G. J. Atchison, *J. Appl. Polym. Sci.*, **7**, 1471 (1963).
9. S. E. Bresler and E. N. Kaxbekov, *Fortschr. Hochpolym.-Forsch.*, **3**, 688 (1964).
10. P. Hedvig and G. Zentai, *Microwave Study of Chemical Structures and Reactions*, CRC Press, Cleveland, Ohio, 1969.

* *Note in proof:* Preliminary ESR results with a spin trapping agent, phenyl *t*-butylnitrone, have confirmed these data.

11. P. Yu. Batyagin, A. M. Dubinskaya, and V. A. Radtsig, *Russian Chem. Rev.* **38,** 290 (1969).

12. P. B. Ayscough, *Electron Spin Resonance in Chemistry*, Methuen, London, 1967, pp. 361–374.

13. W. H. Collins (duPont Instrument and Equipment Division, E. I. duPont de Nemours and Co., Wilmington, Delaware) private communication.

14. J. D. Matlock and A. P. Metzger, *J. Appl. Polym. Sci.*, **12,** 1745 (1968).

15. D. E. Wilson and F. M. Hamaker, in *Thermal Analysis* R. F. Schwenker, Jr., and P. D. Garn, Eds., Vol. 1, Academic Press, New York, 1969, pp. 517–538.

16. R. Salovey and H. E. Bair, *J. Appl. Polym. Sci.*, **14,** 713 (1970).

17. R. T. Conley, Ed., *Thermal Stability of Polymers*, Vol. 1, Dekker, New York, 1970, pp. 273–285.

18. B. G. Gowenlock, *Quart. Rev.*, **14,** 133 (1960).

19. C. Corso, *Chim. Ind.* (Milan), **43,** 8 (1961).

20. M. Menzinger and R. Wolfgang, *Angew. Chem. Intern. Ed.*, 8, 438 (1969).

21. I. J. Goldfarb and A. C. Meeks, AD-678882, U. S. Clearinghouse, Washington, D. C., October 1968.

22. H. L. Friedman, *J. Macromol. Sci. A*, **1,** 57 (1967).

23. J. R. Dharwadkar and M. D. Karkhanavala, in *Thermal Analysis*, R. F. Schwenker, Jr. and P. D. Garn, Eds. Vol. 2, Academic Press, New York, 1969, pp. 1049–1110.

24. J. Sestak, A. Brown, V. Rihak, and G. Berggren, in *Thermal Analysis*, R. F. Schwenker, Jr. and P. D. Garn, Eds. Vol. 2, Academic Press, New York, 1969, pp. 1035–1048.

25. J. H. Sharp and S. A. Wentworth, *Anal. Chem.*, **41,** 2060 (1969).

26. J. J. Maurer, *Rubber Chem. Technol.*, **42,** 110 (1969).

27. H. G. Wiedemann, A. V. Tets, H. P. Vanghan, paper presented at Pittsburgh Conference on Analytical Chemistry and Applied Spectroscopy, February 21, 1966.

28. J. D. Seader, paper presented at Polymer Conference Series, Univ. of Detroit, Detroit, Mich., June 1969.

29. V. D. Furnica, and I. A. Schneider, *Makromol. Chem.*, **108,** 182 (1967).

30. I. A. Schneider, C. Vasile, D. Furnica, and A. Onu, *Makromol. Chem.*, **117,** 41 (1968).

31. I. A. Schneider, *Makromol. Chem.*, **125,** 201 (1969).

32. I. J. Goldfarb, R. McGuchan, and A. C. Meeks, AD-684714, U. S. Clearinghouse, Washington, D. C., December 1968.

33. J. R. MacCallum and J. Tanner, *Europ. Polym. J.*, **6,** 907 (1970).

34. S. A. Liebman, D. H. Ahlstrom, E. J. Quinn, A. G. Geigley, and J. T. Meluskey, *J. Polym. Sci., A-1,* **9,** 1921 (1971).

35. L. Valko, in *Macromolecular Chemistry, Prague 1965 (J. Polym. Sci. C,* **16**), O. Wichterle and B. Sedláček, Eds., Interscience, New York, 1967, pp. 545, 1979.

36. J. P. Gupta and L. E. St. Pierre, *J. Polym. Sci. A-1,* 8, 37–48 (1970).

37. C. H. Bamford and D. F. Benton, *Polymer*, **10,** 63 (1969).

38. R. Salovey, R. J., Albarino, J. P. Luongo, *Macromolecules*, **3,** 314 (1970).

39. I. C. McNeil, *Makromol. Chem.*, **117,** 265 (1968).

40. A. Guyot, M. Bert, A. Michel, and R. Spitz, *J. Polym. Sci., A-1,* 8, 1596 (1970).

41. D. A. Teetsel and D. W. Levi, Plastic Note 20, AD-706811, U. S. Clearinghouse, Wash., D. C., November, 1969 and references therein.

42. R. F. Reinisch, H. R. Gloria, and G. M. Androes, in *Photochemistry and Macromolecules*, R. F. Reinisch, Ed., Plenum Press, New York, 1970, pp. 185–217.

43. D. Campbell, *Macromol. Sci. Rev.*, **4,** 91 (1970).

44. G. Palma and M. Carenza, *J. Appl. Polym. Sci.*, **14,** 1737 (1970).

45. M. M. O'Mara, *J. Polym. Sci., A-1,* **8,** 1887 (1970).

Received December 29, 1970
Revised February 10, 1971

JOURNAL OF POLYMER SCIENCE: PART A-1 VOL. 9, 1835–1852 (1971)

Side-Chain Crystallinity. I. Heats of Fusion and Melting Transitions on Selected Homopolymers Having Long Side Chains

EDMUND F. JORDAN, JR., DONALD W. FELDEISEN, and A. N. WRIGLEY, *Eastern Marketing and Nutrition Research Division, Agricultural Research Service, U. S. Department of Agriculture, Philadelphia, Pennsylvania 19118*

Synopsis

Heats of fusion, melting transitions, and the derived entropies of fusion were obtained by differential scanning calorimetry for examples from three homologous series of homopolymers having long side chains. Homopolymers having side-chain lengths between 12 and 22 carbon atoms were chosen from the poly(*n*-alkyl acrylates), the poly(*N*-*n*-alkylacrylamides) and the poly(vinyl esters). The data demonstrated that only the outer paraffinic methylene groups were present in the crystal lattice. This was concluded because phase diagrams obtained for mixtures of structurally different monomers and homopolymers, as well as for selected copolymers, showed only isomorphism in the polymeric examples. In addition, scanning curves, reflecting the distribution of crystallite sizes, became narrower as the side chains became longer. The critical chain length required to maintain a stable nucleus in the bulk homopolymers was a constant value for each homologous series. It varied between 9 to 12 carbon atoms. When heats of fusion were determined in the presence of methanol, main-chain restraints were freed, thus permitting more methylene groups to enter the crystal lattice. Hence, the heats of fusion, the crystallinity, and melting points increased above that of the bulk state. The magnitude of the contribution to the heats of fusion by each methylene group indicated that the hexagonal paraffin crystal modification prevailed in these homopolymers, in agreement with x-ray data from the literature.

INTRODUCTION

Side-chain crystallinity is usually present in atactic vinyl homopolymers having linear subgroups in excess of 10–12 carbon atoms.[1] This was demonstrated by the first-order melting transitions obtained for largely atactic homologs selected from the poly(*n*-alkyl acrylates and methacrylates)[2,3] and their copolymers,[3] the poly-2-*n*-alkyl-1,3-butadienes,[4] the poly(vinyl esters),[5] the poly-*n*-alkylstyrenes,[6] the poly-*N*-*n*-alkylacrylamides,[7] and the poly(fluoro-*n*-alkyl acrylates).[8] Crystallinity was also shown to be present only in the side chains of the isotactic poly(*n*-alkyl acrylates),[9] by using x-ray diffraction, although the degree of tacticity was not specified in the citation. In highly crystalline isotactic poly-1-alkenes, however, x-ray diffraction demonstrated that both main and side chains were in the crystal.[10]

On rapid quenching of polyoctadecene-1 from the melt and extracting, a fraction melting at 41°C was obtained[11] which was thought to involve only crystallinity in the side chains. This conclusion was reached because most atactic 17- and 18-carbon homopolymers melt at about 45–55°C.

The utilization of vinyl monomers derived from animal fats suffers to some extent because of the rigidity introduced into homopolymers and copolymers by side-chain crystallinity. When they are used as internal plasticizers, brittle failure usually results at high plasticizer content.[7,12] Consequently, a more systematic and quantitative thermodynamic study of the crystallinity phenomenon seemed to be warranted. This paper reports the results of using differential scanning calorimetry to obtain the heats of fusion, melting transitions and derived entropies of fusion for three representative homologous series of homopolymers, namely the poly(*n*-alkyl acrylates) the poly-*N*-*n*-alkylacrylamides, and the poly(vinyl esters). Evidence will be presented indicating that the side chain crystal lattice is entirely paraffinic, with no incorporation of main-chain units. Phase diagrams, constructed for mixtures of homopolymers and for copolymers, will be introduced in support of this view. Estimates of crystallinities will be obtained from the thermodynamic quantities obtained. In subsequent papers the influence of side chain crystallinity on the glass transition[13] and the mechanical properties[14] of copolymers will be treated.

EXPERIMENTAL

Amines and Alcohols

The amines and alcohols, the purest available commercially (specified to be greater than 99% pure by gas-liquid chromatography), were used directly.

Monomer Preparation and Purification

The preparation and purification of *N*-*n*-octadecyl-[12] and *N*-*n*-dodecylacrylamide[7] have been described. The remaining *N*-*n*-alkylacrylamides were prepared[12] and the tetradecyl-,[7] *N*-*n*-hexadecyl-[12] and *N*-*n*-docosylacrylamides[12] purified by the designated literature procedures. Yields, melting points (fused sample), acid number, and purity by gel-permeation chromatography, respectively, were: C_{14}, 82.8%, 63.5–64.0°C, 0.19, 99.9%; C_{16}, 76.4%, 70.0–70.5°C, 99.9%; C_{22}, 67.6%; 80.5–82.0°C, 0.47, 85.8%.

ANAL. C_{14}, Calcd: C, 76.34%; H, 12.44%; N, 5.24%. Found: C_{14}, C, 76.26%; H, 11.99%; N, 5.50%. C_{16}, Calcd: C, 77.23%; H, 12.62%; N, 5.41%. Found: C, 76.71%; H, 12.29%; N, 4.69%. C_{22}, Calcd: C, 79.08%; H, 12.74%; N, 3.69%. Found: C, 78.53%; H, 12.93%; N, 3.61%.

The *n*-alkyl acrylates were prepared by the same procedure used for the *N*-*n*-alkylacrylamides.[12] Each crude ester was taken up in a low-boiling (63–70°C) commercial alkane mixture (3 ml/g) and treated twice with equal volumes of 10% sodium carbonate to remove acid. The isolated C_{12}

and C_{14} were flash-distilled at 0.1 mm Hg and crystallized twice from acetone (3 ml/g), the C_{12} at $-60°C$ and the C_{14} at $-20°C$. The balance of the esters were crystallized from the alkane mixture at $-20°C$ and recrystallized from acetone (3 ml/g), at 0°C, except for the hexadecyl ester which was recrystallized at $-20°C$. Yields were: C_{12}, 77.7%; C_{14}, 62.9%; C_{16}, 61.2%; C_{18}, 53.0%, C_{22}, 45.6%. Purity by gel-permeation chromatography was: C_{12}, 98.3%; C_{14}, 84.6%; C_{16}, 99.7%; C_{18}, 99.5%; C_{22}, 92.7%.

ANAL. C_{12}, Calcd: C, 74.95%; H, 11.74%. Found: C, 75.24%; H, 11.77%. C_{14}, Calcd: C, 76.06%; H. 12.02%. Found: C, 76.22%; H, 11.99%, C_{16}, Calcd: C, 76.98%; H, 12.24%. Found: C, 77.09%; H, 12.02%; C_{18}, Calcd: C, 77.72%; H, 12.42%. Found: C, 77.96%; H, 12.47%. C_{22}, Calcd: C, 78.88%; 12.71%. Found: C, 78.97%; H, 12.77%.

Vinyl laurate and palmitate were prepared[15] and vinyl laurate was purified by a reported procedure.[15] Vinyl palmitate was chromatographed on dry Fluorosil and eluted with hexane. Both esters were 99% pure by gas-liquid chromatography. Vinyl stearate, obtained from commercial sources, was crystallized from acetone (10 ml/g) four times at $-20°C$ and was 98.8% pure by gas-liquid chromatography.

Polymerization Procedure

The monomers were polymerized in benzene (3 mole/mole of monomer) at 60°C for 48 hr in sealed bottles under nitrogen with the use of 0.1 mole-% of azobisisobutyronitrile as initiator. Exceptions were *n*-docosyl acrylate (19 hr) and *N*-*n*-docosylacrylamide (19 hr at 90°C). The homopolymers were precipitated in methanol and extracted free of monomer using this solvent at reflux. All of the homopolymers were freed of solvent by drying under vacuum from thin films. Within experimental error, the elemental analyses gave the expected values for carbon, nitrogen, etc., for each homopolymer.

Molecular Weight Measurements

The osmometric procedure was described;[12] gel-permeation chromatography was performed at the Analytical Service Laboratory of Waters Associates, Inc., Framingham, Mass.

The quantities A_n and A_w are defined as

$$A_n = (1/Q)\bar{M}_n$$
$$A_w = (1/Q)\bar{M}_w$$

where A_n is the number average molecular length and Q is a constant characteristic of the polymer. The ratio A_w/A_n was taken as a quantitative measure of dispersity.

Calorimetric Procedures

A Perkin-Elmer differential scanning calorimeter, DSC-1, was used. A set of standard operating conditions was adopted after a series of trials.

These were: scanning speed 10°C/min, attenuation selector setting 8 mcal/sec, and chart speed 1 in./min. Temperature readings were regulated for direct dial read-out by adjusting the average calibration to the correct melting temperature. For this a series of exceptionally pure fatty-acid derivatives was used as standards, having a spread of melting temperatures from −57 to 112°C. The parabolic calibration curve was then fitted by computer. Heats of fusion were checked using a sample of indium and the exceptionally pure naphthalene and benzoic acid used by Hampson and Rothbart.[16] A weighing procedure similar to that used by those authors was followed and values of the fusion heats close to theirs were obtained. These samples were checked periodically. Solid homopolymers were powdered and viscous samples were weighed into the sealable solvent cups provided with the instrument. Two different sample weights of each homopolymer were programmed, each through three successive heating and cooling cycles, from −73°C to 45°C above the melting transition. No low-temperature polymorphic transitions were observed with any of these homopolymers. Liquid nitrogen cooling was used for all determinations and calibrations. One determination in each set of three was carried out following rapid cooling by manual control, but no differences in melting peak areas were ever noticed by this quenching technique. Fusion endotherms always equaled crystallization exotherms within experimental error. A planimeter was used to measure peak areas; average values of the heats of fusion were reported. Average error in the heats of fusion was estimated to be about 1%. Samples run in methanol or *n*-decane were first melted and weighed as chunks into the solvent cups; the solvent was then introduced and the cups were sealed. No solvent or polymer loss occurred. Mixtures of homopolymers were fused in an oven at 140°C for one hour and then ground and weighed on cooling. The ends of the fusion curves were taken as the temperature of melting in all of the experiments, partly because this procedure gave the most regular value as side-chain length was varied. The last disappearance of crystallinity is the usual criterion for equilibrium melting.[17a] However, at the heating rates employed in this work, equilibrium could only have been approached. All computations were made by use of an IBM 1130 computer.

Refractometric Melting Temperature

Selected samples were run by a refractometric technique,[2] from 15°C below the transition, at an incremental heating rate of 1°C every 30 min. Usually no change occurred in refractive index after 5 min. Consequently, these transitions were considered to be equilibrium melting points.

RESULTS AND DISCUSSION

Thermodynamic Data and Molecular Weight and Size Measurements

The molecular weights, heats of fusion and melting transitions for the three homologous series are listed in Table I. Some melting points obtained at

low heating rates (ca. 1°/30 min) by refractometry are also included. They are usually lower than those by differential scanning calorimetry. They are probably more accurate because the fast scanning speeds (10°C/min) of the latter determination allowed insufficient time to reach equilibrium.[17a] Individual members of a homologous series of homopolymers are often designated in this paper by the number of side-chain methylene groups n.

The molecular weight data is typical of that obtained for the higher homologs.[18] The distribution curves from gel permeation chromatography showed a long tail at high elution volumes, indicating the presence of low molecular weight material in these unfractionated homopolymers. This accounts for the large value of the dispersity index. With the exception of the vinyl esters, the degrees of polymerization show that the samples were high polymers.

Heats of fusion and melting transitions were obtained in bulk for all of the homopolymers and some were determined in the presence of methanol, a non-solvent for the homopolymers. Methanol was used in highly varying amounts from sample to sample; the ratio of methanol to sample changed randomly from 0.16 to 1.4 down the list in Table I. Both types of data are listed in the table. Specific values of the bulk fusion endotherm were similar at each value of n for the poly(n-alkyl acrylates) and the poly(vinyl esters), allowing for the slight difference in n for these two systems, but are considerably lower for the respective poly-*N*-n-alkylacrylamides. However, in the presence of methanol the heats of fusion increased about 2 cal/g for the polyesters and 6 cal/g for the polyamides. In fact the heats of fusion for the poly-*N*-n-alkylacrylamides were similar after treatment to those for the bulk n-alkyl acrylates of the same side-chain length. Of greater significance, the melting transitions for most members of both ester and amide series were higher in methanol than in bulk. Phase-transition theory predicts a small decrease in temperature of melting as nonsolvent is increased,[17b] until the point where liquid–liquid phase separation exists, whereupon no further depression should occur. Consequently another explanation is required for an elevation of melting above that of the bulk state.

It is well known that certain liquids can, by solvation, increase the mobility of chains and thus greatly increase their rates of crystallization.[19–21] However, plasticization and bulk annealing should lead to the same thermodynamic transition[22] when equilibrium conditions prevail. In these systems methanol is thought to solvate the polar groups of the main chain and disrupt intramolecular interactions. This type of interaction is probably responsible for stiffness in these homopolymers[23] because intermolecular interactions are shielded by the side chains. Thus, as chain mobility is increased, more methylene groups in any chain unit can enter the crystal, thereby increasing the equilibrium crystallinity, the melting transitions, and the heats of fusion, as observed. This assumes, of course, that only side chains can crystallize.

Typical scanning curves are shown in Figure 1. These were drawn to equal weights and temperature increments. Insert 1 compares poly(n-

TABLE I
Molecular Weights, Heats of Fusion, and Melting Transition Temperatures for the Long Side-Chain Acrylates, Acrylamides, and Vinyl Esters

n^a	Thermal analysis conditions	Conversion, %	Solution Properties			ΔH_f		T_m, °K	
			$\bar{M}_n$	DP_n	A_w/A_n	cal/g	cal/mole	DSC	Refractometer
			Poly-(*n*-alkyl acrylates)						
12	In bulk	86.8	223,700	930.6	9.12	8.75	2,103	285.0	
14		82.6	169,300	630.7	10.84	14.88	3,994	305.0	298.9
16		93.6	259,000	878.6	8.37	18.19	5,394	316.0	311.3
18		95.6	276,800	852.9	9.91	21.34	6,925	329.0	323.9
22		96.4	253,600	666.3		27.50	10,467	345.0	339.5
22		"	"	"		25.79	9,816	"	
16	In methanol		Same as above			20.37	6,041	321.0	
18						23.70	7,691	332.0	
22						27.85	10,601[b]	342.0	
			Poly-*N*-*n*-alkylacrylamides						
12	In bulk	77.8	448,900	1875.0	11.36	0.95	226	265.0	
14		96.8	505,200	1889.0	7.35	5.43	1,451	291.0	

16		96.6	551,100	1865.0	2.60	11.26	3,327	310.0	
16		"	"	"	"	7.70	2,274[c]	318.0	
18		98.2	244,350	755.2	7.65	12.96	4,193	321.0	
18		"	432,000	1335.0		11.96	3,870[c]	341.0	
22		90.4	199,900	526.5		21.15	8,029	341.0	
12	In methanol		Same as above			5.90	1,406	256.0	
14						12.90	3,450	299.0	306.7
16						16.97	5,015	315.0	317.4
18						20.33	6,578	330.0	327.8
22						23.24	8,823	346.0	
22	In 95% ethanol		Same as above			24.17	9,176	342.0	
				Poly(vinyl Esters)					
11	In bulk	65.3	51,700	228.4	2.23	5.78	1,308	289.0	301.5
15		68.0	59,600	211.0	1.98	17.37	5,150	319.0	316.1
17		82.0	48,900	157.5	2.46	19.82	6,154	331.0	327.6
15	In methanol		Same as above			18.84	5,586	318.0	
17						21.00	6,520	330.0	

[a] The number of side chain methylene groups.
[b] In 95% ethanol.
[c] Not used in the calculation of the parameters of Table III.

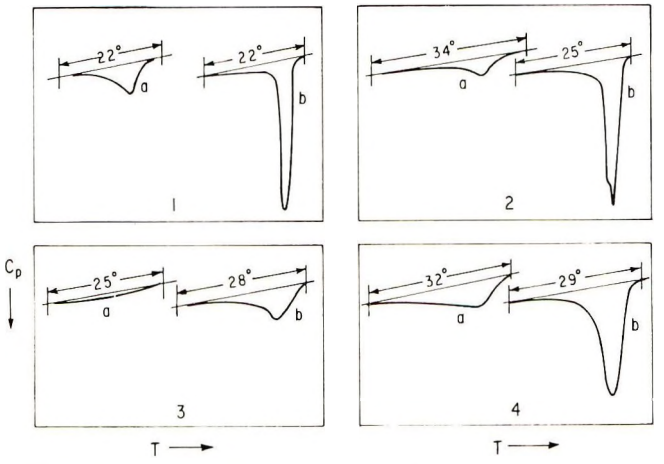

Fig. 1. Comparison of melting point curves for selected homopolymers: (*1a*) poly(*n*-dodecyl acrylate); (*1b*) poly(*n*-octadecyl acrylate); (*2a*) poly(vinyl laurate); (*2b*) poly(vinyl stearate); (*3*) poly-*N*-*n*-dodecylacrylamide, (*a*) in bulk and (*b*) in methanol; (*4*) poly-*N*-*n*-octadecylacrylamide, (*a*) in bulk and (*b*) in methanol.

dodecyl acrylate) with poly(*n*-octadecyl acrylate); insert 2, poly(vinyl laurate) and poly(vinyl stearate); insert 3, poly-*N*-*n*-dodecylacrylamide, in bulk and in methanol, and insert 4, poly-*N*-*n*-octadecylacrylamide in bulk and in methanol. In all of the series, the overall melting range is similar, but there is a marked difference in the scanning curves. These curves qualitatively reflect the distribution of crystallite sizes.[22] In the ester homologs, the crystal-size spectrum becomes narrower and moves toward the higher temperature range of the distribution as the side chain length increases. This supports the view that only side chains crystallized in these systems. The amide crystal-size distributions are broader than those of the corresponding esters. The effect of added solvent in increasing both crystallinity and crystal perfection can be seen in inserts 3 and 4. At higher side chain length, poly-*N*-*n*-alkylacrylamides in methanol resembled the bulk esters of the same side chain length. The melting endotherms for the polyesters in methanol were slightly broader than for the corresponding bulk curves. Again, these data illustrate the effect of increased main-chain mobility on the development of crystallinity and the perfection of the crystals.

Entropies of fusion (listed in Table II) were determined from the usual relation

$$\Delta S_f = \Delta H_f / T_m \tag{1}$$

on the assumption that the melting transition T_m was the true equilibrium melting point, and that the heat of fusion represented that for the entirely crystalline phase.[17b] While melting points (Table I) by refractometry were believed to be equilibrium values, those by scanning calorimetry are not. Consequently, all of the entropies based on DSC measurements (Table II) will be somewhat more in error than those based on refractometry. Never-

TABLE II. Estimation of Crystallinity for the Long Side-Chain Acrylates, Acrylamides, and Vinyl Esters

n	Thermal analysis conditions	Crystallinity per unit x_c or x_c'		Crystalline CH_2 groups in side chain		Amorphous CH_2 groups in side-chain		ΔS_f, cal/mole-deg	
		Eq. (8)	Eq. (14)	Eq. (11)	Eq. (15)	Eq. (12)	Eq. (13)	Per unit	Per bond
				Poly(*n*-alkyl Acrylates)					
12	In bulk	0.17	0.16	2.9	2.8	9.1	9.2	7.38	2.64
14		0.28	0.25	5.4	4.8	8.6	"	13.36	2.78
16		0.35	0.32	7.3	6.8	8.7	"	17.33	2.55
18		0.41	0.38	9.4	8.8	8.6	"	21.39	2.43
22		0.52	0.47	14.2	12.8	7.8	"	32.76	2.56
22		0.49	"	13.4	"	8.6	"	31.23	2.44
16	In methanol	0.39	0.46	8.2	9.7	7.8	6.4	18.82	1.94
18		0.45	0.50	10.5	11.6	7.5	"	23.17	2.00
22		0.53	0.58	14.4	15.7	7.6	"	33.47	2.13
				Poly-*N*-*n*-alkylacrylamides					
12	In bulk	0.02	0.003	0.31	0.10	11.7	12.0	0.85	2.74
14		0.10	0.11	2.0	2.0	12.0	"	4.99	2.50
16		0.22	0.19	4.5	4.0	11.5	"	10.73	2.68
18		0.25	0.26	5.7	6.0	12.3	"	13.06	2.18
22		0.40	0.37	10.9	10.0	11.1	"	23.55	2.36
12	In methanol	0.11	0.15	1.9	2.5	10.1	9.5	5.49	2.20
14		0.25	0.24	4.7	4.5	9.3	"	11.25	2.50
16		0.32	0.31	6.8	6.5	9.2	"	15.80	2.43
18		0.39	0.37	8.9	8.5	9.1	"	20.07	2.36
22		0.44	0.46	12.0	12.5	10.0	"	25.50	2.04
22	In 95% ethanol	0.46	"	12.5	"	9.5	"	26.83	2.15
				Poly(vinyl Esters)					
11	In bulk	0.11	0.11	1.8	1.7	9.2	9.3	4.53	2.66
15		0.33	0.28	7.0	5.7	8.0	"	16.29	2.86
17		0.38	0.35	8.4	7.7	8.6	"	18.79	2.44
15	In methanol	0.36	a	7.6	a	7.4	a	17.57	2.31
17		0.40	a	8.9	a	8.1	a	19.76	2.22

[a] Insufficient data.

theless, a plot of ΔS_f against n for a composite of both types of data was linear, at least within the narrow range of n studied. Linearity is usually observed for correlations of enthalpy or entropy against chain length across short ranges of n.[24]

The relations[24] are

$$\Delta H_f(\text{cal/mole}) = \Delta H_{fe} + \alpha(n) \quad (2)$$

$$\Delta S_f(\text{cal/mole-deg}) = \Delta S_{fe} + \beta(n) \quad (3)$$

In eqs. (2) and (3), α and β represent the contribution of each added methylene group to the heat and entropy of fusion, respectively. Plots of ΔH_f against n in eq. (2) showed that n at $\Delta H_f = 0$ varied between 6.4 and 12.0 for the different systems. These values represent the sequence of methylene groups of a length insufficient to form a stable nucleus.[9] The quantities ΔH_{fe} and ΔS_{fe} are also constants reflecting contributions of the chain ends[24] to the respective enthalpic and entropic changes. The constants of eq. (2) and (3), obtained by curve-fitting the data by computer, are listed in Table III. The entropies of fusion are all very similar and are close to the value for polyethylene, 2.34 cal/mole-deg-CH_2.[17c] Similarly, all of the enthalpies, have like values, the average, 777 cal/mole-CH_2, being close to a value (735 cal/mole-CH_2) found for the α-hexagonal-to-liquid transition ($\alpha_H \rightarrow 1$) exhibited by alkanes close to their melting points.[25] The significance of both of these observations will be treated in the last section of this paper.

TABLE III
Parameters for Various Equations

Homopolymer	Thermal analysis conditions	Equation	Intercept, cal/mole	Slope, cal/mole-CH_2
n-Alkanes ($\alpha_H \rightarrow 1$)[a]		(8)	-2939.0 ± 422.8	734.9 ± 29.3
n-Alkyl acrylates	Bulk	(2)	-7271.0 ± 493.0	791.6 ± 27.8
" "	Methanol	(2)	-5989 ± 454.3	755.4 ± 24.1
N-*n*-Alkylacrylamides	Bulk	(2)	-9262.0 ± 788.6	774.8 ± 47.1
" "	Methanol	(2)	-6994.0 ± 681.3	734.7 ± 38.4
Vinyl esters	Bulk	(2)	-7686.0 ± 1651.0	829.5 ± 113.4
n-Alkyl acrylates	Bulk	(3)	-21.24 ± 1.56[b]	2.41 ± 0.09[c]
" "	Methanol	(3)	-20.78 ± 1.86[b]	2.46 ± 0.10[c]
N-*n*-Alkylacrylamides	Bulk	(3)	-26.14 ± 2.00[b]	2.24 ± 0.12[c]
" "	Methanol	(3)	-16.99 ± 2.39[b]	1.99 ± 0.13[c]
Vinyl esters	Bulk	(3)	-22.02 ± 6.08[b]	2.46 ± 0.42[c]

[a] Data of Broadhurst.[25]
[b] In cal/mole-deg.
[c] In cal/mole-deg-CH_2.

Phase Diagrams for Mixtures of Homopolymers

If only the side chains can crystallize, phase diagrams for mixtures of any two homopolymers should form solid solutions. In contrast, mixtures of

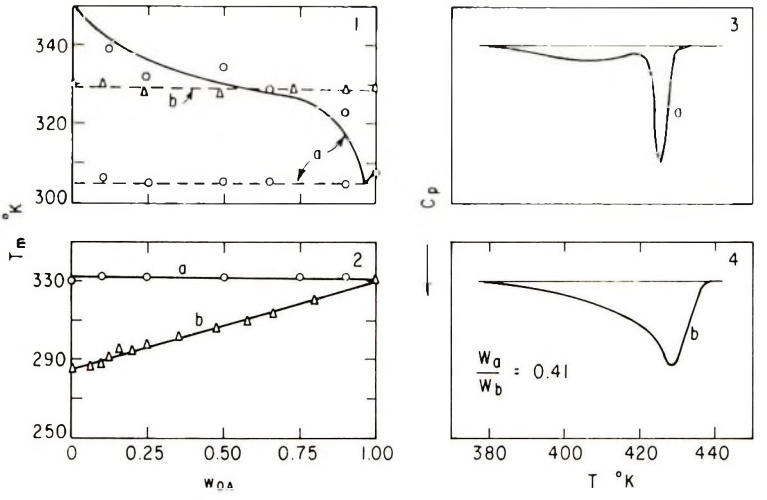

Fig. 2. Phase diagrams and DSC curves: (1) phase diagrams for (*a*) monomeric and (*b*) polymeric mixtures of *n*-octadecyl acrylate and *N*-*n*-octadecylacrylamide; (2) phase diagrams for copolymers of (*a*) *n*-octadecyl acrylate and vinyl stearate and (*b*) octadecyl acrylate and dodecyl acrylate; (3) DSC curves for mixtures, and (4) for copolymers, of *n*-octadecyl acrylate and *N*-*n*-octadecylacrylamide in bulk. w_{OA} is the weigh fraction of *n*-octadecyl acrylate. W is the sample weight.

their monomers should produce eutectic mixtures. Data are shown in Figure 2 for various homopolymer mixtures and copolymers. Insert *1a* shows a phase diagram for a mixture of monomeric *n*-octadecyl acrylate with *N*-*n*-octadecylacrylamide, while *1b* shows the respective homopolymer mixtures. Clearly the monomer mixtures show a eutectic; the homopolymers (curve *b*) only solid solutions, with no T_m depression. Insert 2 shows copolymers of (*a*) *n*-octadecyl acrylate and vinyl stearate and (*b*) copolymers of *n*-octadecyl acrylate and *n*-dodecyl acrylate. Isomorphism persists in both cases. In support of these observations solid solution formation between the higher methacrylate copolymers have long been known.[3] Differential scanning curves are shown in inserts 3 and 4 for (*a*) roughly a 50–50 mixture of poly-*n*-octadecyl acrylate) and poly-*N*-*n*-octadecylacrylamide and (*b*) their copolymers. The broad melting curve, characteristic of the amide homopolymers, persists in the mixtures, but is more diffuse in the copolymers, indicating a tendency toward more similar crystal sizes in the latter. Results like those of the figures were found by constructing phase diagrams for mixtures of poly(*n*-octadecyl acrylate) and poly(vinyl stearate) and by investigating 50–50 mixtures of all combinations of the other homopolymers with $n = 16$ and 22. A significant melting point depression was never found.

Heats of Fusion with a Diluent

The heat of fusion per mole of repeating unit is obtained using a diluent.[17b] When a sequence of methylene groups in the side chain constitutes the repeating unit, as in these homopolymers, the heat of fusion obtained with the

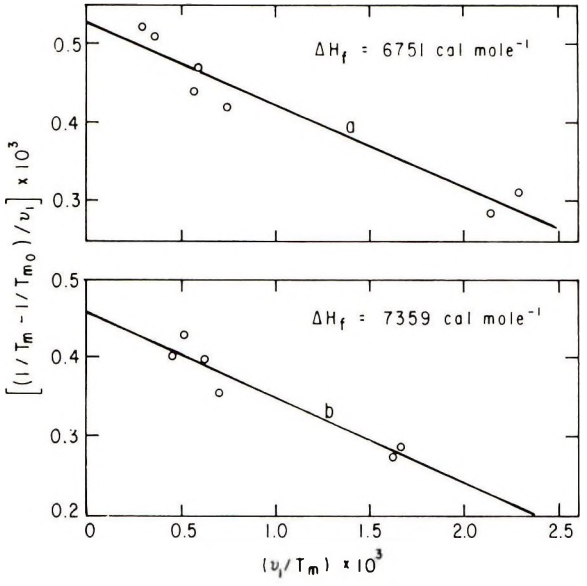

Fig. 3. Plot of the quantity $[(1/T_m) - (1/T_{m0})]/v_1$ against v_1/T_m for (*a*) poly-(*n*-octadecyl acrylate) and (*b*) poly(vinyl stearate) in the diluent *n*-decane.

use of a diluent will be a measure of its crystallinity. The ratio of the calorimetric heat to this quantity will decrease from unity to the extent that chain imperfections introduce sequences of amorphous units. The ratio will therefore represent the overall crystallinity of the sample. Consequently it will give some idea of the reliability of the calorimetric heats as a quantitative measure of the crystallinity present in each unit of the polymer chain.

The diluent method was used to measure the heat of fusion per repeating unit for poly(*n*-octadecyl acrylate) and poly(vinyl stearate). *n*-Decane was the diluent, and the melting point depression was determined by differential scanning calorimetry. The melting point depression was described by the relation

$$[(1/T_m) - (1/T_{m0})]/v_1 = (R/\Delta H_f)(V_u/V_1)[1 - (BV_1/R)(v_1/T_m)] \quad (4)$$

where T_m and T_{m0} are the equilibrium melting points for the homopolymer in the presence of diluent and in bulk, respectively, v_1 is the volume fraction of diluent, V_u/V_1 is the ratio of molar volumes of homopolymer and diluent, respectively, and ΔH_f is the heat of fusion. Densities for the homopolymers were estimated by use of group additivity correlations[26] for crystalline homopolymers; the value for poly(vinyl stearate) was checked by a solvent gradient method. The quantity B is related to the solvent–polymer interaction parameter, χ_1, by the equation

$$\chi_1 = BV_1/RT \quad (5)$$

The data are shown in Figure 3; ΔH_f is given in the figure. The value of ΔH_f for poly(*n*-octadecyl acrylate) was similar to that obtained by calorimetry (Table I); the value for poly(vinyl stearate) was somewhat higher by the diluent method. Consequently over-all crystallinity was nearly unity for poly(*n*-octadecyl acrylate) and 0.83 for poly(vinyl stearate). The high chain-transfer coefficient estimated for poly(vinyl stearate)[27] and its low molecular weight (Table I) suggest that branching caused the decrease in crystallinity. On the other hand, the approximations involving density leave the diluent heats somewhat in doubt. It is considered, however, in view of these experiments, as well as by the observation of the regularity of ΔH_f as n changes (Tables I and II), that most mers are involved in crystal domains. The x-ray data also indicated high levels of crystallinity in poly(vinyl stearate).[28] It remains to establish the extent of crystallinity present in each polymerizing unit.

Some other quantities of interest were obtained from the data using diluents. Heats of fusion were obtained by calorimetry for each point in Figure 3; they agreed with the value in the figure for the indicated homopolymer. Thus evidence is provided that the diluent, as required by theory,[29] was absent from the crystal lattice. In fact, *n*-decane was a thermodynamically rather poor solvent for the homopolymers. The value of B in eq. (4) was positive,[29] being 2.02 for poly-*n*-octadecyl acrylate) and 2.43 2.43 for poly(vinyl stearate).

Estimates of Crystallinity Present in the Side Groups

Crystallinity x_c in polymers can be estimated by calorimetry when the relation

$$x_c = \Delta H_f / \Delta H_{f0} \tag{6}$$

is satisfied.[30] ΔH_f is the observed calorimetric heat of fusion for the unit and ΔH_{f0} is the heat of fusion for the 100% crystalline phase. In these systems the crystalline phase was shown to constitute some fraction of the side chains. The x-ray diffraction has demonstrated[9,31] that the side chains of poly(vinyl stearate), as well as the side chains of the higher polymeric *n*-alkyl acrylates[9] and presumably the methacrylates, are arranged perpendicular to the plane of their chain ends in the rather loose hexagonal modification, assumed by many *n*-paraffins[25] a few degrees below their melting point. However, in poly(vinyl stearate) this crystal form persists down to low temperatures.[9,31] It would seem reasonable, therefore, that enthalpic data from the literature for the fusion of the hexagonal modification of the *n*-alkanes (the $\alpha_H \rightarrow 1$ transition[25]) could represent the crystalline portion of the side chains in these homopolymers. Accordingly, heats of fusion for this transition at various chain lengths,[25] in the range of interest in this paper (n = 9–19), were fitted, with high statistical significance, by a first degree polynomial, in accordance with

$$\Delta H_f(\text{cal/mole}) = C + k(n) \tag{7}$$

where k is ΔH_f cal/mole-CH_2[32] and C is the contribution of the chain ends. The value of k, listed in Table III, clearly shows that the heat of fusion for the hexagonal form is much less than that found for the orthorhombic-to-liquid transition ($\beta_0 \rightarrow 1$)[25] found for the higher n-alkanes through polyethylene. Here k was considered to be 950 cal/mole-CH_2.[24] On substituting ΔH_f from eq. (7) for ΔH_{f0} in eq. (6), the crystallinity fraction is

$$x_c = [\Delta H_f(n)\ 14.026]/[C + k(n)] \tag{8}$$

where ΔH_f is in cal/g, the numerical constant is the molecular weight of a single methylene group, and n is the number of side-chain methylene groups, including the terminal methyl group. C was taken as zero here because the data of interest are the short-range enthalpic changes associated with the fusion of each methylene group.[33] Crystallinity, present in the side-chain only, x_{cs}, is

$$x_{cs} = f x_c \tag{9}$$

with f defined as

$$f = \mathrm{MW_{unit}}/(\mathrm{MW_{side-chain}} - 1.008) = \Delta H_f(\mathrm{cal/mole\text{-}unit})/\Delta H_f(\mathrm{cal/g})(n)14.026 \tag{10}$$

The number of crystalline CH_2 groups, including terminal methyl, in the side chain n_c is

$$n_c = x_{cs}(n) = (x_c \mathrm{MW_{unit}})/14.026 \tag{11}$$

and the number of amorphous methylene groups remaining n_a is

$$n_a = n - n_c \tag{12}$$

The quantities are listed in Table II.

Another approach to estimating crystallinity from these data considers the similarity in magnitude of k [eq. (7)] and α [eq. (2)] (see Table III) for the homopolymers. In eq. (2), the value of n at $\Delta H_{f0} = 0$ is given as

$$n_a' = \Delta H_{fc}/\alpha \tag{13}$$

where n_a' can be defined as the critical side-chain length below which crystallinity is absent. Assuming this value to be constant as side chain length increases without limit, then crystallinity becomes

$$x_c' = [(n - n_a')14.026]/MW_{unit} \tag{14}$$

Again the numbers of crystalline methylene groups is

$$n_c' = n - n_a' \tag{15}$$

If the assumptions inherent in eq. (8) and eq. (14) are correct, then the two methods should yield the same value for the crystallinity fraction. Thus

$$x_c = x_c' \tag{16}$$

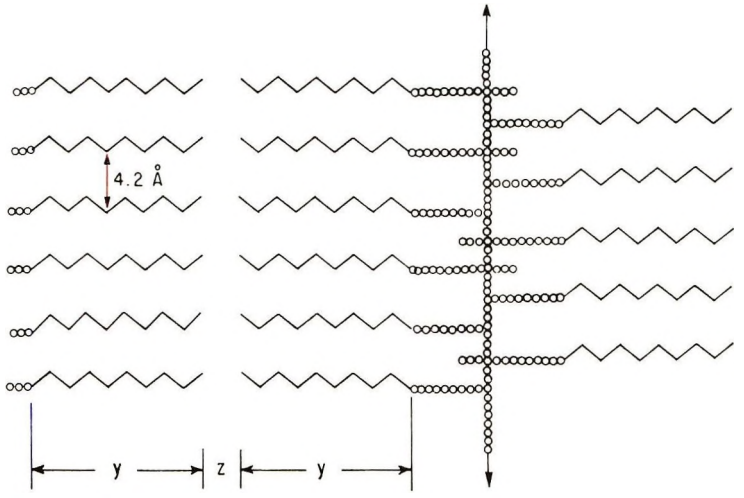

Fig. 4. Diagramatic representation of a proposed structure for poly(vinyl stearate) corresponding to a calculated long spacing of 24.64 Å for $n_c = 8.4$, in comparison to the found[28] long spacing of 27.00 Å.

The appropriate values listed in Table II confirm eq. (16). It is of special interest that the crystallinities obtained by using eqs. (8) and (14) received strong support from values reported by Greenberg and Alfrey[3] for the poly(n-alkyl acrylates) and poly(n-alkyl methacrylates), based on specific volumes; specific volumes should be sensitive to the crystalline order present in each chain unit.

A schematic diagram, illustrating the main features postulated for these homopolymers, is shown in Figure 4. Amorphous main-chain units are connected to 9 to 12 amorphous methylene groups which branch atactically from the main chain (small circles). These connect the ordered alkane chains, arranged in a hexagonal subcell, separated by 4.2 Å, as observed.[3,9,10,28,31] The ordered regions are packed end-to-end as shown and are stacked layer-on-layer to give three-dimensional order. Within the large error in estimating, the illustrated arrangement accounts for the long spacing of 27.0 Å found by Morosoff et al.[31] for poly(vinyl stearate). To calculate this spacing, the values of y and z employed by Jones[10] were used. The failure to observe in poly(vinyl stearate)[31] the low-angle reflections characteristic of the packing of the main chain units in crystalline polyoctadecene-1[10] provides additional confirmation for this structure. Significantly, in quenched polyoctadecene-1, these spacings are missing.[10]

A treatment of the entropy of fusion data in Table II remains. The parameters are listed in Table III. Of special interest are the values of ΔH_f per bond given in the last column of Table II. These were computed by using the ratio, $\Delta S_f/n_e$. The values are only slightly higher than the value of a polyethylene, 2.34 cal/mole-deg-bond.[17c] Quantitative comparisons are probably not warranted because of the differences in obtaining the bond entropy for the two types of homopolymers. It seems reasonable to

conclude that the relatively low values for the homopolymers having long side chains are a manifestation of the high solid-state entropy conferred by the hexagonal packing present in the crystallites.[25] Using eq. (17) to calculate the entropy per bond for the hexagonal crystal form of n-alkanes yields $[(C + kn)/T_m]/n$, where T_m is the melting temperature[25] and C and k are from Table II; this gave an exceptionally low average value of 1.9 cal/mole-deg for the transition.

SUMMARY AND CONCLUSIONS

From the thermodynamic data involving heats and entropies of fusion and melting transitions, for three structurally varied series of homologs having long side chains, it was concluded that only the outer paraffinic methylenes were present in the crystal lattice. Specific information leading to this conclusion were: (a) scanning curves reflecting the distribution of crystallite sizes become narrower as the side chain becomes longer; (b) solvolysis of the main chain by methanol allowed the entrance of more methylene units into the lattice, thereby raising the melting point above that of the bulk state; (c) phase diagrams of mixtures of structurally different monomers and homopolymers, as well as for selected copolymers, showed only isomorphism in the polymeric examples; (d) crystallinity estimates obtained for each structural unit, assuming that only hexagonal paraffinic chains were in the crystal, were in agreement with proposed unit-cell models derived from the literature based on x-ray diffraction measurements.

The authors thank Mr. Bohdan Artymyshyn for determining the molecular weights, Mrs. Ruth D. Zabarsky for operation of the computer, and Dr. Edward S. Rothman for the preparation of the vinyl laurate and palmitate.

References

1. L. E. Nielsen, *Mechanical Properties of Polymers*, Reinhold, New York, 1962, pp. 23–25.

2. R. H. Wiley and G. M. Brauer, *J. Polym. Sci.*, **3**, 647 (1948).

3. S. A. Greenberg and T. Alfrey, *J. Amer. Chem. Soc.*, **76**, 6280 (1954).

4. C. G. Overberger, L. H. Arond, R. H. Wiley, and R. R. Garrett, *J. Polym. Sci.*, **7**, 431 (1951).

5. W. S. Port, J. E. Hansen, E. F. Jordan, Jr., T. J. Dietz, and D. Swern, *J. Polym. Sci.*, **7**, 207 (1951).

6. C. G. Overberger, C. Frazier, J. Mandelman, and H. F. Smith, *J. Amer. Chem. Soc.*, **75**, 3326 (1953).

7. E. F. Jordan, Jr., G. R. Riser, B. Artymyshyn, W. E. Parker, J. W. Pensabene, and A. N. Wrigley, *J. Appl. Polym. Sci.*, **13**, 1777 (1969).

8. A. G. Pittman and B. A. Ludwig, *J. Polym. Sci. A-1*, **7**, 3053 (1969).

9. N. A. Plate, V. P. Shibaev, B. S. Petrukhin, and V. A. Kargin, in *Macromolecular Chemistry, Tokyo-Kyoto, 1966* (*J. Polym. Sci. C*, **23**), I. Sakurada and S. Okamura, Eds., Interscience, New York, 1968, pp. 37–44.

10. A. T. Jones, *Makromol. Chem.*, **71**, 1 (1964).

11. D. W. Aubrey and A. Barnett, *J. Polym. Sci. A-2*, **6**, 241 (1968).

12. E. F. Jordan, Jr., G. R. Riser, W. E. Parker, and A. N. Wrigley, *J. Polym. Sci. A-2*, **4**, 975 (1966).

13. E. F. Jordan, Jr., B. Artymyshyn, A. Speca and A. N. Wrigley, *J. Polym. Sci.*, in press.

14. E. F. Jordan, Jr., G. R. Riser, B. Artymyshyn, J. W. Penabene and A. N. Wrigley, in preparation.

15. D. Swern and E. F. Jordan, Jr., *Org. Syntheses*, **30**, 106 (1950).

16. J. W. Hampson and H. L. Rothbart, *J. Am. Oil Chemists Soc.*, **46**, 143 (1969).

17. L. Mandelkern, *Crystallization of Polymers*, McGraw-Hill, 1964, pp. 20–37; (b) pp. 38–73; (c) pp. 117–145.

18. E. F. Jordan, Jr., H. A. Monroe, B. Artymyshyn, and A. N. Wrigley, *J. Am. Oil Chemists Soc.*, **43**, 563 (1966).

19. H. J. Kolb and E. F. Izard, *J. Appl. Phys.*, **20**, 571 (1949).

20. W. R. Moore and R. P. Sheldon, *Polymer*, **2**, 315 (1961).

21. R. P. Sheldon, *Polymer*, **3**, 27 (1962).

22. P. J. Flory, *J. Chem. Phys.*, **17**, 223 (1949).

23. M. C. Shen and A. Eisenberg, *Rubber Chem. Technol.*, **43**, 95 (1970).

24. P. J. Flory and A. Vrij, *J. Amer. Chem. Soc.*, **85**, 3548 (1963).

25. M. G. Broadhurst, *J. Res. Nat. Bur. Stand.*, **66A**, 241 (1962).

26. D. W. VanKrevelen and P. J. Hoftyzer, *J. Appl. Polym. Sci.*, **13**, 871 (1969).

27. E. F. Jordan, Jr., B. Artymyshyn, and A. N. Wrigley, *J. Polym. Sci. A-1*, **7**, 2605 (1969).

28. D. A. Lutz and L. P. Witnauer, *J. Polym. Sci. B*, **2**, 31 (1964).

29. P. J. Flory, *Principles of Polymer Chemistry*, Cornell Univ. Press, Ithaca, N. Y., 1953, pp. 568–574.

30. M. Dole, in *The Meaning of Crystallinity in Polymers* (*J. Polym. Sci. C*, **18**), F. P. Price, Ed., Interscience, New York, 1967, p. 57.

31. N. Morosoff, H. Morawetz, and B. Post, *J. Amer. Chem. Soc.*, **87**, 3035 (1965).

32. F. W. Billmeyer, Jr., *J. Appl. Phys.*, **28**, 1114 (1957).

33. M. G. Broadhurst, *J. Chem. Phys.*, **36**, 2578 (1962).

Received October 1, 1970
Revised January 14, 1971

JOURNAL OF POLYMER SCIENCE: PART A-1 VOL. 9, 1853–1863 (1971)

Organometallic Polymers I. Solution Polymerization of α-Ferrocenylmethylcarbonium Fluoborate

ALON GAL, MICHAEL CAIS, and DAVID H. KOHN,
Department of Chemistry, Technion-Israel Institute of Technology, Haifa, Israel

Synopsis

The self-condensation of α-ferrocenylmethylcarbonium ion in nitroethane yielded polymers of M_n up to 20,000. The change of $[\eta]$ and $\overline{M_n}$ with the reaction time indicated that the process consisted of a rapid primary growth stage, an induction period, a second growth stage, and a crosslinking stage. The $[\eta]$–$\overline{M_n}$ correlation for a series of polymeric fractions in the $\overline{M_n} = 0.1$–7.2×10^4 range points to a highly branched structure.

INTRODUCTION

Carbonium ions adjacent (α) to metallocene systems possess exceptional stability.[1] With suitable anions, such as the BF_4^- group, it is even possible to isolate these carbonium ions as crystalline salts:[2,3]

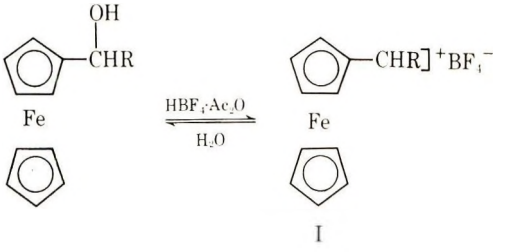

(1)

I

As potential monomer, such an α-ferrocenylcarbonium ion represents a special case of polyfunctionality. While the unsubstituted aromatic cyclopentadienyl ring possesses at least two sites readily available to electrophilic substitution, each α-ferrocenylmethylcarbonium fluoborate (FMCF) molecule holds a single electrophilic group, i.e., the positive carbon atom adjacent to the ferrocene moiety. It has been demonstrated statistically,[4,5] that following a simple polycondensation pattern (i.e. without competitive side reactions) a monomer of this kind yields soluble polymers only, possessing both a highly branched structure and a broad molecular weight distribution.

In this paper we wish to report the synthesis of polymers from the fluoborate salt of the α-ferrocenylmethylcarbonium ion (I), consisting of ferrocene units interconnected by methinyl bridges.

Ferrocenylene-methylene-type polymers were prepared previously by the following general methods: (a) self-condensation of α-ferrocenylcarbinols,[6–8] (b) self-condensation of *N,N*-dimethylaminomethyl ferrocene,[9–11] and (c) polycondensation of ferrocene with various aldehydes.[12–14]

EXPERIMENTAL

Preparation of the Monomer

The monomer, FMCF, which decomposes upon standing, was freshly prepared before each polymerization experiment.

A representative example is given below.

An aqueous solution (48%) of fluoboric acid (210 ml, 0.83 mole) was added slowly under stirring to a flask containing acetic anhydride (650 g, 6.35 mole) cooled in an ice bath. This was followed by the addition of a solution of α-hydroxyethyl ferrocene (140 g, 0.605 mole) in methylene chloride (140 ml). The resulting crimson liquid was immediately transferred to an ice-cooled resin flask, containing anhydrous ethyl ether (3 l.), and fitted with a mechanical stirrer, nitrogen inlet tube, dropping funnel and a teflon tube attached to a suction flask. After 10 min of vigorous stirring at 4°C, the heavy, dark-red precipitate formed, was allowed to settle and the supernatant liquid was removed through the suction tube. The precipitate was washed thoroughly with three portions (700 ml each) of ether under nitrogen, and then dried under reduced pressure (0.5 mm Hg) for 1 hr. The yield was 148 g (82%). The infrared spectrum of the product shows the typical absorption of the BF_4 group between 1030–1110 cm^{-1}; alkaline hydrolysis affords the starting carbinol.

Polymerization

In order to minimize the handling of FMCF, which is sensitive to air, humidity and light, the polymerization was carried out soon after obtaining the dry monomer, in the same flask that served for the synthesis of the monomer.

Nitroethane (260 ml) was introduced into a 4.5-l. resin flask, containing freshly prepared FMCF (110 g) under nitrogen, and the contents were warmed to 60°C. After 2 hr stirring at this temperature, a saturated aqueous solution of sodium carbonate (400 ml) was run in, followed by methylene chloride (800 ml). Stirring was continued for another hour at room temperature, water (1 l.) was added and the phases were allowed to separate. The organic solution was washed with three portions of water (2 l. each), dried with anhydrous $MgSO_4$, and evaporated to dryness in a flash evaporator at about 40°C.

From the dry crude (76 g, $\bar{M}_n$ 4500) a portion of 43.9 g was subjected to reprecipitation, according to the following standard procedure: The poly-

TABLE I
Polymerization of α-Ferrocenylmethylcarbonium Fluoborate (FMCF) in Nitroethane

Expt. no.	Monomer concn, mg/ml solvent	Temp, °C	Reaction time, min	Polymeric products (reduced)					
				Soluble polymer (reprecipitated)					Insoluable polymer, yield from crude, %
				Yield from crude, %	[η], dl/g	$\overline{M}_n$	Elemental analysis[a] C, %	Elemental analysis[a] H, %	
3	100	115	135	77	0.030	1,750			—
6	280	115	20	70	0.033		67.57	5.69	—
9	280	115	320	71	0.041		68.92	5.83	—
13	280	115	660	63.5	0.0565		68.68	5.53	8.7
14	420	25	1	71	0.031				—
17	420	25	1380	82.5	0.041	10,100			—
19	420	60	120	87.5	0.041	20,000[b]			—
20	420	75	6	89.5	0.035	9,200			—
22	420	75	120	88	0.035	10,800			—
27	420	75	1140	91	0.047	16,300			—
28	420	75	1400	56.5	0.032	6,400	67.08	5.68	31.5[c]
32	420	115	280	71.5	0.042	5,000			—
34	420	115	580	75.5	0.058				6.0
35	840	110	5	82.5	0.032	4,500	66.32	6.08	—
36	840	110	20	82	0.035	4,770			—
43	840	110	200	31	0.042	5,770	67.54	6.12	53.0

[a] Calculated for $(C_{12}H_{12}Fe)_n$: C, 67.96%; H, 5.70%.
[b] $\overline{M}_n$ of the reduced crude = 4500.
[c] Elemental analysis: C, 65.11%; H, 6.26%.

mer was dissolved in methylene chloride (6 ml/g), a fivefold volume of petrol ether (40–60°C) was added, and the mixture cooled to −60°C for 15 min. The reprecipitated polymer (38.5 g, 87.5%, $\overline{M}_n$ 20,000) was separated and dried under reduced pressure at 50°C.

Details on the reaction conditions and the products of a number of selected polymerization reactions are summarized in Table I.

Fractionation

Neutralized crude polymer from experiment 19 (20 g, $\overline{M}_n$ 4500) was separated into six more monodisperse fractions by precipitating* with *n*-heptane from benzene solution (5 g/dl) at 20°C (Fig. 1).

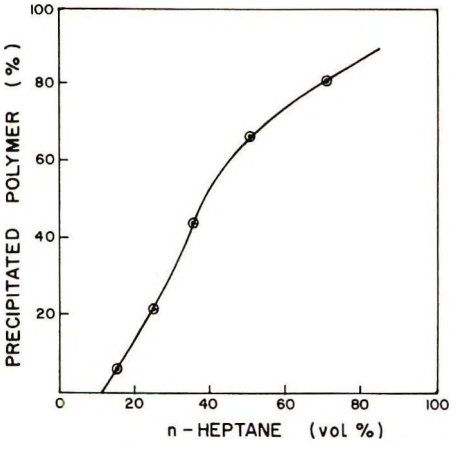

Fig. 1. Fractionation of poly(ferrocenylenemethylmethylene).

Viscosity

Intrinsic viscosities of the polymers $[\eta]$ were determined from measurements of the viscosity of their benzene solutions at 25 ± 0.01°C by using an Ubbelohde viscometer. The values of $[\eta]$ of various polymers are given in Table I.

Molecular Weight

The number-average molecular weight $\overline{M}_n$ was determined for part of the polymers in a vapor-phase osmometer (Model 115, Hitachi Perkin-Elmer).[15] The values are given in Table I.

Infrared Spectra

The spectra were obtained on a Perkin-Elmer 237 grating infrared spectrophotometer with potassium bromide disks.

* The last fraction was obtained by evaporating the mother liquor to dryness.

RESULTS AND DISCUSSION

The course of polymerization of α-ferrocenylmethylcarbonium fluoborate in nitroethane solution was investigated at various constant temperatures and initial monomer concentrations as a function of reaction time.

The results given in Table I suggest that the course of the reaction may consist of several distinct steps, as illustrated in Figures 2 and 3 for two typical cases of solution polymerization of FMCF.

The change of $[\eta]$ and $\bar{M}_n$ with the reaction time indicates that the first growth stage is followed by a relatively long induction period, after which the growth of the polymer starts again. In the next stage, the molecular weight of the sol phase begins to decrease, along with the formation of an insoluble product.

One can assume that the first growth stage represents the self-condensation of FMCF, when pairs of monomer units may react to give a dimer (II).

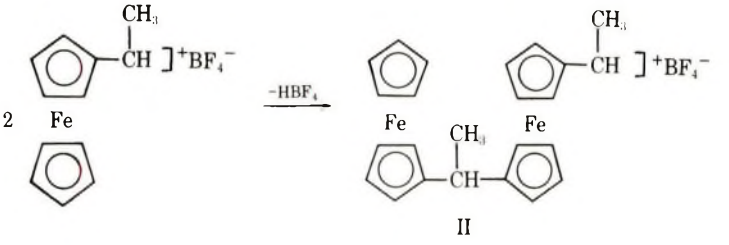

(2)

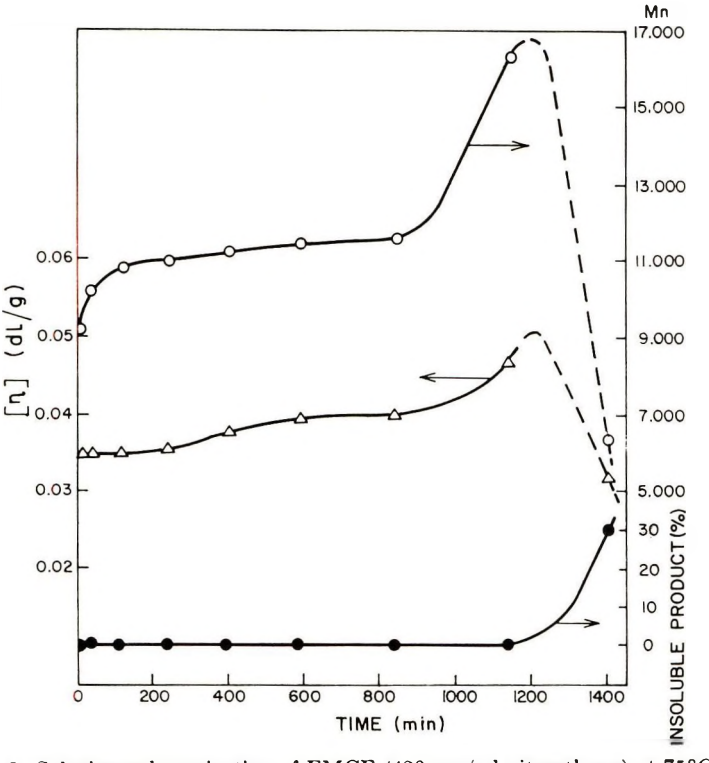

Fig. 2. Solution polymerization of FMCF (420 mg/ml nitroethane) at 75°C.

In its most probable form (II), the dimer contains a heteroannularly disubstituted ferrocenylene unit, due to the deactivating effect of the positive carbon atom on the adjoining ring.

By further increase of the degree of polymerization, the global number of active aromatic sites per growing molecule increases, while the number of electrophilic groups is at best one, at the head of the chain. The reactivity of the polymer toward electrophilic attack as compared with the monomer is also favorably influenced by the presence of electron-releasing methinyl bridges. Thus the great reactivity of the growing chain may be responsible for the quickness of the polycondensation, which was found to reach relatively high conversion and intrinsic viscosity within a few tens of seconds in all the cases investigated.

As a result of the potential polyfunctionality of each repeating unit, the polymer is expected to achieve a highly branched structure, such as shown schematically as (III). For reasons of simplicity this diagram does not show

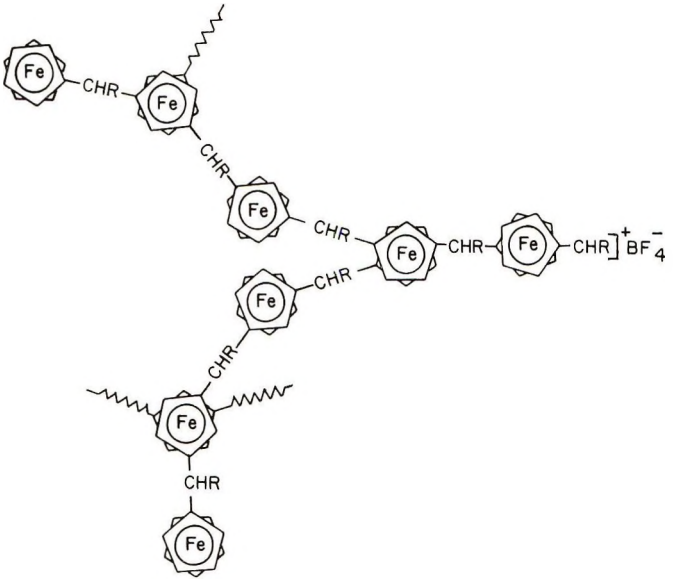

III

the BF_4^- groups which must be associated as counterions with those ferrocene moieties which are in a protonated and/or oxidized (ferricinium ion) state. The existence of a sizable number of such units incorporated into the polymer is suggested by the color, solubility properties and infrared spectrum of the nitroethane-soluble crude. FMCF dissolved in nitroethane gives a reddish solution, turning its color within a few seconds to dark green. The product exhibits a very strong absorption band between 1030 and 1100 cm^{-1}, comparable in intensity to that of the monomeric fluoborate salt. The intensity of this band, characteristic to the BF_4^- anion, did not diminish even in a sample purified by several reprecipitations from methylene chloride solution with excess diethyl ether. This fact

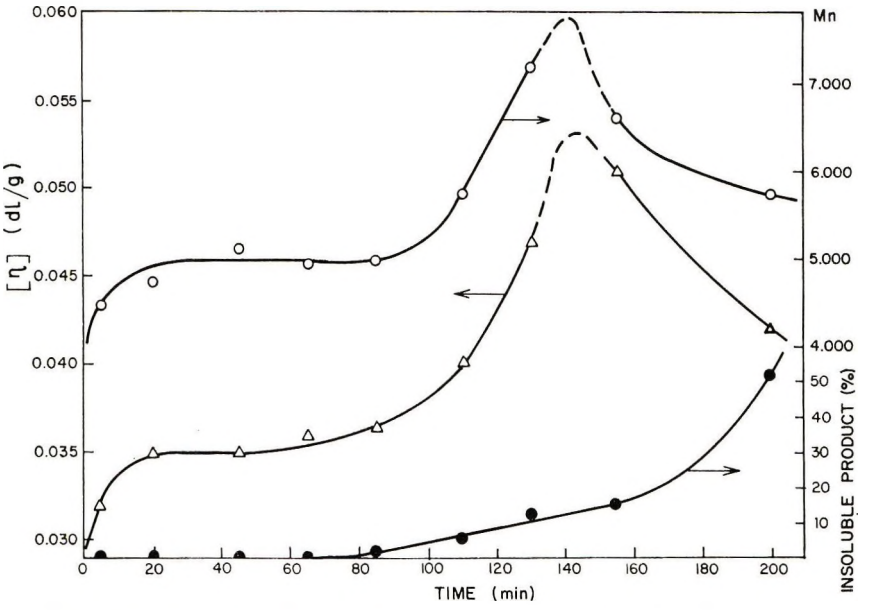

Fig. 3. Solution polymerization of FMCF (840 mg/ml nitroethane) at 110°C.

can hardly be accounted for by the BF_4^- group attached to the sole α-carbonium ion situated at the head of the chain, indicating that the fluoboric acid released during the polycondensation remains—at least partially—associated with the polymeric chain.

Work-up of the crude with alkaline solutions leads to resinous compounds which fail to dissolve in nitroethane and do not exhibit in the infrared spectrum the typical absorption band of the BF_4^- group. The color of these products varies from dark yellow to dark brown, which parallels increasing degrees of polymerization of the respective compounds. Unless the reaction time is prolonged excessively, the neutralized crude is readily soluble in solvents such as 1,2-dichloroethane, chlorobenzene, and dichloromethane.

The elemental composition of the neutralized and reprecipitated polymers correspond (within the experimental error) to molecules composed of ferrocenylene-methylmethylene recurring units, while the two strong peaks exhibited near 1000 and 1100 cm^{-1} in the infrared spectrum demonstrate the existence of unsubstituted cyclopentadienyl rings belonging probably to end groups and to homoannularly polysubstituted ferrocene moieties.

During the observed induction period, $[\eta]$ and $\overline{M}_n$ remain almost unchanged, and from Figures 4 and 5 it is apparent that this stage of the reaction is shortened by increasing the initial monomer concentration and also by raising the reaction temperature.

The existence of such an 'induction period' between the two growth stages suggests that these are qualitatively different processes. In the second growth stage, after reaching a maximum, the average molecular weight of the sol phase decreases rapidly (as shown in Figs. 2 and 3), owing to the

formation of an insoluble material that tends to become the main reaction product. This insoluble product underwent the same color change upon neutralization as the nitroethane-soluble crude. It proved to be insoluble in all solvents tested (e.g. 1,2-dichloroethane, nitrobenzene, dimethyl sulfoxide, sulfuric acid) but it swelled in some of them (1,2-dichloroethane, for instance), giving an elastic gel. When heated up to its decomposition tem-

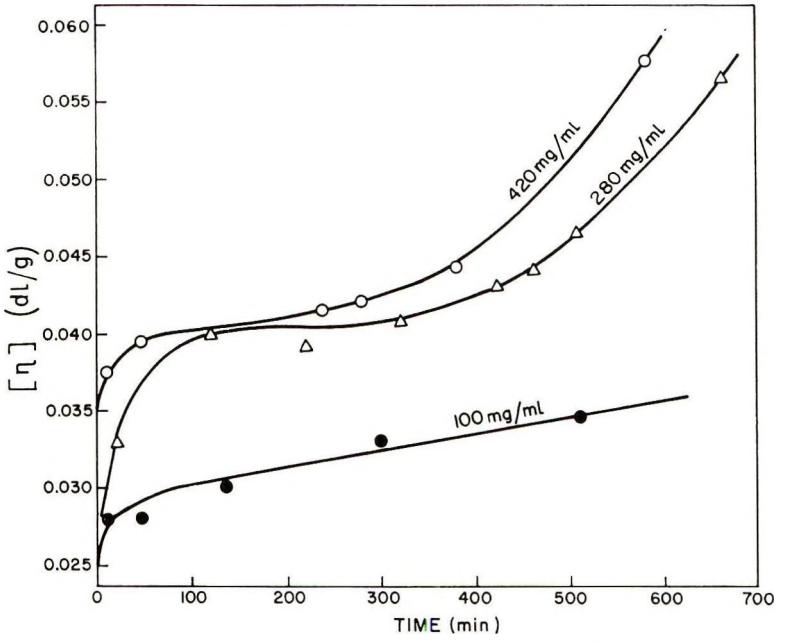

Fig. 4. Effect of reaction time on intrinsic viscosity at 115°C.

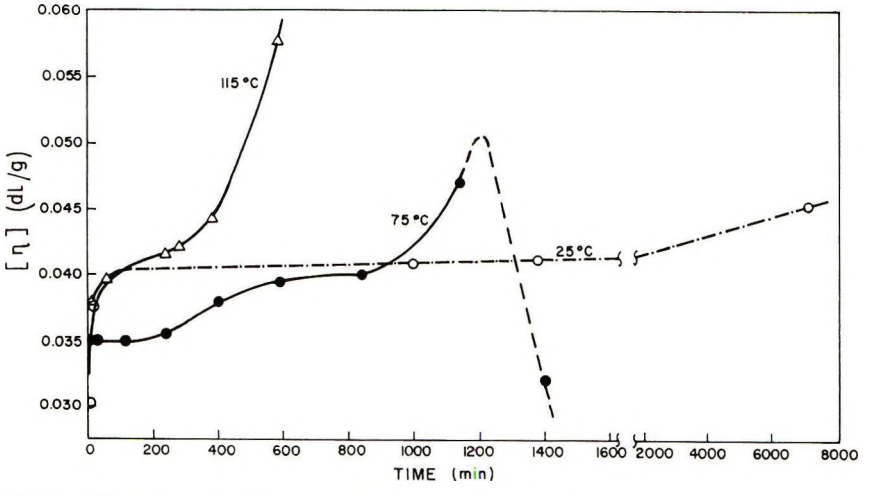

Fig. 5. Effect of reaction time on intrinsic viscosity at an initial monomer concentration of 420 mg/ml nitroethane.

perature (about 230°C), it did not melt or sinter. The infrared spectrum of this product was practically identical with that of the soluble polymer. The quantitative elemental analysis of the insoluble product revealed a somewhat diminished carbon content; on the other hand it was found to contain traces of inorganic iron. These results indicate that the insoluble material may be the crosslinked (gel) form of poly(ferrocenylene-methylmethylene). Based on the behavior of ferrocene and alkylated ferrocenes in protonating media, this second growth stage of the polymer, following the induction period, and the subsequent onset of gelation, are likely to be due to the formation of new interchain bonds and could be brought about by one, or by both of the following two reaction types: (1) the cleavage of the metal-ring bond[16–19] in a number of repeating units, resulting, via intermediary cyclopentadiene or a cyclopentenyl cation, in cyclopentylene-bridged chains of the form IV:

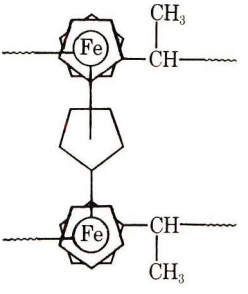

IV

or (2) ligand exchange[20,21] between neighboring ferrocene units belonging to different polymer molecules, leading to the formation of heteroannularly polysubstituted interchain bonding units V, as illustrated by eq. (3).

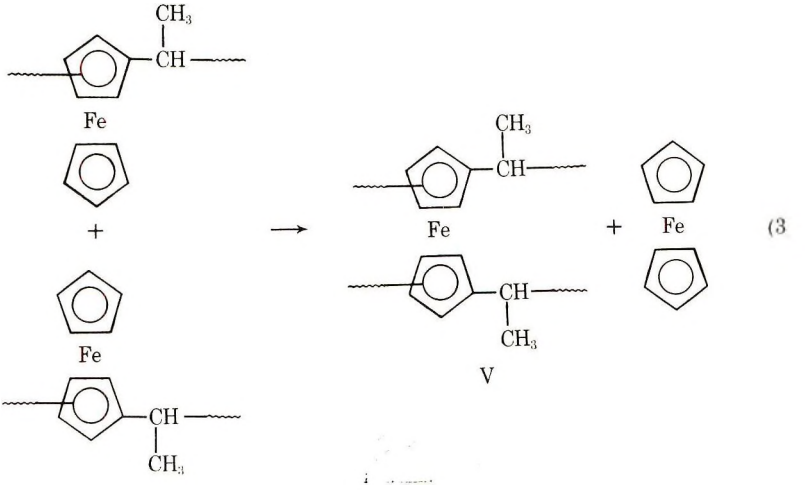

It should be added that the possible intervention of a radical-type mechanism in the crosslink formation cannot yet be excluded.

In order to examine the $[\eta]$-$\overline{M}_n$ relationship, the neutralized crude polymer was fractionated into six fractions and their intrinsic viscosity and number-average molecular weight determined. The double logarithmic plot of $[\eta]$ against $\overline{M}_n$ of the fractionation products was found to be an approximately straight line, as shown in Figure 6.*

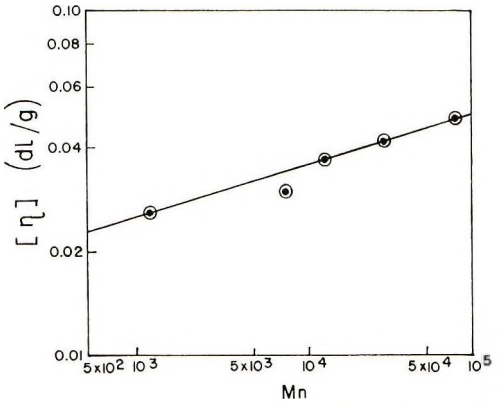

Fig. 6. Intrinsic viscosity of polymeric fractions vs. $\overline{M}_n$.

When the location of this line is calculated by means of the least-squares method, it can be expressed in the form of the following Kuhn-Mark-Houwink-type correlation:

$$[\eta] = 8.84 \times 10^{-3}\overline{M}_n^{0.153}$$

As exponents smaller than 0.5 point to a branched structure, the value of 0.153 seems to confirm the predictions concerning the configuration of the polycondensation products.

The above correlation is different from $[\eta] = 3.95 \times 10^{-3}\overline{M}_n^{0.27}$, reported by Neuse and Trifan[8] for apparently similar polymers prepared by the self-condensation of α-hydroxyethylferrocene. It appears that there is also a considerable discrepancy between $[\eta]$ and $\overline{M}_n$ data of polymers obtained in different reaction conditions (Table I). Thus, for instance, the $\overline{M}_n$ corresponding to the same value of $[\eta] = 0.035$ dl/g is 10,800 in experiment 22 (carried out at 75°C with an initial monomer concentration of 420 mg/ml nitroethane) and 4,770 in experiment 36 (110°C, 840 mg/ml).

The relationship between intrinsic viscosity and molecular weight for nonlinear, polydisperse polymers is dictated both by the geometry of the respective molecules and by their distribution.[22] Differently branched polymers must not necessarily obey the same $[\eta] = K\overline{M}_n^{a}$ equation, so that the

* The highest (first) fraction does not appear in the plot, because it was not completely soluble in the solvent used (benzene) and therefore its $\overline{M}_n$ and $[\eta]$ were not determined.

above-mentioned seeming inconsistencies may be explicable in terms of the effect of reaction conditions on the extent of branching.

This work was supported in part by the Air Force Materials Laboratory, Research and Technology Division, A.F.S.C., European Office of Aerospace Research, United States Air Force, Contract No. AF 61 (052)-752, and in part by the Julius and Irma Schindler Memorial Scholarship.

This paper is taken in part from a dissertation submitted by Alon Gal to the Department of Chemical Engineering, Technion-Israel Institute of Technology, Haifa, in July 1970, in partial fulfillment of the M.Sc. degree.

References

1. M. Cais, *Organometal. Chem. Rev.*, **1**, 435 (1966).
2. M. Cais and A. Eisenstadt, *J. Org. Chem.*, **30**, 1148 (1965).
3. A. Eisenstadt, D.Sc. Thesis, Technion, Haifa, 1967.
4. P. J. Flory, *J. Amer. Chem. Soc.*, **74**, 2718 (1952).
5. P. J. Flory, *Principles of Polymer Chemistry*, Cornell Univ. Press, Ithaca, N.Y., 1953, pp. 348–370.
6. K. Schloegl and A. Mohar, *Monatsh. Chem.*, **92**, 219 (1961).
7. A. Wende and H. J. Lorkowski, *Plaste Kautschuk*, **10**, 32 (1963).
8. E. W. Neuse and D. S. Trifan, *J. Amer. Chem. Soc.*, **85**, 1952 (1963).
9. E. W. Neuse and E. Quo, *J. Polym. Sci. A*, **3**, 1499 (1965).
10. E. W. Neuse, U.S. Pat. 3,238,185 (Mar. 1, 1966).
11. E. W. Neuse and K. Koda, *Bull. Chem. Soc. Japan*, **39**, 1502 (1966).
12. E. W. Neuse and K. Koda, *Organometal. Chem.*, **4**, 475 (1965).
13. E. W. Neuse and K. Koda, *J. Polym. Sci. A-1*, **4**, 2145 (1966).
14. H. Valot, *Double Liaison*, No. **130**, 775 (1966).
15. J. L. Armstrong, in *International Symposium on Polymer Characterization (Appl. Polym. Symp.*, 8), K. A. Boni and F. A. Sliemers, Eds., Interscience, New York, 1969, p. 17.
16. S. G. Cottis and H. Rosenberg, *Chem. Ind.* (London), **1963**, 860.
17. S. G. Cottis and H. Rosenberg, *J. Polym. Sci. B*, **2**, 295 (1964).
18. E. W. Neuse, R. K. Crossland, and K. Koda, *J. Org. Chem.*, **31**, 2409 (1966).
19. E. W. Neuse, *J. Org. Chem.*, **33**, 3312 (1968).
20. D. E. Bublitz, *Can. J. Chem.*, **42**, 2381 (1964).
21. D. E. Bublitz, *Organometal. Chem.*, **16**, 149 (1969).
22. S. Gundiah, *Makromol. Chem.*, **104**, 196 (1967).

Received December 8, 1970
Revised February 26, 1971

JOURNAL OF POLYMER SCIENCE: PART A-1 VOL. 9, 1865–1877 (1971)

Grafting on Wool. I. Electron Microscopic Studies on the Location of Grafted Polymer in Wool Structure

KOZO ARAI and MICHIHARU NEGISHI, *Faculty of Technology, Gunma University, Kiryu, Gunma, Japan*

Synopsis

To determine the location of grafted poly(methyl methacrylate) in orthocortex structure of fine Australian Merino wool fibers, high-resolution electron microscopy was used. Optimal staining conditions for the observation of the deposited polymer were also studied. It was supposed that the grafted polymer is located mainly between the microfibril and matrix and around the protofibrillar subunits, but not in the matrix. The average space occupied by a grafted chain was estimated to be about four times as large as the total residue volume per polymer. It is supposed that the remarkably large space available per polymer chain is related to the excessive swelling seen with respect to the polymer uptake.

Introduction

In a previous report,[1] the relationship between the location of grafted polymer in wool fiber and the rate of grafting of methyl methacrylate in aqueous LiBr–$K_2S_2O_8$ redox systems[2] was clarified. Distribution of polymer was controlled not only by the rate of grafting, but also by the rate of formation of grafting sites. Three distinct cases were observed in dyeing studies: (1) uniform distribution of polymer over the cross section of the fiber, (2) dense deposit of the polymer in the outer zone, (3) much more polymer deposition in the orthocortex than in the paracortex. Relatively uniform deposition of polymer could be seen at lower rates of grafting and at the formation of grafting sites. However, dense distribution of polymer in the outer region was observed at the higher rates.

Studies on the location of grafted polymer in wool fiber have been reported.[3–6] Ingram and his co-workers[7] used electron microscopy and a low-angle x-ray technique to study the location of grafted polystyrene in radiation-grafted wool fibers. It has been postulated that the most of the grafted polymer is located in the keratinous matrix regions between the microfibrils.

The purpose of this investigation is to determine the location and the actual dimensions of a grafted polymer, and to evaluate the possibility of structural research on wool by the use of high resolution electron microscopy.

Experimental and Materials

The tops of fine Australian Merino wool fibers were extracted with acetone in a Soxhlet apparatus for about 24 hr, washed with cold water, and then air-dried.

Wool fibers were grafted with methyl methacrylate (MMA) in the aqueous LiBr–$K_2S_2O_8$ redox reaction system at 30°C without homopolymer. After the reaction period, the wool fibers were only washed with water and dried.

Two typical reaction systems were selected for the preparation of grafted wool fibers. One is the system containing a large amount of diethylene glycol monobutyl ether (BC) as a monomer solubilizer; here, much more polymer occurs in the orthocortex than in the paracortex. The other is a system containing a relatively small amount of BC; the grafted fiber prepared by this system gives dense deposits in the outer region of the fiber. In the former case, the wool (0.5 g) was treated with a solution mixture containing 13.75 g LiBr, 0.1 g $K_2S_2O_8$, 2.5 g MMA, 22.4 g H_2O, and 11.25 g BC (system A) for 3 hr, and the extent of grafting was 101.6% on wool. In the latter case, the wool was treated with a solution mixture containing 13.75 g LiBr, 0.1 g $K_2S_2O_8$, 2.5 g MMA, 22.4 g H_2O, and 7.5 g BC (system B) for 45 min and 4 hr. The extent of grafting of the samples was 54.0% and 113.5% respectively.

The contents of thiol and disulfide groups in the native and the grafted fibers were determined by Leach's polarographic method with methylmercury iodide.[8] All the analyses were carried out twice or three times, and the average value was taken.

Both the native and the grafted fibers were treated with 0.3% potassium permanganate solution for 3 hr at room temperature. These treated samples were dehydrated and embedded in Epon resin. Ultra-thin transverse sections were prepared by use of a JUM-5A ultramicrotome (Japan Optics Lab.) equipped with a glass knife. The ultra-thin sections were followed by poststaining with a saturated solution (7–8%) of uranyl acetate for 10 min and washing. They were then viewed in a JEM 7A electron microscope (Japan Optics Lab.) at 80 kV accelerating voltage.

Wide-angle x-ray diffraction photographs of the grafted samples were obtained from nickel-filtered Cu Kα radiation.

Results and Discussion

Of the amino acids in wool, cystine residues have been found to react with potassium permanganate and to deposit manganese dioxide.[9] Uranyl acetate combines with free carboxyl groups which are present in higher amounts in the crystalline region than in the cystine-rich matrix.[10] As for the staining conditions, it is considered that the same level in electron density between crystalline and matrix regions may be preferable for the observation of the location of unstained polymers. In fact, high contrast in the electron micrographs of the native wool is not achieved by these staining

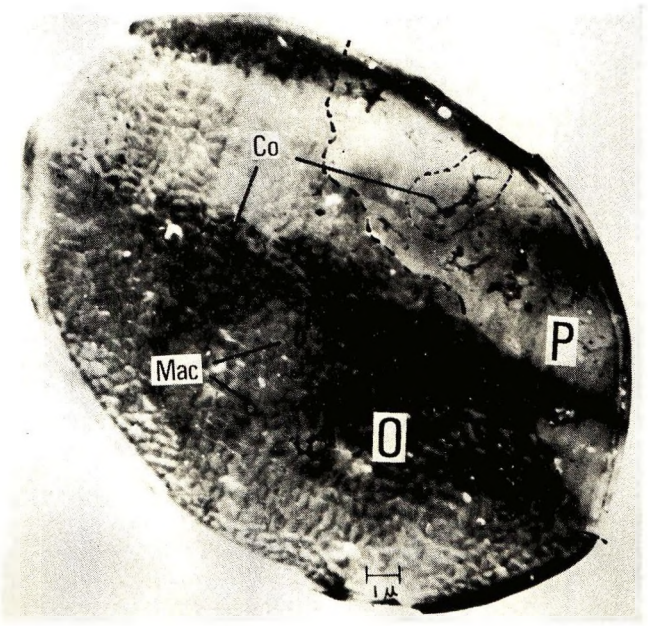

Fig. 1. Electron micrograph of thin cross section of a fine Australian Merino wool fiber, showing the granular macrofibril (Mac) in the orthocortex (O), and the cortical cell (Co) in the orthocortex and paracortex (P). The contrast is due to variations in thickness of the section. Electron micrographs of higher resolution could not be obtained by this staining method.

conditions as shown in Figure 1. However, the cortical cells in the ortho- and paracortex can be distinguished on the cross-sectional view. There is a remarkable difference in the appearance of the two type cells. Approximately circular macrofibrils can be seen in the orthocortical cells. The paracortex is smaller in cross-sectional area than orthocortex (about 1/3).

The electron micrographs of typical whorl-like macrofibrils in the orthocortex of the grafted fiber prepared by the system A are shown in Figures 2 and 3. The light and dense regions correspond with the unstained grafted polymers and the keratinous materials, respectively. The layer structures can be clearly seen in each macrofibril. As is clear in Figure 2, polymer also occurs homogeneously in the macrofibrils at the histological level. On the upper right side in the figure, we can find a single macrofibril surrounded by a large intermacrofibrillar region. Even for such circumstances, the whorly macrofibril is present without any distortion. This facts suggests that the size of the macrofibril increases as the grafting reaction proceeds but the geometric form in the initial state is retained.

On the other hand, for the grafted fiber prepared by the system B, dense deposit of polymer is observed not only in outer regions of the cross section of the fiber, but also of the cross section of the macrofibril (Figs. 4 and 5). The whorled fingerprint-type macrofibrils are partly separated by the grafted intermacrofibrillar materials.

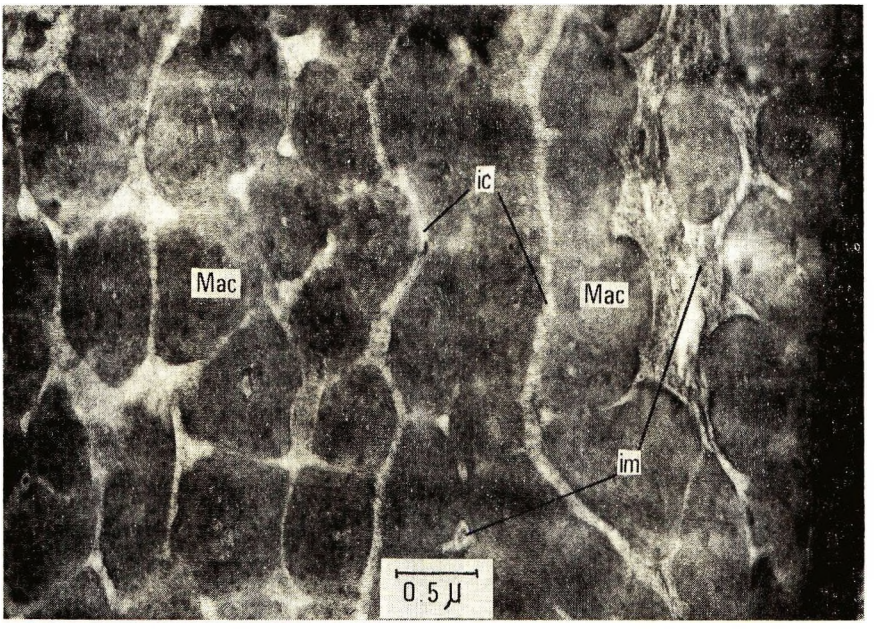

Fig. 2. Electron micrograph of thin cross section of the 101.6% grafted fiber sample obtained by the reaction system A, showing the appearances of the orthocortical macrofibrils. It can be seen that the polymer occurs in each macrofibril (Mac), intermacrofibrillar material (im), and intercellular region (ic).

The average values of cross-sectional area of single fiber and an orthocortical macrofibril in the native and the grafted fiber are listed in Table I. The longitudinal dimensional change was only 1–2% contraction during the reaction period. However, a marked increase in lateral dimensions was observed. A similar result has been reported by Ingram and his co-workers.[7] First, it is interesting to note that the ratio of intermacrofibrillar plus intercellular area to the orthocortex area, which is considered to indicate the uni-

TABLE I
Average Cross-Sectional Area of Single Fiber and Orthocortical Macrofibril for Native and Grafted Wool

Sample	Average cross-sectional area, μ^2 Single fiber (absolute dry)	Orthocortical macrofibril	Ratio of intermacrofibrillar plus intercellular area in orthocortex to orthocortex area
Native wool	300	0.11	0.10
Grafted wool			
54.0% graft	650	0.34	0.08
101.6% graft	930	0.51	0.13
113.5% graft	920	0.63	0.10

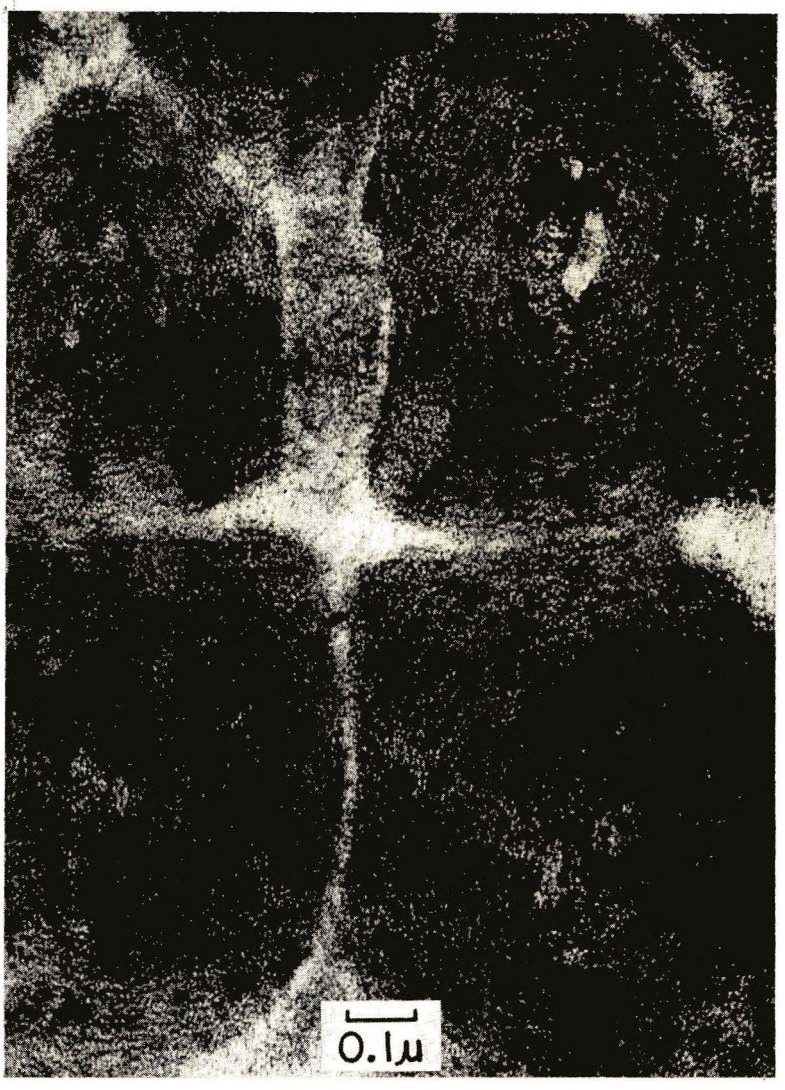

Fig. 3. Higher magnification views of macrofibrils similar to those in Fig. 2, showing that the cylindrical type lamellae in the orthocortical macrofibril can be more clearly seen to be delineated by the electron-light polymer.

formity of the distribution of grafted polymer in the complex morphological structure, is approximately similar for both the native and the grafted samples. The rate of increase in the average values of the cross-sectional area of single fiber is lower than that of a macrofibril. This fact indicates that polymer deposition occurs preferentially in the orthocortex region rather than in the paracortex.[1]

A higher-resolution electron micrograph of the cross-section of the 101.6% grafted sample is shown in Figure 6. The deposited polymers can be clearly differentiated from the electron-dense wool materials in layer structures.

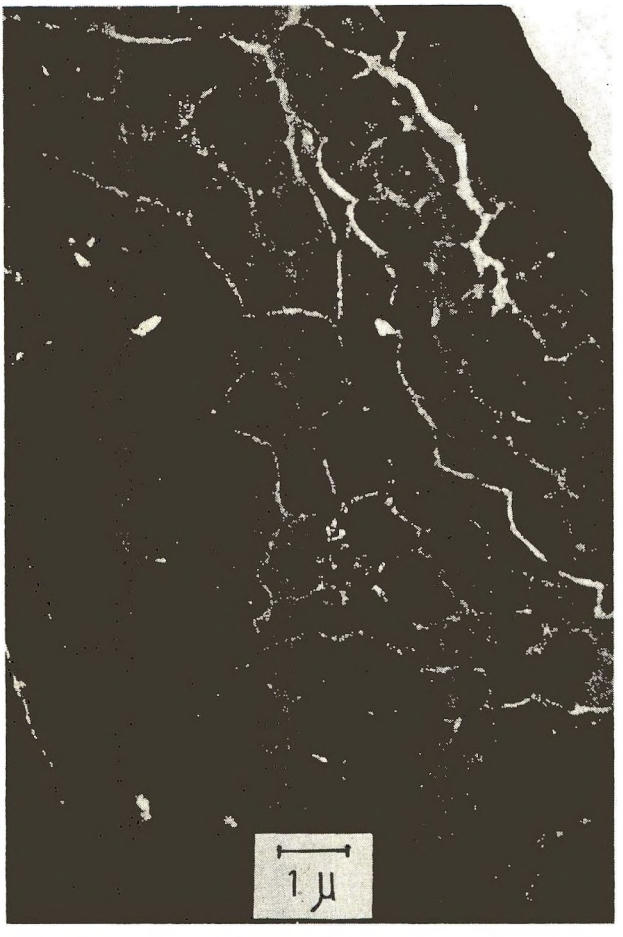

Fig. 4. Electron micrograph of thin cross section of the 54.0% grafted fiber sample obtained by the reaction system B. It can be seen that much polymer is located near the fiber surface and relatively homogeneous deposition in the macrofibrils occurs. On the contrary, in the inner region of the fiber cross section, we can find the dense deposits in the outer zone of the cross section of a macrofibril.

A high-resolution electron micrograph of thin cross section of the 101.6% grafted fiber is shown in Figure 7. A striking feature of the arrangement of semicircular units in sheet structures can be observed. The semicircular units are grafted microfibrils. It can be seen that the microfibril is composed of protofibrillar units[11] which are surrounded by the electron-light polymer. However, it is not possible to determine the exact number o protofibrils. It seems likely that the grafted polymer is located between and around the microfibril and matrix and also around the protofibrillar subunits. This result may be also supported by the following experimental evidence.

First, it was found from the analyses of cystine contents that the disulfide crosslinks remain intact in these grafted wool fibers (Table II). From the

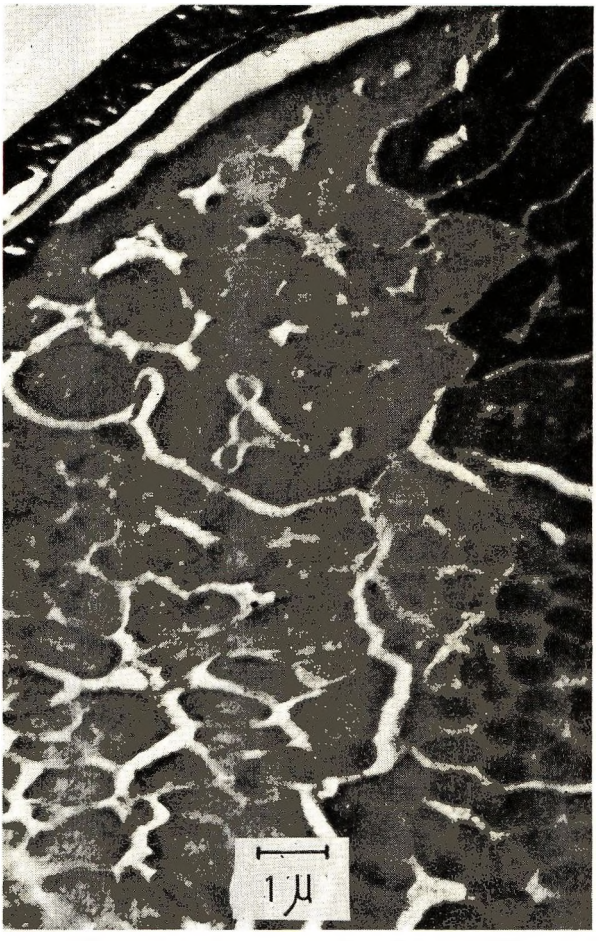

Fig. 5. Electron micrograph of thin cross section of the 113.5% grafted fiber sample prepared by the system B, showing a polymer deposition pattern similar to that in Fig. 4. In the case of the samples with higher amounts of polymer, many cracks tend to occur along the cell boundaries owing to the shear stress during the thin sectioning.

measurements of electron micrographs, the ratio of microfibril to matrix in the orthocortex has been found to be about 4:1.[12] Assuming that all of the disulfide crosslinks are randomly distributed only in the matrix region, the apparent number n of amino acid residues between the crosslinks in the or-

TABLE II
Contents of —SH and —SS— Groups in the Native and Grafted Wool Fibers

Sample	—S—S, μmole/g wool	—SH, μmole/g wool
Native wool	425	39.0
Grafted wool		
54.0% graft	411	32.3
101.6% graft	428	32.1

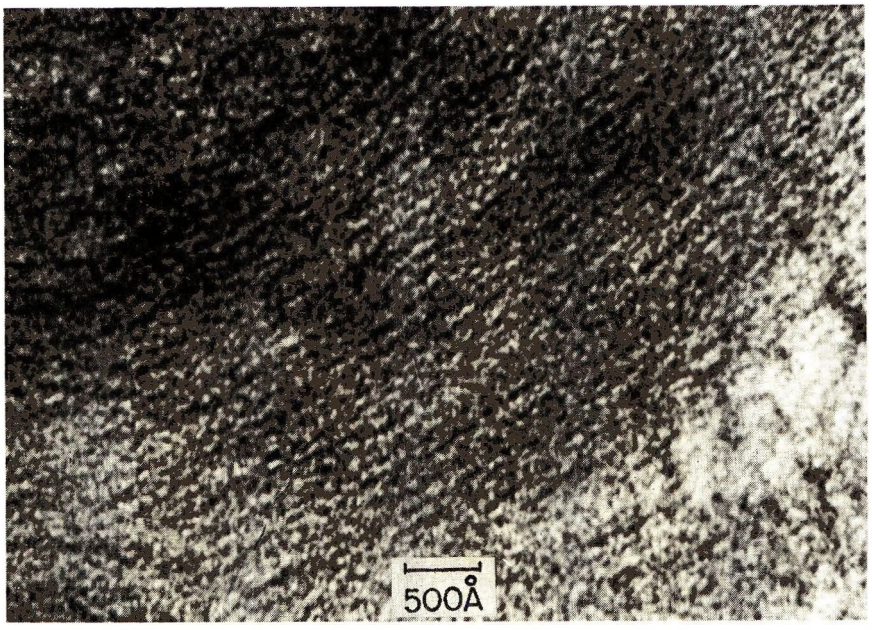

Fig. 6. A higher-resolution electron micrograph of thin cross section of the 101.6% grafted sample showing appearances of the layers in outer region of a macrofibril. A large amount of polymer deposition can be seen on the right side.

thocortex segment is given by $(10^6 \times {}^1/_5 \times {}^1/_{108})/(425 \times 2) = 2.2$, where the average residue weight of matrix molecule is 108.[13] This figure may be too low because the sequence —CyS—CyS— often occurs in the high-sulfur proteins.[14] Corfield et al.[15] reported that the high-sulfur proteins have one —SS— bond per ten residues.

On further details, Bendit[16] presented previously quantitative data for the distributions of high- and low-sulfur proteins in the "microfibril-plus-matrix" unit by combining data from a variety of sources. It has been suggested that a nonhelical portion of SCMKA "tails" spills over into the matrix region, and the region of the tails and the matrix becomes about 50% of the total. On the basis of this suggestion and by using an assumption similar to the above case, n is calculated to be about six. It could be considered that much aggregation arises among the molecules within the matrix which has such a high crosslink density. Therefore, it is not likely that the grafted polymer occurs predominantly within the aggregates.

On the other hand, it was found that some polymer occurs within the aggregated matrix in the partially reduced wool fiber, in which the cystine content has been reduced to 188 μmole/gram wool.[17]

Secondly, the prominent 9.8 Å equatorial and 5.1 Å meridional reflections characteristic of α-keratin are clearly recognized on the high-angle x-ray diffraction photographs of the grafted fibers. Even at high degrees of grafting, superposition of diffraction rings from poly(methyl methacrylate) on the wool were observed, as shown in Figure 8. It was found that the

α-helical components are almost retained within the structure of high levels of grafting.[18] From this x-ray evidence, the grafting is not considered to have an important effect upon the chain conformation of the α-helix forming the protofibril.

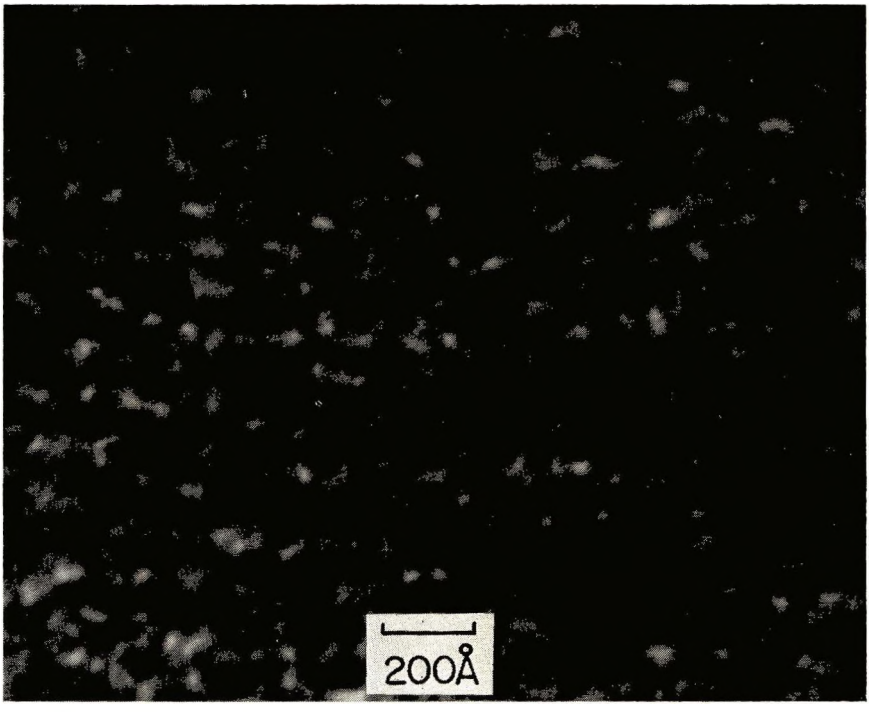

Fig. 7. A high-resolution electron micrograph of thin cross section of the 101.6% grafted fiber, showing the arrangement of semicircular units in sheet structure which are delineated by the electron light polymers. Five sheets can be seen along the horizontal direction of this plate.

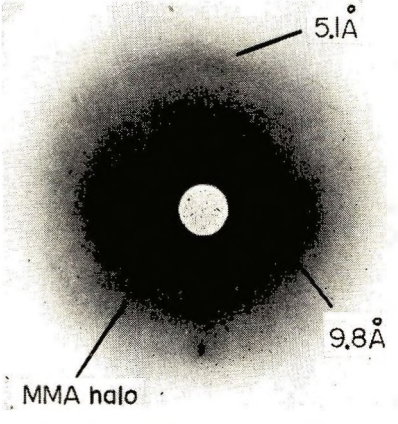

Fig. 8. An x-ray diagram of 111.1% grafted wool fiber prepared by system A.

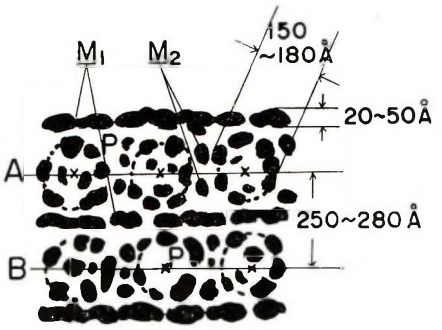

Fig. 9. A schematic diagram of the polymer within lamellar structures in the orthocortical macrofibril of the 101.6% grafted wool fiber: (P) grafted polymer; (M_1) matrix between sheet A and the adjacent sheet B; (M_2) matrix within a sheet.

Thirdly, the results obtained from the longitudinal mechanical behavior[19] also support the above considerations that the nature of the matrix and the α-helical components almost remain intact without being affected very much with the deposited polymer.

From the above results, it is deduced that the location of the grafted polymer is a region in which the polymer can be deposited without disturbing the matrix and protofibrils, that is, the region "between" the matrix and protofibrils.

We turn now to electron microscopic results. A schematic diagram of the polymer-location within lamella structures in orthocortical segment for the 101.6% grafted wool fiber is shown in Figure 9. The spacing between the lines joining the center of microfibrils in adjacent layers (250–280 Å), and the diameter of microfibril (150–180 Å) in a grafted macrofibril are approximately 2.5 times the size of the native wool obtained with the TGA–OsO_4 staining procedure by Fraser and MacRae[20] and Rogers.[21] Figure 9 corresponds well to the average cross-sectional area of the orthocortical macrofibril cited in Table I. It is clear that grafted polymer is located not only around and between microfibril and matrix, but also at the interprotofibrillar and interstitial regions of microfibrils. Here, it is noteworthy that the aggregated matrix between sheets is clearly visible along the linear arrangement of microfibrils (see Fig. 7). In addition, it gives suggestive information regarding the nature of the matrix. The size and shape of the aggregated matrix between sheets are almost the same as reported for the native matrix in the cross-sectional views.[21] It may be reasonable to consider that the matrix between sheets is much more aggregated than the matrix materials between the microfibrils within each sheet. This fact may also imply that the matrix between sheets contains a much higher amount of disulfide crosslinks. On the other hand, the matrix molecules within the sheet may be globules[22] which have little interaction between them, or aggregates having very low levels of disulfide crosslinks. Under such a situation, we could expect uniformly large swelling of each sheet as a result of polymer

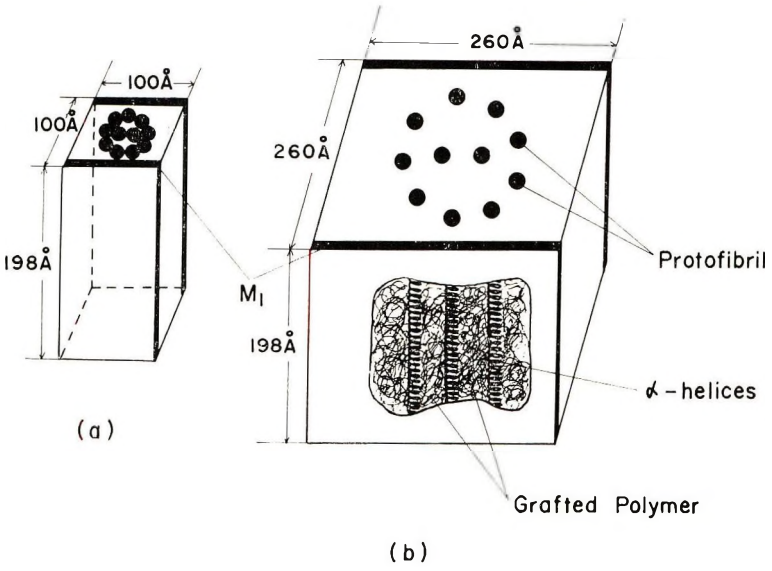

Fig. 10. Schematic representation of the "microfibril-plus-matrix" unit in the orthocortex segment of (*a*), the native wool and (*b*) the 101.6% grafted fiber. The "9 + 2" arrangement[22] of protofibrils in the microfibril is also shown.

deposition. Even if the microfibrils are tilted or are helically arranged with respect to the macrofibril axis, a large swelling effect due to polymer deposition would lead a reduction of the effect of the thickness[23] of the cross-section of the wool structure. It is important that the distribution of polymers reflects characteristically the ultrastructure of wool itself, the discrete x-ray diffraction pattern of α-keratin remaining.

On the basis of electron microscopic evidence and the endgroup analysis of isolated graft polymer,[24] it is possible to estimate the actual dimensions of the grafted polymer and the number of the grafting sites in a unit cell. For native Merino wool, it has been found that each sheet in the orthocortical structure is about 100 Å in thickness.[21] The x-ray diffraction analysis shows that the repeats along the fiber axis give rise to meridional spacings corresponding to the higher-order reflection of the 198 Å spacing.[25] For convenience, a tetragonal type cell may be taken as the "microfibril-plus-matrix" unit in orthocortex. As shown in Figure 10, it is rectangular, with two edges equal in 100 Å length which are normal to the microfibril axis and perpendicular to each other, the other edge being 198 Å in length along the axis direction.

Preferential grafting in orthocortex was observed for the 101.6% grafted sample. The fine texture of Lincoln wool fiber is more or less analogous to the paracortex structure of Merino wool. The degree of grafting reached was only 50% for the Lincoln wool under the similar condition of reaction to that for the Merino wool. The average ratio of orthocortex to paracortex area for the Merino wool is approximately 3:1. Therefore, it is supposed

that preferentially occurring polymer in the orthocortex region is approximately 125% at the level of grafting.

It is known from the results of the DNP endgroup analysis that two DNP amino acid residues are incorporated in both ends of an isolated long polymer chain (average molecular weight $\bar{M} = 50 \times 10^4$).[24] Thus, the number of grafting sites in the orthocortex segment is

$$s = \frac{Z \cdot G}{\bar{M} \times 100}$$

$$= \frac{2(125)}{50 \times 10^4 \times 10^2}$$

$$= 5 \times 10^{-6} \text{ mole/g wool}$$

where Z and G are the number of DNP amino acid endgroups per polymer chain and the extent of grafting, respectively. Therefore, the number of grafting sites per unit cell is

$$s' = \frac{s\rho_w N v}{10^{24}}$$

$$= \frac{5 \times 1.33 \times 6.02 \times 10^{23} \times 100^2 \times 198}{10^6 \times 10^{24}} = 8.0$$

where ρ_w, N and v are density of wool, Avogadro's number, and the volume of microfibril-plus-matrix unit, respectively.

Accordingly, there are four polymer molecules in the unit cell. It is considered that the volume of the wool portion is scarcely changed with grafting, though the dimensions of the plane normal to the microfibril axis in the unit cell are expanded in an isotropic manner. Thus, the increment in volume by the graft polymers is estimated to be 11.5×10^6 Å.^{3} The average space occupied by a single polymer chain is thus 2.9×10^6 Å.^{3} Now, if the polymer density, ρ_p is taken[18] as 1.183 and the molecular weight of the polymer is 50×10^4, the total residue volume of polymer is given by

$$V_p = M/N\rho_p$$

$$= (50 \times 10^4 \times 10^{24})/(6.02 \times 10^{23} \times 1.183) = 7.02 \times 10^5 \text{ Å}^3$$

This value is about a quarter the average space occupied by a grafted polymer. The grafted polymer might be more curled in configuration than the unperturbed molecule because the aqueous reaction medium was a precipitant for poly(methyl methacrylate). On the other hand, the grafted polymer might tend to a more open chain configuration, because of the influences of the interaction between polymers and polypeptide molecules. It is important that there is enough space available for growing high molecular weight polymers in the microfibril-plus-matrix unit.

In conclusion the grafted polymer occurs between the microfibril and matrix or around the protofibrillar subunits. These facts indicate that the in-

teractions between the side-chain groups of residues forming the helices and the matrix molecules and the interactions between the protofibrils are so low that preferential grafting occurs in these regions. Therefore, it is suggested that the region between the protofibrils and matrix is not so much stabilized by chemical crosslinks and secondary bonds as the other. There is a marked difference in the degree of grafting between the two cortex regions. Naturally, the grafting must be severely affected by the crosslinks.

Thanks are due to Dr. F. Bekku, Technical Manager of IWS Japan, for his encouragement, and to the Japan Optics Laboratory Co., Ltd. for their support and the use of the electron microscope.

References

1. M. Negishi, K. Arai, and K. Tabei, *Sen-i Gakkaishi*, **25**, 311 (1969).
2. M. Negisihi, K. Arai, S. Okada, and I. Nagakura, *J. Appl. Polym. Sci.*, **9**, 3465 (1965).
3. E. Mercer, *J. Text. Inst.*, **40**, T629 (1949).
4. M. Horio, K. Ogami, T. Kondo, and K. Sekimoto, *Bull. Inst. Chem. Res. Kyoto Univ.*, **41**, 10 (1963).
5. M. W. Andrews, *J. Roy. Microscop. Soc.*, **84**, 439 (1965).
6. M. W. Andrews, R. L. D'Arcy, and I. C. Watt, *J. Polym. Sci. B*, **3**, 441 (1965).
7. P. Ingram, J. L. Williams, V. Stannett, and M. W. Andrews, *J. Polym. Sci. A-1*, **6**, 1895 (1968).
8. S. J. Leach, *Austral. J. Chem.*, **13**, 547 (1960).
9. M. W. Andrews, A. S. Inglis, F. E. Rothery, and V. A. Williams, *Text. Res. J.*, **33**, 705 (1963).
10. P. Kassenbeck, in *Supramolecular Structure in Fibers* (*J. Polym. Sci.* C, **20**), P. H. Lindenmeyer, Ed., Interscience, New York, 1967, p. 49.
11. B. Filshie and G. E. Rogers, *J. Mol. Biol.*, **3**, 784 (1961).
12. S. J. Leach, G. E. Rogers, and B. K. Filshie, *Arch. Biochem. Biophys.*, **105**, 270 (1964).
13. J. M. Gillespie, *Austral. J. Biol. Sci.*, **15**, 572 (1962); *ibid.*, **16**, 241 (1963).
14. H. Lindley, J. M. Gillespie, and T. Haylett, *Symposium on Fibrous Proteins, Australia*, **1967**, Butterworths (Australia), Sydney, 1968, p. 353.
15. M. C. Corfield, A. Robson, and B. Skinner, *Biochem. J.*, **68**, 348 (1958).
16. E. G. Bendit, *Text. Res. J.*, **38**, 15 (1968).
17. K. Arai et al., unpublished work.
18. K. Arai, M. Negishi, and T. Suda, in preparation.
19. K. Arai, M. Negishi, T. Suda, and K. Doi, *J. Polym. Sci. A-1*, **9**, 1879 (1971).
20. R. D. B. Fraser and T. P. MacRae, *Biochem. Biophys. Acta*, **29**, 229 (1958).
21. G. E. Rogers, *Ann. N.Y. Acad. Sci.*, **83**, 378 (1959).
22. R. D. B. Fraser, T. P. MacRae, and G. E. Rogers, *Nature*, **193**, 1052 (1962).
23. H. P. Lundgren and W. H. Ward, in *Ultrastructure of Protein Fibers*, R. Borasky, Ed., Academic Press, New York, 1963, p. 71.
24. K. Arai, M. Negishi, and S. Komine, *J. Polym. Sci. A-1*, **8**, 917 (1970).
25. I. MacArthur, *Nature*, **152**, 38 (1943).

Received December 14, 1970
Revised February 26, 1971

JOURNAL OF POLYMER SCIENCE: PART A-1 VOL. 9, 1879–1891 (1971)

Grafting on Wool. II. Stress–Strain Behavior of Grafted Fiber in Water

KOZO ARAI, MICHIHARU NEGISHI, TSUTOMU SUDA, and KAZUKO DOI, *Faculty of Technology, Gunma University, Kiryu, Gunma, Japan*

Synopsis

The stress–strain behavior and hysteresis properties of various grafted wool fibers were studied. Three distinct regions on the stress–strain curve and hysteresis properties characteristic of the native wool fiber remain substantially intact, even though a large amount of a rigid polymer occurs. It was suggested that the microfibril and the matrix nature in the native wool fiber exist in the grafted wool structures. The electron microscopic results were also supported. These results can be explained on the basis of Menefee's model that the longitudinal mechanical behavior is more directly controlled by a high modulus matrix.

INTRODUCTION

Studies in this series have been concerned with the location of grafted polymer. On the basis of electron microscopy,[1] it was considered that the grafted polymers might be located not only around and between the microfibril and the matrix, but also at the interprotofibrillar and the interstitial region of the microfibril. The results of x-ray diffraction studies[2] suggested that most of the α-helical components in the grafted fibers remain intact, irrespective of a large diametral swelling by the polymer deposition. The purpose of this work is to study the relationship between the stress–strain behavior in water and the actual location of grafted polymer.

EXPERIMENTAL AND MATERIALS

The tops of fine Australian Merino wool fibers were grafted with ethyl acrylate (EA) and with methyl methacrylate (MMA) in an aqueous Br^-–$S_2O_8^{2-}$ redox reaction system[3] containing diethylene glycol monobutyl ether (BC) as a monomer-solubilizer. Homopolymers were not formed in the system. After the reaction period, the wool fibers were washed only with water and air-dried.

The contents of —SH and —SS— groups in the native and the grafted fibers were determined by Leach's polarographic method.[4]

The samples with different extents of grafting are listed in Table I.

TABLE I
Various Grafted Wool Samples Prepared under Different Reaction Conditions

Sample		Reaction system	Reaction temperature, °C	Reaction time, hr
Monomer	Graft-on, %			
—	Native	—	—	—
—	Control[a]	—	18	18
EA	16.5	A[b]	18	15
EA	36.2	A	18	18
MMA	15.3	A	18	15
MMA	32.0	A	18	18
MMA	54.0	B[c]	30	3/4
MMA	101.6	C[d]	30	3

[a] Wool (1 g) treated with A reaction system in the absence of monomer.
[b] 10 g NH_4Br, 0.3 g $K_2S_2O_8$, 35 g H_2O, 50 g BC, and 5 g monomer.
[c] 27.5 g LiBr, 0.2 g $K_2S_2O_8$, 44.8 g H_2O, 15.0 g BC, and 5 g MMA.
[d] 27.5 g LiBr, 0.2 g $K_2S_2O_8$, 44.8 g H_2O, 22.5 g, BC, and 5 g MMA.

The moisture content was measured at 65% RH and 20°C. Also, water imbibition in liquid water was measured by pressing out the excess water with filter paper until approximately a constant weight was obtained.

A model UTM-II Tensilon tester (Tōyō Measuring Instruments Co., Ltd.) was used for the determination of load–extension properties. Single fibers, 2 cm in length, were mounted on a paper frame and immersed in water at room temperature overnight. The fibers were placed in a jacketed cell filled with water which was maintained at 20°C and extended at rates of 20 and 50%/min. For the determination of the average values of the parameters obtained from load–extension curves, about 200 specimens were tested for each sample.

RESULTS AND DISCUSSION

General

A typical load–extension curve of uniform wool fiber in water exhibits three distinct, approximately linear regions; Hookean, yield, and post-yield, as shown in Figure 1. Points A and B are defined as the intersections of the extrapolations of these regions.[5]

In the Hookean region OA, the stress occurs linearly with a rapid rise in the fiber strain from 0 to about 2% extension, reflecting a deformation in crystal structure of microfibrils.[6]

Beyond 2% extension, the fiber begins to yield, and this continues to around 30% extension. This process of yielding requires only a very small amount of additional stress. This portion of the stress–strain curve is known as the yield region. In this region, it has been considered that the α-helices begin to unfold from the end of the Hookean region.[7] It has been reported by Collins and Chaikin[8] that the slope of the yield region is closely related to the variation of fiber cross-sectional area and to structural non-

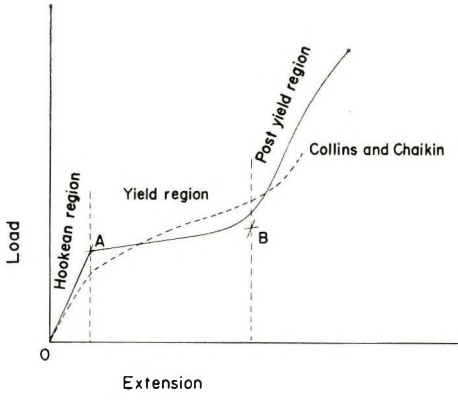

Fig. 1. Schematic representation of the load–extension curve of wool fiber in water. Points *A* and *B* are the intersections of the extrapolation of three distinct, approximately linear regions; Hookean, yield, and post-yield. A load–extension curve characteristic of a nonuniform fiber[8] is also shown (dotted line).

uniformity. A load–extension curve of a nonuniform fiber is shown by the dotted line in Figure 1. Generally, the characteristic feature of the stress–strain curve does not appear clearly, and the yield slope increases with an increase in nonuniformity of fiber cross-sectional area. In addition, breaking load and extension are reduced considerably.

At around 30% extension, the stress in the fiber begins to rise sharply with increase in extension. This region is the post-yield region. Though the behavior of the yield region and the post-yield region have been considered to be more or less viscoelastic, the effect of the rate of loading on the slope of the yield region and the slope of the post-yield region appears to be negligible over the range of 12.5 to 125%/min in water at 20°C.[9,10]

Crewther[11] has demonstrated the effect of thiol and disulfide contents on the stress–strain curve from the systematic study on the reduced and alkylated fibers. The stresses and the yield and post-yield slopes decrease, and the strains increase with decreasing disulfide content; the yield and post-yield slopes appear to be zero at extrapolation to zero disulfide content. When thiol contents are increased, there is a virtual disappearance of the post-yield region as a result of the thiol–disulfide interchange reaction.

Water Content

Considerable increase in diameter occurs with increase in the extent of grafting, but the change in longitudinal dimension was only 1–2% contraction during the reaction, as shown in Table II. This anisotropic swelling by the polymer indicates that the well-oriented units were not disrupted by the polymer deposition. The swelling ratios of diameter increases in wet to dry decrease as the extent of grafting increases. The change in fiber grafted 101.6% with MMA appears to be approximately zero. The values of the moisture regain and the water imbibition for the grafted fibers are markedly decreased as the polymer content is increased. The swelling of a

TABLE II
Variation in Diameter, Thiol and Disulfide Contents, Moisture Regain, and Water Imbibition of the Grafted Fibers

Sample	Average diameter, μ		Increase in swelling ratio (diameter) on going from wet to dry, %	Contraction %	—SH content, μmole/g wool	—SS— content, μmole/g wool	Moisture regain at RH 65%		Water imbibition	
	Dry (65% RH)	Wet (in water)					%	%/wool	%	%/wool
Native	22.0	25.9	18.0	0	39	425	6.52	6.52	52.1	52.1
Control	21.7	25.6	18.0	1.1	22	430	6.27	6.27	—	—
Grafted wool										
EA, 16.5%	22.8	26.5	16.0	—	25	418	4.34	5.06	51.7	60.0
EA, 36.2%	28.1	32.4	15.3	~0	26	394	3.93	5.35	32.3	44.0
MMA, 15.3%	21.5	25.8	19.7	—	28	429	5.35	6.17	45.4	52.4
MMA, 32.0%	25.6	29.0	13.2	~0	31	418	5.18	6.83	46.0	60.7
MMA, 54.0%	28.7	29.5	2.7	1.7	32	411	4.12	6.35	39.8	61.3
MMA, 101.6%	34.4	33.8	~0	2.3	32	428	3.00	6.00	25.8	51.8

wool fiber from dry to wet results from the uptake of the major part of water by the matrix.[12] On assuming the hydrophobic polymer is inert with respect to the equilibrium water content for grafted fibers, the values of the moisture regain and the water imbibition on the basis of the wool portion are shown in Table II. These values appear to be approximately similar to those of the native fibers, even at the higher levels of grafting. Furthermore, the disulfide contents of the grafted fibers are almost the same as those for the native wool fibers, as listed in Table II. As a consequence, with respect to the nature of the matrix for the absorption of water, it might be considered that the matricular chain segments within the grafted structure behave like those of the native wool, being affected very little by the deposited polymer.

Load–Extension Curve

For characterization of the stress–strain behaviors of grafted fibers, if the grafted polymer could be considered as an additional material which interacts with the microfibril and the matrix, it might be preferable to take up the variations on the load–extension curves rather than those on the stress–strain curves on the basis of the fiber cross-sectional area. The load–extension curves of the grafted fibers in water at an extension rate of 20%/min are shown in Figure 2. The load–extension curve for the control fiber is almost the same as that for the native fiber. From Table II, it is known that the change observed for —SH contents of the native and the control fiber has no significant effect on the load–extension curve. No remarkable difference in breaking elongation and in breaking strength between the native and the control fiber is found. These facts also suggest that oxidative chain scission scarcely occurs during the reaction. The load extension curves of all of the grafted fibers show the three regions to be distinctly different. Yield and post-yield slopes tend to increase with increase in the extent of grafting. The fibers grafted with MMA are harder in the Hookean

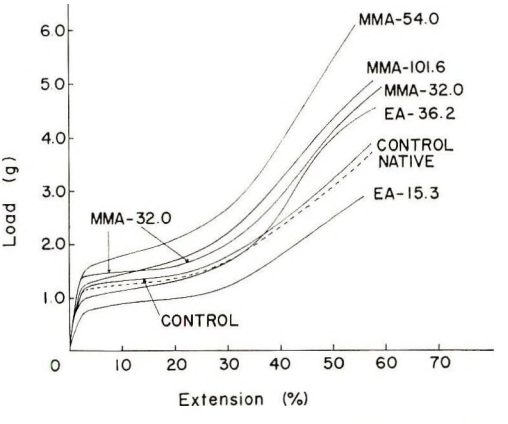

Fig. 2. Load–extension curves of the native, control, and grafted fibers.

TABLE III.
Effect of Rate of Extension on Yield and Post-Yield Slopes of the Load–Extension Curve for Various Grafted Fibers

Sample	Yield slope, g		Strain at point B, %		Post-yield slope, g	
	20%/min	50%/min	20%/min	50%/min	20%/min	50%/min
Control	1.1	1.0	31.6	29.5	7.4	8.2
Grafted wool						
EA, 36.2%	1.5	2.5	30.8	31.8	12.0	10.7
MMA, 32.0%	1.0	4.0	30.5	30.3	12.5	12.5
MMA, 54.0%	2.6	3.1	31.0	32.8	13.5	11.5
MMA, 101.6%	2.3	3.5	30.2	29.8	12.8	12.8

modulus than the control fibers, while the grafted fibers with EA are always softened in the stresses of points A and B.

The results of the electron microscopy[1] and of the x-ray diffraction study[2] indicate that the location of polymer is likely to be the region between and around the microfibril and the aggregated matrix.[13] Therefore, it might be considered that the interactions between the microfibril and the matrix molecules tend to be reduced as the polymer content increases, while the polymer–polymer, polymer–microfibril, and polymer–matrix interactions increase. A decrease in the Hookean modulus of the fiber grafted with EA might be due to the plasticizing effect of poly(ethyl acrylate), which has a low glass transition temperature (about $-22°C$).[14] On the contrary, in fibers grafted with MMA, stiffening in the modulus and an increase in the stress at point A occur. This seems to indicate an increase of internal viscosity resulting from a net excess of the rigid polymer–polymer, polymer–microfibril and polymer–matrix interactions over the reduction in microfibril–matrix interaction resulting from the polymer deposition. The effects of the rate of extension on the yield slope, the post-yield strain, and the post-yield slope are shown in Table III. No significant change in the yield slopes of the control fiber is observed at extension rates from 20 to 50%/min; however, the slopes of the grafted fibers are very rate-sensitive, as shown in Table III. The most marked dependence on the rate of extension is observed for 32.0% grafted (MMA) sample. Furthermore, no marked difference exists in strains at point B in any samples. These facts also suggest that the longitudinal mechanical properties of wool fibers remain substantially intact under the graft modification. Accordingly, an explanation for the changes in the Hookean modulus and in the yield-region slope may be possible in terms of internal viscosity. Therefore, it might be considered that the grafted polymers do not give rise to any variation of distribution of fiber cumulative cross-sectional area, as pointed out by Collins and Chaikin.[15] The grafted polymers may not tend to show additional structural nonuniformity along the fiber axis direction.

Considerable disagreement exists among workers about the structural and molecular interpretation of the post-yield region.[16–18] The post-yield

slopes of the control and the grafted fibers are not changed by the rates of extension. However, the grafted fibers in which over 30% polymer is present have larger values of the slope than the control. Moreover, the increase in the slope appears to be independent of the properties of the grafted polymer. This point is a salient feature of the stress–strain behavior of the grafted fibers. On the contrary, grafting produced no significant change in the post-yield slope of Lincoln wool fiber,[19] whose structure is more or less analogous to the paracortex structure in Merino wool. Although the behavior is too complex to be analyzed in detail at this stage, it seems likely to be related closely to the deformation of the matrix between sheets which are composed of a linear arrangement of microfibrils in the orthocortex region. When a cylindrical layerlike matrix is extended in the lateral direction by the deposition of polymer within a sheet,[1] stress occurs in the matrix segment; this stress might be stored in the cystine-crosslinked network. This stress might play an important role in the slope of the post-yield region.

Hysteresis Curve

When the control and the grafted fibers are stretched and then allowed to retract and subsequent extensions to breaking point are performed, the load–extension curve of the fiber may be suggestive of the occurrence of structural changes caused by the grafting, since this hysteresis curve reflects $\alpha \rightleftarrows \beta$ transformation characteristic of the deformation of α-helices. Figure 3 shows the hysteresis curves of the control and three sets of variously grafted fibers. It is known that, in the case of 15% extension, the second stretching curve after relaxation in water at 20°C for 24 hr is perfectly r - produced on the first stretching curve for all of the fibers except the 101.6% grafted (MMA) fiber. These results indicate that a perfect re-formation to the original structure from the extended state takes place in the hysteresis processes including relaxing. For the 101.6% MMA-grafted fiber, the Hookean modulus and the stress at the end of the Hookean region on the second stretching after relaxation in water at 20°C for 24 hr decrease considerably. However, such a stress-softening scarcely occurs after relaxation at 52°C for 1 hr.[12,20] Accordingly, it is further suggested that reversibility of the longitudinal mechanical properties of a wool fiber substantially exists even in the grafted fiber containing a large amount of polymer. Hysteresis properties of the control and the grafted fibers are summarized in Table IV. As compared with the control fiber in any extension, the 36.2% EA-grafted fiber has similar value in elastic recovery and same level in energy loss. On the other hand, the fibers grafted with MMA have relatively lower values of elastic recoveries, which decrease with increasing the extent of grafting and with increasing extension. The recoveries after relaxation in water appear to be much higher. Considering the strking change in texture by grafting, it is very surprising that the recovery of the 101.6% MMA-grafted sample reached about 90% of the length extended. Moreover, after releasing in water at 52°C for 1 hr, the initial modulus in the

second stretching appears to be approximately the same as the Hookean modulus.

From the x-ray[2] and the electron microscopic evidence,[1] it has been known that about 80% of the original α-components were retained for the 101.6% MMA-grafted sample, and the diameter of a microfibril, being composed of α-helices, expands isotropically to about 2.5 times that of the native.

The grafted fibers with over 32% MMA content have a larger energy loss which is approximately similar over the range of extensions. It is known that the variations of energy loss and reduced work depend largely on the properties of grafted polymer. The fiber grafted with soft polymer, such as the 36.2% EA-grafted sample, has smaller values in energy loss and relatively larger values in reduced work rather than the 32.0% MMA-grafted sample.

As far as the load–extension curve and the hysteresis properties are concerned, the $\alpha \rightleftarrows \beta$ transformation should occur in the grafted structure even

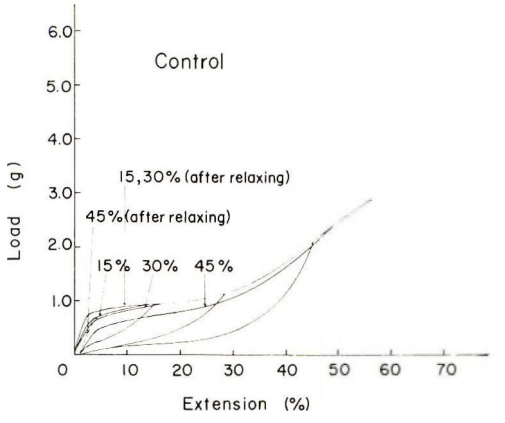

(a)

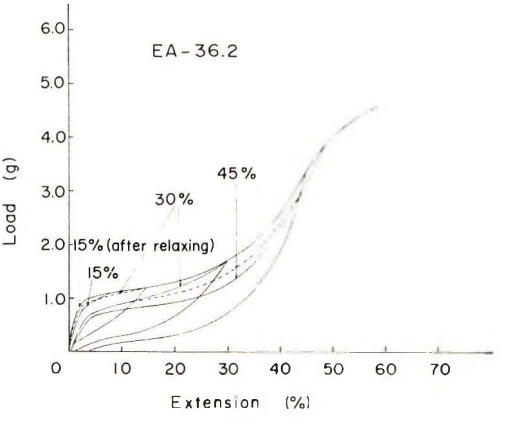

(b)

Fig. 3 (*continued*)

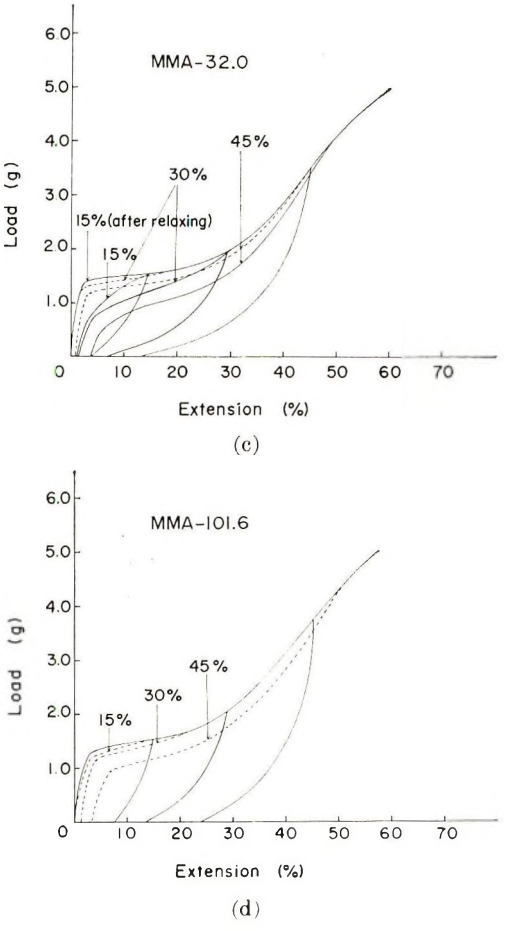

Fig. 3. Hysteresis curves at 15, 30, and 45% extension: (*a*) control; (*b*) EA graft, 36.2%; (*c*) MMA graft, 32.0%; (*d*) MMA graft, 101.6%. Second stretching curves after relaxing in water are shown by dotted lines. Relaxing conditions were 20°C, 24 hr for the control, EA-36.2, and MMA-32.0 samples; and 52°C, 1 hr for the MMA-101.6 sample.

below the glass transition temperature of polymer, provided the molecular interpretations in the Hookean and the yield region are taken as a deformation of bond angle in crystalline microfibril[6] and as an unfolding of α-helices,[7] respectively. However, from the considerations of the variation of peak intensity of the two prominent reflections (equatorial 9.8 Å and meridional 5.1 Å spacing) of the wide-angle x-ray diagram of the 32.0% MMA-grafted sample during extensions from 0 to 50%, it has been suggested that the α-components of microfibrils are markedly stabilized by the deposited polymers.[2] The x-ray photographs of the native and the 32.0% MMA samples at 50% extension are shown in Figure 4. From the quantitative analyses of the diffracted intensities from 9.8 Å spacing, it was found that no significant change occurs over the range of extension of the grafted fibers.[2] In

TABLE IV
Various Parameters Obtained from the Hysteresis Properties

Sample	Extension, %	Hookean modulus, g	Elastic recovery, %[a]	Energy loss %[b]	After relaxing in water at 20°C for 24 hr: Initial modulus, g	Recovery, %	Reduced work %[c]	After relaxing in water at 52°C for 1 hr: Initial modulus, g	Reduced work, %[c]
Control	15		98	49	48.0	100	0	48.0	0
	30	48.0	98	55	48.0	100	0	48.0	0
	45		96	58	44.2	98	3	47.5	2
Graft, EA, 36.2%	15		99	44	47.4	99	4	—	—
	30	47.4	99	52	47.4	99	5	—	—
	45		98	54	44.8	98	15	—	—
Graft, MMA, 32.0%	15		94	68	75.6	100	0	75.6	0
	30	75.6	94	68	75.6	99	3	75.6	2
	45		92	68	75.6	98	9	75.6	5
Graft, MMA, 54.0%	15		88	65	63.4	97	4	63.4	0
	30	63.4	84	67	57.2	95	5	63.4	2
	45		78	67	56.2	89	10	63.4	10
Graft, MMA, 101.6%	15		83	68	60.5	92	17	66.2	8
	30	68.8	69	74	50.6	90	20	66.5	8
	45		67	70	42.2	83	28	50.1	18

[a] After relaxing in water at 20°C for 1 min.
[b] Energy lost in first cycle.
[c] Ratio of the reduction in work to extend a fiber a second time to the work required the first time.

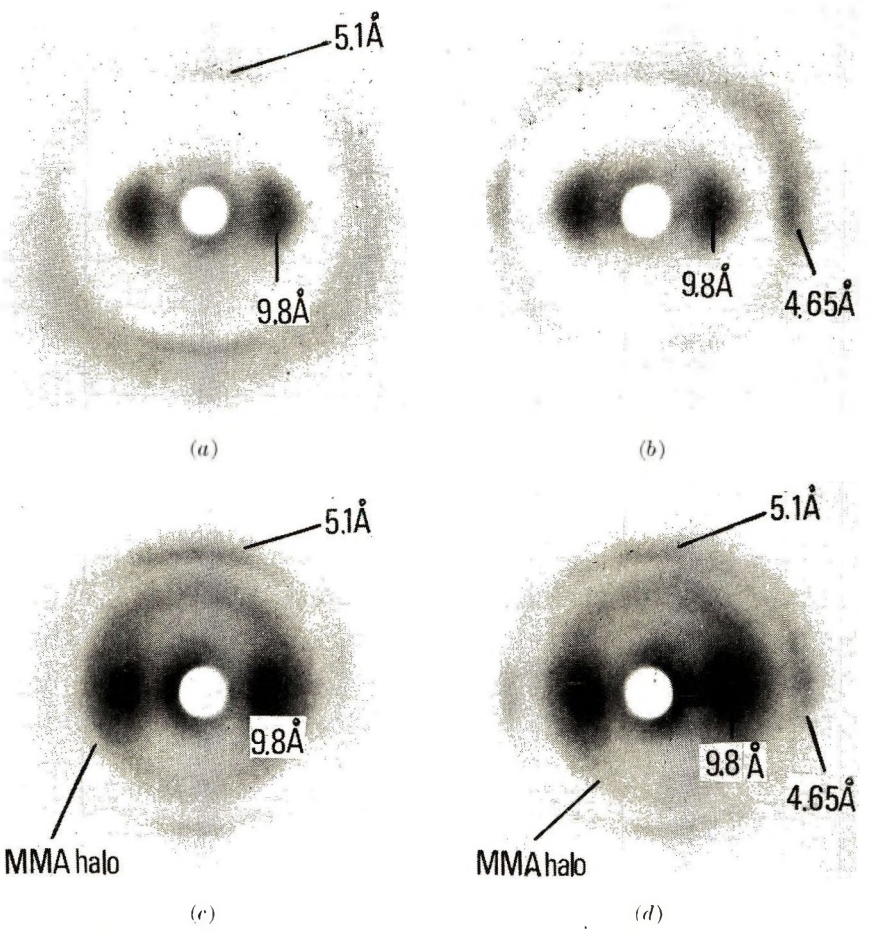

Fig. 4. X-ray photographs of the native and the 32.0% MMA-grafted sample at 50% extension: (*a*) native wool, unstretched; (*b*) native wool, stretched; (*c*) MMA graft, 32.0%, unstretched; (*d*) MMA graft, 32.0%, stretched.

addition to the variation of the 9.8 Å intensity, the disappearance of the 5.1 Å reflection is supposed to give the simplest measure of the decrystallization of the α-keratin. As is clearly seen in Figure 4, the 5.1 Å reflection disappears at 50% extension of the native fiber. However, the reflection arc is substantially retained for the grafted fiber.

The electron microscopic result appears to support this x-ray evidence. The fact that the polymers are located around and between the protofibrillar subunits in microfibrils[1] suggests that an enormous increase in the interaction between the rigid amorphous polymer and the side-chain groups of the α-helix results in a major hindrance to the opening out of an α-helix.

As a consequence, the deformation of a microfibril may not be much concerned with the Hookean and the yield regions of the load–extension curve for either the grafted fiber or for the unmodified wool fiber.

Naturally, some chain scission of the MMA-grafted polymer might occur at localized sites of stress during extension. However, it is considered that modulus for deposited polymer appears to be negligible, since such chain scission is not likely to have a prominent effect on the hysteresis properties at the second extension after relaxing. This fact indicates that little polymer–polymer interaction occurs, while there is an increase in the polymer–matrix and polymer–microfibril interactions which are probably much involved in the stiffening in the modulus of the grafted fiber. With respect to this point, stress relaxation occurring in the native and the grafted fiber stretched to various extensions (15–45%) in 0.1*N* sodium bisulfite solution was studied.[19] The rate of stress relaxation slower in the grafted fiber than in the native fiber. However, the final stresses remaining in the grafted fibers were approximately similar to those (0.2 g) in the native wool fiber. Accordingly, it was supposed that no significant stress is borne by the polymer–polymer interaction. This will be discussed in detail in a future report.

From the results of moduli calculated for the α-helix and extended β-chains, Enomoto and Krimm[21] concluded that the modulus for α-helix is so low that some other high-modulus component must be present in wool. Menefee[22] proposed an extended-matrix model which the matrix acts as the high-modulus component in wool structure. Our results obtained from the stress–strain behavior of grafted fibers support Menefee's view that the mechanical behavior is more directly controlled by a high-modulus matrix.

On the basis of the deviation from the additive property in the two components of the grafted fiber, the measurements of the density and the diffracted x-ray intensity of the grafted fiber prepared by various grafting systems may give information about the polymer–wool interaction.

Finally, quantitative analyses of the appearance of β-keratin in the grafted fiber associated with the 4.65 Å equatorial reflection may give important suggestions regarding the origin of the β-structure.[2]

This research was supported financially in part by the International Wool Secretariat. The authors would like to acknowledge the encouragement of Dr. F. Bekku, Technical Division Manager of IWS Japan.

References

1. K. Arai and M. Negishi, *J. Polym. Sci. A-1*, **9**, 1865–1877 (1971).
2. K. Arai, M. Negishi, and T. Suda, in preparation.
3. M. Negishi, K. Arai, S. Okada, and I. Nagakura, *J. Appl. Polym. Sci.*, **9**, 3465 (1965).
4. S. J. Leach, *Austral. J. Chem.*, **13**, 547 (1960).
5. J. B. Speakman, *J. Text. Inst.*, **18**, T431 (1927).
6. W. T. Astbury and J. W. Haggith, *Biochim. Biophys. Acta*, **10**, 483 (1953).
7. E. G. Bendit, *Text. Res. J.*, **30**, 547 (1960).
8. J. D. Collins and M. Chaikin, *Text. Res. J.*, **35**, 777 (1965).
9. M. Feughelman, *Text. Res. J.*, **29**, 223 (1959).
10. B. J. Rigby, *Austral. J. Phys.*, **8**, 176 (1955).
11. W. G. Crewther, *Text. Res. J.*, **35**, 867 (1965).

12. M. Feughelman, *J. Text. Inst.*, **45,** T630 (1954).
13. G. E. Rogers, *Ann. N.Y. Acad. Sci.*, **83,** 378 (1959).
14. L. A. Wood, *J. Polym. Sci.*, **28,** 319 (1958).
15. J. D. Collins and M. Chaikin, *J. Text. Inst.* **59,** 379 (1968).
16. M. Feughelman, A. R. Haly, and P. Mason, *Nature*, **196,** 957 (1962).
17. L. Mandelkern, J. C. Halpin, A. F. Diorio, and A. S. Posner, *J. Amer. Chem. Soc.*, **84,** 1383 (1962).
18. M. Feughelman, *Text. Res. J.*, **34,** 539 (1964).
19. K. Arai et al., unpublished work.
20. J. B. Speakman, *J. Text. Inst.*, **18,** T431 (1927).
21. S. Enomoto and S. Krimm, *Biophys. J.*, **2,** 317 (1962).
22. E. Menefee, *Text. Res. J.*, **38,** 1149 (1968).

Received December 14, 1970
Revised February 26, 1971

JOURNAL OF POLYMER SCIENCE: PART A-1 VOL. 9, 1893–1899 (1971)

Thermal Bulk Polymerization of Cholesteryl Acrylate

A. C. DE VISSER, K. DE GROOT, J. FEYEN, and A. BANTJES,
Polymer Division, Department of Chemical Technology,
Twente University of Technology, Enschede, the Netherlands

Synopsis

The thermal bulk polymerization of cholesteryl acrylate was carried out in the solid phase, the mesomorphic phase, and the liquid phase to study the effect of monomer ordering on polymerization rate and polymer properties. The rate increased with decreasing ordering (or enhanced mobility) of the monomer. Formation of inhibitive by-products during the polymerization limited conversions to 35%. The sedimentation constant $S_0 = 6.2$ S was the same for the polymers obtained in the three phases. The weight-average molecular weight ($\bar{M}_w$) was 480,000 as determined by ultracentrifugation. Poly(cholesteryl acrylate) formed in bulk is randomly coiled when dissolved in tetrahydrofuran. The thermal properties of the monomer are given.

INTRODUCTION

Liquid crystallinity, a phenomenon discovered in the last century,[1] has begun to attract the attention of polymer chemists only recently. It has been demonstrated that ordering of monomer molecules induced by liquid crystallinity can have an effect on polymerization rate and properties of the prepared polymer.

To study these effects, polymerization can be carried out either in an ordered solution, or in bulk if the monomer exhibits liquid crystallinity by itself. The polymerization in liquid crystalline solution has been described by several authors. Amerik and co-workers[2,3] have studied the polymerization of *p*-methacryloyloxybenzoic acid and the copolymerization of this monomer with styrene, using *p*-cetyloxybenzoic acid as a liquid crystalline solvent. They found that the ordering increased the polymerization rates. Blumstein et al.,[4] working on similar systems, reported an increase in the isotacticity of the polymer obtained. Bulk polymerization of liquid crystalline monomers has been reported also. Paleos and Labes[5] investigated the polymerization of nematic *N*-(*p*-methoxy-*o*-hydroxybenzylidene)-*p*-aminostyrene, but did not find significant effects of the ordered structure on polymerization rate or nature of the product. Amerik and Krentsel[6] found that the rate of polymerization of vinyl oleate was somewhat higher in the liquid crystalline state than in the liquid and solid states. Hardy and co-workers[7] polymerized cholesteryl acrylate in bulk, but it is likely from these results that polymerization took place in the solid phase rather than in the liquid crystalline phase. Toth and

Tobolsky[8] described the bulk polymerization of cholesteryl acrylate and cholestanyl acrylate in the isotropic liquid phase. They found crosslinked, insoluble poly(cholesteryl acrylate) and soluble poly(cholestanyl acrylate) with a molecular weight up to 10^4.

In a previous communication[9] we reported the bulk polymerization of cholesteryl acrylate in the solid, liquid crystalline, and liquid states to molecular weights in the order of 10^5. We wish now to report in more detail the rate of the thermal bulk polymerization of cholesteryl acrylate in its various phases and some properties of the polymers obtained.

EXPERIMENTAL

Materials

Cholesterol (U.S.P., Van Schuppen Chemie N.V.) and acryloyl chloride (Fluka 01780, containing 0.1% hydroquinone) were used without purification. All solvents used were pro analysi grade and dried by standard methods if necessary.

Monomer Preparation and Characterization

Cholesteryl acrylate was prepared in 70% yield by refluxing cholesterol and an excess amount of acryloyl chloride in benzene.

After isolation, the ester was purified by repeated crystallization from ether/ethanol. Elemental analysis yielded the following results.

ANAL. Calcd for $C_{30}H_{48}O_2$ (440.7): C, 81.76%; H, 10.98%; O, 7.26%. Found: C, 81.8%; H, 11.0%; O, 7.3%.

Infrared and mass spectra were consistent with the expected structure. Ebulliometry gave a number-average molecular weight of 440. Phase transitions were determined from thermograms, obtained with a Du Pont differential thermal analyzer, by observation through a hot-stage microscope with crossed nicols and by x-ray diffraction.

Polymerization

The bulk polymerization was studied with small samples (about 50 mg) to avoid temperature increase during the reaction. These portions were still large enough to be investigated by means of ultracentrifugation. The tubes in which the polymerization was carried out were cleaned by treating with concentrated nitric acid. After rinsing several times with demineralized water and with acetone, they were dried. Immediately before use, the tubes were flame-dried while being evacuated. Then about 50 mg monomer was weighed in under nitrogen in a drybox. Each tube was flushed five times with ultrapure nitrogen, evacuated to 2×10^{-2} mm Hg pressure and sealed.

Polymerization was started by immersing the tube in a thermostatted oil bath and was stopped by cooling the tube in liquid nitrogen. The reaction mixture was then dissolved immediately in tetrahydrofuran.

The contact thermometer of the thermostat bath (variability ± 0.01°C) was calibrated to the thermometer of the hot-stage microscope to be sure that polymerization would take place in the phase chosen.

Investigation of the Reaction Mixture

The reaction mixtures were investigated by means of ultracentrifugation with a Beckman-Spinco Model E Analytical Ultracentrifuge equipped with Schlieren optics.

Sedimentation velocity runs of the dissolved samples were performed in Kel-F 12 mm centerpieces at 48,000 rpm. From the areas under the sedimentation peaks the amount of polymer in the reaction mixtures was calculated, the specific refractive index being determined in a Brice-Phoenix differential refractometer.

The results thus found, agreed within experimental error with the results obtained by fractionation. Diffusion experiments were carried out by using double-sector, capillary-type 12 mm Epon-filled centerpieces to measure the amount of crosslinked material. Weight-average molecular weights $\bar{M}_w$ of the polymers obtained by fractionation were determined by sedimentation-diffusion equilibrium, the density being determined pycnometrically.

RESULTS AND DISCUSSION

Thermotropic Properties of Cholesteryl Acrylate

The phase transitions of cholesteryl acrylate as determined by observations through a hot-stage microscope with crossed nicols (M), differential thermal analysis (DTA), and x-ray diffraction (X) are presented in Table I, together with the results of other investigators. The transition at 65°C (D) is a reversible solid–phase transition; on heating the sample to 75°C an endotherm is observed. When the sample is cooled an exothermic peak occurs at the same temperature. The x-ray diffractograms at 14°C, 75°C, and again at 14°C confirmed the findings by DTA. A similar transition has been reported by Barrall et al.[10] for cholesteryl valerate. The transition from the solid into the enantiotropic cholesteric

TABLE I
Thermal Properties of Cholesteryl Acrylate[a]

Source	Temperature of transition, °C, to				
	Solid	Smectic	Cholesteric	Nematic	Isotropic
This	65 (D)		121 (D)		126 (D)
investigation	64 (X)		122.5 (M)		125 (M)
Hardy et al.[7]		<118.7		118.7	125.8
Toth et al.[8]					127

[a] (D): determined by DTA in N_2 atmosphere at 1°C/min heating rate; (M): determined by microscopy; (X): determined by x-ray diffraction in N_2 atmosphere.

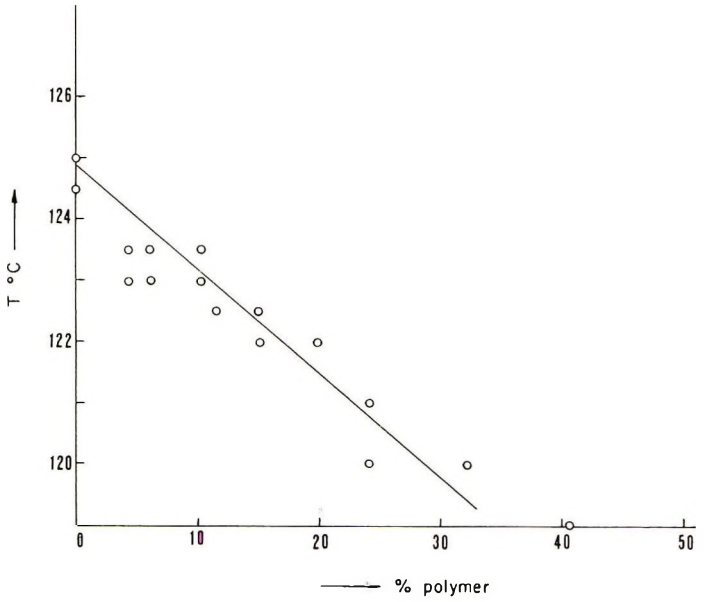

Fig. 1. Effect of the percentage polymer on the mesomorphic–isotropic transition temperature of a monomer–polymer mixture.

mesophase takes place at 122.5°C (M) and the mesomorphic–isotropic transition at 125°C (M). On cooling, the latter transition is precisely reversible, but the former is variable. Toth and Tobolsky[8] observed only on cooling a cholesteric mesophase at 90°C. Hardy and co-workers[9] did not observe any phase transition between −7[8] and 119°C and concluded that cholesteryl acrylate is in the smectic state in this temperature interval. In both publications about the same temperature was reported for transition into the isotropic liquid, more or less in agreement with our observations. The temperature of the mesomorphic–isotropic transition was measured as a function of the composition of various monomer-polymer mixtures to investigate the effect of polymer formation on this transition. The results are given in Figure 1.

Polymerization Kinetics

A kinetic study of the thermal polymerization was conducted in the solid phase at 120°C, the mesomorphic phase at 123°C and the isotropic phase at 126°C. In Figure 2 the amount of polymer formed in the reaction mixture is plotted versus time.

The polymerization in the solid phase takes place at a much slower rate than in the two other phases. The rate in the mesophase becomes equal to the one in the isotropic phase after about 10% polymer has been formed. Figure 1 shows that in a monomer–polymer mixture containing ca. 10% polymer, the transition from the liquid crystalline to the isotropic state

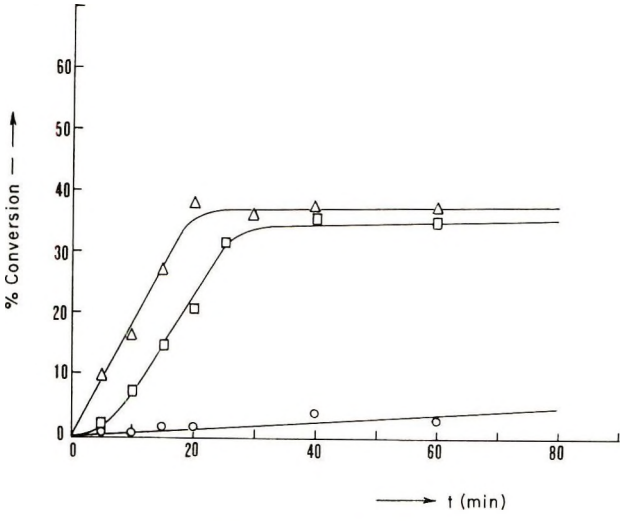

Fig. 2. Conversion–time plots for the bulk polymerization of cholesteryl acrylate: (○) in the solid phase at 120°C; (□) in the mesomorphic phase at 123°C; (△) in the liquid phase at 126°C.

occurs at 123°C. Thus only during the first 10 min the reaction really proceeds in the mesophase at a temperature of 123°C. The polymerization rate increases on going from the solid via the liquid-crystalline to the liquid phase. This result shows that only the mobility, not the ordering of the monomer molecules, enhances the rate. The temperature difference between the polymerizations in the liquid and mesophase does not affect the rate, as follows from the identical slopes of the curves between 10 and 20 min. After about 20 min the reaction stops. At this point, ca. 35% polymer has been formed. Reaction times up to 70 hr did not increase the amount of polymer. Diffusion runs with the ultracentrifuge showed that no appreciable amount of crosslinked material was present and that the reaction mixture beside the polymer only contained low molecular weight, not sedimenting material. This followed also from the number-average molecular weight value of 520, measured by ebulliometry, for the material that remained in solution after the polymer had been removed from the reaction mixture by precipitation. Thin-layer chromatography showed that this material consisted mainly of monomer. Also the transition temperatures of the material were only one or two degrees lower than those of the pure monomer. However, this material did not polymerize thermally anymore in the liquid phase. This suggested that impurities formed in a side reaction inhibited the polymerization. Consequently, when the polymerization rate would be much higher than the rate of the side reaction, one would expect a considerably higher yield. This we confirmed by conducting a polymerization initiated by azobisisobutyronitrile (AIBN): the polymer yield increased to 93%. (AIBN has a half-life time of about 30 sec at 126°C.)

As expected, the yield of the thermal polymerization in the mesomorphic phase was lower than in the isotropic phase because of the lower initial rate of polymerization, favoring the side reaction.

Our conclusions are that the rate of thermal polymerization of cholesteryl acrylate in bulk increases with decreasing order of the monomer system and that the rather low conversions are a result of formation of inhibitive by-products during the polymerization.

Solution Properties of the Polymer

The weight-average molecular weight $\bar{M}_w$ of polymer from the kinetic experiments at 126°C was found to be 480,000 by sedimentation–diffusion equilibrium and did not change with the percentage conversion. The intrinsic sedimentation constant $[S]$, defined as

$$[S] = S_0 \cdot \eta/(1 - \bar{v}d)$$

[where S_0 is the sedimentation constant at zero concentration ($S_0 = 6.2$ S); η and d are, respectively, the viscosity and density of the solvent ($\eta^{20} = 0.487 \times 10^{-2}$ poise), and $\bar{v}$ is the partial specific volume of the polymer ($\bar{v} = 0.95$ cc/g)] was calculated to be 0.195 (S × poise) in tetrahydrofuran. The intrinsic viscosity of the polymer in this solvent is $[\eta] = 0.46$ dl/g. Mandelkern and Flory[11] have derived the following relation for random coils in solution:

$$[S][\eta]^{1/3}/M^{2/3} = \Phi^{1/3}p^{-1}/N_A$$

[where $\Phi^{1/3}p^{-1}$ is a constant, equal to 2.5×10^6 for homogeneous, randomly coiled polymer, and N_A is Avogadro's number. This value may be 30–40% lower, depending on the degree of inhomogeneity, according to Gouinlock et al.[12] and Hunt et al.[13] The values found for $[S]$, $[\eta]$ and $\bar{M}_w$ result in $\Phi^{1/3}p^{-1} = 1.5 \times 10^6$, which value agrees satisfactorily with the value calculated for a heterogeneous polymer.

The sedimentation rate for the polymers obtained in the solid and mesomorphic phase was the same as the S value of the polymer from the liquid phase. Therefore we conclude all three polymers to have the same average molecular weight and to be randomly coiled in tetrahydrofuran.

References

1. F. Reinitzer, *Monatsh*, **9**, 421 (1888).

2. Yu. B. Amerik, I. I. Konstantinov, and B. A. Krentsel, in *Macromolecular Chemistry Tokyo-Kyoto 1966* (*J. Polym. Sci. C*, **23**), I. Sakurada and S. Okamura, Eds., Interscience, New York, 1968, p. 231.

3. A. A. Baturin, Yu. B. Amerik, and B. A. Krentsel, paper presented at Third International Liquid Crystal Conference, Berlin, August 24–28, 1970.

4. A. Blumstein, N. Kitagawa, and R. Blumstein, paper presented at Third International Liquid Crystal Conference, Berlin, August 24–28, 1970.

5. C. M. Paleos and M. M. Labes, paper presented at Third International Liquid Crystal Conference, Berlin, August 24–28, 1970.

6. Yu. B. Amerik and B. A. Krentsel, in *Macromolecular Chemistry, Prague 1965* (*J. Polym. Sci. C*, **16**), O. Wichterle and B. Sedláček, Eds., Interscience, New York, 1967, p. 1383.

7. Gy. Hardy, F. Cser, A. Kallo, K. Nyitrai, G. Bodor, and M. Lengyel, *Acta Chim. Acad. Sci. Hung.*, **65**, 287, 301 (1970).

8. W. J. Toth and A. V. Tobolsky, *J. Polym. Sci. B*, **8**, 289 (1970).

9. A. C. de Visser, J. Feyen, K. de Groot, and A. Bantjes, *J. Polym. Sci. B*, **8**, 805 (1970).

10. E. M. Barrall II, J. F. Johnson, and R. S. Porter in *Thermal Analysis* Vol. I, R. F. Schwenker and P. D. Carn, Eds., Academic Press, New York–London, 1969, pp. 556–570.

11. L. Mandelkern and P. J. Flory, *J. Chem. Phys.*, **20**, 212 (1952).

12. E. V. Gouinlock, P. J. Flory, and H. A. Scheraga, *J. Polym. Sci.*, **16**, 383 (1955).

13. M. L. Hunt, S. Newman, H. A. Scheraga, and P. J. Flory, *J. Phys. Chem.*, **60**, 1278 (1956).

Received February 17, 1971.

JOURNAL OF POLYMER SCIENCE: PART A-1 VOL. 9, 1901–1919 (1971)

Radiation-Initiated Homogeneous Grafting of Styrene to Benzylcellulose*

R. W. BETTY† and W. H. RAPSON, *Department of Chemical Engineering and Applied Chemistry, University of Toronto, Toronto, Ontario, Canada*

Synopsis

Graft copolymers of benzylcellulose and styrene were prepared by direct irradiation of benzylcellulose–styrene solutions with ^{60}Co γ-radiation. The solutions remained homogeneous during irradiation. The amount of styrene grafted to benzylcellulose increased in dilute solutions and was dose-dependent up to 4.0 MR. The graft copolymer consisted of both branched and linear structures with one in every 140–1020 benzylated anhydroglucose units carrying a grafted polystyrene chain. Grafted polystyrene was isolated from the graft copolymer by hydrolysis of the benzylcellulose substrate. The number-average molecular weight and molecular weight distribution of the grafted polystyrene were the same as those for homopolymer formed in the same solution, indicating that the substrate is fully accessible to the monomer and polymerization conditions are uniform throughout the solution during the grafting procedure. The existence of a true graft copolymer was proved by the solubility behavior, intrinsic viscosity, number-average molecular weight, and density-gradient sedimentation of the product of the grafting procedure. Column elution fractionation of the gross products of the grafting procedure failed to isolate the benzylcellulose–styrene copolymer which was eluted with ungrafted benzylcellulose.

INTRODUCTION

During the last decade, considerable effort has been directed towards the preparation of graft copolymers from cellulose or cellulose derivatives and vinyl monomers by high-energy irradiation.[1] Generally, cellulose copolymers have been prepared in liquid–solid or vapor–solid systems by contacting a solid cellulose derivative with a suitable liquid or vapor monomer and irradiating the mixture to initiate graft polymerization. Characterization of the graft copolymers prepared by these heterogeneous methods has shown[2,3] that the molecular weight of the grafted vinyl polymer chains is generally very much larger than that of the substrate, so that while substantial amounts of monomer are grafted, only very few of the substrate molecules actually support a grafted chain. The structural nonrandomness of the graft copolymers is considered to be a result

* Presented at the Fifteenth Canadian High Polymer Forum, Kingston, Ontario, Canada, September 1969.

† Present address: Du Pont of Canada Limited, Central Research Laboratory, Kingston, Ontario, Canada.

of the heterogeneity of the grafting system during polymerization. In order to improve the structural randomness of the graft copolymer, it is necessary to increase the number of substrate molecules supporting grafted chains while reducing the molecular weight of the grafted chains to a range corresponding to that of the substrate. These structural alterations can be achieved by allowing the monomer more uniform access to the substrate during graft polymerization, as would be the case if grafting occurred in a single phase or a homogeneous system.

Several attempts have been made to increase the homogeneity of the grafting system by grafting in solution. Stannett[4] grafted styrene to cellulose acetate in a variety of solvents and Sebban-Danon[5] grafted styrene to polyisobutylene in styrene solutions. Both of these workers, however, found that the solutions become hazy during irradiation. As was first pointed out by Dobry,[6] two different polymers are generally incompatible and when dissolved in the same solution will form two liquid phases, each phase containing practically all of one of the polymers. Stannett and Sebban-Danon attributed the hazy appearance of the solutions to microphase separation of polystyrene, due to its incompatibility with the substrate. Therefore, in both these systems, the solutions separated into two phases upon formation of the second polymer and the grafting conditions were not homogeneous throughout the solutions.

Benzylcellulose and polystyrene are one of very few exceptions to the general rule of incompatibility and will remain in a single phase solution up to total solids concentration exceeding 20%.[6] Therefore, with a benzylcellulose–styrene system, it is possible to carry out a radiation-initiated grafting reaction in a single phase or a homogeneous system. The unhindered and uniform accessibility of styrene to benzylcellulose should lead to the formation of a more random graft copolymer than has yet been prepared by radiation techniques. This investigation was initiated to prepare and characterize a benzylcellulose–styrene graft copolymer in a homogeneous system by irradiation with γ-radiation and to prove that such a copolymer had in fact been formed.

EXPERIMENTAL

Materials

Benzylcellulose was prepared from cotton linters alkali cellulose and benzyl chloride by a two-stage benzylation.[7]

To reduce the chemical and molecular weight heterogeneity, benzylcellulose prepared as above, was extracted with boiling acetone for 72 hr to remove the most soluble fraction. The remaining benzylcellulose was dissolved in 60/40 benzene–cyclohexane. Any undissolved material was rejected as the least soluble fraction of benzylcellulose by centrifugation at approximately 2500 rpm until the solution was clear. The central fraction, recovered by freeze-drying from benzene, was totally soluble in styrene and was used throughout this work.

Inhibitor was removed from Eastman Organic Chemicals highest purity styrene monomer by several successive washings with 10% sodium hydroxide solution. The monomer was then washed several times with distilled water, dried over anhydrous calcium chloride, and fractionally distilled under vacuum immediately prior to use.

Irradiation

All irradiations were carried out in a Gammacell 220 located in the Department of Chemical Engineering and Applied Chemistry of the University of Toronto. Design details of this facility are given elsewhere.[8] This irradiation unit was installed in 1961 with a source of 17,600 Ci of ^{60}Co and a dose rate of $1.44 \times 10^6 \pm 3\%$ rad/hr at the center of the irradiation chamber. The absorbed dose and dose rate were determined by ferrous sulfate dosimetry.[9] The dose rate normally varied between 0.504 and 0.616 Mrads/hr depending on the irradiation geometry and was reduced to 0.058 Mrads/hr by shielding the sample with lead. The irradiation chamber was continuously purged with air to maintain approximately 26°C during irradiations.

Sample Preparation and Recovery

Solutions of styrene and benzylcellulose were prepared gravimetrically. A known volume of solution was sealed under vacuum in an irradiation vial and irradiated in the Gammacell 220 to a specific dose. Following irradiation, a weighed portion of the solution (8–10 g) was selectively precipitated by addition of cyclohexane. The precipitate was filtered on a medium sintered glass filter with the aid of a water aspirator. The filtrate was retained for homopolymer determination by precipitation in excess methanol. The solids were dried under vacuum at 45°C for 48 hr.

Compositional Analysis by Infrared Spectroscopy

Solid samples were intimately ground with dried spectroscopic grade potassium bromide (Mallinckrodt, Infrared grade) to which was added potassium thiocyanate as an internal standard[10] and this mixture pressed to form a disk.

The infrared spectrum of the disk was obtained by using a double-beam Beckman IR 9 spectrophotometer with a pure potassium bromide disk in the reference beam.

The disks were prepared by using Friedlander's method[11] with several modifications. A 0.8–1.0 mg portion of dried sample was weighed accurately (±0.002 mg) into 350 mg of potassium bromide containing the internal standard and dried for 24 hr under vacuum over phosphorus pentoxide. The mixture was ground in a Wig-L-Bug (Crescent Dental Manufacturing Co., Chicago) for 2 min, then for three additional 1-min periods at 1-min intervals and then dried. An accurately weighed 300 mg portion was again dried. Finally, the 300 mg portion was pressed to

form a disk in a Beckman pellet die according to Friedlander's procedure. The pellet was carefully removed and stored under vacuum over phosphorus pentoxide until its spectrum was determined.

Hydrolysis of Benzylcellulose

Benzylcellulose was hydrolyzed to soluble products with trifluoroacetic acid in boiling benzene solutions. A 1% benzylcellulose solution in 2/1 (v/v), benzene–trifluoroacetic acid was refluxed for 24 hr, and polystyrene present during hydrolysis was recovered by precipitation in excess methanol.

Fractionation

Samples were fractionated by column elution fractionation, with the use of a column 128 cm long with an internal diameter of 4.5 cm maintained at 25°C by a water jacket. The column was packed with 100-μ glass beads (Cataphote Corp., Jackson, Mississippi) or Fluoropak 80 (Fluorocarbon Co., Anaheim, California). A 0.1–0.8 g of the polymer sample was deposited on approximately 150 ml of column packing by slow evaporation of benzene solvent. The polymer coated packing was added to the column after pouring in approximately 1800 ml of uncoated support. The column was eluted successively with two linear solvent gradients commencing with 3:1 cyclohexane–hexane through 100% cyclohexane to 3/1 benzene–cyclohexane with a total volume of 2 liters. The flow rate was manually adjusted to 80 ml/hr and fractions 40 ml in volume were collected. The polymer content of each volume fraction was determined by evaporation of the bulk of the solvent and freeze-drying the concentrate. The dried samples were combined to uniform weight fractions of approximately 50 mg following purification by precipitation from dioxane with excess methanol.

Molecular Weight Determination

The number-average molecular weight was determined by using a Mechrolab high-speed membrane osmometer, Model 501, at 37°C with the use of SSO8 membranes (Arro Laboratories, Illinois) and toluene as solvent. The osmotic pressure for each sample was determined at four concentrations (less than 1%) and extrapolated to infinite dilution. Operating procedures were as outlined in the manufacturer's operating and service manual.

Intrinsic Viscosity Determination

Reduced viscosities were determined in toluene at 25°C ± 0.05°C with an Ubbelohde dilution viscometer, size 25, at four concentrations of less than 1%. The intrinsic viscosity was calculated by extrapolation to infinite dilution.

Gel-Permeation Chromatography

The molecular weight distributions of polystyrene samples were obtained with a Waters gel-permeation chromatograph equipped with three columns of maximum rated porosity of 10^5, 10^4, and 800 Å. Deaerated tetrahydrofuran at a flow rate of 3 ml/min was the carrier solvent. A 1-ml portion of 0.05% solution was injected into the carrier solvent and the presence of polymer in the eluent was detected by a differential refractometer.

Ultracentrifugation

A Spinco analytical ultracentrifuge Model E, equipped with Schlieren optics was used at a speed of 52,000 rpm. A bromoform solution, 300 g/l in dimethylformamide was used as the density gradient solvent, and these conditions satisfactorily located the polymers in the cell. The 0.5% (w/v) polymer solutions in the solvent were centrifuged at 25°C. Approximately 36 hr was required for equilibrium to be established. A double-sector aluminum cell facilitated the superposition of the solvent base line on the sample Schlieren photograph. The photographs were taken at a phase angle of 70°.

RESULTS AND DISCUSSION

Degradation of Benzylcellulose

The carbon and hydrogen content, intrinsic viscosity, and number-average molecular weight were determined for benzylcellulose samples irradiated *in vacuo*, and results are shown in Table I. The unusually low values of carbon and hydrogen content for one blank sample and for the sample irradiated to 1.0 Mrads are not consistent with the other samples and are considered a result of experimental error. The number-average molecular weights and the intrinsic viscosities for benzylcellulose samples irradiated up to 5.0 Mrads are generally constant within experimental error

TABLE I
Degradation of Benzylcellulose by Radiation

Total radiation dose MR	C, %	H, %	DS[a]	$\bar{M}_n$	$[\eta]$, dl/g
0.0	73.07	6.42	2.54	41,000	0.675
0.0	68.46	6.04	1.74	39,100	0.661
0.2	73.03	6.34	2.54	40,300	0.682
0.5	72.91	6.32	2.51	—	—
1.0	68.25	5.87	1.72	45,200	0.644
2.0	72.63	6.37	2.45	39,600	0.615
5.0	71.70	6.45	2.27	40,400	0.677

[a]Degree of substitution based on % carbon.

(approximately 4%). These results are in contrast to the severe degradation of cellulose by high-energy radiation[2] and indicate that the highly substituted benzylcellulose used in this work is stable to direct radiation attack up to a dose of 5.0 Mrads.

Grafting Studies

Experimental conditions of preparation for each sample are shown in Table II, along with composition, number-average molecular weight, intrinsic viscosity, etc. of the isolated graft and homopolymer products. Figure 1 shows that the amount of styrene grafted to benzylcellulose in 1 and 5% solutions is dose-dependent, increasing with dose up to 4 Mrads, as would be anticipated for a radiation-initiated process. In addition, the number-average molecular weight and the intrinsic viscosity of the grafted benzylcellulose, shown in Figure 2, increase above that of the substrate with increasing polystyrene content. Polystyrene homopolymer from the same solutions had a maximum molecular weight of 40,800 and therefore occlusion of homopolymer in the precipitate could not account for the observed rise in molecular weight of the benzylcellulose fraction. The parallel increase in the molecular weight and the polystyrene content of the benzylcellulose fraction with dose indicates that a true benzylcellulose–styrene copolymer is formed and that its formation is dose-dependent. This is consistent with the normal kinetic scheme[12] suggested for radiation-initiated graft polymerization.

The effect of benzylcellulose concentration on the amount of styrene grafted to benzylcellulose may be seen from Figure 1, by comparing the amount of styrene grafted in 1 and 5% solutions with that obtained in a 15% solution. While up to 38.2% polystyrene was grafted in 1 and 5% solutions, no detectable polystyrene was grafted in a 15% solution. The observed inverse relationship between yield and solute concentration is not unique in the radiolysis of polymer solutions. A similar effect has been noted in the radiation degradation and crosslinking of poly(methyl

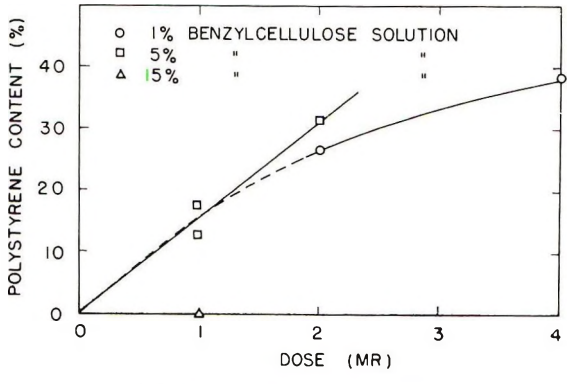

Fig. 1. Styrene grafted to benzylcellulose.

TABLE II

Sample	Preparation conditions			Graft copolymer						Homopolymer	
	Benzylcellulose concentration, %	Dose rate, MR/hr	Dose, MR	Polystyrene, %	$\bar{M}_n$	$[\eta]$, dl/g	Huggins constant	f factor	Benzylated anhydroglucose units per grafted chain	$\bar{M}_n$	$[\eta]$, dl/g
Substrate	—	—	—	—	41,000	0.675	0.61	—	—	—	—
1	0.973	0.588	2.02	26.9	48,100	0.769	0.45	0.584	263	37,800	0.372
2	0.973	0.588	4.20	38.2	60,600	1.03	0.36	0.873	140	33,800	0.356
3	4.89	0.528	1.00	12.9	42,600	0.688	0.56	0.294	704	—	—
4	4.89	0.528	1.00	17.1	42,400	0.704	0.46	0.197	506	40,800	0.308
5	4.76	0.585	2.00	31.1	53,700	0.525	0.70	0.817	176	31,000	0.251
6	5.10	0.616	2.00	—	—	—	—	—	—	—	—
7	4.89	0.556	1.82	23.4[a]	55,200	0.641	0.68	1.09	305	36,400[b]	—
8	4.89	0.556	4.00	—	—	—	—	—	—	—	—
9	14.8	0.504	1.03	0.0	39,400	0.657	0.61	0.0	0	32,700	0.287
10	4.95	0.058	1.00	21.7	46,500	0.802	0.46	−0.220	1020	110,000	0.697

[a] Determined gravimetrically.

[b] Determined by GPC.

methacrylate)[13] and polystyrene[14] in solution. This effect is considered to be due to an indirect attack of the polymer through energy transfer from the radiolysis products of the solvent and has been termed the "indirect" effect.[15] The indirect effect is most evident in dilute solutions and an inverse relationship between yield and concentration, in dilute solutions, has been considered a criterion to distinguish its presence.[15] Therefore, higher yields of benzylcellulose–styrene copolymer obtained in more dilute solutions, indicate an indirect effect by which energy is absorbed by styrene and then transferred to benzylcellulose, yielding macromolecular free radicals capable of initiating graft polymerization.

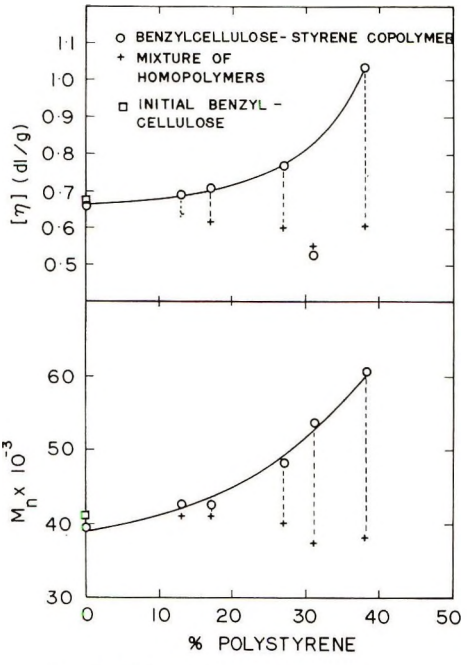

Fig. 2. $\overline{M}_n$ and $[\eta]$ of graft copolymer.

As seen in Figure 1, the inverse relationship between yield and solute concentration apparently does not extend from 5% to 1% solutions. However, during recovery of the graft copolymer by precipitation, difficulties were encountered due to the formation of fine suspensions. This was particularly true for grafted samples prepared in 1% solutions but was also encountered to lesser degrees in all samples. The grafted benzylcellulose products formed in 1% solutions were highly swollen and could not be recovered by filtration. The "precipitate" obtained from a 1% solution, irradiated to a dose of 4 MR, for example, was in a highly swollen, semi liquid state. These samples necessitated recovery by centrifugation at 2600 rpm for up to several hours. Under these conditions complete recovery of the precipitated product was difficult. In contrast, samples

prepared from 5% solutions were successfully recovered by filtration on medium sintered glass filters. The difficulties encountered during selective precipitation and the nature of the precipitate, from 1% solutions, suggest that product losses may account for the apparent similarity of grafting yields in 1 and 5% solutions shown in Figure 1.

The tendency to form stable suspensions during selective precipitation was apparent in all grafted samples but was not encountered during separation of two homopolymers. Stable suspensions have been reported by other workers[16] during fractional precipitation of block and graft copolymers and have been attributed to the selective precipitation of one homopolymeric block of the copolymer. Therefore, the highly swollen precipitate encountered on selective precipitation of 1% solutions after irradiation indicates the presence of large amounts of benzylcellulose–styrene graft copolymer.

The effect of dose rate on the grafting system may be seen by comparing samples 4 and 10 (Table II), prepared from 5% benzylcellulose solutions, irradiated to 1 MR, at dose rates of 0.528 and 0.058 MR/hr, respectively. The polystyrene content of the grafted benzylcellulose is larger at the lower dose rate. This may be accounted for by a higher molecular weight of the grafted polystyrene, as indicated by the corresponding homopolymer, which in turn results from a more efficient initiation of graft and homopolymerization at lower dose rates.[12]

Hydrolysis of Benzylcellulose

Cellulose copolymers lend themselves readily to isolation of the grafted chains due to the ease with which the cellulose portion of the copolymer may be removed by hydrolysis. Gleason and Stannett[17] reported that benzylcellulose, in benzene solution, was hydrolyzed to soluble products by treatment with trifluoroacetic acid under reflux, while polystyrene was unaffected by this treatment. The benzylcellulose portion of sample 7 was removed by hydrolysis in trifluoroacetic acid and the isolated polystyrene chains contained only 6.0% benzylcellulose as determined by infrared spectroscopy. The molecular weight distribution of the polystyrene chains, isolated from the benzylcellulose–styrene copolymer and of polystyrene homopolymer formed in the same solution, was determined by gel permeation chromatography (GPC). The corrected molecular weights and molecular weight distributions were calculated by the method of Pierce and Armonas[18] and are shown in Figure 3.

As seen in Table III, the average molecular weights of the isolated grafted polystyrene chains are almost identical with those of the homopolymer prepared during the grafting reaction. The $\bar{M}_w/\bar{M}_n$ ratio for the polystyrene isolated from the copolymer was 1.63, and that for the homopolymer was 1.66. The corrected GPC chromatograms, shown in Figure 3, demonstrate that both polystyrenes have very similar, relatively narrow, single peak distributions and that no major differences are evident.

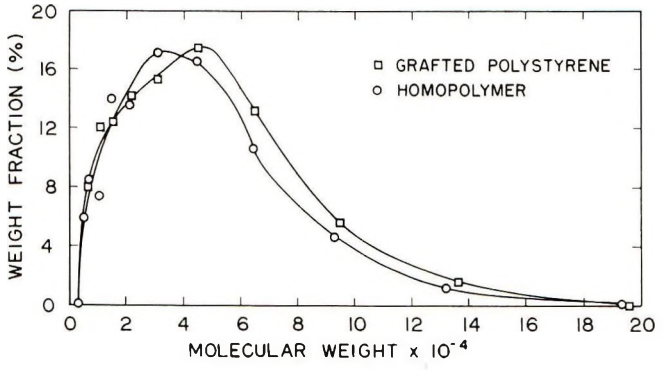

Fig. 3. Molecular weight distribution of grafted and homopolymer polystyrene.

It has been shown[2,3] that heterogeneous grafting processes, in contrast to the homogeneous process of this work, lead to a much larger molecular weight for the grafted chains than for the homopolymer formed in the same system. Stannett[19] isolated and fractionated grafted polystyrene chains from a cellulose acetate-styrene graft copolymer prepared in a heterogeneous system of cellulose acetate film and liquid styrene. Very broad, single and double peaked, molecular weight distributions were obtained. The $\bar{M}_w/\bar{M}_n$ ratios ranged between 9.2 and 28.6, depending on the conditions of preparation. These broad distributions were considered a manifestation of the diffusion controlled nature of the grafting reaction in a heterogeneous system. Heterogeneous solution grafting of styrene to polyisobutylene[5] and of styrene to cellulose acetate[4] yielded conflicting results with the molecular weights of the isolated grafted side chains, smaller and larger, respectively, than the corresponding homopolymer. It was suggested by both authors that these results also were attributable to the heterogeneity of the system during graft polymerization due to phase separation. In the benzylcellulose–styrene, homogeneous system, however, the similarity and relative narrowness of the molecular weight distributions for grafted and homopolymerized polystyrene indicate that graft polymerization and homopolymerization are unaffected by diffusional effects and proceed by similar mechanisms after initiation. The substrate is, therefore, uniformly accessible to monomer, and the polymerization conditions are uniform throughout the solution during the grafting procedure.

TABLE III
Molecular Weights of Grafted and Homopolymer Polystyrene

	Grafted polystyrene	Homopolymer polystyrene
$\bar{M}_n$	36,400	36,400
$\bar{M}_w$	59,200	60,400
$\bar{M}_n/\bar{M}_w$	1.63	1.66

Fractionation

In an effort to isolate the graft copolymer, several samples were fractionated by column elution fractionation. A mixture of homopolymers was also fractionated under identical conditions to determine the efficiency of homopolymer separation by this method. The elution curves for a homopolymer mixture and for a typical grafted sample (sample 6) are shown in Figures 4 and 5, respectively. Analysis of the fractions of sample 6 are shown in Table IV.

An effective separation of the homopolymers was achieved by column elution fractionation, as evidenced by the resolution of two major peaks shown in Figure 4. The first peak eluted corresponds to polystyrene and

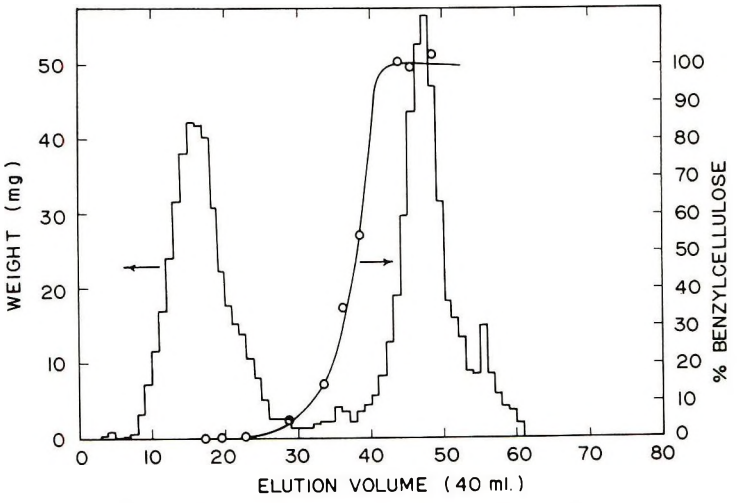

Fig. 4. Elution curve of homopolymer mixture (run 2).

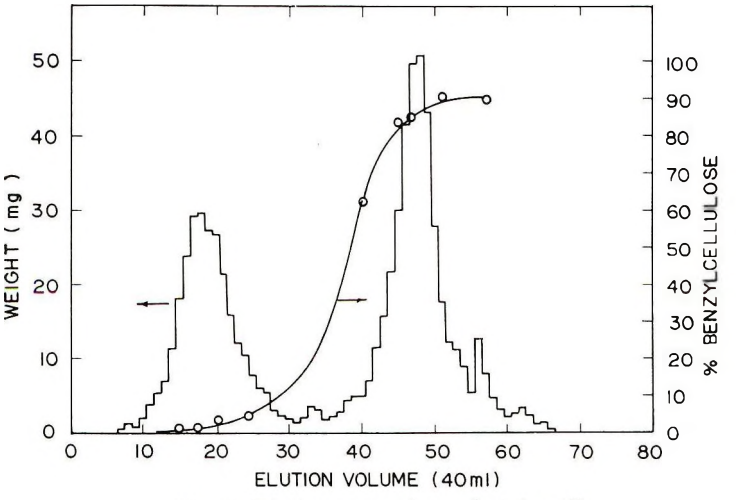

Fig. 5. Elution curve of sample 6 (run 3).

the second to benzylcellulose. Only in the central region, between the major peaks, are the homopolymers eluted simultaneously. This region, however, represents only a small fraction of the total sample weight.

Although column elution fractionation was effective in separating homopolymers, it is apparent from Figure 5 that fractionation of a grafted sample did not produce a third peak corresponding to the copolymer. The elution curve for the grafted sample yielded two major peaks eluted in similar positions to those for homopolymers. The first of these peaks consists of relatively pure polystyrene homopolymer; however, the second contains significant quantities of polystyrene, indicating that the copolymer is eluted in this region along with benzylcellulose.

TABLE IV
Fraction Analysis for Sample 6[a]

Weight fraction number	Average volume fraction	Weight, mg	Benzylcellulose, %	$\bar{M}_n$	$[\eta]$, dl/g
1	12.1	59.0	2.2	10,000[b]	0.195
2	14.9	82.8	2.5	38,800	0.205
3	17.6	70.1	3.9	59,900	0.367
4	21.7	62.6	4.6	56,800	0.315
5	37.4	50.8	62.0	36,100	0.269
6	42.4	69.0	83.8	37,800	0.459
7	44.2	90.4	85.0	46,700	0.566
8	46.0	89.7	86.2	57,500	0.713
9	48.4	67.0	90.2	61,300	0.717
10	54.5	56.8	89.2	47,400	0.713
Combined		698.2	51.8	36,100	0.463
Initial		729.6	58.4	—	—

[a] % Recovery = 95.7%.
[b] Estimated, solute permeated membrane.

Chapiro suggested[20] that fractionation of a previously isolated polyisobutylene–styrene copolymer by gradient elution chromatography occurred primarily by the solubility of the least soluble block of the copolymer. During elution fractionation of a block or graft copolymer, the least soluble block will remain in a collapsed or precipitated form until the solvent composition is capable of dissolving it, even though the more soluble block of the copolymer is completely solvated. Diffusion of the copolymer out of the polymer film on the support will be inhibited by an 'anchor' effect of the as-yet-undissolved, least-soluble block. If the mobility of the copolymer were impaired in this manner, the copolymer would not be released from the film until the least soluble segments were dissolved. Under these circumstances, a third central peak, corresponding to the copolymer, would not be obtained and the copolymer would be retained by the film until the second polymeric species was solvated. This would account for the removal of relatively pure polystyrene homo-

polymer and the elution of the benzylcellulose–styrene copolymer with the ungrafted benzylcellulose.

Characterization

One of the most meaningful parameters for characterizing cellulose graft copolymers is the "grafting frequency," i.e., the number of anhydroglucose units per grafted side chain. This parameter is calculated from the composition of the grafted sample and the molecular weights of the substrate and the grafted polymer. The results are shown in Table II. The number-average molecular weight of the grafted polystyrene, in the benzylcellulose–styrene copolymer, was estimated to be equal to that of the homopolymer formed simultaneously in the same solution. The validity of this estimate was confirmed by hydrolysis of the substrate as discussed above.

As seen in Table II, polystyrene grafted to benzylcellulose in a homogeneous system yielded copolymers where one in every 140–1020 benzylated anhydroglucose units carried a grafted polystyrene chain for a maximum dose of 4 Mrads. Several authors have determined the grafting frequency of other cellulose-based graft copolymers, prepared in contrast to this work, in heterogeneous systems. Krässig[21] compared heterogeneous grafting of styrene to cotton and cellophane by mutual irradiation of cellulose and styrene and by preirradiation of cellulose followed by immersion in styrene. Huang[2] grafted styrene to cellulose by mutual irradiation. The frequency of grafting in these systems varied between 2,540 and 53,000, depending on the conditions of preparation. Both Huang and Krässig irradiated samples up to approximately 4 Mrads. Stannett[4] prepared cellulose acetate-styrene graft copolymers from solutions in pyridine. The solutions were irradiated to 10 Mrads and were always turbid after the grafting procedure, indicating a phase separation, but yielded graft copolymer with one grafted side chain per 234 to 260 acetylated anhydroglucose units. While this grafting frequency is similar to that obtained in a homogeneous system the total dose employed was 2.5 times larger. This suggests that, at a similar dose, the frequency of occurrence of grafted side chains on the substrate in a homogeneous benzylcellulose-styrene system would exceed that in a heterogeneous cellulose acetate–styrene system. In any case, a decided improvement in the grafting frequency was effected in both heterogeneous and homogeneous solutions over that for solid–liquid systems, indicating that the substrate is more accessible to the monomer, resulting in a more efficient utilization of macromolecular radicals formed on the substrate and a more randomly grafted substrate.

The intrinsic viscosity of each sample is plotted against its number-average molecular weight in Figure 6 along with the intrinsic viscosity versus number-average molecular weight relation for the constituent homopolymers as determined in this work. The data for unfractionated benzylcellulose and sample 9, which contained no polystyrene, lie slightly

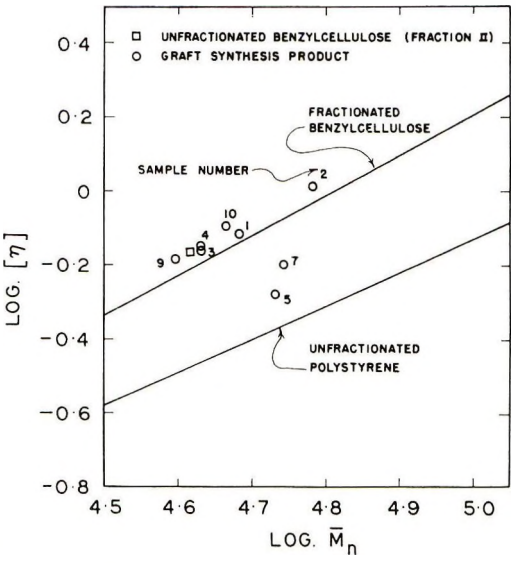

Fig. 6. Viscosity–molecular weight relationship for unfractionated graft copolymer.

above the viscosity-molecular weight correlation for fractionated benzylcellulose, indicating that this relationship is a reasonable approximation for unfractionated benzylcellulose.

The intrinsic viscosity is related to the molecular weight of a macromolecule by the Mark-Houwink equation

$$[\eta] = KM^a$$

The effect of branching is to reduce the value of a, increasing branching causing the viscosity to fall below that for a linear structure of the same molecular weight.[22] This effect is considered a qualitative manifestation of branching[23] and has been applied to graft copolymers.[24]

The intrinsic viscosity–molecular weight data for the benzylcellulose–styrene copolymer, shown in Figure 6, lie equal to or slightly above those for benzylcellulose of a similar molecular weight. If the copolymer were branched, the incorporation of polystyrene into the copolymer would tend to lower its intrinsic viscosity from that of benzylcellulose of a similar molecular weight. The relatively high intrinsic viscosity for the benzylcellulose–styrene copolymers presented in Figure 6 suggests that the copolymer is not branched but alternatively is a linear block copolymer.

Further evidence concerning the structure of the copolymer is obtained from the Huggins' constant shown in Table II and Figure 7. The Huggins' constant is sensitive to the structure of a macromolecule and also has been used as a qualitative indication of branching[23] with an increase in the Huggins' constant corresponding to the presence of branched structures. The Huggins' constant for benzylcellulose–styrene copolymers, with the exception of samples 5 and 7, which are relatively high, lie inter-

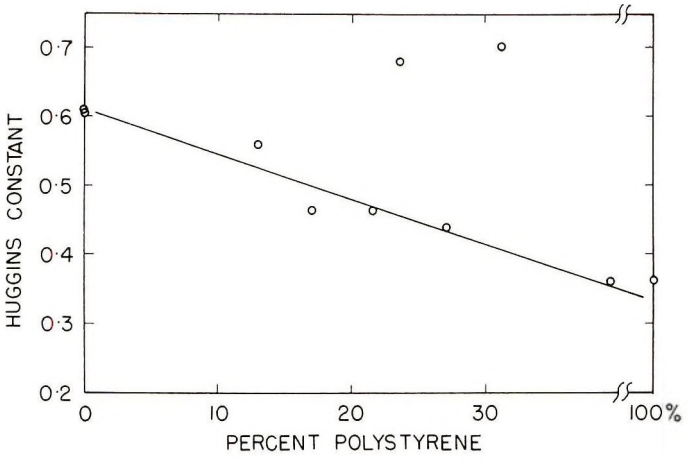

Fig. 7. Huggins constant vs. copolymer composition.

mediate to those for the constituent homopolymers. This behavior is similar to that for linear[25] rather than branched copolymers. Therefore, with the exceptions noted, the Huggins' constants for the benzylcellulose–styrene copolymers support the intrinsic viscosity–molecular weight data and also indicate that a linear block copolymer has been prepared.

It is interesting to note that both the intrinsic viscosity and the Huggins' constant for samples 5 and 7 indicate a relatively more branched structure than is apparent for all other samples. These samples were prepared from 5% solutions at doses of 2 and 4 Mrads, respectively. Indirect solute activation is most evident in dilute solutions and conversely, higher solution concentrations favor direct solute activation. High absorbed dose also increases the relative role of direct activation by reduction of monomer concentration with conversion and possible depletion of substrate sites that present low energy pathways for energy transfer from styrene. The combination of relatively high solution concentration and radiation dose in samples 5 and 7 would tend to favor direct activation and possibly lead to a change in polymer structure related to a change in the relative importance of direct and indirect activation of benzylcellulose. Unfortunately, the data are too limited to clarify this point more fully.

Proof of Grafting

Direct evidence of the existence of a chemical bond between benzylcellulose and polystyrene was elusive and therefore several experimental approaches were explored to establish the fact that a true copolymer had been formed.

Qualitative evidence supporting the belief that a copolymer is formed is apparent from the solution behavior of the irradiation products. The grafted products were recovered by selective precipitation to minimize occlusion of homopolymer with the precipitated graft copolymer. A series

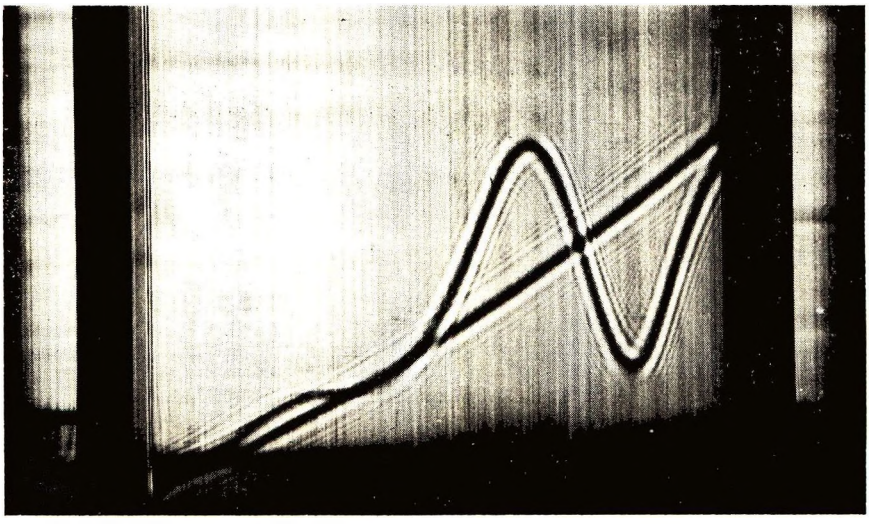

Fig. 8. Density gradient Schlieren diagram for homopolymer mixture.

of experiments showed that benzylcellulose and polystyrene are separated quantitatively by selective precipitation, whereas the precipitate obtained from irradiated solutions consistently contained significant quantities of polystyrene and the amount was dose dependent. The failure to separate all polystyrene from the benzylcellulose precipitate after irradiation indirectly supports the belief that the polystyrene was in fact grafted to the benzylcellulose. In addition, difficulties were often encountered during selective precipitation of the grafted benzylcellulose due to the formation of stable suspensions, while separation of homopolymers was accomplished without difficulty. Ceressa[16] considered the occurrence of stable turbidity during fractional precipitation an almost certain indication of the presence of a graft or block copolymer. Therefore, the formation of a stable turbidity during selective precipitation of irradiated solutions also indicates the presence of a benzylcellulose–styrene copolymer.

More quantitative proof of grafting was obtained from the intrinsic viscosity and the number-average molecular weight of the graft copolymers, which are plotted as a function of their polystyrene content in Figure 2. In all but one case, both the intrinsic viscosity and the molecular weight of the grafted sample are greater than that of a mixture of homopolymers of the same composition, indicating the presence of a graft copolymer. In addition, the magnitude of the discrepancy between the grafted samples and the homopolymer mixtures, for both these parameters, increases with increasing polystyrene content, indicating that the polystyrene is participating in a benzylcellulose–styrene graft copolymer.

Stannett[26] has successfully used density gradient centrifugation to prove the existence of a cellulose acetate-styrene graft copolymer. He observed a third peak of intermediate density to the two homopolymers, corresponding to a cellulose acetate–styrene copolymer. Fraction 9 of sample 6

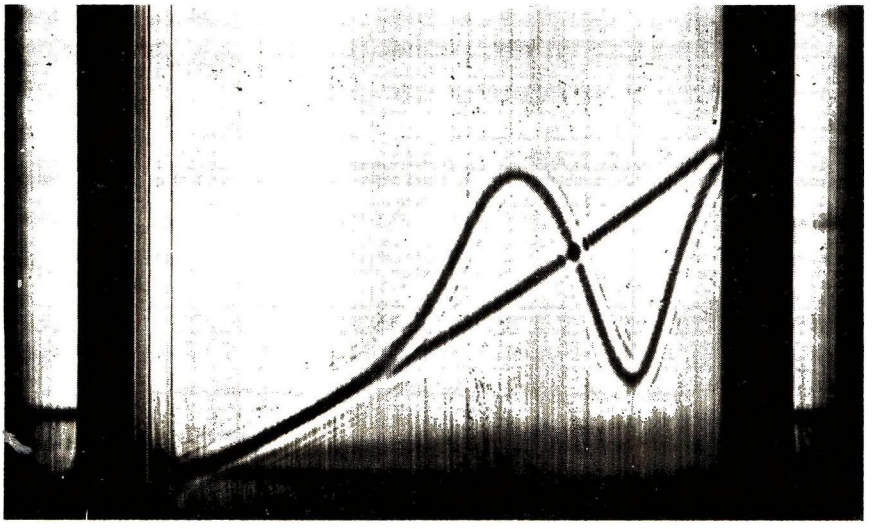

Fig. 9. Density gradient Schlieren diagram for grafted sample.

was subjected to density-gradient centrifugation under conditions that resolved a mixture of homopolymers of the same composition into two, partly overlapping, but clearly discernible bands. The Schlieren diagrams for the homopolymer mixture and the grafted sample are shown in Figures 8 and 9, respectively. The smaller, left-hand band in Figure 8 corresponds to polystyrene similar to that found by Stannett[26] and the larger right-hand band to benzylcellulose in Figure 8 at 1.083 and 1.195 g/ml, respectively. The polystyrene used in this experiment was obtained from the homopolymer isolated from sample 5, prepared under similar conditions to sample 6, and the benzylcellulose was the initial benzylcellulose used as the substrate throughout this work.

The Schlieren diagram for the grafted sample is shown in Figure 9. When compared to that for the homopolymer mixture, shown in Figure 8, the most obvious feature is the total lack of a band at a density corresponding to polystyrene. Since infrared analysis showed that the grafted sample contained 9.8% polystyrene, it is clear that polystyrene does not exist as free homopolymer. In addition, some alteration of the benzylcellulose band is apparent. The band maximum has shifted slightly to a lower density of 1.188 and the band has become more skewed towards the lower-density regions. The suggestion of a slight shoulder on the extreme left-hand side of the band and the skewness in this region indicate the presence of a component of intermediate density to that of the two homopolymers, as would be anticipated for a benzylcellulose–styrene copolymer. Therefore, the grafted sample shows no evidence of free polystyrene, and irregularities in the Schlieren diagram compared to that of the corresponding homopolymer mixture suggest the presence of a benzylcellulose–styrene copolymer.

Finally, Glaudemans and Passaglio[27] developed an interesting technique based on molecular weight determinations which could yield an unequivocal answer on the existence of a true graft. This method is based on knowledge of the molecular weights of the substrate, the grafted side chains and the total sample, in addition to the fraction add-on. The fraction add-on is defined as the weight ratio of the grafted side chains to the substrate. Glaudemans and Passaglio calculated a factor f, equal to the fraction of secondary polymer chains attached to the substrate, which has a value 0.0 for no grafting and 1.0 for complete grafting:

$$f = \{M_m[g + (M_p/M_s)] - M_p(1 + g)\}/gM_m$$

where M_m denotes the molecular weight of the total sample, g is the fraction add-on, M_p is the molecular weight of the grafted chains (and homopolymers), and M_s is that molecular weight of the substrate. M_s was taken as that of the initial benzylcellulose, M_p as that of the homopolymer formed simultaneously with the graft, and M_m was determined from each sample. g was calculated from the composition of the sample determined by infrared spectroscopy. The results are given in Table II. All samples except number 10 showed positive values of f, varying between 0.197 and 1.09, indicating the formation of a true graft copolymer. These calculations do not take into consideration copolymer formation by chain scission or substrate degradation during irradiation and therefore constitute a severe test for the existence of a copolymer. A negative result would have been indeterminate, but a positive result, as found here, proves the existence of a true benzylcellulose–styrene graft or block copolymer.

The authors wish to thank Prof. J. Guillet and D. Kells of the Department of Chemistry, University of Toronto, for the Ultracentrifuge analysis and Prof. A. E. Hamielec and S. Balke of the Department of Chemical Engineering, McMaster University, for the GPC analysis.

One of us (R. W. Betty) wishes to express his gratitude to Rayonier Canada (B.C.) Ltd. and the University of Toronto for financial assistance during the course of his Ph.D. program at the University of Toronto.

References

1. H. A. Krässig and V. Stannett, *Adv. Polym. Sci.*, **4**, 111 (1965).
2. R. Y-M. Huang, B. Immergut, E. H. Immergut, and W. H. Rapson, *J. Polym. Sci. A*, **1**, 1257 (1963).
3. J. C. Arthur and D. J. Daigle, *Text. Res. J.* **34**, 653 (1964).
4. V. Stannett, J. D. Wellons, and H. Yasuda, in *Macromolecular Chemistry, Paris 1963* (*J. Polym. Sci., C*, **4**), M. Magat, Ed., Interscience, New York, 1964, p. 551.
5. J. Sebban-Danon, *J. Chim. Phys.*, **58**, 263 (1961).
6. A. Dobry and Boyer-Kowenoki, *J. Polym. Sci.*, **2**, 90 (1943).
7. E. C. Worden, *Technology of Cellulose Ethers*, General Publishing Co., Toronto, 1933.
8. F. G. Rice and W. D. Smythe, *Ind. Eng. Chem.*, **52**, No. 5, 47A (1960).
9. H. Fricke and S. Morse, *Phil. Mag.*, **7**, 129 (1929).
10. S. E. Wiberley, J. W. Sprague, and J. E. Campbell, *Anal. Chem.*, **29**, 210 (1957).

11. B. I. Friedlander, Ph.D. Thesis, Department of Chemical Engineering and Applied Chemistry, University of Toronto, 1966.

12. A. Chapiro, *Radiation Chemistry of Polymeric Systems*, Interscience, New York, 1962.

13. S. Okamura, T. Manabe, S. Futami, T. Iwasaki, A. Nakajima, K. Odan, H. Inagaki, and I. Sakurada, *Proc. 2nd Intern. Conf. Peaceful Uses Atomic Energy, Geneva, 1958*, Vol. 29, United Nations, p. 176.

14. A. Henglein and C. Schneider, *Z. Physik, Chem.* (Frankfurt), **18**, 56 (1958).

15. A. Charlesby, *Atomic Radiation and Polymers*, Pergamon Press, New York, 1960.

16. R. J. Ceresa, *Block and Graft Copolymers*, Butterworths, London, 1962.

17. E. Gleason and V. Stannett, *J. Polym. Sci.*, **44**, 183 (1960).

18. P. E. Pierce and J. E. Armonas, in *Analytical Gel Permeation Chromatography*, (*J. Polym. Sci. C*, **21**), J. F. Johnson and R. S. Porter, Eds., Interscience, New York, 1968, p. 23.

19. J. D. Wellons, A. Schindler, and V. Stannett, *Polymer*, **5**, 499 (1964).

20. A. Chapiro and P. Cordier, in *Macromolecular Chemistry, Paris 1963* (*J. Polym. Sci. C*, **4**), M. Magat, Ed., Interscience, New York, 1964, p. 491.

21. H. A. Krässig, *Tappi*, **46**, 654 (1963).

22. C. D. Thurmond and B. H. Zimm, *J. Polym. Sci.*, 8, 477 (1952).

23. W. Cooper, G. Vaughan, D. E. Eaves, and R. W. Madden, *J. Polym. Sci.*, **50**, 159 (1961).

24. J. Sebban-Danon, *J. Chim. Phys.*, **58**, 246 (1961).

25. D. J. Angier, R. J. Ceresa, and W. F. Watson, *J. Polym. Sci.*, **34**, 699 (1959).

26. A. Ende and V. Stannett, *J. Polym. Sci. A*, **2**, 4047 (1964).

27. C. P. J. Glaudemans and E. Passaglia, in *Fourth Cellulose Conference* (*J. Polym. Sci. C*, 2), R. H. Marchessault, Ed., Interscience, New York, 1963, p. 189.

Received December 22, 1970

JOURNAL OF POLYMER SCIENCE: PART A-1 VOL. 9, 1921–1935 (1971)

Thermal Decomposition of Poly(vinyl Chloride) and Chlorinated Poly(vinyl Chloride). II. Organic Analysis

S. A. LIEBMAN, D. H. AHLSTROM, E. J. QUINN, A. G. GEIGLEY, and J. T. MELUSKEY, *Armstrong Cork Company, Research and Development Center, Lancaster, Pennsylvania 17604*

Synopsis

A concerted study of poly(vinyl chloride), chlorinated poly(vinyl chloride), and poly(vinylidene chloride) polymers by spectroscopy, thermal analysis, and pyrolysis–gas chromatography resulted in a proposed mechanism for their thermal degradation. Polymer structure with respect to total chlorine content and position was determined, and the influence of these polymer units on certain of the decomposition parameters is presented. Distinguishing differences were obtained for the kinetics of decomposition, reactive macroradical intermediates, and pyrolysis product distributions for these systems. It was determined that chlorinated poly(vinyl chloride) systems with long-chain —CHCl— units were more thermally stable than the unchlorinated precursor, exhibited increasing activation energy for the dehydrochlorination, and produced chlorine-containing macroradical intermediates and chlorinated aromatic pyrolysis products. The poly(vinyl chloride) polymer was relatively less thermally stable, exhibited decreasing activation energy during dehydrochlorination, and produced polyenyl macroradical intermediates and aromatic pyrolysis products.

The mechanism of PVC degradation has been a controversial and extensively studied topic, whereas no detailed studies are found in the literature for the comparative mechanism of thermal decomposition for chlorinated PVC polymers. Few coordinated mechanistic or kinetic analyses of thermal decomposition using the tools of modern organic analysis to study the effects of polymer structure and important physical parameters have been reported for either polymer system.[1,2] Our studies[1] allow a concerted interpretation leading to a proposed thermal decomposition scheme for the PVC and Cl-PVC systems that demonstrates certain similarities and differences observed under the experimental conditions used.

In our polymer degradation and characterization program, it was necessary to obtain specific analyses of PVC and Cl-PVC systems in the fields of spectroscopy, chromatography, and thermal analysis. The information obtained from infrared (IR), nuclear magnetic resonance (NMR), electron spin resonance (ESR), pyrolysis gas–liquid chromatography (PGLC), and derivative thermogravimetric analysis (dTGA) was used to study

certain parameters operative in the thermal degradation of those systems with respect to the effect of chloride content and polymer structure.

EXPERIMENTAL

Infrared Spectra

Infrared spectra were obtained by using a Perkin-Elmer 457 spectrometer, with samples examined in KBr pellets.

NMR Spectra

Samples were dissolved in *o*-dichlorobenzene and the spectra recorded at 150°C by using a Jeol JNM-4H 100-MHz high-resolution spectrometer and tetramethylsilane (TMS) as internal standard.

ESR Spectra

A Varian 4500-10A, X-band ESR spectrometer, 100-kHz field modulation with a variable temperature insert was used to obtain first-derivative spectra for the above series under identical conditions. Detailed experimental conditions are given in Part I.[1]

PGLC

Pyrograms were reproducibly recorded for samples placed in capillary tubes (ca. 1–2 mg sample weights) and pyrolyzed at approximately 550°C for 10 sec in an Aminco pyrolyzer attachment to an F&M Model 500 chromatograph equipped with a thermal-conductivity detector. Analyses were performed on the products swept directly from the pyrolyzer by using an 8-ft × $^1/_4$-in. stainless-steel column packed with 3% SE-52 on AW-DMCS Chromosorb W with a helium flow of ca. 30 cc/min. A precolumn of NaOH on firebrick removed the HCl evolved in the pyrolysis and did not noticeably affect the product distribution within the retention-time range examined. Identification of peaks was made by comparison of retention times with authentic compounds placed in the unknown samples and pyrolyzed in an identical manner. Previous literature identifications based on mass-spectral data and retention times were used for comparative evidence.[3–7] A twofold decrease of sample size and use of a flame-ionization detector with a Hewlett-Packard Model 5750 chromatograph gave pyrogram patterns analogous to those obtained above with larger sample size and less sensitive detection.

dTGA

Samples were examined in the denoted temperature ranges and atmospheres by using an Aminco thermogravimetric analyzer. Computer programs and kinetic treatment of the weight-loss data are discussed in detail separately.[1,2]

RESULTS AND DISCUSSIONS

Infrared Studies

The 600–700 cm^{-1} region has definitive assignments available for C-Cl stretching bands in PVC and Cl-PVC.[8–14] As the chlorination level increased in our sample series, the intensities for the 602 cm^{-1} (B_1 mode) and the 640 cm^{-1} (A_1 mode) peaks due to C-Cl syndiotactic *trans* sequences in the crystalline phase decreased, while there was increased absorption at 690, 750, and 800 cm^{-1}. Band-absorption overlap was apparent as the CHCl units exhibited absorption at the 690 cm^{-1} region where original isotactic C-Cl bands appear. The overall pattern in Figure 1 for the Cl-PVC series demonstrates this general trend as chloride content increased from the control PVC (56%) to Cl-PVC (75%). Poly(vinylidene)chloride ($PVCl_2$) C-Cl band absorptions are significantly different from any in the above series, which emphasized the varied environment of these C-Cl units in the $PVCl_2$ system (72.2% Cl) relative to that of Cl-PVC (72.8% Cl) with essentially the same total chloride content. It had been concluded previously that chlorinated PVC is closer structurally to poly-1,2-dichloroethylene than to poly-1,1-dichloroethylene.[10–12] The 530 cm^{-1} peak[14] in the $PVCl_2$ spectrum has been tentatively assigned to in-phase stretching vibrations of $C\text{-}Cl_2$ units.

Development of a corresponding peak at 525 cm^{-1} in the Cl-PVC series from 64–75% Cl content is noted, with constant intensity achieved between 72 and 75%. This implies that the 1,1-dichloro units in Cl-PVC are formed not necessarily as a result of exhaustion of replaceable hydrogen atoms on CHCl units, but rather under other directing structural influences within the polymer system, since they apparently are produced at the lower chlorination levels and do not increase proportionately with chloride content. Alternatively, should the assignment be made to tertiary-Cl units[8] at 530 cm^{-1}, this band may indicate such initial levels being produced. However, failure of increased intensity for this peak as chlorination increases to yield large amounts of CHCl units (by NMR) makes the former assignment the preferred one.

NMR Studies

Tacticity determination for PVC has been well established, and chlorination sites are identifiable by observation of decreased peak intensities of the CH_2 groups in the isotactic portion,[15,16] with concurrent increase of peak intensities in the lower field region. The CH_2 protons with neighboring C-Cl bonds (3 ppm) show increased absorption as do the number of CHCl protons (4.95 ppm). Figure 2 shows the effects of increasing chlorination of PVC on the NMR spectrum in the CH_2 and CHCl proton absorption regions. Our sample of 70.2% Cl-PVC from Diamond 450 precursor is essentially identical in NMR peak positions and intensities to the 70.2% Cl-PVC obtained by Sobajima et al.[17] from PVC precursor Geon EP

(Japanese Geon Co., Ltd.). However, the 72–75% Cl-PVC samples prepared from different PVC polymer precursors have a notably higher number of CHCl(CHCl)$_n$ units, as determined by the analysis of absorption intensity at 4.95 ppm. Svegliado and Grandi[18] have calculated the number-average sequence length (l_n) of such 1,2-dichloroethylenic units and concluded that a random distribution for the chlorination process is followed. The 72–75% Cl-PVC samples display an exceptionally high l_n value for a completely random distribution, and theoretical calculations at this laboratory do not support such a conclusion.[16] NMR spectra for chlorinated samples in the 64–70% range obtained from our specially prepared PVC polymers may aid in the explanation, since the samples of higher Cl content (72–75%) are reflecting a different chlorination pattern that is due apparently to the structural influences of the precursor PVC. All other chlorination conditions were identical for the entire series.

ESR Studies

The initial detection temperature of free radicals in thermally treated PVC is reported separately in conjunction with kinetic data from weight-loss measurements by TGA.[1] Figure 3 presents the first-derivative ESR curve recorded for control PVC and Cl-PVC (72.2%) at the denoted temperatures under nitrogen. It is evident that the control sample and

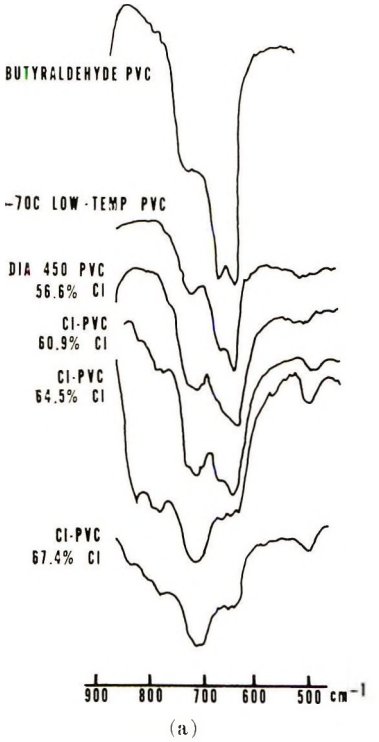

(a)

Fig. 1 (*continued*)

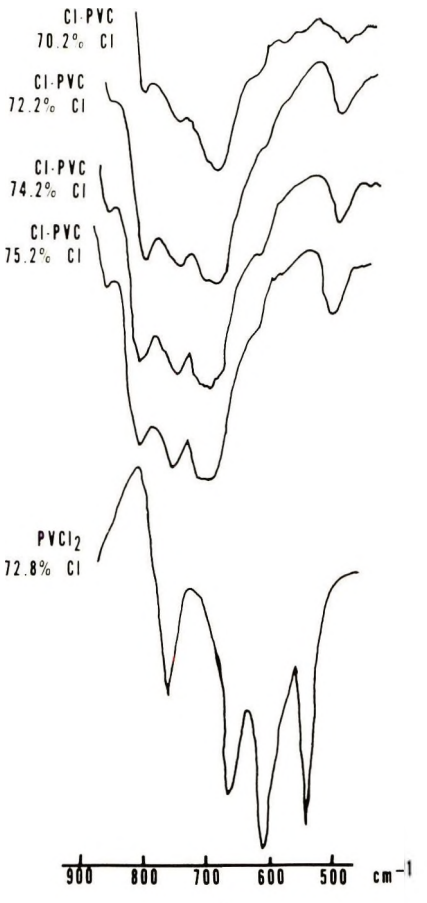

(b)

Fig. 1. Infrared spectra in 500–700 cm^{-1} region; KBr pellets.

chlorinated sample display different ESR curve shapes and, hence, macroradical behavior under these experimental conditions. The use of a duPont curve resolver[19] allowed comparative analysis of the curve shapes which resulted in the conclusion that a minimum of three different macroradicals are present in PVC throughout the range studied, while at least two species are present in Cl-PVC. Thus, although radical identification is not possible from these data, the distinctness in curve shape and decay behavior of the macroradical(s) produced in control PVC from those of chlorinated PVC is demonstrated, and one may infer that the difference is due to the presence of Cl atoms remaining along the polymer chain. The ESR spectral patterns and macroradical behavior were similar throughout the chlorinated PVC series, and no subtle influences were noted by this method as being derived from the different distributions of Cl atoms (infrared and NMR data). Therefore, the main distinction for these ESR spectral parameters was based on a comparison of the three polymer

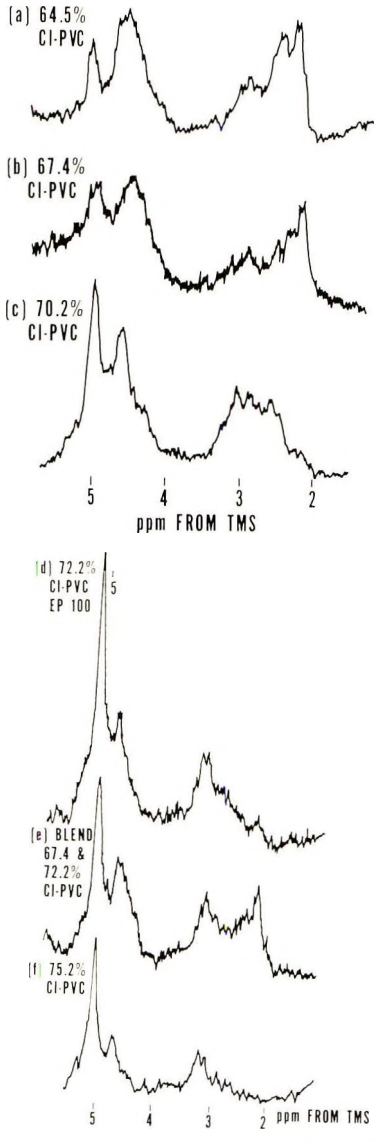

Fig. 2. Nuclear magnetic resonance spectra, 100 MHz, *o*-dichlorobenzene solvent at 150°C; Tetramethylsilane (TMS) internal standard.

groups (control PVC samples, chlorinated-PVC samples with 64–75% Cl, and $PVCl_2$ with 72.8% Cl). The last of these polymers had a distinctly lower temperature of radical detection[1] and a faster rate of radical generation.

Pyrolysis Gas-Liquid Chromatography

Some product analyses by gas–liquid chromatography (GLC) for PVC and Cl-PVC samples which had been pyrolyzed under varied experimental con-

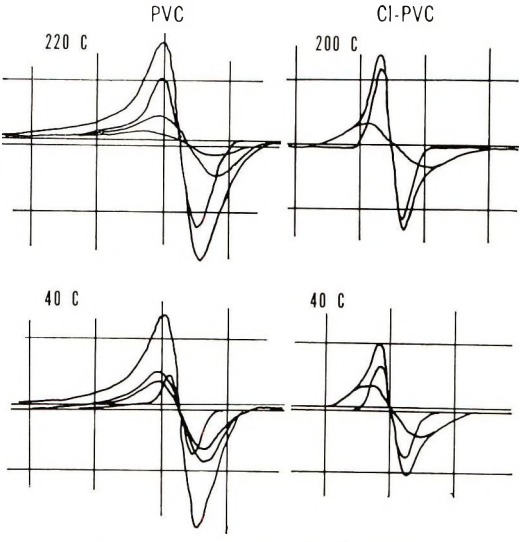

Fig. 3. First-derivative ESR signals analyzed with the duPont curve resolver. Diamond 450 PVC compared to 72.2% Cl-PVC at 220, 200, and 40°C.

ditions have been reported by other workers.[3–7] A definitive change of product type was determined for PVC relative to Cl-PVC, as well as for $PVCl_2$. Representative pyrograms are presented in Figure 4 for our series.

The control PVC resulted in essentially complete aromatic hydrocarbon species within the defined retention-time range, while the chlorinated systems produced chlorinated aromatics. Similar tetralin/naphthalene ratios were routinely observed for PVC polymers, while mono- and dichlorobenzenes resulted from the Cl-PVC systems and negligible tetralin or naphthalene species. The $PVCl_2$ system provided Cl-aromatic products[4] but not the analogous mono-/dichlorobenzene ratios seen for Cl-PVC. The fact that a simple change from tetralin/naphthalene product ratios to chlorinated tetralin/naphthalene ratios was not observed demonstrates the major influence on the degradative mechanism incurred by chlorination, even at low Cl content (64% Cl). The cyclization steps following dehydrochlorination show some dependence on sequence length, since high mono-/dichlorobenzenes product ratios are noted from polymers of low Cl content where shorter internal CHCl units are present, while lowered ratios resulted at the higher Cl contents (70–75%).

Several specially prepared PVC control polymers gave PGLC results similar to those of the Diamond 450 polymer. However, vinyl chloride polymerized with a free-radical initiator and excess butyraldehyde did not show the characteristic tetralin/naphthalene ratio (Fig. 4). It is anticipated from the above results that more detailed PGLC studies on PVC systems may give useful information about the presence of defect structures, Cl types and positions, and end-groups, as well as their influence in the degradative processes.

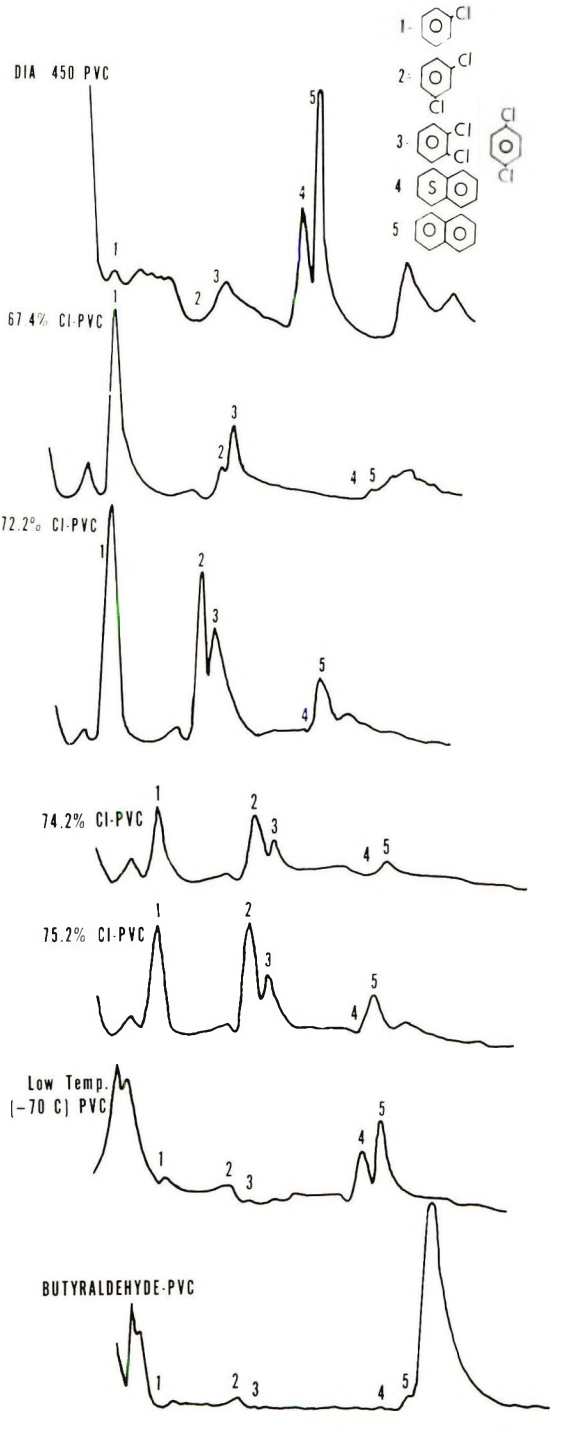

Fig. 4. Representative pyrograms from pyrolysis gas–liquid chromatography.

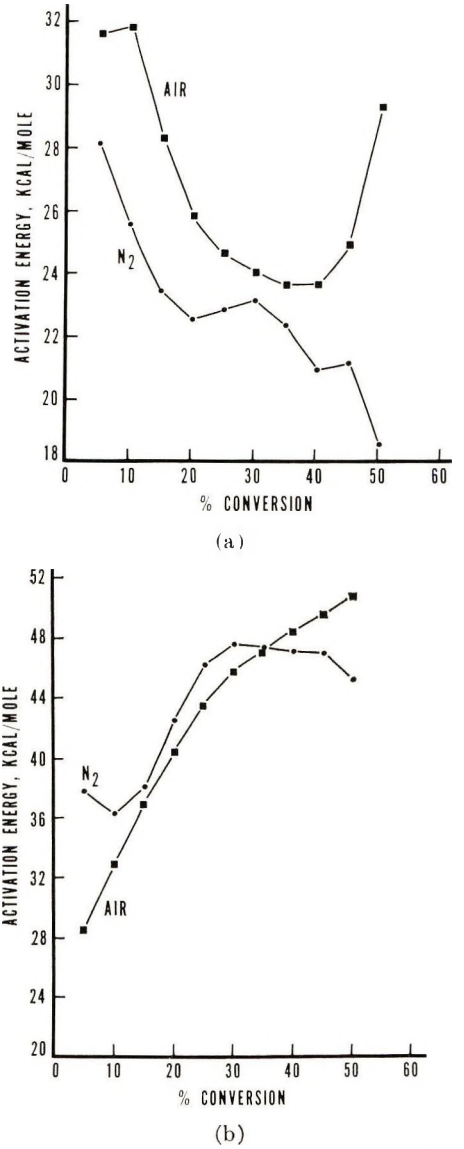

Fig. 5. Variation of apparent Arrhenius activation energy E_a with extent of dehydrochlorination in air and N_2 at heating rates of 3, 10, and 18°C/min from TGA data: (*a*) Diamond 450 PVC; (*b*) 75.2% Cl-PVC.

Thermogravimetric Analysis

Derivative plots for the weight losses recorded for certain of the above samples are presented in Figure 5. The calculated kinetic factors for PVC and Cl-PVC samples showed consistent variations with Cl content and oxidative atmosphere.[1] It was shown that chlorination throughout the Cl range studied (64–75%) provided increased thermal stability

TABLE I
Residues at 500°C

Sample	Heating rate, °C/min	Residue, wt-%	
		N_2	Air
Dia 450 PVC	3	16.5	26.2
	6	18.5	30.0
	10	21.0	32.5
	15	23.0	31.8
	18	23.0	32.5
64.5% Cl-PVC	3	36.4	24.0
	10	36.4	32.0
	18	37.5	31.5
67.4% Cl-PVC	3	36.0	16.0
	10	30.2	29.0
	18	35.2	33.8
70.2% Cl-PVC	3	37.2	13.5
	10	37.0	18.0
	18	37.2	28.0
72.2% Cl-PVC	3	37.9	16.0
	10	38.0	33.0
	18	37.8	33.0
75.2% Cl-PVC	3	35.0	14.0
	10	38.9	33.0
	18	40.0	32.5
72.8% $PVCl_2$	3	36.5	4.5
	10	41.6	27.0
	18	43.3	38.5
48% Cl PE	3	39.6	—
	10	38.5	—
	18	41.5	—
−70°C low-temp PVC	3	19.7	—
	10	25.5	—
	18	26.0	—

(TGA breakpoint temperatures), higher activation energies, and variable frequency factors for the dehydrochlorination process with increasing Cl content.

The effect of heating rate on the control PVC could be assessed by the data in Table I, which lists weight-per cent residues in air and nitrogen atmospheres. There was a slight decrease in residue from 23% to 16.5% at a decrease in heating rates from 18 to 3°C/min. In an oxidative environment, while the total residue was higher (32–26%), there was only a slight effect at the lower two heating rates. For the Cl-PVC (70.2% Cl) sample the higher residue levels persisted for all heating rates in nitrogen, while the oxidative decompositions showed a significant lowering of residue amounts and a more marked effect at the low (3 deg/min) heating rate. It is seen that more volatilization resulted in the latter decomposition than in nitrogen, and the lowest heating rate in air (longest thermal input) gave more degradative weight loss: thus the Cl-PVC attained

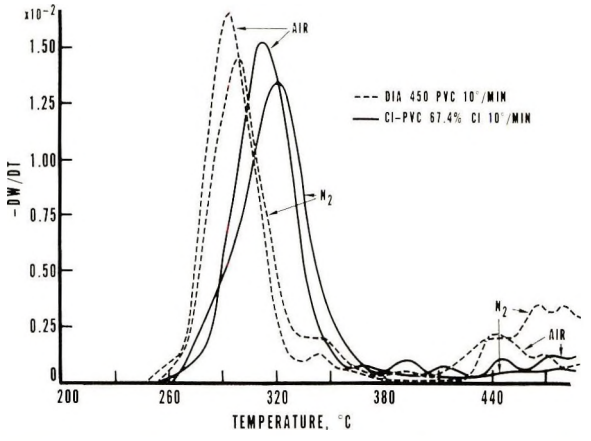

Fig. 6. Derivative thermogravimetric analysis in air and N_2 at heating rate of 10°C/min: (--) Diamond 450 PVC; (——) 67.4% Cl-PVC.

approximately the same residue as did the control PVC under nonoxidative conditions. The effect of heating rate was also demonstrated for both series by calculations of activation energies, frequency factors, and reaction order by using three distinct methods for data treatment.[1]

In addition, the change of activation energy with per cent weight loss demonstrated the important difference between PVC and Cl-PVC polymer (Fig. 5). PVC showed a decreasing activation energy for dehydrochlorination as the process continued, whereas Cl-PVC had an increasing value. Since the effects of oxidative and nonoxidative environments on the amounts of residues were also opposite for the PVC and Cl-PVC systems, the fundamental importance of that parameter on the degradative mechanisms is noted in the high-temperature (~400°C) region. No such effect was seen at the 3°C/min heating on the temperature of initial weight loss for the dehydrochlorination process (248–250°C) when air/nitrogen atmospheres were used during decompositions of PVC and Cl-PVC, respectively.[1] However, the dehydrochlorination process did show generally slightly decreased activation energies when an oxidative environment was used in either polymer system.

One may note (Fig. 6), that the control PVC in nitrogen showed more volatilization (greater weight loss) for the high-temperature degradation step than when decomposed in air at the same heating rates. Comparative dTGA plots are shown (Fig. 6) for a corresponding chlorinated PVC (67.4% Cl). The higher temperatures at which the Cl-PVC system reached maximum rates of weight loss is an additional indication of its increased thermal stability[1] relative to PVC (Fig. 6). It is interpreted that increased crosslinking and inhibition of volatilization by various mechanisms occur in air, and increased residues result. The temperature for this degradative step, when it does occur, is approximately 450°C for all systems, but the oxidative decomposition had a less steep weight-loss

slope. Contrary to control PVC, the Cl-PVC compounds in nitrogen show essentially no weight loss at 450°C, but in air the dTGA plots do show some increased rate of weight loss in the high-temperature region, i.e., Cl-PVC systems are more stable in an inert environment, but sensitive to an oxidative one in a manner that resulted in increased volatilization. Therefore, a crosslinking mechanism is not likely, but a bond scission and/or cyclization mechanism is probable.

The effect of inert or oxidative environment may also be seen in the data from the ESR experiments. The control PVC sample in nitrogen demonstrated a less steep ESR signal generation slope at 220°C, but, once generated, gave a stronger signal when monitored at 40°C. The signal had increased slope at 220°C in the presence of air. The Cl-PVC sample behavior was contrary to that seen with PVC, however, giving essentially the same generation slope in air or nitrogen and, once generated, exhibited a decreased macroradical signal when monitored at 40°C; i.e., free-radical decay, not growth, was noted, which likely resulted from recombination, termination, and processes which lead to high percentage of residues in nitrogen. In air, a steady ESR signal intensity was monitored at 40°C, so that an oxidative environment may lead to a slight increase in free-radical activity, resulting in increased bond scission, electron transfer, and subsequent increased volatilization (decreased residues). It may be inferred that bond scission was not accomplished easily in nitrogen, since free-radical activity decreased once the radicals were generated, which resulted in higher weight-per cent residues. In air, bond scission has a lower activation energy, and radical activity is increased, leading to increased volatilization and low residue weights.

There was no apparent systematic influence on the TGA or ESR parameters arising from the structure variations in the PVC control or in the specially prepared PVC precursor systems with different contents of internal $CHCl(CHCl)_n$ units.

Conclusions

The structural characterization of PVC and Cl-PVC polymers by infrared and NMR spectra has allowed the effect of chloride content and position on thermal degradation to be assessed in subsequent analyses. Although certain of these methods (TGA, ESR) were relatively insensitive to subtle structural changes as internal sequence length of chloromethylene units, they did provide information on the activation energy, reactive intermediates, and oxidative influences present during thermal decomposition of PVC, Cl-PVC, and $PVCl_2$ systems. The pyrolysis-GLC method demonstrated inherent sensitivity to position and number of chlorine atoms in the Cl-PVC systems. The ESR monitor provided conclusive evidence for the presence of free radicals at low levels of dehydrochlorination ($\leq 5\%$) and essentially no variation in initiation temperatures or generation rates of macroradicals under certain conditions. However, important changes were observed in ESR curve shape, macro-

radical decay behavior, and response of the radicals to an oxidative environment. The following conclusions thus may be made.

(1) Thermal stability of PVC in oxidative and nonoxidative environments as seen by dTGA is relatively increased by chlorination,[1] which provides long internal (CHCl) sequences (by NMR) in the polymer chain. The $—CCl_2$ unit is known to be more thermally labile, and comparative data on $PVCl_2$ demonstrates this fact.

(2) Free-radical intermediates were detected by ESR at low levels of dehydrochlorination during thermal decomposition for control PVC, Cl-PVC, and $PVCl_2$ samples; such macroradicals behave differently in the three systems with respect to decay rates and extent of response to an oxidative environment.

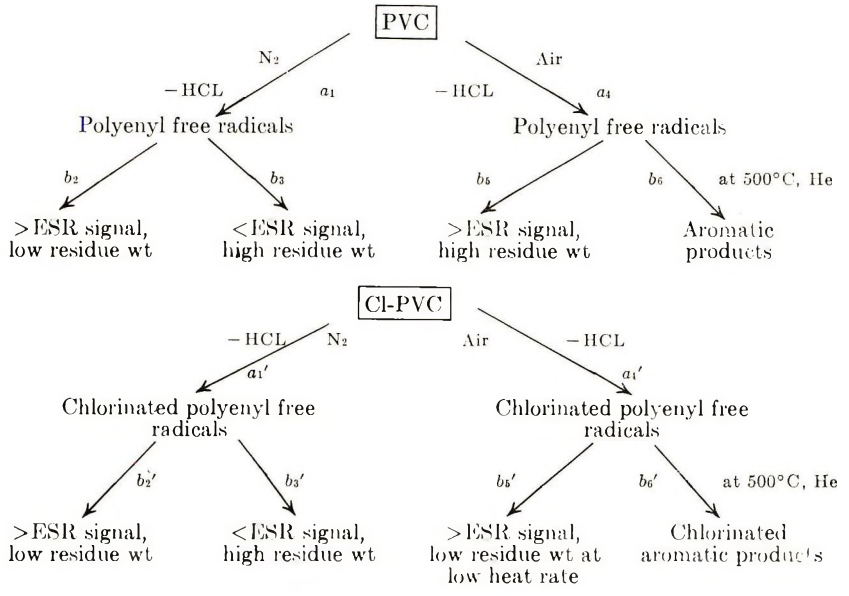

Fig. 7. Steps in thermal degradation of PVC and Cl-PVC.

(3) Thermal analysis (TGA, dTGA) established different kinetic patterns and response to an oxidative environment for the three basic systems.

(4) Product analysis by PGLC demonstrated the importance of chlorine number and position on the pyrolytic degradation of the above three basic systems.

On the basis of the information presented here concerning polymer structure and physical parameters, in conjunction with specific identification of polyenes in low-level degradation of PVC by resonance-enhanced Raman spectroscopy,[20] it is reasonable to postulate the sequence shown in Figure 7.

It was found for PVC that pathways $a_1 \cong a_4$, $b_2 > b_3$, and $b_6 > b_2$; correspondingly, for Cl-PVC systems, $a_1' \cong a_4'$, $b_2' < b_3'$, and $b_5' \leqq b_2'$; notably, steps b_6 and b_6' distinguish between PVC and Cl-PVC systems.

In summary, our data support the thermal-degradative sequence of initial dehydrochlorination with early production[1] of macroradicals, both in air and nitrogen for PVC, Cl-PVC, and $PVCl_2$ systems. Polyenyl free radicals produced in PVC polymers exhibit increasing numbers in both air ($b_2 > b_3$), and nitrogen atmospheres ($b_5 > b_2$), but Cl-PVC macroradicals show a decrease in ESR signal intensity ($b_2' < b_3'$) and only a small effect of atmosphere ($b_5' \leqq b_2'$). PVC macroradicals lead to high volatilization in N_2 resulting in low residues ($b_2 > b_3$), while in an oxidative atmosphere a high residue weight results. This is apparently from increased crosslinking and general inhibition of volatilization of products. Cl-PVC macroradicals showed opposite results with respect to residues in air and nitrogen, i.e., residues were larger in N_2 than in air. Hence, the tendency to crosslink and inhibition to volatization were not enhanced in the oxidative environment.

The different product analyses upon pyrolytic treatment at 500°C in a helium atmosphere were definitive for the two series. PVC gave essentially aromatic compounds in the temperature range examined, whereas Cl-PVC gave chlorinated aromatic compounds.

The individual techniques employed (spectroscopy, thermal analysis, and chromatography) have enabled the investigation of polymer structure, decomposition kinetics, reactive intermediates during the thermolysis, and the resulting product analyses to be conducted in an internally consistent manner for the denoted polymers. Discrete differences in certain of these stages were noted in the comparative study for PVC and Cl-PVC polymers. The presentation of free-radical thermal-decomposition mechanisms for both systems is given. Different macroradical species are postulated based on spectroscopic parameters, decomposition kinetics, response to an oxidative or inert environment, and product analyses.

More complete characterization of PVC polymer systems is planned with respect to "defect" structures by pyrolysis-GLC, as well as the effects of oxygen concentration, pyrolytic temperatures, stabilizers, and other additives. The influence of these factors on the kinetics and mechanism will be studied also.

Such interdisciplinary organic analysis of the complex structural and physical factors inherent in decomposition phenomena, as shown in this work, may reasonably lead to predictions which aid in the synthesis of more thermally stable polymers, optimized stabilization for existing polymer systems, and a better understanding as to the role various additives may have in the degradation process.

We appreciate the cooperation of the personnel in the Analytical, Computer and Technical Information sections, respectively, of the Armstrong Cork Company. Acknowledgment is gratefully made to George G. Kemmerer, Jr., Physics Department, Temple University, Philadelphia, Pa., for assistance in the ESR experiments.

References

1. S. A. Liebman, J. F. Reuwer, Jr., K. A. Gollatz, and C. D. Nauman, *J. Polym. Sci. A-1*, **9**, 1823 (1971).

2. P. Berticat, *J. Chim. Phys.*, **1967**, 887, 892.

3. S. Tsuge, T. Okumoto, and T. Takeuchi, *Macromolecules*, **2**, 200 (1969).

4. D. Noffz, W. Benz, and W. Pfab, *Z. Anal. Chem.*, **235**, 121 (1968).

5. E. A. Boettner, paper presented at Polymer Conference Series, Univ. of Detroit, Detroit, Michigan, June 16–20, 1969.

6. M. M. O'Mara, *J. Polym. Sci. A-1*, **8**, 1887 (1970).

7. Y. Tsuchiya and K. Sumi, *J. Appl. Chem.*, **17**, 364 (1967).

8. S. Krimm and S. Enomoto, *J. Polym. Sci. A*, **2**, 669 (1964).

9. B. Schneider, J. Stokr, D. Doskocilova, M. Kolinsky, S. Sykora, and D. Lim, *Molecular Chemistry, Prague 1965* (*J. Polym. Sci. C*, **16**), O. Wichterle and B. Sedláček, Eds., Interscience, New York, 1968, p. 3891.

10. C. G. Opaskar and S. Krimm, *J. Polym. Sci. A-1*, **7**, 57 (1969).

11. R. D. Young, and V. R. Allen paper presented at American Chemical Society 158th Meeting, September 1969; *Polym. Preprints*, **10**, No. 2, 038 (1969).

12. G. Ajroldi, G. Gatta, P. Gugelmetto, R. Rettore, and G. P. Talamini, paper presented at American Chemical Society Meeting, Houston, Texas, February 1970; *Polym. Preprints*, **11**, No. 1, 357 (1970). We appreciate receipt of a preprint of the full paper from the authors.

13. V. Heidingsteld, V. Kuska, and J. Zelinger, *Angew. Makromol. Chem.*, **3**, 141 (1968).

14. S. Krimm and V. Liang, *J. Polym. Sci.*, **22**, 95 (1956).

15. A. M. Hassan, Armstrong Cork Co., personal communication, 1970.

16. J. L. Work, Ph.D. Thesis, Univ. of Delaware, Newark, Delaware, 1970.

17. S. Sobajima, N. Takagi, and H. Watase, *J. Polym. Sci. A-2*, **6**, 223 (1968).

18. G. Svegliado and F. Z. Grandi, *J. Appl. Sci.*, **13**, 1113 (1967).

19. William E. Collins (duPont Instrument and Equipment Division, E. I. duPont de Nemours, Inc., Wilmington, Delaware), private communication.

20. S. A. Liebman, J. F. Reuwer, Jr., C. R. Foltz, and R. J. Obremski, *Macromolecules*, **4**, 134 (1971).

Received December 29, 1970
Revised February 10, 1971

JOURNAL OF POLYMER SCIENCE: PART A-1 VOL. 9, 1937–1945 (1971)

Thermal Stability of Hydrogen Networks by Chemical Stress Relaxation

MONTGOMERY T. SHAW and ARTHUR V. TOBOLSKY,
Frick Chemical Laboratory, Princeton University,
Princeton, New Jersey 08540

Synopsis

The thermal stability of hydrocarbon networks by chemical stress relaxation was investigated *in vacuo* and in the temperature range 300–350°C. The polymers studied were low-density polyethylene, high-density polyethylene, and ethylene–propylene terpolymer. Carbon-carbon crosslinked networks were produced either by dicumyl peroxide or by radiation. The results show that the overall thermal stability is in the order: peroxide-cured EPT > peroxide-cured LDPE > peroxide-cured HDPE > radiation-cured HDPE. The results are in apparent contradiction to the belief that linear structures are more stable than branched structures. We believe that this can be explained in terms of weak linkages introduced during curing.

Introduction

The technique of chemical stress relaxation is a popular method for comparing the thermal and thermo-oxidative stabilities of elastomeric networks.[1,2] In experimental terms, the technique consists of imposing a fixed strain on the elastomeric sample, which is exposed to the desired thermal and chemical environment, and measuring the force required to maintain the strain. If conditions are such that chemical scission reactions can occur in the network chanins, the measured force will decay in proportion to the severing of the chains. These conditions can be made to approximate an actual use situation as closely as desired, or may be designed for answering theoretical questions.

The relaxation data are often presented as a semilogarithmic plot of the relative force (force at time t, divided by the initial force) versus time. This allows a quick comparison of the relative stabilities of different elastomers and an accurate estimate of the lifetimes of the materials used under similar conditions.

The development of saturated hydrocarbon elastomers, as exemplified by the ethylene–propylene terpolymers (EPT), has made available a class of networks exhibiting outstanding thermal stability.[2] Calorimetric or thermogravimetric pyrolysis studies in vacuum have consistently shown that saturated hydrocarbon polymers such as polyethylene and polypropylene are essentially unaffected by temperatures below 300°C.[3] Similar

studies have demonstrated that branched structures are generally less stable than linear molecules when decomposition (random cleavage) does occur.[4] Many saturated hydrocarbon polymers can be crosslinked by peroxides[5] or radiation[6,7] to yield network structures containing only carbon-carbon bonds in the polymer chains and crosslinkages. These networks will, of course, always be "branched" at the crosslink site, but other disturbances in the structures are thought to be negligible.

As high-temperature, vacuum stress relaxometers have developed,[8] it has become logical to compare the thermal stabilities of saturated hydrocarbons in network form, allowing detection of scission reactions, possible exchange-type reactions (which need not change molecular weight or lead to volatiles), or weak crosslinkages or other weaknesses introduced during crosslinking. In this study, crosslinked low- and high-density polyethylene (LDPE and HDPE, respectively) were the principal network materials, with some peroxide-cured EPT included for comparison. The results were not altogether as anticipated.

Experimental

HDPE samples, cured with 2.5 and 5% dicumyl peroxide (DiCuP), were prepared by Dr. R. Schaffhauser of Allied Chemical Corporation, Morristown, New Jersey. Radiation-cured (12 and 17 Mrad, electron beam) HDPE was supplied through the courtesy of Dr. R. Brand of Mobil Chemical Company, Metuchen, New Jersey, while Mr. I. L. Hopkins of Bell Telephone Laboratories, Murray Hill, New Jersey provided LDPE samples crosslinked with 2, 4, 8, and 16% dicumyl peroxide. The latter were extracted with benzene before use to remove peroxide inevitably remaining at such high cure levels. The EPT (Enjay 3509) was cured with ~1% dicumyl peroxide and extracted before use.

The stress relaxometer, previously described,[8] was operated under vacuum ($<0.5\ \mu$), with the exception of the EPT at 300 and 325°C, where a nitrogen atmosphere was used. All samples were held for not less than 12 hr of conditioning at 250°C under vacuum to eliminate oxygen and hydroperoxides, followed by 1 hr at the experimental temperature before force–time data were recorded.

Results and Discussion

The chemical stress relaxation curves are presented in Figures 1, 2, and 3 for runs at 300, 325, and 350°C, respectively. These temperatures cover the range of relaxation times for the networks which is practical experimentally. At temperatures much below 300°C, relaxation is negligibly slow, while at temperatures higher than 350°C degradation is so rapid that manipulation becomes impossible.

Relaxation times for the various materials at the temperatures studied are recorded in Table I as the times required for the force to decay to half of its initial value ($t_{1/2}$) and $1/e$ of its initial value ($t_{1/e}$), where reached.

TABLE I
Chemical Stress Relaxation of Hydrocarbon Networks *in Vacuo*

Polymer	Crosslinking agent	Crosslinker dose	Temp, °C	$n_e(0) \times 10^{-20}$ chains/cm³	$t_{1/2}$, sec $\times 10^{-4}$	$t_{1/e}$, sec $\times 10^{-4}$
High-density polyethylene (HDPE)	Dicumyl peroxide	2.5%	300	1.38	4.7	9.8
			325	0.71	0.59	0.98
			350	0.055	0.07	0.12
		5%	300	2.25	13	—
			325	1.24	0.72	1.1
			350	0.19	0.15	0.23
	Radiation	12 Mrad	300	0.26	1.3	—
			325	0.076	0.13	0.22
			350	0.007	0.02	0.03
		17 Mrad	300	0.47	2.3	—
			325	0.22	0.24	0.42
			350	0.033	0.053	0.083
Low-density polyethylene (LDPE)	Dicumyl peroxide	2%	300	0.27	0.56	0.96
			325	0.11	0.19	0.32
			350	0.014	0.047	0.073
		4%	300	0.36	1.7	—
			325	9.23	0.29	0.47
			350	0.023	0.075	0.11
		8%	300	0.78	5.8	—
			325	0.77	0.82	1.5
			350	0.22	0.19	0.29
		16%	300	2.45	~30	—
			325	1.82	2.9	5.6
			350	1.10	0.82	1.3
EPT	Dicumyl peroxide	~1%	300	—	12	—
			325	0.23	2.0	—
			350	0.13	0.37	0.8

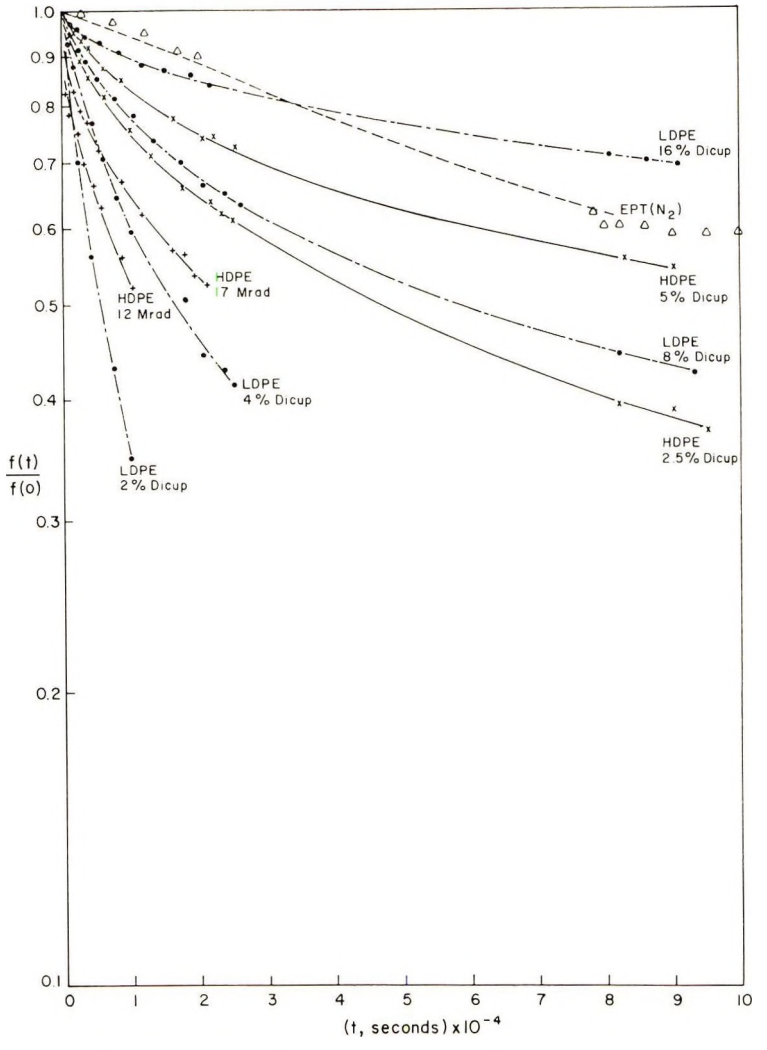

Fig. 1. Stress relaxation of hydrocarbon networks at 300°C *in vacu*.

The initial network chain densities, $n_e(0)$, are also included in Table I. The units of $n_e(0)$ are chains per cubic centimeter, computed from rubber elasticity theory.

The relaxation curves of Figures 1, 2, and 3 are, in nearly every case, with EPT as the possible exception, concave upwards; that is the relative force decay is less rapid than exponential. This is especially evident at the lower temperatures. Network theory requires that first-order, irreversible cleavage of main chain linkages, crosslinkages, or both should give a force relaxation which is exponential or faster than exponential.[9] The slower-than-exponential behavior under the conditions of these experiments means any or all of the following: additional crosslinking reactions during the experi-

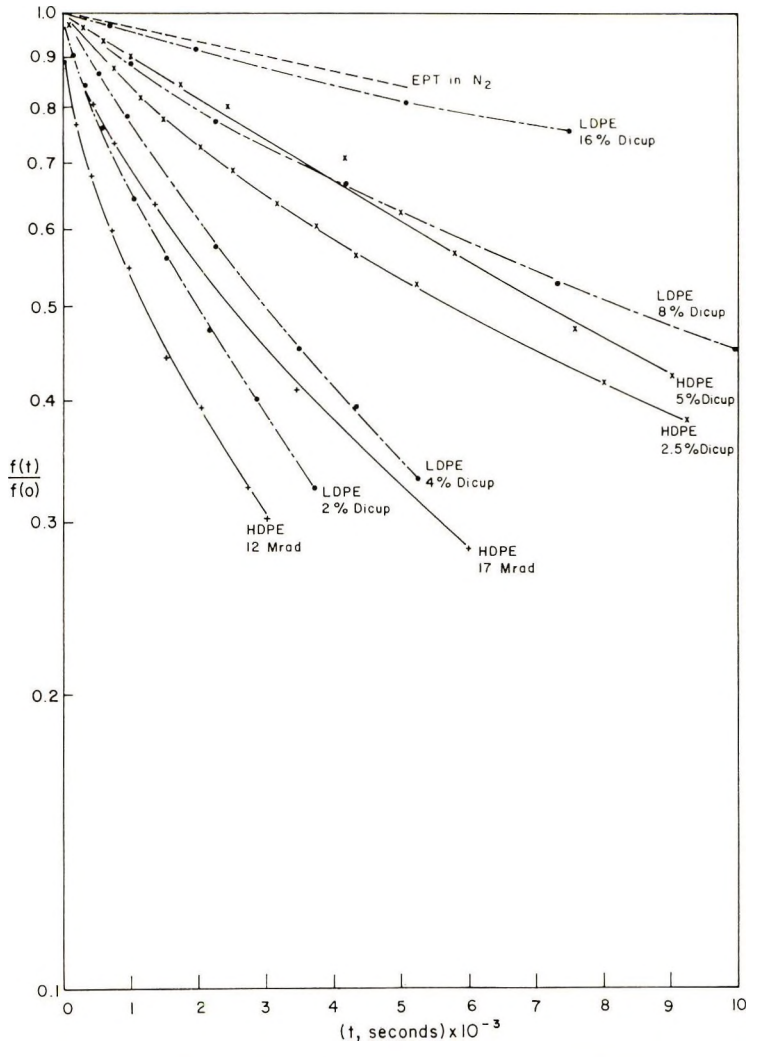

Fig. 2. Stress relaxation of hydrocarbon networks at 325°C in *vacu*.

ment, non-first-order reactions (weak linkages), or weight loss. The latter was excluded because correction for the weight loss (generally less than 1%) had little effect on the shape or the placement of the curves. Additional crosslinking or reversible reactions in these networks is generally quite small but cannot be discounted entirely. Weak linkages, we believe, can most easily account for much of the behavior of these networks, as will be explained.

In Figure 4, the relaxation half-times, $t_{1/2}$, are plotted against the initial network-chain density, $n_e(0)$. Log scales are used to permit inclusion of all data on a single plot. Figure 4 shows a definite, positive correlation between network stability and initial chain density, which is expected for

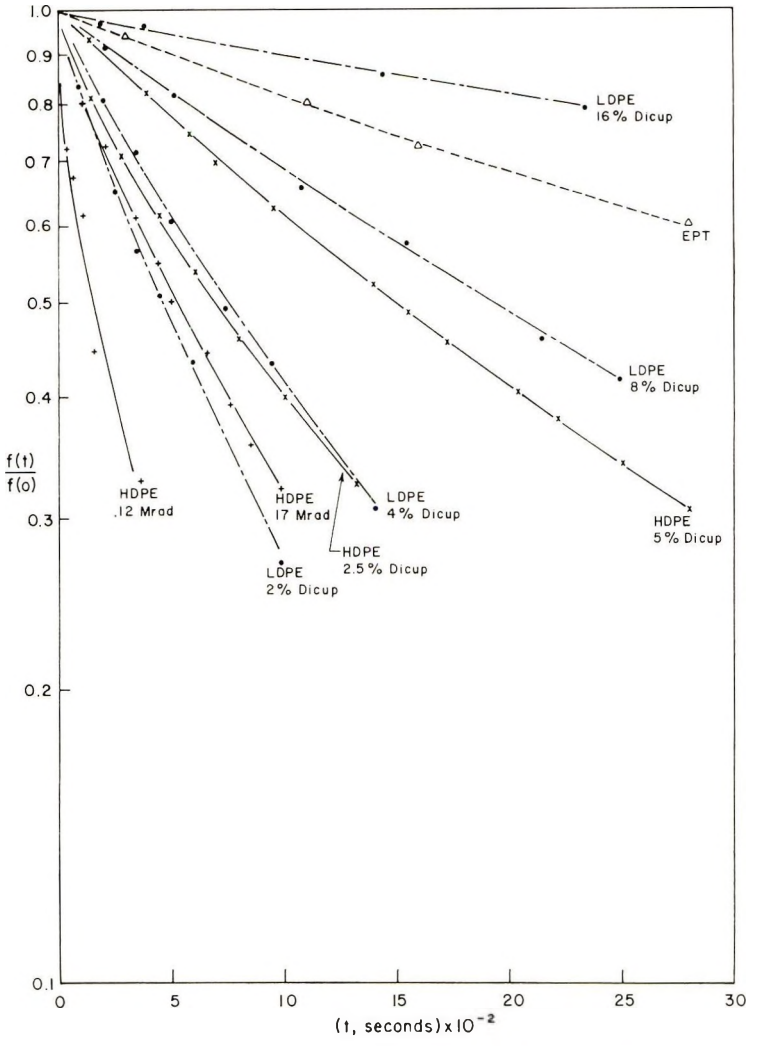

Fig. 3. Stress relaxation of hydrocarbon networks at 350°C *in vacu*.

elastomers where scissions occur along the main chains of the network.[1] More importantly, Figure 4 gives, at a glance, the order of stability of the networks at any given crosslink density and temperature. Surprisingly, HDPE (radiation-cured) is the least stable hydrocarbon network studied, while EPT, with the greatest branching frequency, is the most stable.

Figure 4 reveals some additional, less obvious generalizations which provide important clues. Taken by temperature groups, the curves in Figure 4 suggest an increasing dependence of $t_{1/2}$ on $n_e(0)$ at low temperatures, a dependence which even appears to exceed the first power of $n_e(0)$ at 300°C. In addition, the stability of the materials at 350°C is higher than what might be predicted from their behavior at 300°C and 325°C. (Note also

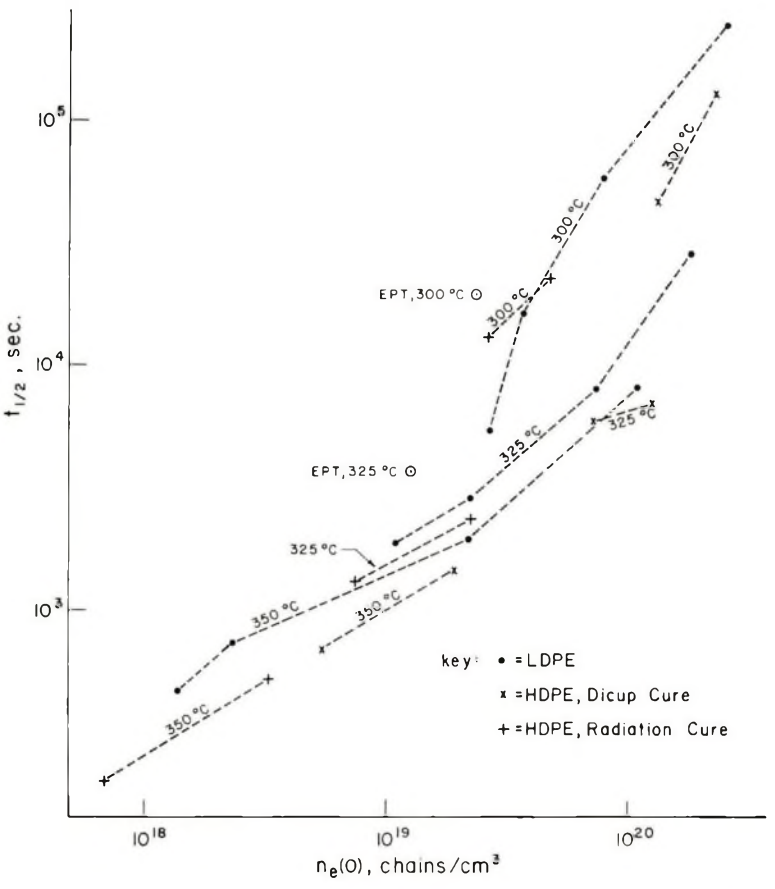

Fig. 4. Relaxation half-times as a function of network chain density at various temperatures.

that the crosslinking efficiency of DiCuP appears to be greater for HDPE than for LDPE.)

All of the foregoing results can be explained most realistically in terms of significantly weaker linkages present or introduced during the initial parts of the cure. The amounts need not be a large fraction of the total number of linkages, but the "weak links" present in the original hydrocarbon polymer molecules are probably not sufficiently numerous to produce all the observed effects.

Relating this premise to the experimental observations is not difficult. As mentioned earlier, a slowing of the force decay, especially at low temperatures, is good evidence for weak linkages. The weak linkages cause a rapid initial force decay, and as they disappear the network stabilizes. At higher temperatures the weak linkages break before the experiment begins: the log $f(t)/f(0)$ versus t curves show less upward curvature, and the networks possess unexpected stability. Curvature due to crosslinking reac-

tions would also lessen at higher temperatures (higher activation energy for scission than for crosslinking) but stabilization would not be expected.

The apparent greater-than-first-power dependency of $t_{1/2}$ on $n_e(0)$ at 300°C would be very difficult to rationalize in terms other than weak linkages. An explanation based upon additional crosslinking, which would have the greatest effect at low crosslink densities, is particularly inadequate.

Required for all explanations is a proportionally greater number of weak linkages at the low crosslink densities, implying that (a) weak crosslinkages are introduced first, followed by stronger crosslinks, or (b) weak linkages are present in the molecules before any crosslinking, among other possibilities. Case a is most plausible for LDPE, which is a branched structure. The peroxide curing agent removes preferentially the hydrogen atoms at the branch points, giving tertiary radicals. The small proportion of these which do combine (disproportionation dominates, giving unsaturation and lowering crosslinking efficiency)[5] could form the weak crosslinkages. Additional weak crosslinkages might result from radical crosslinking reactions at the allyl sites produced by the disproportionation. As these sites are exhausted, secondary radicals are dominantly formed, which combine to yield stronger crosslinkages. These strong crosslinkages provide the observed stabilization of the networks with time, temperature, and crosslink density.

A structure-behavior relationship for HDPE, a simpler molecule, is not obvious. The relaxation curves for HDPE do show marked curvature, and Figure 4 does show evidence of temperature stabilization. Weak linkages may be present in HDPE in sufficient numbers before crosslinking (case b above) or there may be a tendency for weak unsaturated structures to congregate in some chains (by radical migration),[6] leaving others unweakened. In any case, the instability of network HDPE relative to LDPE is good evidence for an abundance of weak linkages in radiation and peroxide-cured LDPE.

EPT, with its built-in crosslinking sites, apparently weathers the cure unscathed, developing a minimum of weak linkages. The thermal stability of EPT would probably show little increase (or even a decrease) if an overcure were forced by using large amounts of peroxide.

Conclusions

Networks based on saturated hydrocarbon polymers cured with peroxide or radiation decompose thermally at measurable rates (by chemical stress relaxation) in the temperature range 300–350°C. Overall thermal stability is in the order: peroxide-cured EPT > peroxide-cured LDPE > peroxide-cured HDPE > radiation-cured HDPE. The apparent inconsistency of this result with the known greater stability of linear versus branched structures can be explained in terms of weak linkages introduced during curing.

The partial support of the Office of Naval Research is gratefully acknowledged.

References

1. A. V. Tobolsky, *Properties and Structure of Polymers*, Wiley, New York, 1960, pp. 223–265.

2. T. C. P. Lee, L. H. Sperling, and A. V. Tobolsky, *J. Appl. Polym. Sci.*, **10,** 1831 (1966).

3. J. V. Schooten and P. W. O. Wijga in *Thermal Degradation of Polymers*, (S.C.I. Monograph No. 13), Soc. Chem. Ind., London, 1961, p. 433.

4. R. H. Hansen in *Thermal Stability of Polymers*, Vol. 1, R. T. Conley, Ed., Dekker, New York, 1970, p. 155.

5. L. D. Loan, *J. Polym. Sci. A*, **2,** 3053 (1964).

6. S. Ohnishi, S. Sugimoto, and I. Nita, *J. Polym. Sci. A*, **1,** 605 (1963).

7. Y. Okada in *Irradiation of Polymers* (*Advan. Chem. Ser.*, **66**) American Chemical Society, Washington, D.C., 1967, p. 44.

8. M. T. Shaw, *Rev. Sci. Instr.*, in press.

9. J. Scanlan, *J. Polym. Sci.*, **43,** 501 (1960).

Received March 11, 1971
Revised March 29, 1971

JOURNAL OF POLYMER SCIENCE: PART A-1 VOL. 9, 1947–1958 (1971)

Polyesters. I. Rate of Polyesterification of γ-Arylitaconic Acids with Ethylene Glycol

F. G. BADDAR, M. H. NOSSEIR, G. G. GABRA, and N. E. IKLADIOUS,
Faculty of Science, Ain Shams University, and Polymer and Pigment Laboratory, National Research Centre, Cairo, U.A.R.

Synopsis

A kinetic study of the polyesterification reaction of γ-phenyl- γ-*p*-methoxyphenyl-, and γ-*p*-chlorophenylitaconic acids (1 mole) with ethylene glycol in the presence or in absence of *p*-toluenesulfonic acid as a catalyst has been carried out in order to show the effect of substituents on the rate and degree of polymerization. The reaction of 1 mole of the acid and an excess of ethylene glycol has also been studied. In all cases the reaction is found to follow the second-order rate equation. The mechanism of polyesterification has been discussed. In catalyzed polyesterification electron-withdrawing groups (Cl) decrease the velocity of the reaction. The low values of ρ in both the autocatalyzed and catalyzed reaction indicate that this polyesterification is slightly sensitive to the polar nature of the substituent.

INTRODUCTION

Many experimental studies on the polyesterification reactions between aliphatic dibasic acids and glycols have been reported by many authors among them Menshytkin,[1] Dostal and Raff,[2] Flory,[3] Rafikov and Korshak,[4] Colonge and Stuchlik,[5] Davies,[6] and Tang and Yao[7] but quite varied results were obtained. Flory[3] reported that polyesterification in the absence of a foreign acid is a third-order reaction. Other authors, however, pointed out that polyesterification follows a second-order rate equation, at least at the early stage of the reaction, and the reaction may be third order in the later stages.

In the present investigation the kinetics of polyesterification of substituted phenylitaconic acids (*trans*-COOH)

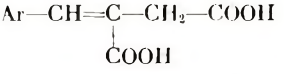

with ethylene glycol were determined in order to study the effect of substituents on both the rate and degree of polymerization.

EXPERIMENTAL

Materials

γ-Phenylitaconic acid,[8] γ-*p*-methoxyphenylitaconic acid,[9] and γ-*p*-chlorophenylitaconic acid[10] were prepared by the methods described in the litera-

ture and were used after being crystallized twice. Ethylene glycol was carefully fractionally distilled, and the fraction boiling at 197°C was collected.

Apparatus and Procedure

The apparatus consisted of a two-necked, round-bottomed flask provided with an inlet for dry carbon dioxide gas and an outlet provided with a calcium chloride tube. The flask was heated in an oil bath maintained at constant temperature within ±0.5°C throughout any one experiment. The data were taken at 140, 160, and 180°C. The reaction was followed by the titration of the total free carboxyl in samples (ca. 20 mg) removed from the mixture at suitable intervals with 0.04 *N* alcoholic potassium hydroxide, phenol red being used as an indicator (grade A automatic buret was used in the titration). The end points were very sharp. Reactions catalyzed with *p*-toluenesulfonic acid were carried out in the same manner, except that the calculated amount of the catalyst needed for the three runs was dissolved in the glycol in order to keep the catalyst concentration constant, and then the calculated amount of glycol for each temperature was taken from the mixture. Each experiment was repeated twice and the results were reproducible. The amount of the catalyst was very small compared with that of the itaconic acid derivatives, and accordingly no correction was made in determining the amount of the unreacted acid in the kinetic runs. The correction was found to fall within the range of the experimental error.

Ozonolysis of the Polyester

A chloroform solution of the polyester from γ-phenylitaconic acid (IVa) (1.8 g) was treated with ozone for 3 hr, then the formed ozonide was decomposed with water, zinc dust and dilute acetic acid. The product was steam-distilled in a stream of carbon dioxide, and the distillate, was extracted with ether, dried, and the solvent removed to give benzaldehyde (0.8 g). This was identified and estimated as its 2,4-dinitrophenylhydrazone (2.1 g), mp 237°C, undepressed with an authentic specimen. The amount of DNP isolated is equivalent to

$$2.1 \times \frac{\text{MW of } C_7H_6}{\text{MW of DNP}} = 2.1 \times \frac{90}{285}$$

$$= 0.663 \text{ g benzylidene}$$

i.e., 1.8 g of polymer contains 0.663 g of benzylidene residue.

RESULTS AND DISCUSSION

The unbranched nature of the polyesters was established by ozonolysis and NMR spectra.

Ozonolysis

Isolation of benzaldehyde by ozonolysis of the polyester (IVa) shows that it contains a benzylidene group. The experimental result shows that the ratio of the polyester (IVa) or its segmer (A) to the benzylidene residue is 1.8/0.663 = 2.7. The calculated ratio is

$$\frac{\text{MW of segmer of IVa}}{\text{MW of } C_7H_6} = \frac{232}{90} = 2.6$$

This shows that each segmer contains one benzylidene residue, i.e., there is no branching.

NMR Spectrum

The integrated NMR spectrum of IVa (Fig. 1) shows the following signals: singlet at τ 6.4 (2p), triplet at τ 5.6 (4p), singlet at τ 2.6 (5p), and nonsymmetrical singlet at τ 2.0 (1p). These signals are characteristic of C_6H_5—C=C—CH_2—CO—,[11a] —CO—O—CH_2—CH_2—O—CO—,[11b] aromatic protons and olefinic proton in C_6H_5—CH=C—CO—,[11c] respectively. The nonsymmetry of the signal for the olefinic protons may be due to weak coupling with the *trans* CH_2.

Both these observations substantiate the structure assigned to the polyester and prove that it contains no branching. The failure of branching may be attributed to steric factors.

As in simple esterification the reaction between substituted γ-arylitaconic acids and ethylene glycol is found to be acid-catalyzed. In the absence of an added foreign acids, a second molecule of the acid undergoing esterification functions as a catalyst and the rate constant is given by the rate expression

$$-d[\text{COOH}]/dt = k[\text{COOH}]^2[\text{OH}]$$

The hydrogen ion comes from the ionization of the dibasic acid and the esterification is supposed to take place according to the mechanism reported by Tang and Yao.[7]

In the uncatalyzed polyesterification of γ-arylitaconic acids (1 mole) and ethylene glycol (1 mole), the relation between $[1/(1-p)]$, $[1/(1-p)]^{3/2}$ and $[1/(1-p)]^2$ has been plotted graphically against t. The best straight lines were obtained by plotting $1/(1-p)$ versus t, i.e., the reaction could be described as a second-order one (bimolecular). From the slope of the straight line the value of k_2 has been calculated as shown in Table I by using eq. (1):

$$C_0k_2t = [1/(1-p)] - 1 \qquad (1)$$

where C_0 is the initial concentration in equivalents of OH or COOH group per liter, k_2 is the velocity constant in liters per equivalent per minute, t

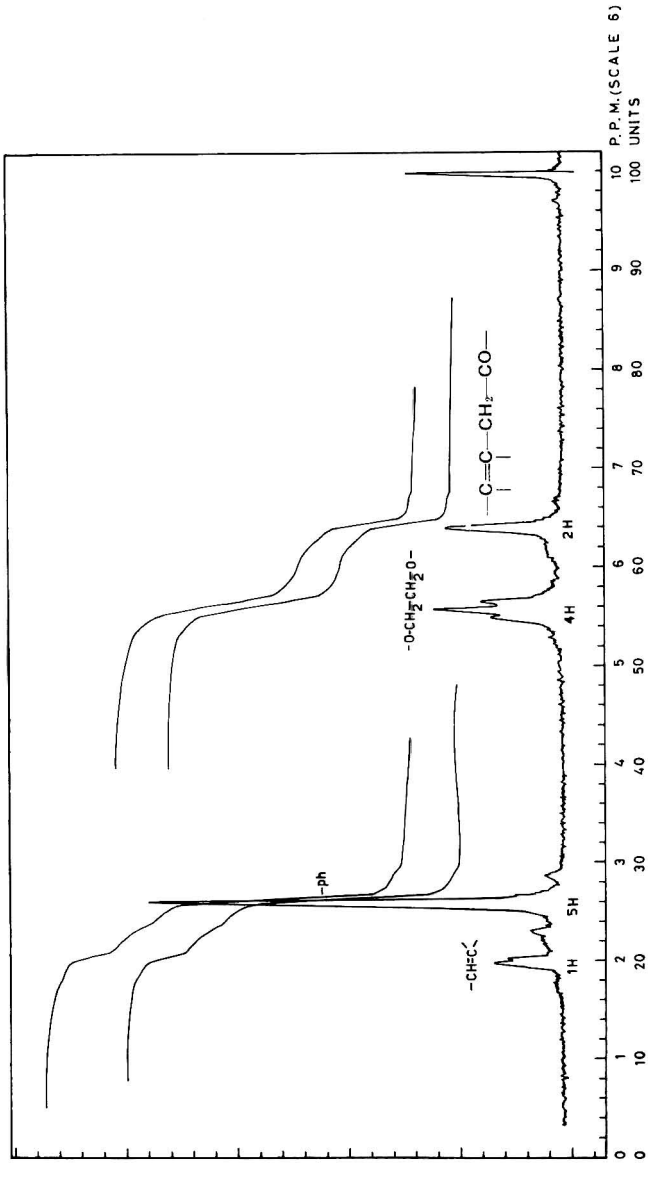
P.P.M.(SCALE 6)
UNITS
-CH=C<
-ph
-O-CH2-CH2-O-
-C=C-CH2-CO-
1H
5H
4H
2H
COMPOUND: [CO-C-CH2-CO-O-CH2-CH2-O]n
CH
Ph

Figure 1.

TABLE I
Velocity Constants and Energies of Activation for the Uncatalyzed Polyesterification of Arylitaconic Acids with Ethylene Glycol

Acid	$k_2 \times 10^4$, l./eq.-min			ΔE, kcal/mole
	140°C	160°C	180°C	
γ-Phenylitaconic	1.606	4.136	12.048	18.8
γ-*p*-Methoxyphenylitaconic	1.216	2.834	7.649	17.2
γ-*p*-Chlorophenylitaconic	2.008	4.460	10.030	15.2

TABLE II
Velocity Constants and Energies of Activation for the Catalyzed Polyesterification of γ-Arylitaconic Acids and Ethylene Glycol

Acid	$k_2 \times 10^4$, l./eq-min			ΔE^* kcal/mole
	140°C	160°C	180°C	
γ-Phenylitaconic	4.015	7.445	12.048	11.5
γ-*p*-Methoxyphenylitaconic	4.015	8.036	16.867	13.7
γ-*p*-Chlorophenylitaconic	3.476	6.024	10.030	10.0

is the time in minutes, and p is the extent of the reaction, i.e., the fraction of the COOH groups which has reacted at time t.

As one molecule of the acid acts as a catalyst, one should expect the reaction to follow the third-order rate equation [eq. (2)]:[12]

$$2C_0k_3t = [1/(1 - p)]^2 - 1 \quad (2)$$

where k_3 is in (liters per equivalent)^2 per minute. This, however, could be explained by the fact that since the protonation step is reversible, then although such a reaction should show a third order kinetics, Schulz[13] reported that it may follow the second-order rate eqution.

The rates of polyesterification of γ-arylitaconic acids with ethylene glycol catalyzed by a small amount of *p*-toluenesulfonic acid (0.004 mole/mole glycol) were determined, and the reaction was found to follow the second-order rate equation. Table II shows the k_2 values for the catalyzed reactions.

Mechanism of Polycondensation

Substituted γ-arylitaconic acids contain two carboxyl groups, one of them attached to the methylene group and the other attached to C=C; therefore, one must follow whether esterification takes place first on the carboxyl group attached to the α- or β-carbon atom. On simple esterification of these acids with methanol in presence of sulfuric acid the α-half ester (Ia) is obtained; this shows that at the beginning of esterification the α-half ester (I) is formed, i.e., the carboxyl group not conjugated with the benzene is more rapidly esterified than the second carboxyl group. Accordingly the latter step can be considered to be the rate-determining step

in the diesterification of γ-arylitaconic acid. The conclusion that the formation of the α-half ester (Ib) is a rapid process was also inferred from the observation that the reaction is very rapid in the first 30 min, nearly half of the phenylitaconic acid being consumed.

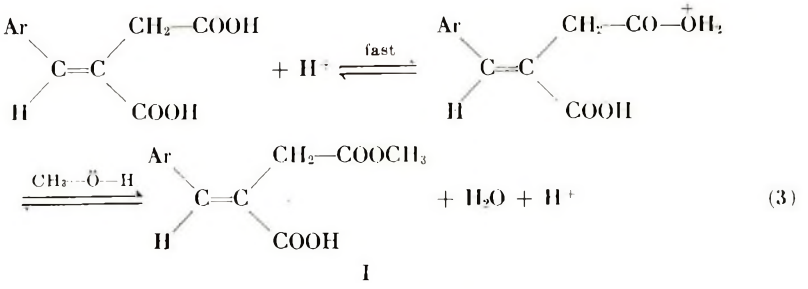

I

In the reaction with ethylene glycol, the first step is supposed to take place according to eq. (3) to give II.

The mechanism (4)–(5) is supposed for the following steps:

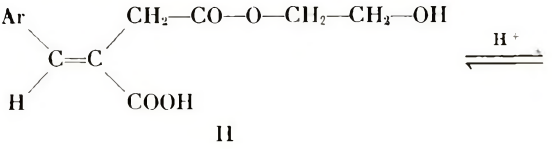

II

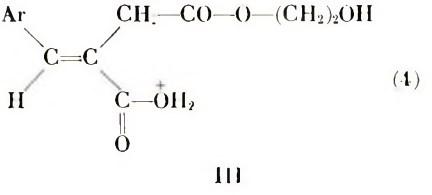

(4)

III

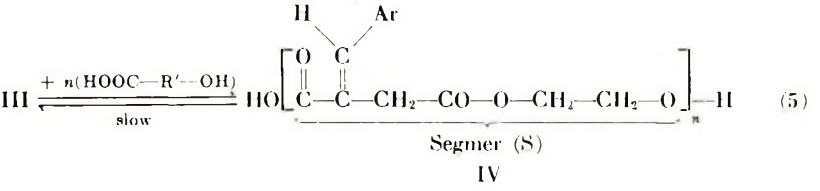

(5)

Segmer (S)

IV

(a) Ar = C_6H_5
(b) Ar = p-$CH_3O.C_6H_4$
(c) Ar = p-$Cl.C_6H_4$

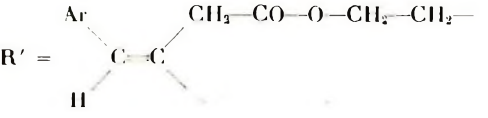

Polycondensation occurs by the repetetion of step (5).

In catalyzed polyesterification the reaction takes place by the same mechanism, the only difference being that the proton catalyzing the reaction comes from p-toluenesulfonic acid.

Effect of the Nature of Substituent on Reaction Rate

Since the esterification of the carboxyl group conjugated with the aromatic nucleus, i.e., the β-carboxyl group, is considered to be the rate-determining step, the effect of substitution on the rate of polyesterification could be compared with that observed in the esterification of benzoic and cinnamic acids.

Hartman and Borders[14] found that the velocity of hydrion-catalyzed esterification of substituted benzoic acids decreased in the following order:

$$p\text{—}CH_3 > H > p\text{—}Cl > p\text{—}NO_2$$

Anomalies in the order of the effect of halogen substituents upon the velocity of side chain reactions have been noted by Evans et al.,[15] who stated that the *para* halogen substituents often give peculiar velocity effects.

This order agrees very closely with that found in the catalyzed polyesterification of substituted γ-arylitaconic acids, i.e., electron-withdrawing groups (e.g. Cl) decreased the velocity of polyesterification (cf. Table II).

On comparing the autocatalyzed with the catalyzed reaction it is concluded that the reaction velocity in the autocatalyzed polyesterification of substituted γ-arylitaconic acids is much slower than the catalyzed reaction, in spite of the fact that the activation energy is not much greater (Table I). This indicates that the factor P in Arrhenius equation is much greater for the reaction involving a charged catalyst.

Also, the autocatalytic polyesterification of γ-*p*-chlorophenylitaconic acid at 140 and 160°C is more rapid than that of γ-*p*-methoxyphenylitaconic acid, and the activation energy is correspondingly lower (Table I). This is what would be expected from the polar effect of chlorine atom in facilitating the attack of the alcoholic oxygen atom on the carbonyl carbon atom of the acid. The effect may be also attributed to the higher degree of ionization of the γ-*p*-chlorophenylitaconic acid (electron-withdrawing groups increase the degree of ionization, i.e., greater concentration of hydrogen ions).

The deviation in the velocity of the polyesterification of γ-*p*-chlorophenylitaconic acid at 180°C (Table I) may be attributed to the fact that at this temperature the acid loses water to form the corresponding anhydride[17] more easily than γ-phenylitaconic acid. Since the rate of the uncatalyzed polyesterification of the anhydride is lower than that of the corresponding acid (Table III), then the conversion of the acid into its anhydride at this high temperature will cause a decrease in the rate of polyesterification.

The fact that the anhydrides are known to be more easily monoesterified than the corresponding acids[19] could be considered to be good evidence that the first step in the polyesterification is not the rate-determining step, since the rates of polyesterification of the anhydrides are found to be much lower than those of the corresponding acids (Table III).

It appears from the present investigation that the rate of the reaction of the catalyzed polyesterification at 140 and 160°C is always faster than

TABLE III
k_2 Values for the Uncatalyzed Polyesterification Reaction of Arylitaconic Acids and Their Anhydrides with Ethylene Glycol at 160 and 180°C

	$k_2 \times 10^4$, l./eq-min			
	Acids		Anhydrides[a]	
	160°C	180°C	160°C	180°C
γ-Phenylitaconic	4.136	12.048	1.79	5.60
γ-*p*-Methoxyphenylitaconic	2.834	7.649	1.14	2.44
γ-*p*-Chlorophenylitaconic	4.46	10.03	1.93	6.79

[a] Data of Faltus.[18]

TABLE IV
k_2 Values for the Catalyzed Polyesterification of Arylitaconic Acids and Their Anhydrides with Ethylene Glycol at 160 and 180°C

	$k_2 \times 10^4$, l./eq-min			
	Acids		Anhydrides[a]	
	160°C	180°C	160°C	180°C
γ-Phenylitaconic	7.445	12.048	2.09	6.996
γ-*p*-Methoxyphenylitaconic	8.036	16.867	1.574	3.740
γ-*p*-Chlorophenylitaconic	6.024	10.030	3.754	—

[a] Data of Faltus.[18]

TABLE V
Log k_2 and ρ Values for the Polycondensation of *p*-Substituted Arylitaconic Acids and Ethylene Glycol at 140, 160, and 180°C

	log k_2			
Temperature, °C	*p*-Methoxyphenyl derivative	Phenyl	*p*-Chlorophenyl derivative	ρ
140	−3.9151	−3.7943	−3.6973	+0.4
160	−3.5476	−3.3834	−3.3504	—
180	−3.1164	−2.9191	−2.9988	—

TABLE VI
Log k_2 and ρ Values for the Catalyzed Polycondensation of *p*-Substituted Arylitaconic Acids and Ethylene Glycol at 140, 160, and 180°C

	log k_2			
Temperature, °C	*p*-Methoxyphenyl derivative	Phenyl	*p*-Chlorophenyl derivative	ρ
140	−3.3964	−3.3964	−3.4593	−0.133
160	−3.0950	−3.1281	−3.2201	−0.24
180	−2.7729	−2.9191	−2.9988	−0.4

that of the uncatalyzed one. However, this is not the case in the polyesterification of γ-phenylitaconic and γ-*p*-chlorophenylitaconic acids at 180°C, since the catalyzed and uncatalyzed polyesterification were found to have the same rate. This abnormal result may be attributed to the ease of conversion of these acids into their anhydrides. As mentioned before, the anhydrides were found to undergo polyesterification much more slowly than the corresponding acids (Tables III and IV), and the rate of their polyesterification is not appreciably affected by the presence of the catalyst.

In autocatalyzed polyesterification the Hammett equation[20] is obeyed only at 140°C (Table V) and ρ has a positive value, which is consistent with experimental fact that electron-withdrawing groups enhance esterification.

The negative sign of the ρ values for the catalyzed polyesterification (Table VI) confirms the experimental data that the reaction is enhanced by electron-releasing groups and retarded by electron-withdrawing groups. The low values in both cases indicate that this polyesterification is slightly sensitive to the polar nature of the substituent.

Relation between log k and ΔE^*

It is apparent that for the acids studied the range of velocities was not sufficient to permit accurate analysis of the factors of the Arrhenius equation. All of the acids fall within a range in which the ratio of velocities of the fastest to the slowest is about 6:1. If the change in velocity of polyesterification produced by the substituents was entirely due to change in ΔE^*, the points on the graph for log k versus ΔE^* should lie on a straight line having a slope of $2.303RT$.[14] From the data it was found that the slope differs from the theoretical one, from which it may be concluded that the factor P also varies.

As shown in Table II, the energies of activation for the polyesterification reactions fall between 10 and 13.7 kcal/mole. The values agree with those obtained in case of substituted benzoic acid.[14]

ΔS for the reaction is very low (Table VII), which may be due to the restricted movement of the molecule in the transition state due to the viscosity of the reaction medium.

Properties of the Polyesters

The polyesters produced by heating γ-arylitaconic acids with ethylene glycol to an advanced stage of esterification contain at least 6–8 condensa-

TABLE VII
ΔS Values for the Autocatalyzed and Catalyzed Reactions at 160°C

Acid	ΔS, eu	
	Autocatalyzed	Catalyzed
γ-Phenylitaconic	−33.2	−49.11
γ-*p*-Methoxyphenylitaconic	−37.8	−43.7
γ-*p*-Chlorophenylitaconic	−41.4	−52.8

TABLE VIII
Molecular Weight by the Endgroup Method

Temperature, °C	Molecular weight		
	IVa	IVb	IVc
	Polyesters obtained without catalyst		
140	602	636	710
160	934	858	1064
180	1318	1188	1654
	Polyesters obtained with catalyst		
140	704	850	898
160	1236	1188	1460
180	1664	1846	1996
	Polyester obtained with excess of ethylene glycol		
160	5283		

TABLE IX

Compound	MW[a]	λ_{max}, mμ	Absorbance of $10^{-5}M$ soln of acid A_a	Absorbance of $10^{-5}M$ soln of polymer A_p	$n = \frac{A_p}{A_a}$	MW = $n \times$ MW of segmer + H_2O
γ-Phenylitaconic acid	206	265	0.19			
Polymer IVa at 160°C with catalyst	1236	265		0.9545	5.0	1178
Polymer IVa at 180°C with catalyst	1664	265		1.43	7.5	1740
γ-*p*-Methoxyphenyl-itaconic acid	236	290	0.203			
Polymer IVb at 180°C	1188	292		0.855	4.2	1118
γ-*p*-Chlorophenyl-itaconic acid	241.5	265	0.2388			
Polymer IVc at 140°C	710	267		0.49	2.3	615

[a] The molecular weight of the polymer is that determined by the end group method.

tion units per mole. Higher molecular weight polyesters up to 2000 have been obtained when the polycondensation was carried out in presence of *p*-toluenesulfonic acid. The produced polyesters are in the form of crystalline, yellow, glasslike fibers which can be easily crushed. They are soluble in most organic solvents, insoluble in carbon tetrachloride, *n*-hexane and light petroleum.

These polyesters can not be crosslinked even with styrene or methyl methacrylate, or with benzoyl peroxide. No appreciable change in the physical properties was observed when these polyesters were subjected to γ-radiation (0.3053×10^6 rad/hr).

The failure of these polyesters to undergo free radical polymerization may be attributed to steric factors. It may also be due to the neighbouring electron-withdrawing carboxyl group, since the polymerization of itaconic acid itself is rather difficult.[21]

Their molecular weights were determined by the end group method[22–24] (cf. Table VIII) and compared with those obtained from the ultraviolet data (cf. Table IX), which proved to be in fairly good agreement.

Determination of Molecular Weight from Electronic Spectral Data

It is a known fact that the absorbance at λ_{max} of a molecule containing several identical isolated chromophores is given by the term nA (where n is the number of chromophores and A is the absorbance of a single chromophore at the same molar concentration).

Since the polymer (IV) consists of several isolated γ-arylitaconic acid chromophores, then absorbance (A_p) of a known concentration of the polymer (say 10^{-5} mole/l.) in dioxane is given by $A_p = n$[average number of γ-arylitaconic acid residues (or segmers, s, see IV) × absorbance (A_a) of 10^{-5} mole/l. of the solution of γ-arylitaconic acid in dioxane.

On taking the molecular weight of the polymer determined by the end-group method for preparing the 10^{-5} M solution of the polymer and determining the absorbances of the polymer and the γ-arylitaconic acid at λ_{max}, n can be calculated:

$$\text{MW of polymer} = n \times \text{MW of segmer (s)} + H_2O$$

The results are reported in Table IX.

The authors wish to express their thanks to Dr. J. Webber, Department of Chemistry, The University of Birmingham, U.K., for running the NMR spectrum.

References

1. N. N. Menshytkin, *Ber.*, **15**, 562 (1882).
2. H. Dostal and R. Raff, *Monatsh.*, **68**, 117, 188 (1936).
3. P. J. Flory, *J. Amer. Chem. Soc.*, **59**, 466 (1937).
4. S. R. Rafikov and V. V. Korshak, *Dokl. Akad. Nauk SSSR*, **64**, 211 (1949).
5. J. Colonge, and P. Stuchlik, *Bull. Soc. Chim. France*, **17**, 267 (1950).
6. M. Davies, *Research* (London), **2**, 544 (1949).
7. Tang A.-C. and Yao K.-S., *J. Polym. Sci.*, **35**, 219 (1959).
8. H. Stobbe, *Ber.*, **41**, 4350 (1908).
9. A. M. El-Abbady, and L. S. El-Assal, *J. Chem. Soc.*, **1959**, 1024.
10. A. M. El-Abbady, S. H. Doss, H. H. Mousa, and M. Nosseir, *J. Org. Chem.*, **26**, 4871 (1961).
11. D. W. Mathieson, *Nuclear Magnetic Resonance*, Academic Press, New York–London, 1967, (a) spectrum 4, p. 253; (b) spectrum 5, p. 253; (c) Table 4, p. 183.
12. T. Skwarski, *Zeszyty Nauk. Politech. Lodz*, **4**, 41 (1956).
13. G. V. Schulz, *Z. Physik Chem.*, *A* **182**, 127 (1938).
14. R. J. Hartman and A. M. Borders, *J. Amer. Chem. Soc.*, **59**, 2107 (1937).
15. D. P. Evans, V. G. Morgans, and H. B. Watson, *J. Chem. Soc.*, **1933**, 1168.
16. A. Michael and K. J. Oechslin, *Ber.*, **42**, 317 (1909).
17. A. Brooke, *Ann.*, **305**, 21 (1899).

18. Polyesters II. F. G. Baddar, M. H. Nosseir, N. N. Messiha and B. M. Faltas, accepted for publication in Europ. Polym. J.

19. E. F. Siegel and M. K. Moran, *J. Amer. Chem. Soc.*, **69**, 1456 (1947).

20. L. P. Hammett, *Chem. Revs.*, **17**, 125 (1915).

21. D. Braun, and A. El-Sayed, *Makromol. Chem.*, **96**, 100 (1966).

22. K. G. Cunningham, W. Dawson, and F. S. Spring, *J. Chem. Soc.*, **1951**, 2305.

23. J. C. P. Schwarz, *Physical Methods in Organic Chemistry*, Oliver and Boyd, London, 1964, pp. 163, 260.

24. P. W. Allen, *Techniques of Polymer Characterisation*, Butterworths, London, 1959.

Received May 12, 1970
Revised June 29, 1970

JOURNAL OF POLYMER SCIENCE: PART A-1 VOL. 9, 1959–1970 (9171)

Constitutive Equations for Elastomers

NICHOLAS W. TSCHOEGL, *Division of Chemistry and Chemical Engineering, Pasadena, California 91109*

Synopsis

General relations were derived by expanding the strain-energy density function in terms of the invariants of the deformation tensor. Some constitutive equations obtained by keeping a third term in the expansion in addition to the two terms retained in the Mooney-Rivlin equation were tested in the light of currently available experimental data. It is shown that by the retention of the third term the upswing in the Mooney stress at low values of λ^{-1} is successfully predicted, and the stress–strain behavior can be described with excellent accuracy up to break, even in carbon black-filled rubber which is notoriously difficult to describe by the Mooney-Rivlin equation.

INTRODUCTION

The continuum mechanical derivation of constitutive equations for elastomeric materials is based on the concept of a strain energy density function or elastic potential W, representing the change in the Helmholtz free energy of the material upon deformation. Expanding W in terms of the invariants of the deformation tensor,

$$I_1 = \lambda_1^2 + \lambda_2^2 + \lambda_3^2 \tag{1a}$$

$$I_2 = \lambda_1^2\lambda_2^2 + \lambda_2^2\lambda_3^2 + \lambda_3^2\lambda_1^2 \tag{1b}$$

and

$$I_3 = \lambda_1^2\lambda_2^2\lambda_3^2 \tag{1c}$$

leads,[1] for an imcompressible body (for which $I_3 = 1$), to

$$W = \sum_{i,j=0}^{\infty} c_{ij}(I_1 - 3)^i(I_2 - 3)^j \tag{2}$$

where the c_{ij} are material constants ($c_{00} \equiv 0$). In eqs. (1) λ_1, λ_2, and λ_3 are the stretch ratios in the three principal directions.

In simple tension, the stress σ (calculated on the undeformed cross section), is the derivative of the strain energy density, W, with respect to the principal stretch ratio λ, i.e.,

$$\sigma = \partial W/\partial\lambda \tag{3}$$

Retention of the first two terms, ($i, j \leq 1$) in the expansion of W, eq. (2), yields the Mooney-Rivlin equation

$$\sigma = 2(c_1 + c_2\lambda^{-1})(\lambda - \lambda^{-2}) \tag{4}$$

where $c_1 = c_{10}$, and $c_{01} = c_2$.

According to the infinitesimal theory of elasticity, for an incompressible body

$$\sigma = 3G\epsilon \tag{5}$$

where G is the shear modulus, and $\epsilon = \lambda - 1$ is the Cauchy strain. Any constitutive equation must, therefore, reduce to eq. (5) as $\lambda \to 1$, i.e., it must obey the relation

$$\lim_{\lambda \to 1} [\sigma/(\lambda - 1)] = 3G \tag{6}$$

Inserting eq. (4) into eq. (6) and applying L'Hospital's rule shows that

$$2(c_1 + c_2) = G \tag{7}$$

Statistical mechanical considerations based on Gaussian chain statistics lead to the constitutive equation[2]

$$\sigma = G(\lambda - \lambda^{-2}) \tag{8}$$

Equation (8) may also be obtained from eq. (3) by retaining only the first term, c_{10}, in the expansion of W. Inserting eq. (8) into eq. (6) gives

$$2c_1 = G \tag{9}$$

Equations (4) and (8) are thus mutually exclusive.

Experimental data, when plotted as σ versus λ or $\lambda - \lambda^{-2}$ (i.e., in stress–strain coordinates) reasonably well obey eq. (8) in simple tension and simple compression with the same value of the modulus, G, for moderate deformations.[2] The same data, however, when plotted as $\sigma/(\lambda - \lambda^{-2})$ versus λ^{-1} (i.e., in Mooney coordinates), commonly obey eq. (4) for values of λ^{-1} greater than about 0.4–0.5, albeit different values of the modulus are usually obtained when the data are fitted in the two sets of coordinates. Data obtained in simple tension and compression cannot generally be fitted in Mooney-Rivlin coordinates with the same value of G. For small values of λ^{-1} (less than about 0.4–0.5), the Mooney stress, $\sigma/(\lambda - \lambda^{-2})$, generally shows an upswing not predicted by eq. (5).

These inadequacies must be the result of neglecting higher terms in the expansion, eq. (3). No investigation appears to have been made, however, of constitutive equations derived by keeping higher terms. In the following sections we will deduce and then put to the test constitutive equations in which higher terms in the expansion are retained. It will be shown that one or the other of several possible three-term expansions predicts the upswing successfully, and that the stress-strain curve can be described with three constants with satisfactory accuracy up to break.

An extension of the statistical mechanical theory of rubber elasticity[1] also predicts the upswing. This theory, however, fails to account for the decrease of the Mooney stress with a decrease in λ^{-1} and thus does not represent experimental data.

GENERAL RELATIONS

When cartesian coordinates are used to describe both the undeformed and the deformed state, the stress tensor for an incompressible material is

$$\bar{\sigma}_{ij} = 2[C_{ij}(\partial W/\partial I_1) - (C_{ij})^{-1}(\partial W/\partial I_2)] - P\delta_{ij} \tag{10}$$

where the bar on σ denotes true stress, C_{ij} is the right Cauchy-Green deformation tensor, and P is an arbitrary hydrostatic pressure.

We consider a general biaxial deformation for which the principal stretch ratios are

$$\begin{aligned} \lambda_1 &= \lambda \\ \lambda_2 &= \lambda^a \\ \lambda_3 &= \lambda^{-a-1} \end{aligned} \tag{11}$$

Equations (11) yield the principal stretch ratios in simple tension for $a = -1/2$, those in equibiaxial tension for $a = 1$, and those in pure shear for $a = 0$.

The Cauchy-Green tensor for this deformation is

$$C_{ij} = \begin{bmatrix} \lambda^2 & 0 & 0 \\ . & \lambda^{2a} & 0 \\ . & . & \lambda^{-2a-2} \end{bmatrix} \tag{12}$$

and its reciprocal becomes

$$(C_{ij})^{-1} = \begin{bmatrix} \lambda^{-2} & 0 & 0 \\ . & \lambda^{-2a} & 0 \\ . & . & \lambda^{2a+2} \end{bmatrix} \tag{13}$$

Substituting eqs. (12) and (13) into eq. (10), eliminating the hydrostatic pressure, and making use of the relation $\bar{\sigma}_i = \sigma_i\lambda_i$, we obtain the two principal true stress differences in terms of the nominal stresses as

$$\lambda\sigma_1 - \lambda^{-a-1}\sigma_3 = 2(\lambda^2 - \lambda^{-2a-2})[(\partial W/\partial I_1) + \lambda^{2a}(\partial W/\partial I_2)] \tag{14a}$$

and

$$\lambda^a\sigma_2 - \lambda^{-a-1}\sigma_3 = 2(\lambda^{2a} - \lambda^{-2a-2})[(\partial W/\partial I_1) + \lambda^2(\partial W/\partial I_2)] \tag{14b}$$

Substitution of eq. (2) into eqs. (14) yields, after division by λ or λ^a, respectively,

$$\sigma_1 - \sigma_3\lambda^{-a-2} = 2(\lambda - \lambda^{-2a-3}) \sum_{i,j=0}^{\infty} c_{ij}F_{ij}(\lambda) \tag{15a}$$

and

$$\sigma_2 - \sigma_3\lambda^{-2a-1} = 2(\lambda^a - \lambda^{-3a-2}) \sum_{i,j=0}^{\infty} c_{ij}f_{ij}(\lambda) \tag{15b}$$

where

$$F_{ij}(\lambda) = i(I_1 - 3)^{i-1}(I_2 - 3)^j + j(I_1 - 3)^i(I_2 - 3)^{j-1}\lambda^{2a} \tag{16a}$$

and

$$f_{ij}(\lambda) = i(I_1 - 3)^{i-1}(I_2 - 3)^j + j(I_1 - 3)^i(I_2 - 3)^{j-1}\lambda^2 \qquad (16b)$$

The invariants of the deformation tensor in terms of the principal stretch ratios, eqs. (11), become

$$I_1 - 3 = (\lambda^{2a} + \lambda^2 - 3 + \lambda^{-2a-2}) \qquad (17a)$$

and

$$I_2 - 3 = (\lambda^{2a+2} - 3 + \lambda^{-2} + \lambda^{-2a}) \qquad (17b)$$

SPECIAL CASES

Equations (15) together with eqs. (16) are the constitutive equations for the general biaxial deformation considered. They can now be specialized by assigning appropriate values to the exponent a.

Simple Tension

In simple tension $a = -1/2$, $\sigma_1 = \sigma$, and $\sigma_2 = \sigma_3 = 0$. Substitution into eqs. (15a) and (16a) yields

$$\sigma = 2(\lambda - \lambda^{-2})\left[c_1 + c_2\lambda^{-1} + \sum_{i,j=1}^{\infty} c_{ij}F_{ij}^{s}(\lambda)\right] \qquad (18a)$$

or

$$\sigma/(\lambda - \lambda^{-2}) = 2\left[c_1 + c_2\lambda^{-1} + \sum_{i,j=1}^{\infty} c_{ij}F_{ij}^{s}(\lambda)\right] \qquad (18b)$$

where $\sigma/(\lambda - \lambda^{-2})$ is the Mooney stress and $F_{ij}^{s}(\lambda)$ indicates the special form of $F_{ij}(\lambda)$ for simple tension. In eqs. (18) the first two terms of the expansion were written out explicitly.

To obtain specific forms of $F_{ij}^{s}(\lambda)$ we first express the invariants as

$$I_1 - 3 = (\lambda - 1)^2(1 + 2\lambda^{-1}) \qquad (19a)$$

and

$$I_2 - 3 = (\lambda - 1)^2(2 + \lambda^{-1})\lambda^{-1} \qquad (19b)$$

Equations (19) are readily obtained from eqs. (17). Substituting into eq. (16a) we find

$$F_{ij}^{s}(\lambda) = (\lambda - 1)^{2(i+j-1)}[i(1 + 2\lambda^{-1})^{i-1}(2 + \lambda^{-1})^j + j(1 + 2\lambda^{-1})^i(2 + \lambda^{-1})^{j-1}]\lambda^{-j} \qquad (20)$$

Because of the factor $(\lambda - 1)^2$ in eq. (20), $F_{ij}^{s}(1) = 0$, and hence $\sigma/(\lambda - \lambda^{-1})$ is always $2(c_1 + c_2)$ for $\lambda = 1$, regardless of the number of terms retained in the expansion.

Keeping the c_{11} term as the third term in addition to the first two terms, we find

$$\sigma/(\lambda - \lambda^{-2}) = 2[c_1 + c_2\lambda^{-1} + 3c_3(\lambda - 1)^2(1 + \lambda^{-1})\lambda^{-1}] \qquad (21)$$

This equation is mentioned by van der Hoff and Buckler.[3] The expression obtained by retaining the c_{20} term is:

$$\sigma/(\lambda - \lambda^{-2}) = 2[c_1 + c_2\lambda^{-1} + 2c_3(\lambda - 1)^2(1 + 2\lambda^{-1})] \tag{22}$$

This equation has been derived previously by Signorini[4] and also follows from the theory of Bernstein et al.[5] It has also been derived by Sato.[6] Both eqs. (21) and (22) predict an upswing in the Mooney stress for small values of λ^{-1}.

Equibiaxial Tension

In equibiaxial tension $a = 1$, $\sigma_1 = \sigma_2 = \sigma$, and $\sigma_3 = 0$. Substitution into eqs. (15a) and (16a) yields

$$\sigma = 2(\lambda - \lambda^{-5})\left[c_1 + c_2\lambda^2 + \sum_{i,j=1}^{\infty} c_{ij}F_{ij}^{E}(\lambda)\right] \tag{23}$$

or

$$\sigma/(\lambda - \lambda^{-5}) = 2\left[c_1 + c_2\lambda^2 + \sum_{i,j=1}^{\infty} c_{ij}F_{ij}^{E}(\lambda)\right] \tag{24}$$

where we will call $\sigma/(\lambda - \lambda^{-5})$ the Mooney stress in equibiaxial tension. Equation (23) is the analog of the Mooney-Rivlin equation in simple tension.

Since now

$$I_1 - 3 = (\lambda - \lambda^{-1})^2(2\lambda + \lambda^{-1})\lambda^{-1} \tag{25a}$$

and

$$I_2 - 3 = (\lambda - \lambda^{-1})^2(\lambda + 2\lambda^{-1})\lambda \tag{25b}$$

we obtain for $F_{ij}^{E}(\lambda)$

$$F_{ij}^{E}(\lambda) = (\lambda - \lambda^{-1})^{2(i+j-1)}[i(2\lambda + \lambda^{-1})^{i-1}(\lambda + 2\lambda^{-1})^{j} + j(2\lambda + \lambda^{-1})^{i}(\lambda + 2\lambda^{-1})^{j-1}]\lambda^{j-i+1} \tag{26}$$

Again, because of the $(\lambda - \lambda^{-1})$ factor in eq. (26), $F_{ij}^{E}(1) = 0$, and $\sigma/(\lambda - \lambda^{-5})$ reduces to $2(c_1 + c_2)$ for $\lambda = 1$ regardless of the number of higher terms which have been retained.

For the c_{11} term as the third term in addition to the c_1 and c_2 terms we have

$$\sigma/(\lambda - \lambda^{-5}) = 2[c_1 + c_2\lambda^2 + 3c_3(\lambda - \lambda^{-1})^2(\lambda + \lambda^{-1})\lambda] \tag{27}$$

Pure Shear

In pure shear, $a = 0$, $\sigma_1 = \sigma$, $\sigma_2 = \sigma'$, and $\sigma_3 = 0$. We have, for the maximum principal stress,

$$\sigma = 2(\lambda - \lambda^{-3})\left[c_1 + c_2 + \sum_{i,j=1}^{\infty} c_{ij}F_{ij}^{P}(\lambda)\right] \tag{28}$$

or

$$\sigma'/(\lambda - \lambda^{-3}) = 2\left[c_1 + c_2 + \sum_{i,j=1}^{\infty} c_{ij}F_{ij}^{\mathrm{P}}(\lambda)\right] \tag{29}$$

and for the intermediate principal stress,

$$\sigma' = 2(1 - \lambda^{-2})\left[c_1 + c_2\lambda^2 + \sum_{i,j=1}^{\infty} c_{ij}F_{ij}^{\mathrm{P}}(\lambda)\right] \tag{30}$$

or

$$\sigma'/(1 - \lambda^{-2}) = 2\left[c_1 + c_2\lambda^2 + \sum_{i,j=1}^{\infty} c_{ij}f_{ij}^{\mathrm{P}}(\lambda)\right] \tag{31}$$

Since

$$I_1 - 3 = I_2 - 3 = (\lambda - \lambda^{-1})^2 \tag{32}$$

we find

$$F_{ij}^{\mathrm{P}}(\lambda) = (i + j)(\lambda - \lambda^{-1})^{2(i+j-1)} \tag{33a}$$

and

$$f_{ij}^{\mathrm{P}}(\lambda) = (i + j\lambda^2)(\lambda - \lambda^{-1})^{2(i+j-1)} \tag{33b}$$

Because of the factor $(\lambda - \lambda^{-1})$, $F_{ij}^{\mathrm{P}}(1) = f_{ij}^{\mathrm{P}}(1) = 0$. The Mooney stress in pure shear with c_{11} as the third coefficient becomes

$$\sigma/(\lambda - \lambda^{-3}) = 2[c_1 + c_2 + 2c_2(\lambda - \lambda^{-1})^2] \tag{34}$$

for the maximum principal stress, and

$$\sigma'/(1 - \lambda^{-2}) = 2[c_1 + c_2\lambda^2 + c_3(\lambda - \lambda^{-1})^2(1 + \lambda^2)] \tag{35}$$

for the intermediate principal stress.

Simple Shear

Simple shear is a pure shear plus a rotation. For simple shear in the 1,3-plane parallel to the 1-direction, the right Cauchy-Green tensor and its reciprocal become

$$C_{ij} = \begin{bmatrix} 1 & k & 0 \\ . & 1 + k^2 & 0 \\ . & . & 1 \end{bmatrix} \tag{36a}$$

and

$$(C_{ij})^{-1} = \begin{bmatrix} 1 + k^2 & -k & 0 \\ . & 1 & 0 \\ . & . & 1 \end{bmatrix} \tag{36b}$$

where k is the amount of shear. The principal stretches are the same as in pure shear, i.e., $\lambda_1 = \lambda$, $\lambda_2 = 1$, and $\lambda_3 = \lambda^{-1}$. The amount of shear is

$$k = \lambda - \lambda^{-1} = \tan \epsilon \tag{37}$$

in terms of the major principal stretch ratio, and the angle of shear, respectively.[7] Equation (10) now gives

$$\sigma_{12} = 2k[(\partial W/\partial I_1) + (\partial W/\partial I_2)] \tag{38}$$

and, hence, substituting eq. (2) yields

$$\sigma_{12} = 2k \sum_{i,j=0}^{\infty} c_{ij} F_{ij}^{\mathrm{P}}(k) \tag{39}$$

where

$$F_{ij}^{\mathrm{P}}(k) = (i + j)k^{2(i+j-1)} \tag{40}$$

because

$$I_1 - 3 = I_2 - 3 = k^2 \tag{41}$$

The equations for simple shear are thus seen to be formally identical with those for the maximum principal stress in pure shear, with k replacing $\lambda - \lambda^{-1}$.

Normal Stresses

The three normal stress differences in shear are easily derived from eq. (10) with eqs. (36). They become

$$\sigma_{11} - \sigma_{22} = -2k^2[(\partial W/\partial I_1) + (\partial W/\partial I_2)] \tag{42a}$$

$$\sigma_{22} - \sigma_{33} = 2k^2(\partial W/\partial I_1) \tag{42b}$$

$$\sigma_{33} - \sigma_{11} = 2k^2(\partial W/\partial I_2) \tag{42c}$$

Substituting eq. (2) and using (41) yields

$$\sigma_{11} - \sigma_{22} = -2k^2 \sum_{i,j=0}^{\infty} c_{ij} F_{ij}^{\mathrm{I}}(k) \tag{43a}$$

$$\sigma_{22} - \sigma_{33} = 2k^2 \sum_{i,j=0}^{\infty} c_{ij} F_{ij}^{\mathrm{II}}(k) \tag{43b}$$

and

$$\sigma_{33} - \sigma_{11} = 2k^2 \sum_{i,j=0}^{\infty} c_{ij} F_{ij}^{\mathrm{III}}(k) \tag{43c}$$

We have

$$F_{ij}^{\mathrm{I}}(k) = (i + j)k^{2(i+j-1)} \tag{44a}$$

$$F_{ij}^{\mathrm{II}}(k) = ik^{2(i+j-1)} \tag{44b}$$

and

$$F_{ij}^{\mathrm{III}}(k) = jk^{2(i+j-1)} \tag{44c}$$

$F_{ij}^{I}(k)$ is identical with $F_{ij}^{II}(k)$. The three Mooney normal stress differences for the c_{11} term as the third term become

$$(\sigma_{22} - \sigma_{11})/k^2 = 2[c_1 + c_2 + 2c_3k^2] \tag{45a}$$

$$(\sigma_{22} - \sigma_{33})/k^2 = 2[c_1 + c_3k^2] \tag{45b}$$

and

$$(\sigma_{33} - \sigma_{11})/k^2 = 2[c_2 + c_3k^2] \tag{45c}$$

EXPERIMENTAL RESULTS

The equations derived from the expansion of the strain energy density function [cf. eqs. (15)] are linear in the coefficients, c_{ij}. They can, therefore, be obtained easily by least squares fitting of experimental data on a computer. Such calculations were made with a program which fits experimental data in simple tension to equations containing three coefficients,

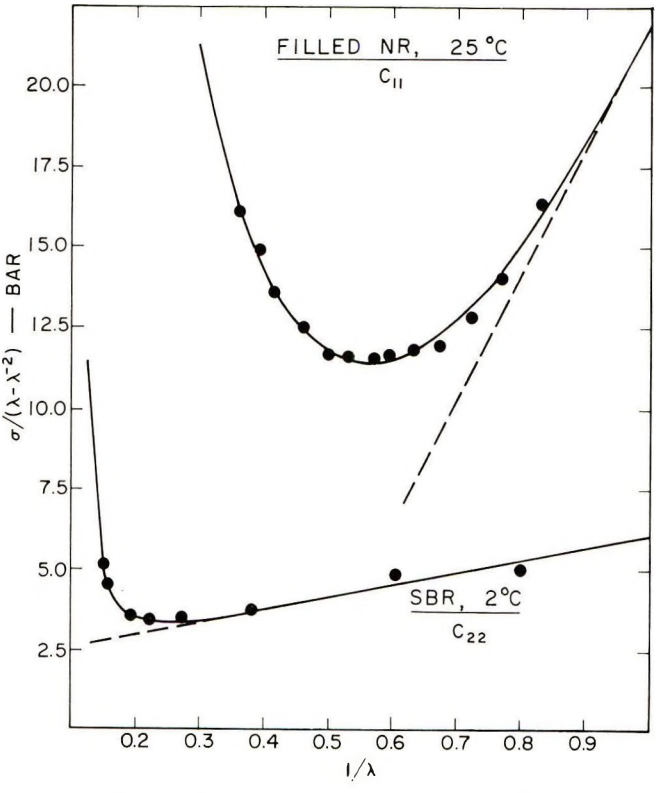

Fig. 1. Mooney stress as a function of λ^{-1} for: (*a*) pure gum SBR at 2°C (solid curve represents fit with $c_3 = c_{22}$) and (*b*) carbon black-filled natural rubber at 25°C (solid curve represents fit with $c_3 = c_{11}$)

the first two of which are the c_1 and c_2 coefficients of the Mooney-Rivlin equation, eq. (4). The third coefficient is c_{11}, c_{20}, c_{21}, c_{22}, c_{02}, or c_{12}. The corresponding functions of the stretch ratio λ are tabulated in the Appendix.

Data on a pure gum SBR[2b] gave the best fit (lowest χ^2 value) when fitted with $c_3 = c_{22}$, i.e., to

$$\sigma/(\lambda - \lambda^{-2}) = 2[c_1 + c_2\lambda^{-1} + 6c_3(\lambda - 1)^6(1 + 2\lambda^{-1}) \times (2 + \lambda^{-1})(1 + \lambda^{-1})\lambda^{-2}] \quad (46)$$

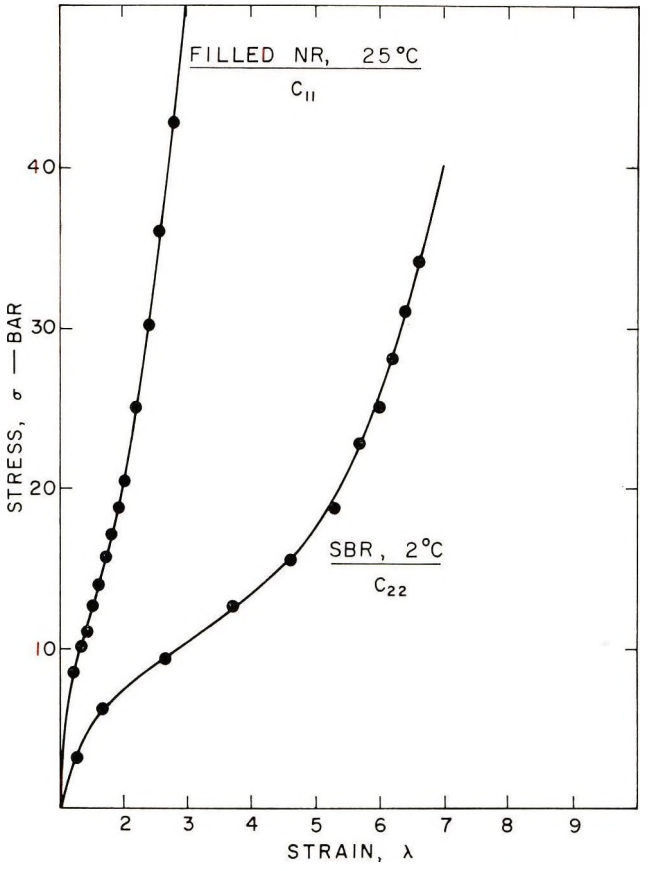

Fig. 2. Stress–strain curve of (*a*) pure gum SBR at 2°C (solid curve represents fit with $c_3 = c_{22}$) and (*b*) carbon black-filled natural rubber at 25°C (solid curve represents fit with $c_3 = c_{11}$).

The numerical values of the coefficients thus obtained were: $c_1 = 1.11$, $c_2 = 1.95$, and $c_3 = 0.0001$. Figure 1 shows the resulting Mooney-Rivlin plot. The corresponding stress-strain curve is shown in Figure 2. The broken line in Figure 1 represents the Mooney-Rivlin equation, eq. (4) with the same values for coefficients c_1 and c_2.

Data on a carbon black-filled natural rubber sample[8] are also shown in Figures 1 and 2. These data present a particularly severe test. Because the upswing is quite marked and begins at rather high values of λ^{-1}, data like these are virtually impossible to describe by the Mooney-Rivlin equation. In this case, the best fit was obtained with $c_3 = c_{11}$. The numerical values of the coefficients from which the solid curve was calculated, were: $c_1 = -8.54$, $c_2 = 19.4$, and $c_3 = 2.10$. The stress–strain curve is shown in Figure 2 and is seen to give an excellent fit to the data up to the break point. The broken line in Figure 1 represents the Mooney-Rivlin equation, again with the same values for c_1 and c_2.

CONCLUSIONS

The foregoing results have shown that a very reasonable fit to simple tension data on both filled and unfilled elastomers can be obtained by retaining another term in addition to the c_1 and c_2 terms in the expansion of the strain energy function. Terms higher than the six listed above may be required in some cases. The limited results obtained so far indicate that the form of the constitutive equation (i.e., which of the higher terms should be retained) may well depend on the material. One might then expect the numerical values of the coefficients to change with temperature while the form of the constitutive equation remains invariant. To clarify this point a study will be made of the isochronal uniaxial tension data of Smith[9] on Viton A-HV vulcanizates at different temperatures in which well defined upswings appear in the Mooney stress at low values of λ^{-1}. The crucial test of a constitutive equation, however, is to apply the same equation to data obtained in different modes of deformation. An investigation of the equilibrium data of Dickie and Smith[10] on SBR in simple tension, equibiaxial tension, and pure shear has been started.

Some interesting theoretical observations may be made. Since $F_{ij}^{s}(\lambda)$ is always positive [cf. eq. (20)], one cannot account simultaneously for the behavior normally observed in both tension and compression[11] unless at least one more coefficient, c_4, is retained. Since both c_2 and either c_3 or c_1 must be positive to represent the behavior in simple tension, at least one coefficient must be negative to describe the behavior in simple compression. Our computer program is being modified to allow for the calculation of c_4 terms in addition to c_3 terms. The results will be presented elsewhere.

Finally, it should be noted that if a constitutive equation contains a cross term (i.e, a term in which both i and j have nonzero values, such as c_{11}, c_{12}, c_{21}, or c_{22}) it is inconsistent with the theory of Valanis and Landel[12] which assumes that the strain energy density function can be represented by

$$W = w(\lambda_1) + w(\lambda_2) + w(\lambda_3) \tag{47}$$

in which $w(\lambda)$ is the same function for all three principal stretch ratios.

APPENDIX

Functions of the Stretch Ratio Associated with the Coefficients $c_{ij}(i,j = 0, 1, 2)$.

In simple tension:

$$F_{10}^{S}(\lambda) = 1 \tag{A-1}$$

$$F_{01}^{S}(\lambda) = \lambda^{-1} \tag{A-2}$$

$$F_{11}^{S}(\lambda) = 3(\lambda - 1)^2(1 + \lambda^{-1})\lambda^{-1} \tag{A-3}$$

$$F_{20}^{S}(\lambda) = 2(\lambda - 1)^2(1 + 2\lambda^{-1}) \tag{A-4}$$

$$F_{02}^{S}(\lambda) = 2(\lambda - 1)^2(2 + \lambda^{-1})\lambda^{-2} \tag{A-5}$$

$$F_{21}^{S}(\lambda) = (\lambda - 1)^4(1 + 2\lambda^{-1})(5 + 4\lambda^{-1})\lambda^{-1} \tag{A-6}$$

$$F_{12}^{S}(\lambda) = (\lambda - 1)^4(2 + \lambda^{-1})(4 + 5\lambda^{-1})\lambda^{-2} \tag{A-7}$$

$$F_{22}^{S}(\lambda) = 6(\lambda - 1)^6(1 + 2\lambda^{-1})(2 + \lambda^{-1})(1 + \lambda^{-1})\lambda^{-2} \tag{A-8}$$

In equibiaxial tension

$$F_{10}^{E}(\lambda) = 1 \tag{A-9}$$

$$F_{01}^{E}(\lambda) = \lambda^2 \tag{A-10}$$

$$F_{11}^{E}(\lambda) = 3(\lambda - \lambda^{-1})^2(\lambda + \lambda^{-1})\lambda \tag{A-11}$$

$$F_{20}^{E}(\lambda) = 2(\lambda - \lambda^{-1})^2(2\lambda + \lambda^{-1})\lambda^{-1} \tag{A-12}$$

$$F_{02}^{E}(\lambda) = 2(\lambda - \lambda^{-1})^2(\lambda + 2\lambda^{-1})\lambda \tag{A-13}$$

$$F_{21}^{E}(\lambda) = (\lambda - \lambda^{-1})^4(2\lambda + \lambda^{-1})(4\lambda + 5\lambda^{-1}) \tag{A-14}$$

$$F_{12}^{E}(\lambda) = (\lambda - \lambda^{-1})^4(\lambda + 2\lambda^{-1})(5\lambda + 4\lambda^{-1})\lambda^2 \tag{A-15}$$

$$F_{22}^{E}(\lambda) = 6(\lambda - \lambda^{-1})^6(2\lambda + \lambda^{-1})(\lambda + 2\lambda^{-1})(\lambda + \lambda^{-1}) \tag{A-16}$$

In pure shear, for the maximum principal stress,

$$F_{10}^{P}(\lambda) = F_{01}^{P}(\lambda) = 1 \tag{A-17}$$

$$F_{11}^{P}(\lambda) = F_{20}^{P}(\lambda) = F_{02}^{P}(\lambda) = 2(\lambda - \lambda^{-1})^2 \tag{A-18}$$

$$F_{21}^{P}(\lambda) = F_{12}^{P}(\lambda) = 3(\lambda - \lambda^{-1})^4 \tag{A-19}$$

$$F_{22}^{P}(\lambda) = 4(\lambda - \lambda^{-1})^6 \tag{A-20}$$

and for the intermediate principal stress

$$f_{10}(\lambda) = 1 \tag{A-21}$$

$$f_{01}(\lambda) = \lambda^2 \tag{A-22}$$

$$f_{11}(\lambda) = (\lambda - \lambda^{-1})^2(1 + \lambda^2) \tag{A-23}$$

$$f_{20}(\lambda) = 2(\lambda - \lambda^{-1})^2 \tag{A-24}$$

$$f_{02}(\lambda) = 2(\lambda - \lambda^{-1})^2\lambda^2 \tag{A-25}$$

$$f_{21}(\lambda) = (\lambda - \lambda^{-1})^4(2 + \lambda^2) \tag{A-26}$$

$$f_{12}(\lambda) = (\lambda - \lambda^{-1})^4(1 + 2\lambda^2) \tag{A-27}$$

$$f_{22}(\lambda) = 2(\lambda - \lambda^{-1})^6(1 + \lambda^2) \tag{A-28}$$

Finally, for the second and third normal stress differences

$$F_{10}^{II}(k) = 1 \qquad F_{10}^{III}(k) = 0 \tag{A-29}$$

$$F_{01}^{II}(k) = 0 \qquad F_{01}^{III}(k) = 1 \tag{A-30}$$

$$F_{11}^{II}(k) = k^2 \qquad F_{11}^{III}(k) = k^2 \tag{A-31}$$

$$F_{20}^{II}(k) = 2k^2 \qquad F_{20}^{III}(k) = 0 \tag{A-32}$$

$$F_{02}^{II}(k) = 0 \qquad F_{02}^{III}(k) = 2k^2 \tag{A-33}$$

$$F_{21}^{II}(k) = 2k^4 \qquad F_{21}^{III}(k) = k^4 \tag{A-34}$$

$$F_{12}^{II}(k) = k^4 \qquad F_{12}^{III}(k) = 2k^4 \tag{A-35}$$

$$F_{22}^{II}(k) = 2k^6 \qquad F_{22}^{III}(k) = 2k^6 \tag{A-36}$$

This research was supported by the Air Force Rocket Propulsion Laboratory, Edwards, California, Air Force Systems Command, United States Air Force.

References

1. R. S. Rivlin, *Large Elastic Deformations*, in *Rheology*, Vol. 1, F. R. Eirich, Ed. Academic Press, New York, 1956, p. 351 ff.
2. L. R. G. Treloar, *The Physics of Rubber Elasticity*, 2nd ed., Clarendon Press, Oxford, 1958, (a) general; (b) p. 121.
3. B. M. E. van der Hoff and R. J. Buckler, *J. Macromol. Sci. (Chem.)* **A1**, 797 (1967).
4. A. Signorini, *Ann. Mat. Pura Appl.* [4], **39**, 147 (1955).
5. B. Bernstein, E. A. Kearsley, and L. J. Zapas, *Trans. Soc. Rheol.*, **7**, 391 (1963).
6. Y. Sato, *Reprts. Progr. Polym. Phys. Japan*, **9**, 369 (1969).
7. A. S. Lodge, *Elastic Liquids*, Academic Press, New York, 1964.
8. S. Kusamizu, Japan Synthetic Rubber Co., Kawasaki, Japan, unpublished results.
9. T. L. Smith, in *Macromolecular Chemistry, Prague* **1965** (*J. Polym. Sci. C*, **16**), O. Wichterle and B. Sedláček, Eds., Interscience, New York, 1967, p. 841.
10. R. A. Dickie and T. L. Smith, *Trans. Soc. Rheol.*, **15**, 91 (1971).
11. P. Thirion and R. Chasset, *Rev. Gen. Caoutchouc Plastiques*, **45**, 859 (1968).
12. K. C. Valanis and R. F. Landel, *J. Appl. Phys.*, **38**, 2997 (1967).

Received January 20, 1971
Revised March 10, 1971

JOURNAL OF POLYMER SCIENCE: PART A-1 VOL. 9, 1971–1981 (1971)

π-Allyl Nickel Halide–Oxygen System as a Catalyst for Polymerization of Butadiene

TSUYOSHI MATSUMOTO,* JUNJI FURUKAWA, and HIROHISA MORIMURA, *Department of Synthetic Chemistry, Kyoto University, Kyoto, Japan*

Synopsis

The π-allyl nickel halide-oxygen system was found to be active as catalyst for stereospecific polymerization of butadiene. The catalyst from π-allyl nickel chloride or π-allyl nickel bromide yields the polymer of 90% *cis*-1,4 content with high activity, whereas the catalyst from π-allyl nickel iodide affords a polymer of 70% or less *cis*-1,4 content. The catalyst systems can be fractionated into two parts on the basis of solubility in benzene. It is concluded that the catalyst activity originates essentially from the benzene-insoluble nickel complex which is composed of oxygen, halogen, σ-allyl group, and nickel. The structure of growing polymer terminal is discussed in relation to the mechanism of the stereospecific polymerization.

INTRODUCTION

The authors have studied the stereospecific polymerization of butadiene by various nickel catalysts. They have reported various types of catalyst and investigated the nature of active sites and the mechanism of stereospecific polymerization.[1–7]

The present study, which was briefly reported in part in letter form,[5,6] is concerned with the activity of a new catalyst obtained by the reaction of π-allyl nickel halide and oxygen and deals with the structure of the catalyst in relation to the mechanism of the stereospecific polymerization.

The stereospecific polymerization of butadiene with a transition metal–oxygen system has been also studied by Oreshkin et al.[8] They reported the π-allyl chromium–oxygen system initiates the butadiene polymerization to yield predominantly the *trans*-1,4 polymer but did not of the catalyst structure.

Many oxygen complexes of transition metals are known, but this might be the first report describing the preparation of the allyl or alkyl complex having oxygen.

* On leave of absence from Japan Synthetic Rubber Co., Ltd., Kyobashi, Tokyo, Japan.

EXPERIMENTAL

Materials

π-Allyl or π-crotyl nickel halides were prepared from nickel carbonyl and allyl or crotyl halides according to the method of Fisher.[9] Oxygen was of 99.999% purity and dried by passing through molecular sieves. Butadiene was of BR (butadiene rubber) grade as supplied by Japan Synthetic Rubber Company and dried over molecular sieves. Benzene was freed of oxygen and water by distillation over the metal ketyl prepared from benzophenone and sodium.

Polymerization

Polymerizations were carried out in glass reaction bottles under a nitrogen atmosphere. Dry butadiene was introduced by distillation to the bottle by use of a vacuum–nitrogen apparatus. Polymerizations were terminated by addition of methanol containing aqueous hydrochloric acid.

Reaction of π-Allyl Nickel Halide with Oxygen

A two-necked flask was connected through a stopcock to a gas buret which was filled with oxygen gas. A solution of the π-allyl nickel halide under nitrogen was introduced to the flask. The flask was evacuated after it was cooled with Dry Ice–methanol. After the bottle was warmed to the desired temperature, a given volume of oxygen was gradually introduced by opening the stopcock with stirring. A precipitate formed when benzene was used as solvent.

The reaction was usually carried out at room temperature (20–30°C) and was stopped by cooling again to about −70°C followed by replacing unreacted oxygen with nitrogen after the check of the volume of reacted oxygen. When the reaction mixture was used as catalyst, the procedure was carried out in polymerization bottles. The benzene-insoluble solid nickel complexes were isolated by filtering the reaction mixtures under nitrogen, followed by washing several times with benzene and drying *in vacuo*. They were transferred to polymerization bottles in a nitrogen box.

Spectroscopy, and Elemental Analysis of Nickel Complexes

The samples were prepared under nitrogen. Infrared spectra were recorded on Hitachi grating infrared spectrometer, EPI-G. Elemental analysis was done with separate samples for each element.

Hydrolysis of Nickel Complexes

The nickel complexes were placed in a flask equipped with two necks, one connected with a gas buret and a vacuum–nitrogen apparatus and the other closed with a rubber stopper. Aqueous hydrochloric acid was added by a syringe through the rubber stopper. Evolved gas was identified by vapor-phase chromatography with activated charcoal.

Microstructure of the Polymers

The polymers were examined in carbon disulfide solution. The method of analysis is that reported by Morero et al.[10]

RESULTS AND DISCUSSION

Polymerization

π-Crotyl nickel nickel chloride itself is poorly active for the *cis*-1,4 polymerization. The addition of oxygen was found to enhance the activity, as shown in Table I. The addition of water altered the microstructure of the resulting polymer from predominantly *cis*-1,4 to predominantly *trans*-1,4 without any change in the activity.

Further studies were done on the π-crotyl nickel chloride–oxygen system. As summarized in Table I, the polymerization activity was highest at an O/Ni molar ratio of 0.5, whereas the *cis*-1,4 content of the polymer increased to 93–94% with the increasing molar ratio. The molecular weight of the polymer also increased with increasing molar ratio.

A brown precipitate formed in the reaction of π-crotyl nickel chloride with oxygen in benzene. The precipitate was found to be a nickel complex containing oxygen. Polymerization activities of the reaction mixture, the benzene-insoluble part, and the soluble part were measured. Results are shown in Table II. It is to be noticed that the benzene-insoluble part separated from the mixture afforded a polymer of high molecular weight

TABLE I
Polymerization of Butadiene with π-Crotyl Nickel Chloride–Oxygen or Water System[a]

Cocatalyst		Polymerization time, hr	Polymer				
Type	Concn mmol		Yield, %	*cis*-1,4, %	*trans*-1,4, %	1,2, %	$[\eta]^{30}_{\text{tol.}}$
—		88	6	79	18	3	—
—[b]		60	5	76	20	4	—
O_2	0.1	3	17	78	18	4	Low
O_2	0.3	3	33	86	12	3	0.4
O_2	0.5	3	70	88	11	3	0.6
O_2	0.75	3	64	91	5	4	1.1
O_2	1.0	3	42	94	3	3	2.2
O_2	1.25	4	14	93	4	3	2.8
O_2	1.50	4	8	94	3	3	3.1
H_2O	0.5	70	2	42	50	8	—
H_2O	1.0	70	2	60	32	2	—
H_2O	2.0	70	2	0	72	28	—

[a] Conditions: catalyst concn $[\pi\text{-}C_4H_7NiCl]_2$, 1.0 mmole except as otherwise noted; butadiene, 7.2 g; benzene, 16 ml; reaction between two components at room temperature for 30 min; polymerization temperature, 40°C.

[b] Catalyst $[\pi\text{-}C_4H_7NiCl]_2$, 2.3 mmole.

TABLE II
Activity of Catalyst of Benzene Soluble and Insoluble Parts[a]

Fraction	O_2/$[C_4H_7NiCl]_2$ ratio	Polymerization, hr	Polymer				
			Yield, %	*cis*-1,4, %	*trans*-1,4, %	1,2, %	$[\eta]^{30}_{tol.}$
Mixture	0.3	3	33	78	18	4	0.4
Mixture	0.5	3	70	88	11	3	0.6
Mixture	1.0	3	42	94	3	3	2.2
Insoluble	0.3	3	21	93	3	4	2.6
Insoluble	0.5	3	52	94	3	3	2.0
Insoluble	1.0	3	37	94	3	3	2.3
Soluble	0.3	—	—	—	—	—	—
Soluble	0.5	70	trace	—	—	—	—
Soluble	1.0	72	trace	—	—	—	—

[a] Polymerization conditions same as described for Table I.

TABLE III
Polymerization of Butadiene with the Catalyst Prepared from π-Allyl Nickel Bromide and Oxygen[a]

Fraction	O_2/$[C_3H_5NiBr]_2$ ratio	Polymerization time, hr	Polymer				
			Yield, %	*cis*, 1,4, %	*trans*, 1,4, %	1,2, %	$[\eta]^{30}_{tol.}$
—	0	87	40	0	89	11	–
Mixture	0.3	3	35	72	24	4	0.5
Mixture	0.5	3	55	75	16	4	1.0
Mixture	0.75	3	41	89	7	3	2.5
Mixture	1.0	3	21	90	6	4	3.3
Insoluble	0.3	4	54	93	5	2	2.0
Insoluble	0.5	4	82	91	6	3	2.0
Insoluble	0.75	4	49	92	5	3	2.4
Insoluble	0.70[b]	5.5	60	93	4	3	2.2

[a] Conditions: catalyst concn.: $[\pi\text{-}C_3H_5NiBr]_2$, 1 mmole; butadiene, 7.2 g; benzene, 16 ml; reaction between two components at room temperature for 30 min; polymerization temperature, 40°C except as otherwise noted.

[b] Conditions: Catalyst concn $[\pi\text{-}C_3H_5NiBr]_2$, 5 mmole; butadiene, 72 g; benzene, 160 ml.

containing 92–94% *cis*-1,4 configuration in all cases, regardless of amount of added oxygen. It is clear that the polymerization activity of π-crotyl nickel chloride–oxygen system originates from the benzene-insoluble part. Since the microstructure is not affected by the amount of oxygen added, the nature of the active species is considered to be independent of the amount of oxygen.

Table III summarizes the results of experiments with π-allyl nickel bromide. π-Allyl nickel bromide alone yielded a polymer of predominantly *trans*-1,4 configuration. On the other hand, the π-allyl nickel

bromide–oxygen system afforded a polymer of *cis*-1,4 configuration. As in the case with π-crotyl nickel chloride, the reaction of π-allyl nickel bromide with oxygen in benzene formed a brown precipitate, which was found to be a nickel complex as described later. The data in Table III indicate that the benzene-insoluble precipitate is the active species in the above system. Regardless of mole ratio of oxygen added to π-allyl nickel bromide, the same kind of active site is formed in the benzene-insoluble nickel complex. Run b shows the activity of the catalyst prepared on a large scale.

In the polymerization catalyzed by the π-crotyl or allyl nickel iodide–oxygen system, as shown in Table IV, the *cis*-1,4 content of the polymer

TABLE IV
Polymerization of Butadiene with Catalyst Prepared from π-Crotyl or Allyl Nickel Iodide and Oxygen[a]

No.	Fraction	$O_2/[C_4H_7NiI]_2$ ratio	Polymerization time, hr	Polymer			
				Yield, %	*cis*, 1,4, %	*trans*-1,4, %	1,2, %
1	—	0	29	41	0	96	4
2	Mixture	0.5	29	75	35	63	2
3	Mixture	0.75	20	94	50	45	5
4	Mixture	1.0	20	96	57	38	5
5	Insoluble	0.3	23	36	69	25	6
6	Insoluble	0.5	23	59	70	25	5
7	Insoluble	0.8	23	39	67	28	5
8[b]	Insoluble	0.5	25	73	67	30	3

[a] Polymerization conditions same as described under Table III.

[b] π-Allyl nickel iodide was used.

was about 60% at most. A blackish violet complex insoluble in benzene was formed. The complex separated from the reaction mixture yielded a polymer of 65–70% *cis*-1,4 content at various ratios of added oxygen to π-crotyl nickel iodide, although the activity was much lower than in the case of the reaction mixture as catalyst. Polymer of 65–70% *cis*-1,4 structure produced by the benzene-insoluble complex was solid and resembled Japanese paper in appearance.

Table V shows the effect of polar solvent on polymerization. The benzene-insoluble part was also insoluble in diethyl ether but soluble in more polar solvents such as tetrahydrofuran and methanol. When the reaction of π-allyl nickel chloride or bromide with oxygen was carried out in tetrahydrofuran, no precipitate was formed, and the color of the solution changed from reddish brown to brown. The polymerization in tetrahydrofuran proceeded in homogeneous phase and afforded a polymer of high *trans*-1,4 content. The polymerization in diethyl ether proceeded in heterogeneous phase and yielded a polymer of high *cis*-1,4 content, the *cis*-1,4 content and catalyst activity being lower than those in benzene.

TABLE V
Effect of Polar Solvents[a]

No.	Catalyst	Solvent	Polymerization time, hr	Polymer			
				Yield, %	*cis*-1,4, %	*trans*-1,4- %	1,2, %
1	π-AllylNiBr—O_2 (bz.-insol.)	Benzene	4	82	91	6	3
2	π-AllylNiBr—O_2 (bz.-insol.)	Diethyl ether	3.7	44	85	11	4
3	π-AllylNiBr—O_2 (bz.-insol.)	Tetrahydrofuran	150	9	16	78	6
4	π-AllylNiBr—O_2 (mixture)	Benzene	3	55	75	16	4
5	π-AllylNiBr—O_2 (mixture)	Benzene–THF, 5:3 (vol)	20	10	9	79	12
6	π-AllylNiBr—O_2 (mixture)	Methanol	60	trace			
7	π-CrotylNiCl—O_2 (mixture)	Benzene	3	70	88	11	3
8	π-CrotylNiCl—O_2 (mixture)	Methanol	70	trace			

[a] Conditions: catalyst mole ratio $O_2/[C_3H_5$ or $C_4H_7NiX]_2$, 0.5; catalyst concentration, conditions of reaction of two components, and polymerization temperature same as described under Table I.

Structure of Catalyst in Relation to Stereospecificity of the Polymerization

In general, the active species of the π-allyl nickel halide–oxygen system exists in the benzene-insoluble part as described in the previous section. The part is considered to have the same active site regardless of the mole ratio of oxygen added to π-allyl nickel halide. The effect of oxygen on the microstructure of the polymer was the most profound in the case of π-allyl nickel bromide. Thus, the structure of the benzene-insoluble part formed from π-allyl nickel bromide and oxygen was investigated in relation to the mechanism of the stereospecific polymerization of butadiene.

The benzene-insoluble part is a yellowish-brown, amorphous solid. It dissolves in tetrahydrofuran, giving a brown solution, but is not soluble in diethyl ether. This suggests that the solid is a polar complex.

In order to obtain the complex in a crystalline form, the preparation at a low temperature in toluene or ether with reprecipitation from tetrahydrofuran solution was attempted, but this was not successful. Accordingly, the complex was analyzed in an amorphous form.

The complex was stable at room temperature for 48 hr and for a week at 0°C in nitrogen atmosphere. There was no change in appearance, polymerization activity, and infrared spectrum under the above conditions.

The following studies were carried out with the benzene-insoluble precipitate formed when 0.5 mole O_2 was added to $[\pi\text{-}C_3H_5NiBr]_2$. The polymerization activity was highest at this ratio. Under these conditions no oxygen remained in the gas phase after the reaction. Since the benzene-soluble part was reddish brown, it is suggested that unreacted π-allyl nickel bromide remained in the benzene-soluble part. These observations are compatible with the following results of the elemental analysis of the complex.

The elemental analysis for Ni, C, H, Br, and O was done with separate samples. The data agreed reasonably well with a composition of NiC_3H_5BrO.

Calcd for NiC_3H_5BrO: Ni, 30.00%; C, 18.41%; H, 2.57%; Br, 40.84%; O, 8.17%. Found: Ni, 30.18%; C, 17.31%; H, 2.57%; Br, 41.90%; O, 7.17%.

It is supposed on the basis of the above results that the benzene-insoluble complex was formed by the addition of oxygen to allyl nickel bromide without expelling any ligand.

On hydrolysis with aqueous hydrochloric acid in nitrogen atmosphere, the complex evolved gas, leaving a brownish black viscous substance. The gas was found to be pure propylene containing no propane by gas chromatography. These data confirm that the complex contains an allyl group.

The complex and its tetrahydrofuran solution were paramagnetic, and therefore NMR measurements were impossible. The gram susceptibility of the complex was 28.5×10^{-6}, suggesting that two unpaired electrons are present per nickel atom.

Figure 1 shows the infrared spectrum of the oxygen complex in comparison with that of π-allyl nickel bromide. The authors reported previously that the infrared spectra of two π-allyl nickel complexes, π-crotyl nickel chloride and iodide, much resembled each other.[4] On the contrary, the two spectra in Figure 1 are different from each other.

The oxygen complex has bands at 2955–2855, 1660, 1093, 913, and 678 cm^{-1} but no band at 1010–1020, 740–790 or 495–540 cm^{-1}, the latter being characteristic of the π-allyl ligand.[11] The band at about 1010–1020 cm^{-1} has been observed in $[RPdCl]_2$, $[RNiX]_2$, $RMoCp(CO)_2$, $RFe(CO)_3X$,

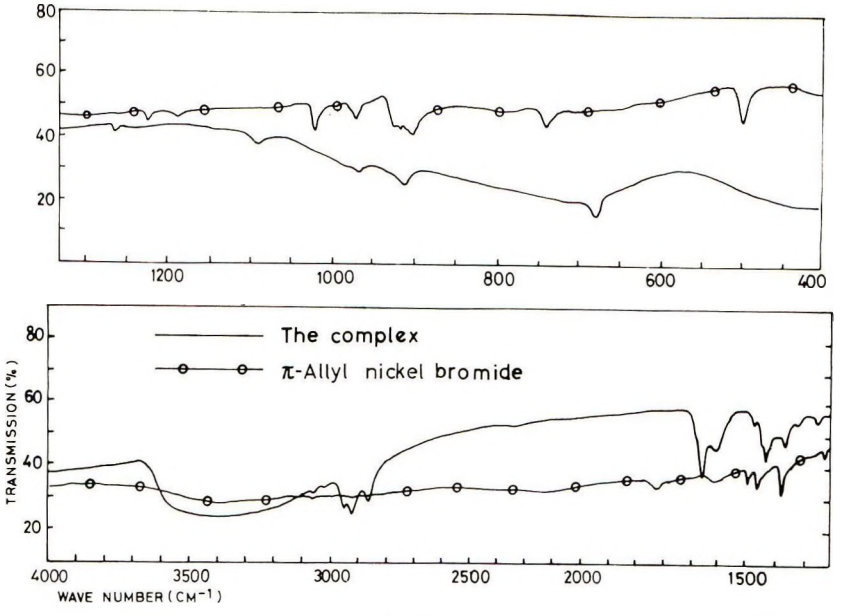

Fig. 1. Infrared spectrum of the benzene-insoluble complex prepared from π-allyl nickel bromide and oxygen, compared with that of π-allyl nickel bromide. KBr disk.

RPdCp, RNiCp, $RCo(CO)_3$, and $RFe(CO)Cp$, R, X, and Cp being π-allyl, halogen, and cyclopentadienyl, respectively and attributed to the symmetrical C-C stretching of the π-allyl ligand. The band at about 495–540 cm^{-1} has been attributed to the C-C-C deformation of π-allyl ligand in $[RPdCl]_2$, $[RNiX]_2$ and RPdCp. The band at about 740–790 cm^{-1} has been attributed to C-H deformation of π-allyl ligand in $[RPdCl]_2$, $[RPdCl]_2$, $[RNiX]_2$, RPdCp, $RCo(CO)_3$, $RFeCp(CO)$, $RMoCp(CO)_2$, and $RWCp(CO)_2$. In regard to bands observed in the oxygen complex, the band at about 1660 cm^{-1} may be assigned to the C=C stretching, the bands at 2855, 2920, and 2955 cm^{-1} to the CH stretching of $-CH_2-$ and $=CH_2$ groups, and the band at 913 cm^{-1} to the CH_2 deformation of $=CH_2$ group.

Martin et al.[12] pointed out in their report on $CpZr(C_3H_5)_2$ that σ-allyl complexes have fairly intense bands in the range of C—H stretching (2800–3000 cm^{-1}), whereas π-allyl complexes have very weak ones. The relation

between the two spectra in Figure 1 coincides with Martin's indication, if the oxygen complex is assumed to be an σ-allyl complex.

The same bands were also observed in spectra in Nujol and hexachlorobutadiene. These data lead to a conclusion that the allyl group in the oxygen complex is not π-allyl but σ-allyl.

The bands in a region from about 3600 to 2800 and about 1600 cm^{-1} in Figure 1 are assigned to the water absorbed on the surface of the precipitate during operations. These bands almost disappears in the spectrum of the

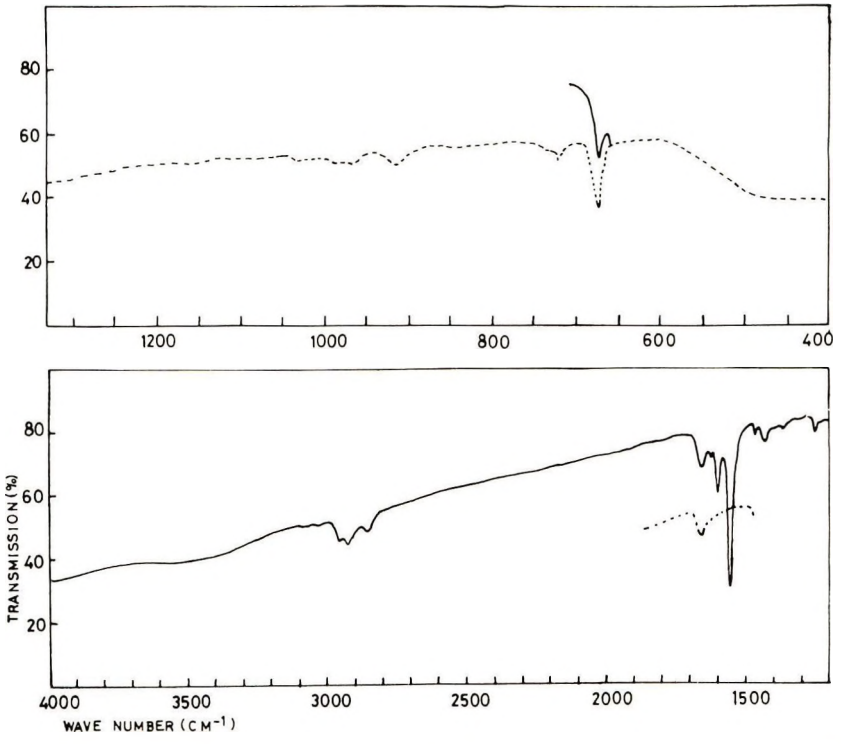

Fig. 2. Infrared spectrum of the benzene-insoluble complex prepared from π-allyl nickel iodide and oxygen: (——) in hexachlorobutadiene; (– – –) Nujol.

benzene-insoluble complex prepared from π-allyl nickel and oxygen, as shown in Figure 2.

The complex prepared from π-allyl nickel iodide and oxygen afforded the polymer whose structure was 70% *cis*-1,4 and differed from that of the polymer yielded by π-allyl nickel iodide alone (*trans*-1,4 95%). When π-allyl nickel iodide was allowed to react with one half mole oxygen, almost no oxygen remained in the vapor phase. The infrared spectrum of the resulting complex is shown in Figure 2. It is essentially the same as that of the complex from π-allyl nickel bromide and oxygen, the band at about 680 cm^{-1} being more sharp and strong. Therefore, the benzene-insoluble

complex prepared from π-allyl nickel iodide and oxygen is also considered to be a σ-allyl complex containing oxygen.

To study the complex mode of oxygen in the oxygen complex, the following experiments were carried out. The complex prepared from π-crotyl nickel chloride and oxygen was allowed to react with triphenylphosphine at a mole ratio of 1:1 (Ni:P) in a dry oxygen atmosphere in tetrahydrofuran. Triphenylphosphine oxide was obtained with an yield of 30% by the reaction for $^1/_2$ hr at room temperature. The reaction of π-crotyl nickel chloride with triphenylphosphine (1:1) in benzene followed by the exposure to air with agitation of the solution for one day resulted in the formation of triphenylphosphine oxide almost quantitatively. The oxygen complex did not liberate oxygen when it was treated with iodine or tetracyanoethylene at a temperature lower than about 40°C.

The polymerization in benzene catalyzed by the oxygen complexes proceeded in a heterogeneous system, and no change occurred in color and appearance of the catalyst system as the result of the addition of butadiene. Butadiene seems to coordinate to vacant sites in the oxygen complex without displacement with oxygen, halogen and allyl group and then to be inserted between the nickel–σ-allyl bond. Accordingly, the living polymer terminal is considered to be σ-allyl nickel.

The mechanisms of the stereospecific polymerization of butadiene are classified into two kinds. One is based on the assumption that the active polymer terminal is attached to metal with a π-allyl bond and that consequently the formation of *cis*-1,4 structure depends on the ratio of *anti* to *syn* isomer of π-allyl terminal, the ratio being affected by other ligands. The other mechanism is based on the mode of monomer coordination to metal, and the *cis*-1,4 structure is considered to be derived from the monomer bidentately coordinated to the catalyst.

It is well known that π-allyl nickel chloride initiates the *cis*-1,4 polymerization, whereas π-allyl nickel iodide initiates *trans*-1,4 polymerization. Previously, we reported[4] NMR and infrared studies indicating that π-crotyl nickel chloride and iodide are both of the *syn* form. The result seems to rule out the former mechanism as discussed in the previous report.[4]

In this study, it is to be noticed that the oxygen addition to π-allyl nickel halide causes the change of π-allyl to σ-allyl, together with the change of the *trans*-1,4 to the *cis*-1,4 polymerization or with much increase of the *cis*-1,4 polymerization activity. This is taken to a support for the latter mechanism at least in the *cis*-1,4 polymerization.

In conclusion, the data support the second of these two mechanisms for the stereospecific polymerization of butadiene by a transition metal catalyst. The bidentate coordination of butadiene to a transition metal catalyst will be discussed elsewhere in terms of the molecular orbital theory.

The authors are thankful to Dr. S. Hashimoto for the elemental analysis and the measurement of magnetic susceptibility.

References

1. T. Matsumoto and S. Ohnishi, *Kogyo Kagaku Zasshi*, **71**, 1709 (1968).
2. K. Ueda, S. Ohnishi, T. Yoshimoto, J. Hosono, K. Maeda, and T. Matsumoto, *Kogyo Kagaku Zasshi*, **66**, 1103 (1963).
3. T. Matsumoto and S. Ohnishi, *Kogyo Kagaku Zasshi*, **71**, 2059 (1968).
4. T. Matsumoto and J. Furukawa, *J. Polym. Sci. B*, **5**, 935 (1967).
5. T. Matsumoto, J. Furukawa, and H. Morimura, *J. Polym. Sci. B*, **6**, 869 (1968).
6. T. Matsumoto, J. Furukawa, and H. Morimura, *J. Polym. Sci. B*, **7**, 541 (1969).
7. T. Matsumoto, J. Furukawa, and H. Morimura, *J. Polym. Sci. A*, in press.
8. I. A. Oreskin, E. I. Tinyakova, and B. A. Dolgoplosk, *Vysokomol. Soedin. A*, **11**, 1645 (1969).
9. O. Fisher and G. Burger, *Z. Naturforsch.*, **16b**, 77 (1961).
10. D. Morero, A. Santambrogio, L. Porri, and F. Ciampelli, *Chim. Ind.* (Milan), **41**, 758 (1969).
11. E. O. Fisher and H. Werner, *Metal-Complex, Vol. 1, Complexes with Di- and Oligo-Olefinic Ligands*, Elsevier, Amsterdam, 1966, pp. 181–183.
12. H. A. Martin, P. J. Lemaire, and F. Jellinek, *J. Organometal. Chem.*, **14**, 149 (1968).

Received December 28, 1970

JOURNAL OF POLYMER SCIENCE: PART A-1 VOL. 9, 1983–1991 (1971)

Equilibrium Anionic Polymerization of α-Methylstyrene in *p*-Dioxane

J. LÉONARD and S. L. MALHOTRA, *Département de Chimie, Université Laval, Québec 10, Canada*

Synopsis

The equilibrium anionic polymerization of α-methylstyrene in *p*-dioxane, with potassium as initiator, has been investigated at 5, 15, 25, and 40°C by using high-vacuum techniques. The comparison of these results with those obtained previously for the equilibrium polymerization of α-methylstyrene in tetrahydrofuran revealed that, although the values of ΔG_{lc}, the free-energy change upon the polymerization of 1 mole of liquid monomer to 1 base-mole of liquid amorphous polymer of infinite chain length, are the same for both systems, there is a distinct effect of the solvent. This effect is reflected in the value of monomer equilibrium concentration and its variation with polymer concentration and is explained in terms of a solvent–monomer and solvent–polymer interaction parameter.

INTRODUCTION

Recently it has been shown[1] that in the case of anionic polymerization of α-methylstyrene in tetrahydrofuran at a given temperature, the equilibrium monomer concentration is not unique but varies with concentration of polymer present under equilibrium conditions. It has been also suggested[2] that, in the range of temperature under investigation, interactions between monomer and solvent may play an important role in determining the state of equilibrium, this being reflected in the value of the equilibrium monomer concentration as well as in its variation with polymer concentration.

The effect of solvent on equilibrium polymerization may be checked by comparing results obtained for the polymerization of a given monomer in two different solvents. Because the equilibrium polymerization of α-methylstyrene in tetrahydrofuran has been studied in detail, it was decided to investigate the equilibrium polymerization of the same monomer in *p*-dioxane. Dielectric constants and propagation rate constants[3,4] for the same counterion differ to a considerable extent for these two solvents so that a solvent effect on the equilibrium position is expected. In order to check the magnitude of that effect, we wish to report the determination of equilibrium monomer concentrations for the anionic polymerization of α-methylstyrene in *p*-dioxane at 5, 15, 25, and 40°C.

EXPERIMENTAL

Materials

1,4-Dioxane (Baker analyzed) was purified by percolation through a column of activated alumina (80 g/100–200 ml of solvent) and distilled. The middle fraction was kept over CaH_2 and degassed over vacuum line for three weeks. It was further refluxed with and distilled over a sodium–potassium alloy. A small amount of naphthalene was distilled into the container, and the green sodium naphthalene complex was formed. The retention of the green color was used as an indicator for the purity of dioxane. The flask containing dioxane was covered with an aluminum foil and degassed from time to time. Even with all these precautions, it was observed that after a period of about three weeks the green complex decomposed and a brown crust was formed. In order to avoid this, the contents were distilled on fresh sodium–potassium alloy after about every two weeks.

Tetrahydrofuran (Anachemia) was kept over CaH_2 and degassed on the vacuum line for three weeks. It was refluxed with and distilled over a sodium–potassium alloy. A small amount of naphthalene was distilled

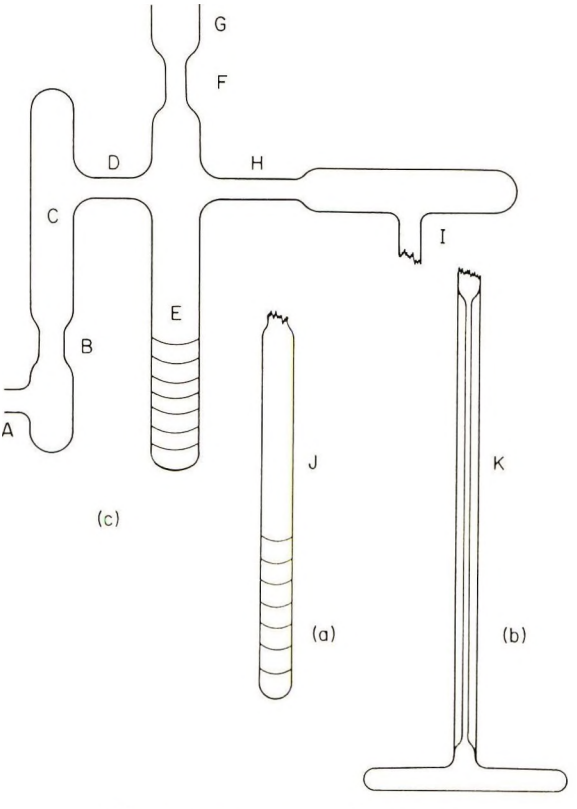

Fig. 1. Apparatus for polymerizations.

into the flask and the retention of the green color was used as a test for the purity of the solvent.

α-Methylstyrene (Baker analyzed) was kept over CaH_2 and degassed on the vacuum line for two to three weeks. It was distilled under vacuum, the head and the tail fractions being discarded. Vapor-phase chromatography (VPC) of the middle fraction showed it to contain small amounts of cumene, but the presence of no other material could be detected.

Calibration of the Ampoules

Polymerization runs were carried out in calibrated ampoules of the type shown in Figure 1. These ampoules were calibrated by filling them up to a definite reference mark with mercury at 25.00 ± 0.05°C and from the weight of mercury required to fill them, the total volume was deduced. Further the cross-section of the capillary (Fig. 1*b*) and the tubing (Fig. 1*a*) were checked at different points by filling them with mercury at different levels and noting the differences of their levels and the reference mark. At each level mercury was weighed, and from the density of mercury at 25°C, the corresponding volume was calculated. As the total volume at the reference mark and the cross section were known, the volume at any level in the ampoules could be deduced. Ampoules of type shown in Figure 1*a* were easy to handle and therefore more frequently used for polymerizations. The volume of these ampoules was approximately 6 ml and determined within an error of ±0.03%. The use of dilatometers was restricted to the study of the kinetic curve as the polymerization progressed toward equilibrium; in this case the accuracy on the volume (6 ml) was around ± 0.005%.

Polymerization

Polymerizations were carried out in the reaction vessel shown in Figure 1*c* with an ampoule or dilatometer attached to it at point I. The reaction vessel was cleaned by filling with chromic acid and left overnight. It was then washed successively with distilled water and methanol and dried. A piece of potassium was introduced at A and the end was sealed. The reaction vessel was connected to the vacuum line at G and degassed. The potassium metal was heated with a cold flame, a mirror formed in C, and the glass was collapsed at B, the lower part being discarded.

The monomer and the solvent were then distilled into E which had been previously graduated for a rough estimate of the starting monomer concentration. The mixture of monomer and solvent was frozen with liquid nitrogen and the reaction vessel sealed off the line at F. The mixture was then poured on to the potassium mirror and the reaction vessel was rinsed with it till the red color indicating the presence of poly-(α-methylstyryl) anions was persistent. The solution was transferred to E, frozen, and sealed off at D, part C, being discarded, and then transferred from E to J (or K) up to a level slightly lower than the reference mark. The glass was collapsed at H and the dilatometer (or the ampoule) was immersed in a con-

stant temperature bath set at a desired temperature. Progress toward equilibrium was followed through the variation of the meniscus height in dilatometer K with time. It was observed that in the case of the α-methylstyrene–dioxane system at 5°C, equilibrium was reached after 8 days.

After equilibrium had been reached, the dilatometer (or the ampoule) was inverted and opened to air at H in presence of methanol, the whole process being carried out at equilibrium temperature. After the red color had disappeared, the solution was quantitatively removed and the polymer precipitated in methanol. The precipitated polymer was filtered through a weighed sintered glass filter, thoroughly washed with methanol and dried in a vacuum oven at 60°C to constant weight. The filtrate and the washings were collected in a measuring flask and preserved for the analysis of the unreacted α-methylstyrene.

Monomer Analysis

Determination of unreacted monomer was carried out through gas chromatography with cumene as an internal standard. Analyses were performed with a Perkin-Elmer chromatograph at 170° on a UCON oil column LB-550-X with the use of a thermal conductivity detector with helium as a carrier.

Molecular Weights

Molecular weights of poly-α-methylstyrene were determined by viscometry in toluene at 25°C in a modified Ubbelhode viscometer. Molecular weights were computed from the relation:[5]

$$[\eta] = 7.81 \times 10^{-5} \bar{M}_v^{0.73}$$

where $\bar{M}_v$ is the viscosity-average molecular weight ($\bar{M}_v > 3 \times 10^4$). The intrinsic viscosity $[\eta]$ was determined by a one-point method.[6] For the present system, results obtained by the one-point method are in good agreement with those obtained through the extrapolation of η_{sp}/c.

RESULTS

Equilibrium monomer concentrations $[M]_e$ and equilibrium polymer concentrations [P] for the anionic polymerization of α-methylstyrene in *p*-dioxane at 5, 15, 25, and 40°C are shown in Table I together with molecular weights, $\bar{M}_v$, and "living end" concentrations [LE]. Assuming two "living ends" per chain, [LE] is obtained through the relation

$$[\text{LE}] = 2w/\bar{M}_v V_e = 2 \times 118.2\ [\text{P}]/\bar{M}_v \text{ mole/l} \qquad (1)$$

where w is the weight of polymer (in grams) present at equilibrium in the volume V_e (in liters).

TABLE I
Equilibrium Values of Monomer and Polymer Concentrations, Molecular Weights and Living End Concentrations at Various Temperatures

Solvent	Temperature, °C	$[M]_e$, mole/l.	[P], base-mole/l.	$\bar{M}_v \times 10^{-4}$, g/mole	[LE] $\times 10^3$, mole/l.
Dioxane	5	0.864	0.422	18.5	0.54
		0.677	1.140	8.7	3.1
		0.761	1.823	18.8	2.3
		0.671	2.131	14.7	3.4
		0.565	2.532	16.7	3.6
		0.532	3.200	14.7	5.1
		0.540	3.810	16.0	5.6
Dioxane	15	1.40	0.86	5.5	3.7
		1.42	0.980	12.9	1.8
		1.29	1.300	6.9	4.4
		1.13	1.96	6.7	6.9
		1.13	2.04	12.4	3.9
		1.05	2.080	5.6	8.7
		1.13	2.300	10.6	5.1
		0.84	2.960	11.0	6.3
		0.91	3.670	16.0	5.4
		0.80	3.830	20.9	4.3
		0.75	4.420	21.8	4.8
Dioxane	25	1.863	0.890	2.9	7.1
		1.920	1.140	7.3	3.7
		2.040	1.330	6.4	4.9
		1.750	2.174	6.4	8.0
		1.700	2.220	4.0	13.2
		1.600	2.600	9.5	6.4
		1.670	2.680	10.0	6.3
		1.610	3.230	10.1	7.6
		1.350	4.600	15.5	7.2
Dioxane	40	3.510	0.860	3.0	6.7
		3.380	1.600	9.7	3.9
		3.400	1.620	13.7	2.8
		3.250	2.800	4.9	13.5
		3.050	4.330	17.7	5.8

TABLE II
Experimental Values of A, B, ϕ_m^0, and b at Various Temperatures

Temperature, °C	A, mole/l.	$-B$ mole/base-mole	V_m, l./mole	V_p, l./base-mole	ϕ_m^0	$-b$
5	0.866	0.097	0.128	0.106	0.111	0.117
15	1.50	0.180	0.129	0.107	0.193	0.217
25	2.10	0.164	0.130	0.107	0.273	0.199
40	3.607	0.129	0.132	0.108	0.476	0.158

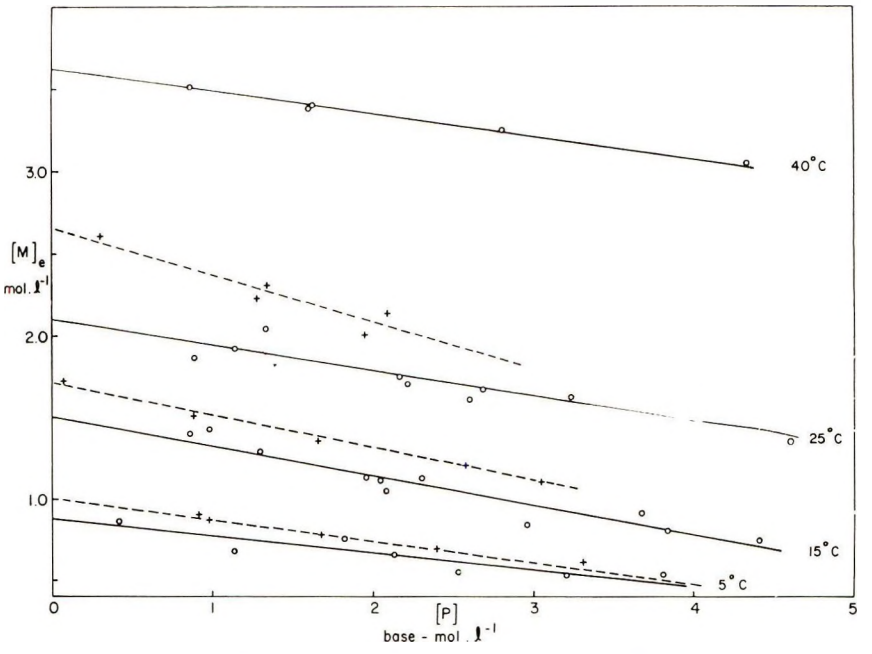

Fig. 2. Variation of equilibrium monomer concentration $[M]_e$ with polymer concentration [P] for the anionic polymerization of α-methylstyrene: (●) in p-dioxane, (+) in THF.

From Figure 2 it can be seen that, as in the case of tetrahydrofuran (THF), the variation of $[M]_e$ with [P] is linear for the concentration range studied here and this variation may be expressed by

$$[M]_e = A + B[P] \tag{2}$$

Parameters A and B are computed by the method of least squares and results are shown in Table II.

In order to relate the experimental results to the thermodynamic properties of the polymerization system, eq. (2) is written in terms of monomer volume fraction, ϕ_m, and polymer volume fraction, ϕ_p;

$$\phi_m = AV_m + B(V_m/V_p)\,\phi_p = \phi_m^0 + b\phi_p \tag{3}$$

where V_m is the monomer molar volume and V_p, the volume of one base-mole of polymer. Values of V_m are obtained from data in the literature,[7] and values of V_p are assumed to be identical to values obtained in THF.[1] Values of V_m, V_p, ϕ_m^0, and b are shown in Table II.

The variation of ϕ_m with ϕ_p may be expressed by[2]

$$\phi_m = \frac{-(\Delta G_{le}/RT) + \ln a + \beta}{\beta + \chi_{mp} - (1/a)} + \frac{\chi_{mp} - \beta}{\beta + \chi_{mp} - (1/a)}\,\phi_p \tag{4}$$

where χ is the free-energy interaction parameter between any two components, the subscripts m, s, and p referring to monomer, solvent, and polymer,

respectively; $\beta = \chi_{ms} - \chi_{sp}\ (V_m/V_s)$ where V_s is the solvent molar volume; ΔG_{1c} is the free-energy change upon conversion of 1 mole of liquid monomer to 1 base-mole of liquid amorphous polymer of infinite chain length, and since the molecular weights $\bar{M}_n$ listed in Table I are all above 11,800 ($\bar{DP}$ = 100), the infinite chain length assumption is valid. a is a constant which, ideally, should coincide with $\phi_m{}^0$. Assuming $a = \phi_m{}^0$ and $\chi_{mp} = 0.4$ for the present range of polymer concentrations,[8] β and $-(\Delta G_{1c}/RT)$ may be computed by comparing eq. (3) with eq. (4). Results are shown in Table III.

TABLE III
Values of β and $\Delta G_{1c}/RT$ Deduced from Equations (3) and (4)

Temperature, °C	Dioxane		Tetrahydrofuran	
	β	$-\Delta G_{1c}/RT$	β	$-\Delta G_{1c}/RT$
5	−0.69	1.85	−0.81	1.82
15	−0.81	1.38	−0.80	1.22
25	−0.31	0.63	−0.75	0.68
40	0.16	−0.15	—	—

DISCUSSION

The consistency of the equations used for the computation of ΔG_{1c} may be checked by comparing results obtained for the polymerization of α-methylstyrene in *p*-dioxane and THF. As ΔG_{1c} refers essentially to the conversion of liquid monomer to liquid amorphous polymer of infinite chain length, this quantity should be independent of the polymerization system at a given temperature for a given monomer. If this is so, although the equilibrium monomer and polymer concentrations in *p*-dioxane and THF are different, eqs. (3) and (4) should yield identical values of ΔG_{1c} for the polymerization of α-methylstyrene. Table III shows comparative values of ΔG_{1c}/RT for both systems. In Figure 3, values of $\Delta G_{1c}/RT$ available for both systems are plotted against $1/T$. It can be seen that agreement between the two sets of values is quite satisfactory; by using the least-mean-squares method (the value at −20°C being omitted), a value of −10.6 kcal for ΔH_{1c} is obtained, which confirms the value of −10.8 determined previously.[1]

The effect of solvent on the equilibrium position can be checked empirically by comparing the variation of $[M]_e$ with [P] in THF and *p*-dioxane. From Table II and Figure 2 it can be seen that for a given temperature, the equilibrium monomer concentration in *p*-dioxane is approximately 20% lower than the corresponding monomer concentration in THF, together with the variation of $[M]_e$ with [P]. These two different behaviors cannot be explained through $\Delta G_{1c}/RT$ since for a given monomer at a given temperature, this thermodynamic value is independent of the polymerization system. This difference may be expressed in terms of β, a parameter which

is the sum of two parameters describing the solvent–monomer and solvent–polymer interactions. Values of β for both polymerizations systems at various temperatures are shown in Table III. It can be seen that for the 5–25°C temperature range, this parameter varies considerably with temperature in *p*-dioxane whereas it is relatively constant in THF. As expected

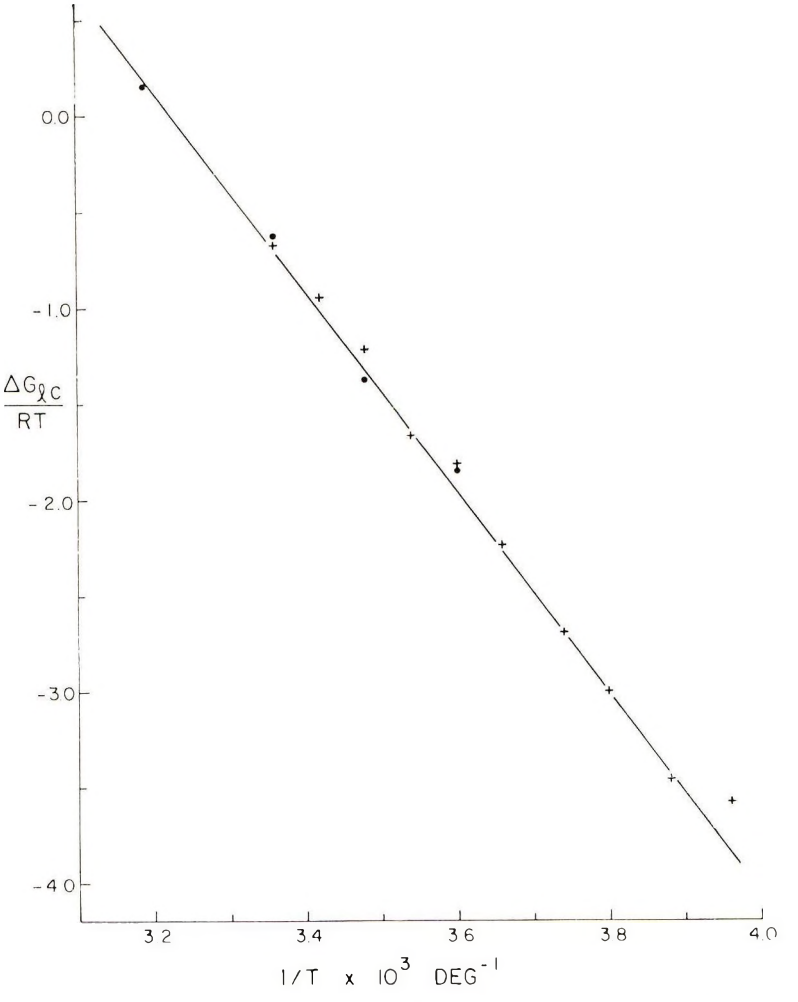

Fig. 3. Variation of $\Delta G_{1c}/RT$ with $1/T$ for the polymerization of α-methylstyrene. $\Delta G_{1c}/RT$ computed from data obtained (●) in *p*-dioxane, (+) in THF.

from the above considerations, values of β at 5 and 25°C differ quite appreciably. At 15°C both values of β are similar but this is also the temperature where the discrepancy for $\Delta G_{1c}/RT$ estimated from the *p*-dioxane system and the THF system is the largest; this would indicate that the similarity between the two values of β is only apparent. This result seems to confirm the effect of solvent on the equilibrium position and works are

now being carried out for the determination of χ_{sp} and χ_{ms}, and hence β, in an independent way in order to get more information about this effect.

The authors gratefully acknowledge financial support fron the National Research Council of Canada. S. L. M. wishes to thank the Université Laval for a post-doctoral fellowship. Special thanks are due to Dr. L. P. Blanchard and Mrs. F. Tahiani of Département de Génie Chimique for making the use of gas chromatograph possible.

References

1. K. J. Ivin and J. Leonard, *Europ. Polym. J.*, **6**, 331 (1970).
2. J. Leonard, *Macromolecules*, **2**, 661 (1969).
3. M. Van Beylen, D. N. Bhattacharrya, J. Smid, and M. Szwarc, *J. Phys. Chem.*, **70**, 157 (1966).
4. F. S. Dainton, G. C. East, G. A. Harpell, N. R. Hurworth, K. J. Ivin, and R. T. La Flair, *Makromol. Chem.*, **89**, 257 (1965).
5. H. W. McCormick, *J. Polym. Sci.*, **41**, 327 (1959).
6. A. A. Berlin, *Vysokomol. Soedin.*, **8**, 1336 (1966).
7. R. H. Boundy and R. F. Boyer, *Styrene*, Reinhold, New York, 1952, p. 698.
8. S. G. Canagaratna, D. Margerison, and J. P. Newport, *Trans. Faraday Soc.*, **62**, 3058 (1966).

Received December 31, 1970
Revised February 25, 1971

JOURNAL OF POLYMER SCIENCE: PART A-1 VOL. 9, 1999–2007 (1971)

Radiation-Induced Polymerization at High Pressure of 2,3,3,3-Tetrafluoropropene in Bulk and with Tetrafluoroethylene

DANIEL W. BROWN, ROBERT E. LOWRY, and LEO A. WALL,
Institute for Materials Research, National Bureau of Standards, Washington, D. C. 20234

Synopsis

The radiation-induced polymerization of 2,3,3,3-tetrafluoropropene was studied as a function of temperature (22–100°C) and pressure (autogenous to 10^4 atm). Rates have varied 100-fold for the same reaction conditions probably because of trace impurities. The most rapidly polymerizing material has a rate of 4.5%/hr at 6000 atm, 22°C, and 1500 rad/hr. The activation enthalpy and volume are 4 kcal/mole and −13 cc/mole, respectively. Rates are proportional to the square root of the radiation intensity. Degrees of polymerization varied between 2×10^3 and 2×10^6. In copolymerization with tetrafluoroethylene the reactivity ratios at 22°C and 5000 atm are 0.37 (the ratio for addition to the tetrafluoroethylene-ended radical) and 5.4 (the ratio for addition to the tetrafluoropropene-ended radical). Comparison of ratios for the copolymerization of other fluorine-containing monomers with tetrafluoroethylene shows that they generally disfavor incorporation of the latter.

INTRODUCTION

Previously, studies were made of the radiation-induced polymerization at high pressure of propene,[1] 3,3,3-trifluoropropene,[2] and hexafluoropropene.[3] 2,3,3,3-Tetrafluoropropene has now been studied similarly. The polymerization appears sensitive to trace impurities, and the uncertainty of the results in bulk polymerizations caused us to study the copolymerization with tetrafluoroethylene. A preliminary description of our work has been given.[4]

Other workers using 2,3,3,3-tetrafluoropropene have homopolymerized and copolymerized it by emulsion techniques,[5] telomerized it with various halogen-containing alkanes at 150–200°C,[6] and polymerized it at autogenous pressure under radiation from ^{60}Co.[7] This last is pertinent to our work. The number of tetrafluoropropene molecules polymerized per 100 eV absorbed was reported to be 350 at 10^5 rad/hr. The polymer had a number-average degree of polymerization (DP_n) of seven whether prepared at 10^5 or 8×10^5 rad/hr.

EXPERIMENTAL

2,3,3,3-Tetrafluoropropene was prepared by deiodofluorinating 2,2,3,3,3-pentafluoropropyl iodide, samples of which were purchased from Columbia

Organic Chemical Company, Peninsular Chem Research, and Pierce Chemical Company. The deiodofluorinations are described below. Tetrafluoroethylene was purchased from Peninsular Chem Research. Inhibitor was removed by low-temperature distillation.

Both monomers were degassed, condensed on Ascarite, then on phosphorus pentoxide, and finally condensed into the reaction vessels. High-pressure polymerizations were performed in steel bombs as before.[8] Glass tubes were used for runs at autogenous pressure. An external radiation source of ^{60}Co was used. Rates in each run were calculated from the conversion and time in the source.

In copolymerizations the monomer compositions were calculated by use of the perfect gas law from the pressure and volume of each component. Copolymer compositions were calculated from their carbon contents. Mole fractions of the components are within 0.02 of correct values.

Intrinsic viscosities $[\eta]$ at 29.8°C were determined as before in acetone and hexafluorobenzene.[9] No corrections were made for the effect of the shear rate (2500–5000 sec^{-1}). Fractions were prepared by precipitating the polymer from solutions of acetone with benzene (high DP) or with methanol (low DP) by successive temperature reductions. The ratio of osmotic pressure to concentration was determined at four concentrations each in acetone for four of the fractions. Plots of the square roots of these ratios versus concentration for each fraction were linearly extrapolated to zero concentration. The intercepts were squared and used in the van't Hoff equation to calculate the molecular weights of the fractions.

RESULTS

Preparation of 2,3,3,3-Tetrafluoropropene

Three dehalogenation methods were used. These are listed in Table I. Conditions and general techniques were similar to those used by others in analogous preparations.[10–12] In the zinc and magnesium methods the iodide was added dropwise to the stirred, refluxing, solvent–metal mixture, and the fluoropropene was collected as it evolved. When methyl lithium was used, it was added dropwise to the cold, stirred, ether–iodide mixture;

TABLE I
Deiodofluorination of 2,2,3,3,3-Pentafluoropropyl Iodide

Agent/solvent temp	Yield, % $CF_3CF = CH_2$	Yield, % $C_2F_5CH_3$
Zn/HAc, reflux	50	15
Mg, I_2/ether, reflux	25	1.0
CH_3Li/ether, −80°C	65	0.8

this was stirred for 6 hr at −80°C and allowed to warm to room temperature overnight. Some fluoropropene collected in an attached cold trap during this warmup but the bulk remained in the ether from which it was later driven by distillation.

The low-boiling material from each preparation was redistilled, taking as the fluoropropene the fraction boiling between −29 and −28°C. (The boiling point of 2,3,3,3-tetrafluoropropene is reported as −28.3°C.[13]) The molecular weight measured by vapor density on a portion of one fluoropropene fraction was 114; elemental analysis of polymer formed from it gave 1.69% H, 31.5% C, and 67.2% F. Theoretical values are 114 for the monomer molecular weight and 1.77% H, 31.59% C, and 66.64% F for the composition.

The yields of fluoropentene fraction are given in Table I. Unconverted iodide was recovered from the methyl lithium reaction. The propene yield, based on iodide consumed, was 90%. In the other reactions, essentially no iodide was recovered.

These different syntheses were used because of byproduct formation, poor yields, and apparent retardation in the polymerization of the fluoropropene. 1,1,1,2,2-Pentafluoropropane was formed in all dehalogenations; its yields are included in Table I. Identification was based on the boiling point, −17°C,[14] and the vapor density of the portion of a distillation cut from the zinc dehalogenation, collected between −28 and −15°C, that did not undergo bromination. Chromatographic and mass spectrographic analyses were used to establish fluoropropane yields in the other reactions. A 1-m, Perkin-Elmer column (treated silica gel) at 110°C resolved the fluoropropane and fluoropropene satisfactorily, the former having a 50% greater retention time. SE 30, in the 1-m column, did not resolve these components at −10°C.

Chromatographic analysis on the silica gel column of the fluoropropene from the zinc reaction showed a fluoropropane content of 5%. The propane contents of the other cuts were about 0.5%. Except for that of air, no other impurity peaks were present in the chromatogram of the distillate from the zinc reaction. The magnesium-prepared fluoropropene on SE 30 showed an unidentified impurity with a low retention time in its chromatogram, approximating 0.1% of the total peak area. The silica gel chromatogram of the propene from the methyllithium reaction contained a peak with 0.05% of the total area that had the same retention time as 3,3,3-trifluoropropyne. No peak appeared at the retention time of 2-(trifluoromethyl)-propene. (Authentic samples of these two compounds were obtained from Peninsular Chem Research.) In our reaction one might expect such compounds following transfer and addition reactions, respectively, of methyllithium with 2,3,3,3-tetrafluoropropene.

Earlier,[4] peaks in the mass spectrum at masses 36, 37, 38, 55, 56, 57, 81, 82, and 83 were mentioned as possibly being due to impurities. Additional work indicates that they probably arise from the propene or propane. Other small peaks were sometimes found at masses 39, 40, and 41. Their

origin is unknown, but they may be associated with poor polymerizability, as discussed below.

Bulk Polymerization

At 5000 atm* and 22°C, the polymerization rate without radiation was less than 10^{-3}%/hr. (As this is only 2% of the lowest radiation-induced rate that we observed, the contribution of thermal polymerization is not considered further.)

In contrast, exposure to γ-radiation under these conditions readily produces polymer. Figure 1 shows for different samples at 22°C how polymerization rate varies with pressure. The conversions to polymer ranged from 0.1 to 20%. Numbers near the points in the figure are values of $[\eta]$ in acetone.

The polymerizations were done first with the fluoropropene from the zinc reaction (filled circles in Fig. 1). As noted above, this reactant contained 5% pentafluoropropane. It polymerized well to form polymers with large $[\eta]$ values, indicating that this propane neither inhibits polymerization nor is a labile transfer agent. However, it was desired to effect the polymerization in the absence of the fluoropropane, and additional fluoropropene was prepared by use of the magnesium reaction, since separating the propene from the propane was impractical.

This material polymerized very slowly (flagged open circle, in Fig. 1); $[\eta]$ was not determined. The run was repeated, and about the same result was obtained. This propene was then purified by preparative-scale chromatography with the use of SE 30 at −10°C in a 5/8-in. diameter, 9-ft column. About 10% was cut from the front and back of the propene peak; the unidentified impurity, mentioned earlier, came off well before the propene peak. The shape of the main peak indicated overloading, and it is unlikely that there were large reductions in the concentrations of any impurities having retention times about equal to that of the propene. Nevertheless, the polymerization rate of the purified monomer (open circles in Fig. 1) was almost two orders of magnitude higher than before the chromatography. The rates and intrinsic viscosities are higher throughout the pressure range than those obtained with the product of the zinc reaction.

Mass spectra were secured using the magnesium-prepared propene from the original distillation, from that recovered after the first two polymerizations and after chromatographic purification; also, the material rejected in this chromatographic purification was run. Certain small peaks, whose size correlates inversely with polymerization rate, were found. These peaks and their heights are listed in Table II. Comparison of the results from the as distilled and recovered samples shows a 50% decrease in their heights which may indicate that an impurity had been consumed. The chromatographed sample contained no peaks at these masses whereas the sample denoted reject did. The second comparison appears particularly significant,

* 1 atm equals 1.013×10^6 dyne/cm^2 or 1.013×10^5 N/m^2.

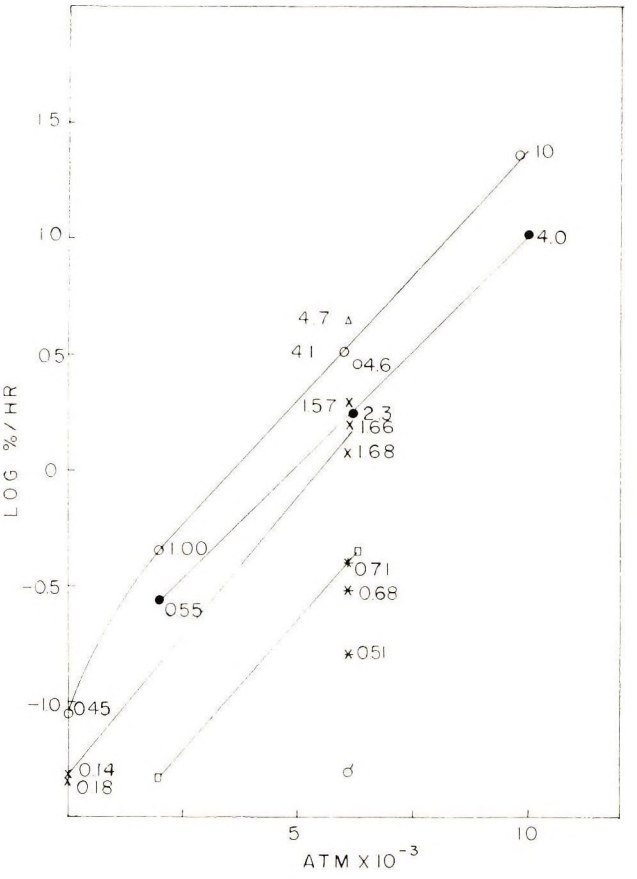

Fig. 1. Polymerization rate at 22°C, 1500 rad/hr vs. pressure: (●) Zn reaction; (♂) Mg reaction; (○) Mg reaction chromatographed; (□) MeLi reaction; (×) MeLi reaction chromatographed; (*) MeLi reaction sodium treated; (△) MeLi reaction chromatographed. The numbers near the points are intrinsic viscosities in acetone (dl/g).

since the chromatographed and rejected samples were run on the same day in the order listed, with only a background run in between. Masses 39, 40, and 41 presumably come from fragments containing three carbons and three, four, and five hydrogens, respectively, but these cannot arise from $C_3H_2F_4$. If they come from doubly charged ions of masses 78, 80, and 82, then peaks 10-fold higher should be found at these masses. Such was not the case; additionally, masses 78 and 80 cannot arise from $C_3H_2F_4$.

The supply of the fluoropropene from the magnesium reaction was exhausted before all the desired work was accomplished. More fluoropropene was prepared, this time by the methyllithium reaction in the hopes of bettering the yield and avoiding a need for chromatographic purification. However, the polymerization rate of this product was low (squares in Fig. 1). After chromatographic purification (crosses, Fig. 1), rates were higher

TABLE II

Ion Currents in Per Cent of That at Mass-to-Charge Ratio m/e Equal to 69 in the Mass Spectra of 2,3,3,3-Tetrafluoropropene Prepared by Use of Iodine-Activated Magnesium

Sample	Ion currents		
	m/e = 39	m/e = 40	m/e = 41
As distilled	0.50	0.22	0.60
Recovered	0.28	0.12	0.30
Chromatographed	0	0	0
Rejected	0.10	0.10	0.10

but not as high as with the purified fluoropropene from the magnesium reaction. Several repeat polymerizations using recovered propene were performed at 6100 atm to test whether the rate would become greater each time, as might be expected if a retarder were being consumed. This did not occur; instead, rates varied randomly from 1 to 2%/hr.

Analytical chromatograms had shown that a little 3,3,3-trifluoropropyne was present in the methyllithium-prepared propene after being chromatographed on a preparative scale. Treatment with sodium amalgam removed this impurity. In three separate runs the resulting fluoropropene polymerized very slowly to polymer of relatively low intrinsic viscosity (asterisk in Fig. 1). This fluoropropene was then chromatographed on a 30-ft (SE 30, Nester Faust, biwall) preparative column at -10°C, and the polymerization rate and intrinsic viscosity now found (triangle in Fig. 1) were the largest yet obtained in runs at 6000 atm.

The analytical chromatogram of the material rejected in the preparative-scale purification showed two impurity peaks with 0.2 and 0.02 area-% coming out after the fluoropropene peak. As the rejected material represented about 10% of the total chromatographed, these contents before chromatographing would have been about one tenth as large. These impurities have not been identified. Mass spectrograms were obtained as before but

TABLE III

Effect of Radiation Intensity at 6100 atm on the Polymerization of 2,3,3,3-Tetrafluoropropene

Dehalogenation agent	Temperature, °C	(Intensity)$^{1/2}$, (rad/hr)$^{1/2}$	Rate, %/hr	$[\eta]$, dl/g[a]
Zn[b]	98	38	6.8	1.18
Zn[b]	98	210	42	0.53
Zn[c]	22	92	6.8	0.27
Zn[c]	22	368	36	0.22
Mg[d]	22	38	2.8, 3.3	4.6, 4.1
Mg[d]	22	210	18.3	1.85

[a] In acetone at 29.8°C.
[b] 5% $CF_3CF_2CH_3$.
[c] 50% $CF_3CF_2CH_3$.
[d] Chromatographed, 0.6% $CF_3CF_2CH_3$.

no significant differences in impurity peaks were found in samples of the original distillate, the chromatographed main peak and rejecta and the amalgam-treated material. No additional efforts were made to achieve more reproducible polymerization rates because each new approach we tried seemed to bring new problems.

An exploration has been made of the effects of varying the intensity of γ-radiation. Results in Table III show that the polymerization rate increases about as the square root of radiation intensity. At the high intensities, values of $[\eta]$ are much less except in those samples of the zinc-prepared propene to which additional pentafluoropropane had been added.

Figure 2 is a modified Arrhenius plot of results at 9200 atm and 6000 atm for magnesium- and zinc-prepared 2,3,3,3-tetrafluoropropene, respectively.

Copolymerization

Table IV contains results of the copolymerizations. Arithmetic means of the initial and final monomer compositions are listed since the change during polymerization was less than 0.02. The intrinsic viscosities were determined in hexafluorobenzene because the polymers containing more than 19% tetrafluoroethylene do not dissolve in acetone. The polymer containing 86% tetrafluoroethylene is insoluble but swells greatly in hexafluorobenzene. Presumably, this behavior is due to crystallinity. Polymer containing 68% tetrafluoroethylene or less is soluble in the monomer.

Polymerization continues after removal from the radiation source. Two homopolymerizations are listed. These differed in that the second had a 23-hr post-irradiation storage period at 5000 atm. Almost three times as much polymer was formed as without storage. A volume decrease at

TABLE IV
Copolymerization of C_2F_4 and CF_3CFCH_2 at 5000 atm, 22°C, and 1500 rad/hr

C_2F_4, mole fraction		Irradiation time, hr	Polymer yield, mole-%	Rate, %/hr	$[\eta]$, dl/g[a]
In monomer	In polymer				
0.95	0.86	2.0	2.37	1.20	
0.91	0.79	3.0	2.47	0.83	4.04
0.89	0.68	2.0	1.20	0.60	3.19
0.81	0.50	3.0	1.61	0.54	2.34
0.53[b]	0.19	2.33	3.81	1.66	
0.51	0.18	5.0	1.79	0.36	1.29
0.43[b]	0.14	3.0	4.38	1.49	
0.16	0.032	3.25	2.10	0.65	
0	0	4.0	3.95	1.01	2.05
0	0	4.0	11.1		4.28
0.81[a]	0.48	1.0	0.92	0.93	3.98
0.81[d]	0.60	1.0	4.11	4.20	6.70

[a] In C_6F_6.
[b] Stored 18–24 hrs at 5000 atm, 22°C after removal from source.
[c] Polymerized at 10000 atm, 22°C.
[d] Polymerized at 5000 atm, 73°C.

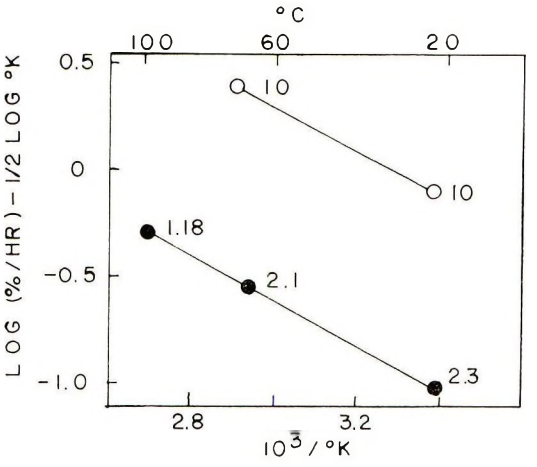

Fig. 2. Modified Arrhenius plot. (●) Zn reaction (6000 atm); (○) Mg reaction, chromatographed (9200 atm). Rates were at 1500 rad/hr. The numbers near the points are intrinsic viscosities in acetone (dl/g).

constant pressure during storage was observed, confirming that a reaction was going on. The intrinsic viscosity also is higher than that of the polymer formed without storage. These phenomena are the same as found with 3,3,4,4,5,5,5-heptafluoropentene-1 and presumably have the same cause: a radiation-formed thermal catalyst.[15] Before this was discovered the copolymerizations designated (b) had been performed. The vessels had been removed from the source late in the afternoon and not opened until the next day. Presumably, polymerization during storage accounts for the high values of the listed rates, which are based on time in the source. Values of $[\eta]$ were not determined because the samples were consumed in elemental analysis.

Intrinsic Viscosity–DP_n Relation

Figure 3 shows the variation of intrinsic viscosity $[\eta]$ in acetone and hexafluorobenzene with DP for four fractions. The equations for the least-squares fit to the data are:

Acetone:

$$[\eta] = 3.6 \times 10^{-3} (DP)^{0.58}$$

Hexafluorobenzene:

$$[\eta] = 2.6 \times 10^{-3} (DP)^{0.65}$$

The low exponent in acetone indicates that 29.8°C is near the theta temperature. Consistent with this, polymer having an intrinsic viscosity of 10 dl/g is not completely dissolved at 20°C.

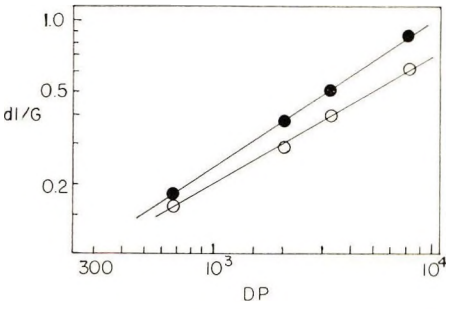

Fig. 3. Intrinsic viscosity at 29.8°C vs. DP for fractions of poly-2,3,3,3-tetrafluoropropene. (●) in C_6F_6; (○) in acetone. DP from osmotic pressure measurements.

DISCUSSION

The differences in polymerization rate found among the various preparations appear too large and too consistent to be due to random scatter, which might result simply from an irreproducible loading technique. *A priori*, the differences might come from the presence of retarders or accelerators. In Figure 1 it is seen that, at constant pressure, higher rates are generally associated with higher intrinsic viscosities. If the higher rates were due to the presence of accelerators lower intrinsic viscosities would be expected. Since rates increased with temperature (Fig. 2) and about as the square root of the radiation intensity (Table III), a free-radical mechanism appears applicable to the unretarded, propane-free polymerization:

Initiation:

$$\mathrm{M} \xrightarrow{\gamma} \mathrm{R}$$

$$d[\mathrm{R}]/dt = 1.18 \times 10^{-10} I G_i [\mathrm{M}]$$

Propagation:

$$\mathrm{R}_n + \mathrm{M} \xrightarrow{k_2} \mathrm{R}_{n+1}$$

$$-d[\mathrm{M}]/dt = k_2[\mathrm{M}] \sum_1^\infty [\mathrm{R}_n]$$

Transfer:

$$\mathrm{R}_n + \mathrm{M} \xrightarrow{k_3} \mathrm{P}_n + \mathrm{R}$$

$$d[\mathrm{P}]/dt = k_3[\mathrm{M}] \sum_1^\infty [\mathrm{R}_n]$$

Termination:

$$\mathrm{R}_n + \mathrm{R}_m \xrightarrow{k_4} \mathrm{P}_n + \mathrm{P}_m$$

$$d[\mathrm{P}]/dt = 2k_4 \left(\sum_1^\infty [\mathrm{R}_n] \right)^2$$

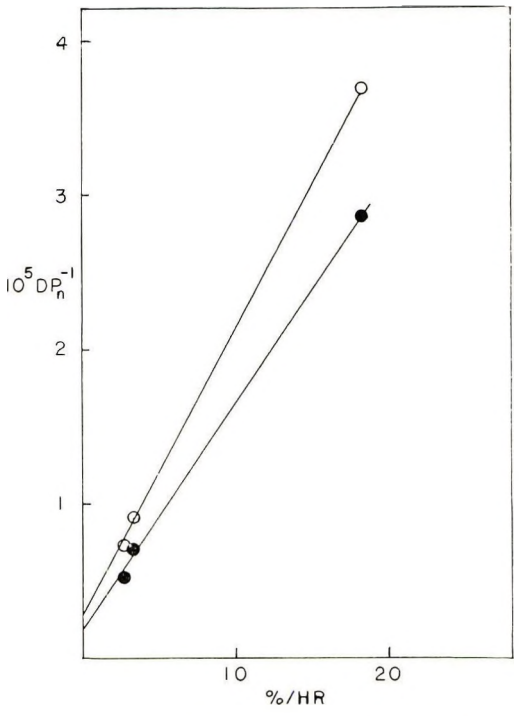

Fig. 4. Reciprocal DP_n vs. rate at different intensities: (○) disproportionation; (●) combination. Chromatographed 2,3,3,3-tetrafluoropropene from Mg reaction, 22°C, 6100 atm.

The letters M, R, and P denote the monomer, radicals, and polymer, respectively, and the terms in brackets are their molar concentrations. Subscripts denote the number of monomer units and the k's are rate constants. I is the radiation intensity in rads per hour and G_i is the number of radicals formed per 100 eV absorbed. The factor 1.18×10^{-10} gives $d[\mathrm{R}]/dt$ in moles/l.-hr when I is in rad/hr.

Assuming that there is a long kinetic chain and that the steady state approximation for $\sum_1^\infty [\mathrm{R}_n]$ is valid, the equations for R_p, the fraction of monomer polymerized per hour, and DP_n^{-1} are:

$$R_p = \frac{-d[\mathrm{M}]}{[\mathrm{M}]dt} = k_2[\mathrm{R}] = 1.09 \times 10^{-5}\left(\frac{IG_i[\mathrm{M}]}{2k_4}\right)^{1/2} k_2 \qquad (1)$$

$$DP_n^{-1} = \frac{2k_4R_p}{k_2^2[\mathrm{M}]} + \frac{k_3}{k_2} \qquad (2a)$$

$$DP_n^{-1} = \frac{1.18 \times 10^{-10}G_iI}{R_p} + \frac{k_3}{k_2} \qquad (2b)$$

If termination is by combination, the first term on the right side of eqs. (2a) and (2b) is half as large.

The presence of fluoropropane and retarders superimposes additional steps. We have no certain evidence concerning these and so will assume that the mechanism above applies to the polymerization of the chromatographed product of the magnesium prepared propene. This has little fluoropropane and gave high rates and intrinsic viscosities. The other products will be considered only where special comment is indicated.

Data from the magnesium-prepared sample in Table III were used to calculate k_3/k_2 and G_i by use of eqs. (2a) and (2b). The intrinsic viscosity–DP relation found in acetone was used to calculate the DP; viscosity-average values being obtained for whole polymer. These were assumed to be 1.8 times DP_n for termination by disproportionation and 1.4 times DP_n for termination by combination. Figure 4 is a plot of DP_n^{-1} versus 100 R_p. The intercept, k_3/k_2, is about 2×10^{-6} for both methods of termination. G_i was calculated by use of eq. (2b) from the rate at 44,000 rad/hr, since the importance of transfer decreases as intensity is increased. Depending on whether termination is by disproportionation or combination, G_i is 1.2 or 1.9 rad/100 eV, respectively. Values of about this size are normal for radical formation from small molecules.

The kinetic chain length is R_p divided by $1.18 \times 10^{-10} I G_i$. Assuming G_i is 1.2 under all polymerization conditions, this length ranges from 4×10^3 at autogenous pressure to 2×10^6 at 70°C and 10^4 atm. DP_n, calculated as above, ranges from 3×10^3 to 0.5×10^6. Considering that values of $[\eta]$ above about 4 dl/g should be higher than found, because of the effect of the shear rate, we conclude that kinetic chain length is about equal to DP_n. Khramchenkov's[7] observations that DP_n was only 2% of the G value for monomer consumption and that DP_n was independent of radiation intensity imply that there was much transfer at autogenous pressure. Our data show that the transfer was not with the propene.

Activation volumes and enthalpies may be calculated from the data in Figures 1 and 2, respectively.[2] For the chromatographed magnesium-prepared propene, these are −13 cc/mole at 22°C between 2000 and 9800 atm and 4 kcal/mole at 9200, respectively.* The low value of the latter is consistent with a temperature-independent rate of initiation. The activation entropy may be calculated from any rate, once the activation enthalpy is known.[2] The value at 9200 atm is about −16 cal/mole-degree. The slopes of the lines for different products in Figures 1 and 2 are nearly the same, showing that the overall activation volumes and enthalpies of each product are similar to the values above.

Although much effort has been put into purifying this fluoropropene there is no way of proving that a completely unretarded polymerization has been achieved. (This is also true of other polymerizations.) For this and other reasons, it is felt that a table of copolymerization reactivity ratios with a common monomer better reveals the correlation between monomer activity and structure than bulk polymerization rates. Provided that the kinetic chain for the incorporation of each monomer is long, retardation will not

* 1 kcal equals 4.184 kJ.

affect the copolymer composition which will depend on the monomer composition and four propagation rate constants. The latter are denoted k_{AA}, k_{AB}, k_{BB}, and k_{BA}, where A and B refer to tetrafluoroethylene and 2,3,3,3-tetrafluoropropene, respectively. In each constant the first subscript indicates the kind of radical end and the second indicates the monomer added. An equation relating the instantaneous polymer and monomer compositions is[16]

$$F_A = (r_1 f_A^2 + f_A f_B)/(r_1 f_A^2 + 2 f_A f_B + r_2 f_B^2) \quad (3)$$

where F_A and f_A are the mole fractions of tetrafluoroethylene in polymer and monomer, respectively, f_B is the mole fraction of the propene in the monomer, and r_1 and r_2 are the rate constant ratios k_{AA}/k_{AB} and k_{BB}/k_{BA}, respectively.

The composition data from polymerizations at 5000 atm and 22°C in Table IV were used to calculate r_1 and r_2, by the Fineman-Ross method.[17] The values obtained were entered in eq. 3 which was then used to generate the line in Figure 5. Symbols indicate experimental points; they approach the line closely throughout the composition range. Single runs at higher pressure and temperature also give points close to the line, indicating little effect of those variables on the reactivity ratios.

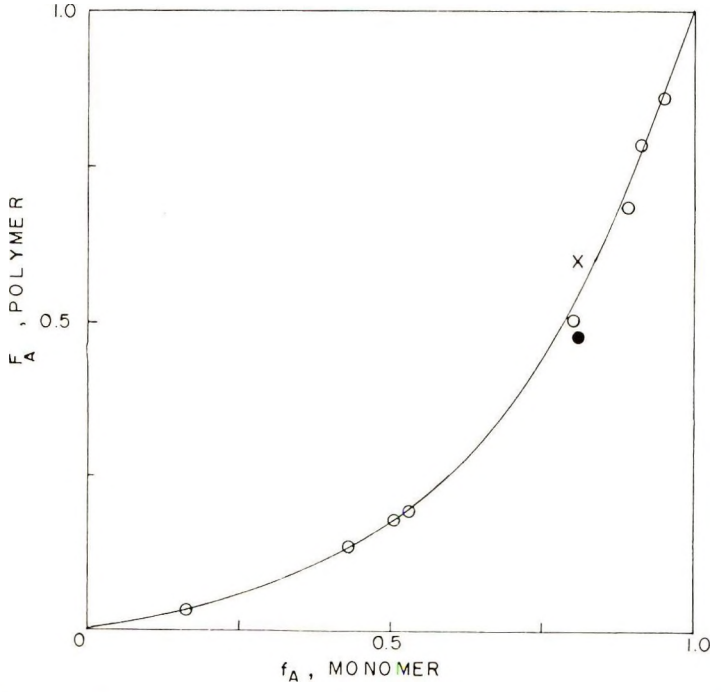

Fig. 5. Mole fraction C_2F_4 in polymer (F_A) vs. that in monomer (f_A): (○) 5000 atm, 22°C; (●) 10000 atm, 22°C; (×) 5000 atm, 73°C. Line according to eq. (3) with r_1 = 0.37, r_2 = 5.4.

Table V lists the reactivity ratios for other B monomers copolymerized with tetrafluoroethylene at high pressure. Ratios for 3,3,3-trifluoropropene and 3,3,4,4,5,5,5-heptafluoropentene-1 were published previously.[9,18] Ratios for 2-trifluoromethyl-3,3,3-trifluoropropene and for *trans*-1,3,3,3-tetrafluoropropene are from work in progress. The reciprocals of the r's represent relative rate constants for the addition of the monomers to a radical ending in a tetrafluoroethylene unit using a scale on which the rate constant for addition of tetrafluoroethylene is one. Considering the first three B monomers in Table V the reciprocals increase as the number of electron-withdrawing groups on the vinyl group is decreased. Steric effects appear to be involved to a minor extent since the reciprocals for the hexafluoroisobutylene and 3,3,4,4,5,5,5-heptafluoropentene-1 are not much

TABLE V
Rate Constant Ratios r_1, r_2 at 5000 atm and 22°C[a]

B	r_1	$1/r_1$	r_2	$-d[B]/[B]dt$,[b] %/hr
C_2F_4	1	1	1	—
$CH_2{=}CF(CF_3)$	0.37	2.7	5.4	3.2
$CH_2{=}CH(CF_3)$	0.12	8.3	5.0	1.5
$CH_2{=}C(CF_3)(CF_3)$[c]	0.58	1.7	0.09	
$CH_2{=}CH(C_4F_7)$	0.21	4.8	2.3	0.05
trans-$CHF{=}CH(CF_3)$	22	0.046	0.18	0.001

[a] A = C_2F_4; $r_1 = k_{AA}/k_{AB}$; $r_2 = k_{BB}/k_{BA}$.
[b] At 3000 rad/hr, [A] = 0.
[c] 10^4 atm. Monomer supplied by Dr. M. H. Kauffman, Naval Weapons Center, China Lake, California.

less than those for 2,3,3,3-tetrafluoropropene and 3,3,3-trifluoropropene, respectively. The *trans*-1,3,3,3-tetrafluoropropene has a very low reciprocal. This implies that polar effects are very important, since the tendency of fluorine to withdraw electrons should be about the same in both the one and two positions.

The r_1's show much less variation with structure than do the homopolymerization rates. The latter involve rate constants for the addition of each monomer to a different active end as well as initiation and termination rate constants. In each case these constants are combined as in eq. (1), provided no retarder is present.

The variation of the r_2 can not be correlated simply with monomer structure because different B-ended radicals are involved. Where the

value exceeds one, the ratio favors the incorporation of monomer B. This is the case except with the hexafluoroisobutylene and *trans*-1,3,3,3-tetrafluoropropene.

The copolymer rate equation can be used to calculate R_p/R_B, the copolymerization rate relative to the homopolymerization rate of 2,3,3,3-tetrafluoropropene under the same conditions, if values are assumed for R_A/R_B, the ratio of the two homopolymerization rates, and for the cross-termination parameter ϕ.[9] Results of this calculation are shown in Figure 6. Lines are according to eq. (2) of reference 9; points are experimental rate ratios.

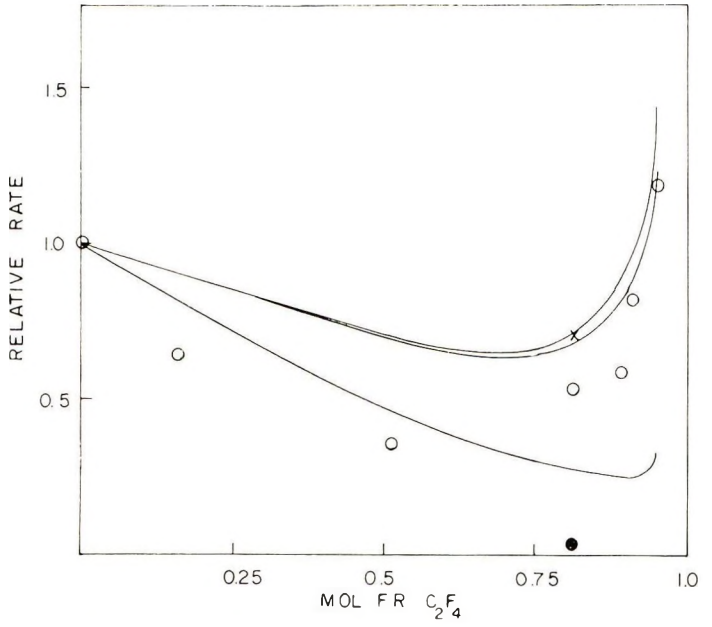

Fig. 6. Copolymerization rate relative to the homopolymerization rate of 2,3,3,3-tetrafluoropropene vs. the mole fraction of C_2F_4 in the monomer: (○) 5000 atm, 22°C; (●) 10000 atm, 22°C; (×) 5000 atm, 73°C. Lines according to eq. (2) of ref. 9: (upper) $R_A/R_B = 10$, $\phi = 1$; (middle) $R_A/R_B = 4$, $\phi = 1$; (lower) $R_A/R_B = 10$, $\phi = 100$.

It was not possible to choose a ϕ and R_A/R_B that gave substantial agreement between lines and points throughout the composition range. Somewhat better agreement with theoretical curves was obtained in copolymerizations of tetrafluoroethylene with 3,3,3-trifluoropropene[9] and 3,3,-4,4,5,5,5-heptafluoropentene-1.[18] Presumably, the copolymerizations studied here are retarded to different extents, accounting for the great disagreement observed.

This study was supported by the U.S. Army Research Office, Durham, North Carolina.

Certain commercial materials are identified in this paper in order to adequately specify the experimental procedure. In no case does such identification imply recommendation or endorsement by the National Bureau of Standards, nor does it imply that the materia identified is necessarily the best available for the purpose.

References

1. D. W. Brown and L. A. Wall, *J. Phys. Chem.*, **67**, 1016 (1963).
2. D. W. Brown, paper presented at 150th Meeting, American Chemical Society, Sept. 1965, Atlantic City, N. J.; *Polym. Preprints*, **6**, 965 (1965).
3. R. E. Lowry, D. W. Brown, and L. A. Wall, *J. Polym. Sci. A-1*, **4**, 2229 (1966).
4. D. W. Brown, R. E. Lowry, and L. A. Wall, paper presented at 160 Meeting, American Chemical Society, Sept. 1970, Chicago, Ill.; *Polym. Preprints*, **11**, 1042 (1970).
5. E. S. Lo, U.S. Pat. 2,970,988 (Feb. 7, 1961).
6. M. Hauptschein, M. Braid, and F. Lawlor, U.S. Pat. 3,240,825 (March 15, 1966).
7. V. A. Khramchenkov, *Dokl. Akad. Nauk SSSR*, **149**, 230 (1963), Consultants Bureau translation.
8. L. A. Wall, D. W. Brown, and R. E. Florin, paper presented at 140th Meeting, American Chemical Society, Sept. 1961, Chicago, Ill.; *Polym. Preprints*, **2**, 366 (1961).
9. D. W. Brown and L. A. Wall, *J. Polym. Sci. A-1*, **6**, 1367 (1968).
10. E. T. McBee, D. H. Campbell, and C. W. Roberts, *J. Amer. Chem. Soc.*, **77**, 3149 (1955).
11. H. Gilman and R. G. Jones, *J. Amer. Chem. Soc.*, **65**, 2037 (1943).
12. O. R. Pierce, E. T. McBee, and G. F. Judd, *J. Amer. Chem. Soc.*, **76**, 474 (1954).
13. A. L. Henne and T. P. Woolkes, *J. Amer. Chem. Soc.*, **68**, 496 (1946).
14. R. L. Shank, *J. Chem. Eng. Data*, **12**, 474 (1967).
15. D. W. Brown, R. E. Lowry, and L. A. Wall, *J. Polym. Sci., A-1*, **8**, 3483 (1970).
16. P. J. Flory, *Principles of Polymer Chemistry*, Cornell Univ. Press, Ithaca, N.Y., 1953, p. 178.
17. M. Fineman and S. D. Ross, *J. Polym. Sci.*, **5**, 259 (1950).
18. D. W. Brown, R. E. Lowry, and L. A. Wall, *J. Polym. Sci. A-1*, **8**, 2441 (1970).

Received February 9, 1971

JOURNAL OF POLYMER SCIENCE: PART A-1 VOL. 9, 2009–2029 (1971)

Thermal and Photochemical Oxidation of 2,6-Dimethylphenyl Phenyl Ether: A Model for Poly(2,6-dimethyl-1,4-phenylene Oxide)

ROBERT A. JERUSSI,* *General Electric Research & Development Center, Schenectady, New York 12301*

Synopsis

The oxygenation of 2,6-dimethylphenyl phenyl ether (I) at 260°C has resulted in the formation of 4-methylxanthone (II), 2-hydroxy-3-methylbenzophenone(III), 2-phenoxy-3-methylbenzaldehyde (IV), 2-phenoxy-3-methylbenzoic acid (V), 2-phenoxy-3-methylbenzyl *o*-cresotinate (VI), 2-phenoxy-3-methylbenzyl alcohol (VII), and 2-phenoxy-3-methylbenzyl 2-phenoxy-3-methylbenzoate (VIII), The photochemical oxidation at 75° produced compounds II, III, IV, VII, and VIII. Oxidation of poly(2,6-dimethyl 1,4-phenylene oxide) film at 200°C and photochemically at 50°C produced a carbonyl band at ca. 1730 cm^{-1}. The gel content of the photochemically aged film could be significantly reduced and the 1730 cm^{-1} peak in the thermally aged specimen could be moved to longer wavelength by base treatment. The isolation of compound VIII in both processes with the model compound and the results with the polymer allows us to propose an ester group as a crosslinking unit in thermally and photochemically aged polymer film.

INTRODUCTION

The thermal oxidation of poly(2,6-dimethyl-1,4-phenylene oxide) films at 125°C in air has revealed[1] the development of a broad —OH absorption in the infrared region along with two other bands at 1660 and 1695 cm^{-1}. The latter was assigned to a carboxylic acid carbonyl group. These spectral changes were accompanied by large amounts of gel formation, indicating crosslinking. A mechanism was proposed where an initially formed hydroperoxide decomposed to a mixture of benzyl and benzyloxy type radicals. It was further suggested that these intermediates combined to form crosslinked products with bibenzyl or dibenzyl ether bridges and that the benzyloxy radical also could react further to benzaldehyde and benzyl alcohol type units. The origin of carboxylic acid was suggested as arising from oxidation of these latter two groups.

A similar study in this laboratory[2] at 125, 150, 175, 200, and 250°C indicated the formation of —OH and three peaks in the carbonyl region at 1722, 1689, and 1661 cm^{-1}. The 1689 cm^{-1} peak was assigned to carboxylic acid

* Present address: Food and Drug Administration, Bureau of Drugs, Rockville, Md. 20852.

and it was suggested that the 1722 cm^{-1} peak may be due to ester carbonyl. The rate with which these peaks developed increased with temperature.

The photo oxidation of the polymer was also studied.[1] Within 180 hr, a broad band at ca. 1740 cm^{-1} was produced, and almost the maximum amount of gel formation had occurred, ca. 10%. Although this band was not assigned by the authors, at least part of it is in the aromatic ester region.

Poly(2,6-dimethyl-1,4-phenylene oxide) is primarily a molding material with a melting peak having a maximum at 267°C.[3] With this in mind, and the aforementioned work on the polymer, an investigation was begun to study the oxidation of 2,6-dimethylphenyl phenyl ether (I), the simplest model for the polymer, at about 270°C. Specific information was sought about the reactions occurring and the functional groups being developed during the oxidation. The photochemical oxidation of I was also investigated, along with thermal and photochemical aging of polymer films.

RESULTS

Thermal Oxidation of Compound I

Compound I was oxidized at reflux (ca. 260°C) by passing a slow stream of oxygen through the system for 11 hr. After the reaction, the ether-soluble material was converted into a neutral and basic fraction. The neutral fraction was primarily unreacted starting material, which was separated from the oxo products by column chromatography and recovered in 56% yield. The oxo products were separated into a number of compounds by preparative thin layer chromatography.

One of the oxidation products was isolated as a yellow solid in 3.9% crude yield. The recrystallized material had mp 124–124.2°C and exhibited strong carbonyl absorption at 1650 cm^{-1} and rather weak aryl-oxygen stretching vibrations at 1220 and 1235 cm^{-1}. The material also failed to give the characteristic color of a 2,4-dinitrophenylhydrazone when a silica gel TLC plate containing it was sprayed with 2,4-dinitrophenylhydrazine. These facts were suggestive of a xanthone, a class of compounds which has a strong carbonyl absorption at 1660 cm^{-1} and gives carbonyl derivatives with difficulty.[4,5] Comparison of the compound isolated with an authentic sample of 4-methylxanthone (II), mp 125–126°C, confirmed its identity as II.

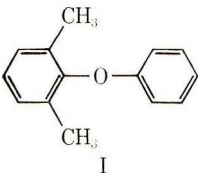

I

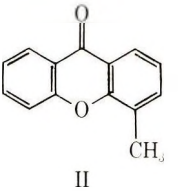

II

Another compound was isolated as a yellow oil. The infrared spectrum revealed a bonded hydroxyl at 3200 cm^{-1}, a strong carbonyl absorption at 1620 cm^{-1}, and a strong aryl-oxygen stretching vibration at 1240 cm^{-1}.

Conversion of the hydroxyl to a silyl ether shifted the carbonyl to 1670 cm^{-1}. The NMR spectrum indicated only one $—CH_3$ group at 2.25 ppm. The yellow color and the fact that the carbonyl absorption could be shifted by converting the hydroxyl group to an ether suggested 2-hydroxy-3-methylbenzophenone (III). Synthesis of III and comparison of it with the yellow compound isolated confirmed its identity. Compound III was isolated from the oxidation reaction in 3.0% yield.

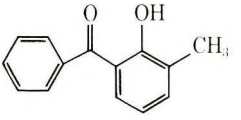

III

A third product was isolated as an amber oil. The infrared spectrum indicated a carbonyl band at 1700 cm^{-1}, a strong aryl-oxygen stretching vibration at 1230 cm^{-1}, and a band at 2730 cm^{-1}, which could be assigned to the carbon-hydrogen stretching vibration of an aldehyde.[6] The nuclear magnetic resonance spectrum of the crude material indicated one $—CH_3$ group at 2.17 ppm and a sharp singlet at 10.25 ppm for one hydrogen. The latter lent further support to an aldehyde and 2-phenoxy-3-methylbenzaldehyde (IV) was considered. Short path distillation gave a colorless oil which gave a satisfactory analysis for IV. The mass spectrum indicated the molecular ion at m/e 212, the correct molecular weight for IV, and it also contained a large M-1 peak, also indicative of an aldehyde.[7a] Finally, the material was oxidized by chromium trioxide to 2-phenoxy-3-methylbenzoic acid (V), which was identical to authentic material. The crude aldehyde was isolated in 2.7% yield.

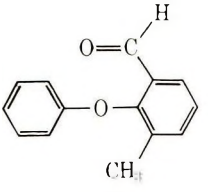

IV

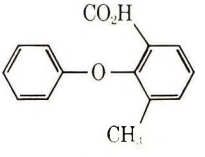

V

Several other products were isolated in trace quantities (<1%) from the neutral fraction and identified. One of these was an oil which had a longer vapor-phase chromatography retention time than II, III, or IV and exhibited infrared bands at 1670 and 3200 cm^{-1}. The nuclear magnetic resonance spectrum indicated the presence of two $—CH_3$ groups at 2.15 and 2.28 ppm, possibly a benzylic methylene unit at 5.33 and possibly a phenolic —OH at 10.9 ppm. A high-resolution mass spectrogram indicated the mass peak to be 348.1368 ($C_{22}H_{20}O_3$). This information suggested 2-phenoxy-3-methylbenzyl *o*-cresotinate (VI). Further support was given structure VI by the observation of a 214.0986 ($C_{14}H_{14}O_2$) peak in the mass spectrogram

which is very likely due to the benzyl alcohol VII. The production of alcohol is a known fragmentation process for salicylates via the path shown.[7b]

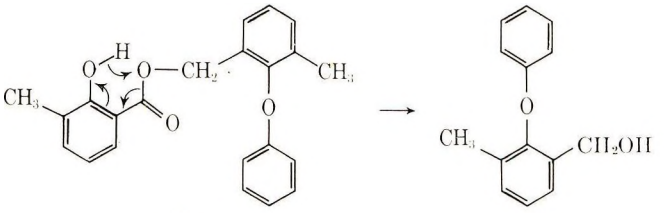

VI VII (1)

Compound VI was confirmed as the structure of the unknown compound by synthesis of authentic material via the route outlined in eq. (2). Oxidation of I with potassium permanganate in pyridine gave 2-phenoxy-3-methylbenzoic acid (V). Compound V was converted to the methyl ester,

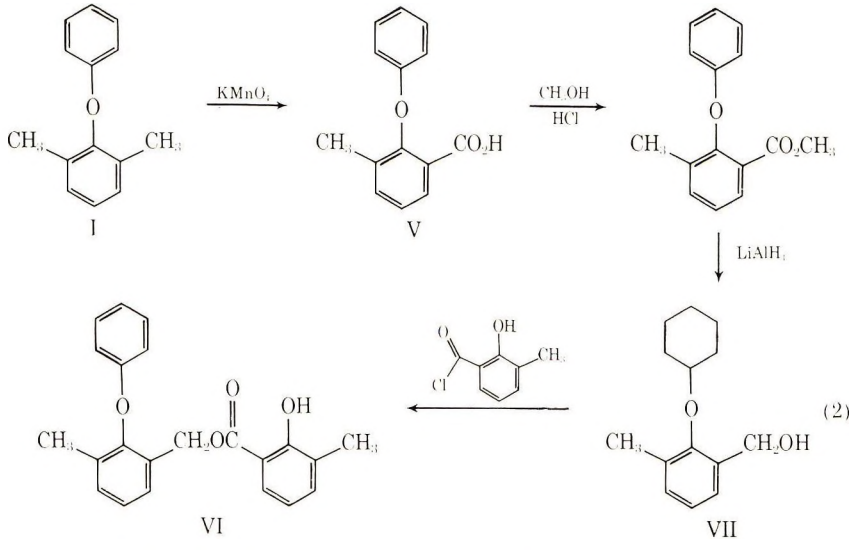

(2)

which was reduced with lithium aluminum hydride to 2-phenoxy-3-methylbenzyl alcohol (VII). Reaction of VII with 2-hydroxy-3-methylbenzoyl chloride gave VI in 47% yield. This was identical to the material isolated in the oxidation reaction. Finding VI in the neutral fraction is probably due to its insolubility in aqueous base.

Having authentic VII helped in identifying it as a trace product in the oxidation mixture. The infrared spectra and vapor phase chromatography retention times of the two samples were identical.

Another material isolated as a trace product had a carbonyl band at 1730 cm^{-1} in the infrared and a molecular ion m/e 424 in the mass spectrogram. The mass spectrogram also had major peaks at m/e 211 and 197. These facts are suggestive of a benzyl benzoate such as VIII, which has a molecular weight of 424. Benzyl benzoates produce the two ions of the type shown[7b]

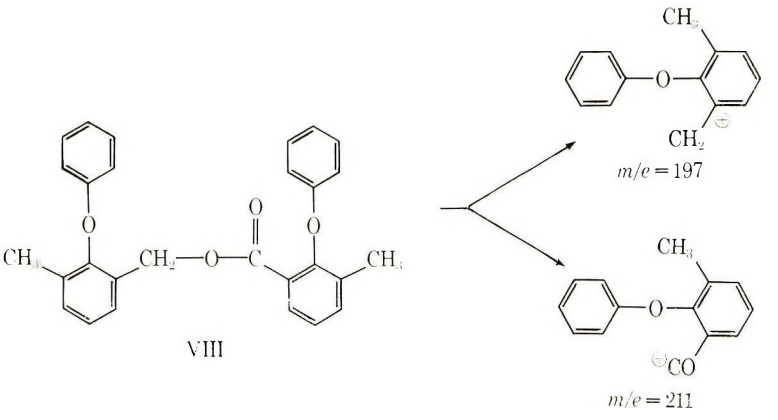

and their presence is support for structure VIII. Unfortunately, not enough of this material was isolated for further characterization. However, VIII was synthesized by the thermal reaction of V and VII. Although VIII could not be obtained crystalline, a correct analysis was obtained and its infrared spectrum was identical to that of the material isolated.

Vapor-phase chromatography of the crude fraction soluble in aqueous sodium hydroxide indicated that the ether I was the major component. The next largest constituent had the same retention time as 2,6-dimethylphenol. However, an attempt to isolate this phenol by TLC failed, perhaps due to its evaporation from the plate with the solvent in the drying step. However, having authentic V in hand helped in identifying it as a trace constituent in this fraction.

Photochemical Oxidation of Compound I

Molten I (ca. 75°C) was irradidated with a sunlamp for a total of 25.5 hr, during which most of the material sublimed. The infrared spectra changes of the remaining 7% at the end of the reaction are shown in Figure 1. This material was submitted to vapor-phase chromatography and individual peaks trapped and identified by infrared spectroscopy. This revealed that the following compounds were present in the reaction yields given: compound IV, 0.9%; VII, 0.95%; III, 0.3%; II, 0.3%; VIII, trace.

Thermal Oxidation of Poly(2,6-dimethyl-1,4-phenylene Oxide) Film

Poly(2,6-dimethyl-1,4-phenylene oxide) film was heat aged at 200°C in a forced air oven. The infrared changes accompanying the heat aging are recorded in Figure 2. The increase in intensity of the carbonyl and hydroxyl bands are similar to those already described.[1,2] This material was 95% gel after the 45 hr test. It was treated for 12 hr with aqueous NaOH in refluxing tetrahydrofuran and the reaction terminated by acidifying with HCl.

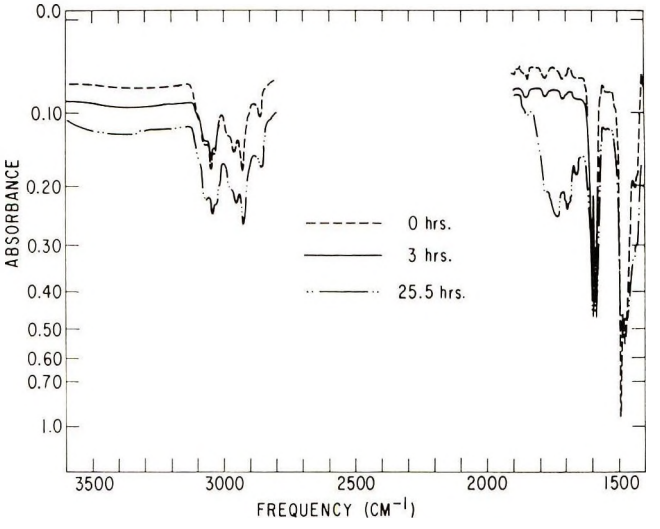

Fig. 1. 2,6-Dimethylphenyl phenyl ether, sunlamp, 75°C.

The gel content was now 81%. The infrared curve of the insoluble material in KBr is shown in Figure 3. The distinct carbonyl peaks found in Figure 2 are no longer present and the spectrum appears to be that of a carboxylate ion. When the same material was slurried with HCl for 10 hr, a shift could be detected in the carbonyl region (Fig. 3). The peaks at 1690 and 1730 cm^{-1} began to reappear.

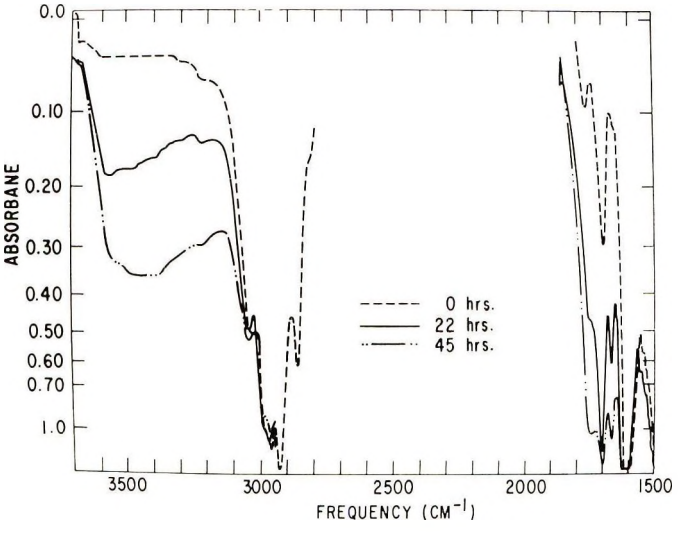

Fig. 2. Poly(2,6-Dimethyl-1,4-phenylene oxide) film, heat-aged at 200°C.

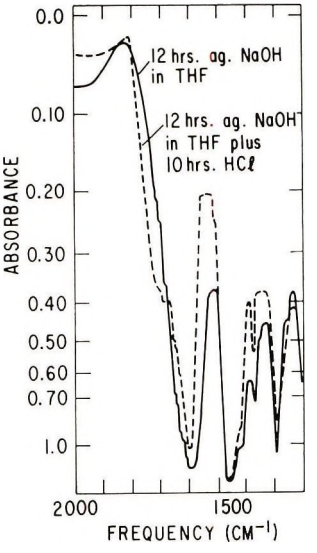

Fig. 3. Poly(2,6-Dimethyl-1,4-phenylene oxide) in KBr, film after base treatment.

Photochemical Oxidation of Poly(2,6-dimethyl-1,4-phenylene Oxide) Film

Poly(2,6-dimethyl-1,4-phenylene oxide) film oxidized by air under a sunlamp developed the infrared changes with time shown in Figure 4. In addition to the formation of a broad hydroxyl absorption, a broad carbonyl band developed centered at about 1740 cm^{-1} as was previously found.[1] Also, early in the oxidation, a peak could be seen at 1660 cm^{-1}. This sample contained 66% gel.

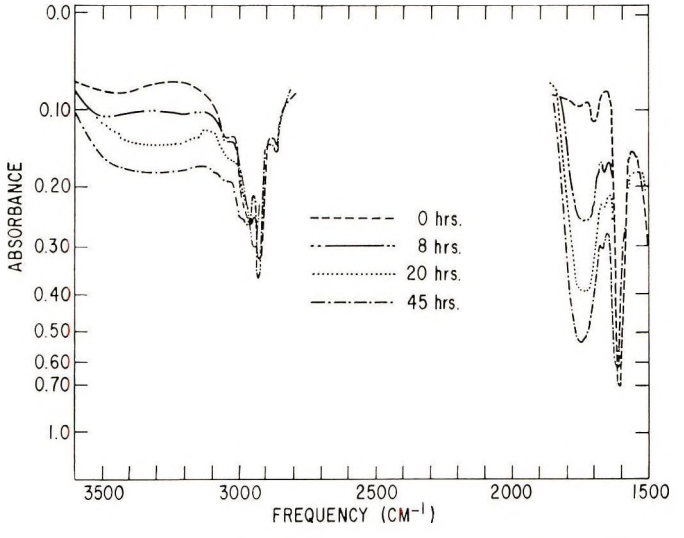

Fig. 4. Poly(2,6-Dimethyl-1,4-phenylene oxide) film, sunlamp aging at ca. 50°C.

Figure 5 also shows a photochemically oxidized polymer film. With this thicker film, the changes in the carbonyl region are more distinct than those in Figure 4 and resemble those observed in the thermal oxidation (Fig. 2).

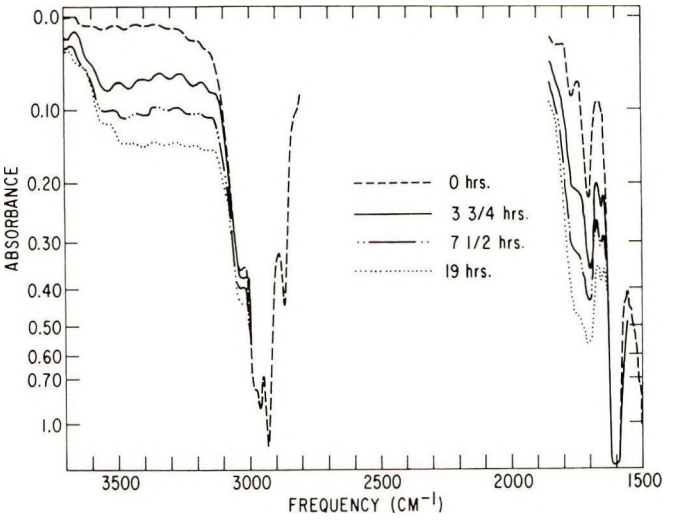

Fig. 5. Poly(2,6-dimethyl-1,4-phenylene oxide) film, sunlamp aging at ca. 50°C. This film was thicker than the one in Fig. 4.

This film was 56% soluble in benzene (44% gel). However, when treated with $NaOCH_3$ in methyl alcohol–benzene, it was 74.4% soluble (25.6% gel).

DISCUSSION

Formation of Products by Thermal Reaction

The three sequential oxidation products of a methyl group, the alcohol (VII), the aldehyde (IV), and the carboxylic acid (V), have all been isolated, and their presence lends support to the postulate[1] that an alkyl hydroperoxide is formed in the oxidation of such a methyl group in the polymer. The likely sequence of events is outlined in eq. (3).

$$-CH_3 \rightarrow -CH_2OOH \rightarrow -CH_2OH \rightarrow -\overset{\overset{O}{\|}}{C}H \rightarrow -\overset{\overset{O}{\|}}{C}OH \qquad (3)$$

The formation of the xanthone (II) and benzophenone (III) were unexpected products. However, they can be readily explained. It is known that the ether (I) will rearrange thermally at 370°C to 2-benzyl-6-methylphenol (IX) in good yield, and that the presence of an oxidant will speed up the reaction (lower the reaction temperature).[8] If such a process occurred in our oxidation reaction, IX might be oxidized to III, as shown in eq. (4).

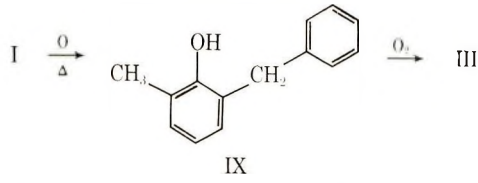

IX (4)

To test the possibility of the second half of the reaction occurring, IX was oxidized at 280°C (bath temperature) for 1 hr under the same conditions as for the oxidation of I. Although only ca. 45% of the material was ether-soluble, this consisted primarily of an equal mixture of compounds IX and III. Therefore, eq. (4) is a possible path for the production of compound III.

Another possible route to both II and III is by thermal rearrangement of the aldehyde IV. White has shown that *o*-phenoxybenzaldehydes rearrange above 300°C to a mixture of *o*-hydroxybenzophenones and xanthones, the latter being a minor product.[9] When an oxidizing agent is present, the amount of xanthone is increased.

Two other potential routes exist for xanthone formation: (1) oxidative ring closure of compound III and (2) thermal ring closure of compound V. The first of these routes seemed attractive, since both chemical and biogenetic transformations of this type have been reported.[10,11] However, in these reported cases, the ring which oxygen is attacking (the monosubstituted ring in III) also contains an oxygen atom. Our attempt to convert III to II with oxygen at 280°C failed [eq. (5)]. About 1% of a product

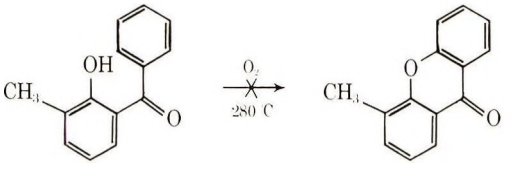

(5)

was isolated which did not have the correct infrared spectrum for II. However, the thermal reaction of the acid V, did give an 8% yield of xanthone [eq. (6)].

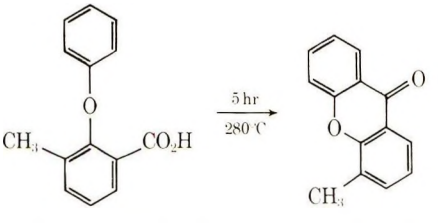

(6)

The ester VIII can be rationalized as forming by a thermal esterification and/or by the reaction of the benzyl hydroperoxide from I and the aldehyde IV. Proof that thermal esterification can occur was obtained when the reaction of the alcohol VII and the acid V in a sealed tube at 280°C resulted in a 63% yield of VIII. The hydroperoxide-aldehyde route is suggested by

the reported oxygenation of *p*-xylene in the liquid phase at 138–150°C in the presence of a cobalt salt to give *p*-methylbenzyl toluate X among the products.[12] The authors consider that compound X is formed via the reaction of *p*-methylbenzyl hydroperoxide and *p*-methylbenzaldehyde. The latter was also a product of the reaction. In fact, Farrissey has produced *p*-methylbenzyl *p*-toluate X from the thermal decomposition of *p*-methylbenzyl hydroperoxide in inert solvents.[13] When *p*-methylbenzaldehyde was added, the yield of X increased. The reaction is thought to pass through a hydroxyperoxide [eq. (7)].

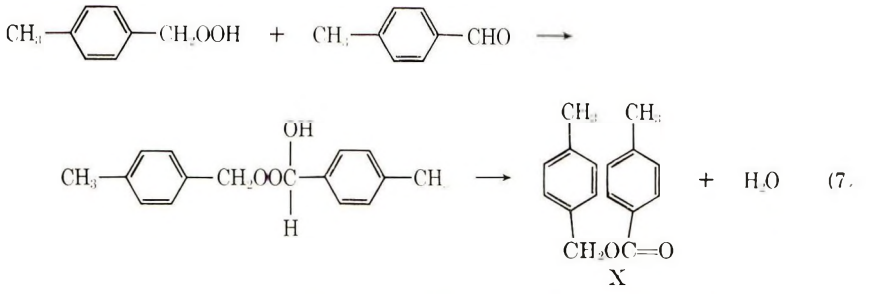

Compound VI may be formed by cleavage of VIII or by esterification of cresotic acid and VII. However, cresotic acid was not an isolated product from this reaction. In either case, the isolation of VI and the identification of 2,6-dimethylphenol is indicative of ether cleavage in the oxidation.

Formation of Products by Photochemical Reaction

The products identified, compounds II, III, IV, VII, and VIII were all isolated in the thermal reaction. There were other materials produced which were not identified, but none were major. The amount of compound VIII produced was not enough to agree with the intensity of the 1730 cm^{-1} band in Figure 1. This may mean that polymeric ester formed which is not being vaporized in the gas inlet port of the gas chromatographic instrument.

The aldehyde IV and alcohol VII are probably formed from decomposition of a photochemically produced benzyl hydroperoxide. Compounds III and II are very likely not formed thermally at 75°C but rather may be produced by a photochemical equivalent of White's thermal aldehyde rearrangement.[9] The ester VIII is very likely not produced thermally but may be formed by the hydroperoxide–aldehyde route discussed above.

Relevance to Polyphenylene Oxide

The three carbonyl bands found in the polymer after heat aging in air, 1722, 1689–1695, 1660–1661 cm^{-1}, are close to those of the three oxo products isolated in the thermal study.[1,2] They are the ester VIII, 1730 cm^{-1}, the acid V, ca. 1695 cm^{-1} (KBr) and the xanthone II, 1660 cm^{-1}. The aldehyde III has a carbonyl band at 1700 cm^{-1} which could be under the carboxyl band in the polymer and the ester type group in compound VI could

be under the xanthone band. A carbonyl band at 1620 cm^{-1} in a hydroxybenzophenone structure such as III would not be seen in the polymer since it would be under the strong aryl in-plane stretching vibration at ca. 1600 cm^{-1} and therefore not detected.

The identification of five of the same compounds in the photochemical oxidation of I may indicate that both oxidations proceed by the same mechanism. The formation of compound VIII in the photochemical oxidation is interesting in that its carbonyl absorption, 1730 cm^{-1} is in the range of the broad band formed in the reported photochemical oxidation of polymer film.[1] The esters VI and VIII in the thermal oxidation and VIII in the photochemical oxidation of I are interesting in that they are the only products isolated that involved intermolecular reaction.

This isolation of intermolecular oxo products in the model and the presence of "ester" carbonyl bands in the thermal and photochemical aged polymer films[1,2] prompted us to investigate the oxidation of polymer film to determine whether an ester group is present or not and if it is crosslinking.

Thermal and Photochemical Oxidation of Polyphenylene Oxide Film

We interpret the results with the thermally aged film as follows. The peak that develops at 1730 cm^{-1} is very likely due to a benzyl benzoate ester and the 1695 cm^{-1} is probably due to an acid. The base treatment converts the latter to carboxylate ions and also saponifies the ester groups to carboxylate ions. The acidification at the end of the reaction only destroys the base solution, but the film pieces were isolated before the carboxylate ions could be converted to carboxylic groups in the insoluble polymer. In order to carry out the latter reaction, a longer reaction time is necessary, e.g., 10 hr HCl treatment. However, the material now has both a carboxyl, 1695 cm^{-1}, and an ester band, 1730 cm^{-1}. This is somewhat surprising, in that one would not have expected the 1730 cm^{-1} band. The disappearance of an ester band by base treatment and its reappearance after acid treatment is suggestive of a lactone. The feature that allows for lactone formation on acid treatment of a hydroxy acid is the stereochemical requirement that the carboxyl and hydroxy groups be in close proximity. Since the polymer sample is 95% gel, a great amount of solubilization does not occur on saponification. This may be due to crosslinking units other than ester[1] and/or the possibility that linear polymer with more than a few carboxyl groups per chain is insoluble in the solvent system used. At any rate, the polymer chains are in a rigid environment and in close proximity to one another. Thus, a crosslinked ester group on saponification will retain the carboxylate ion and alcohol close to one another so that on acidification, an ester is formed with the same ease as lactonization.

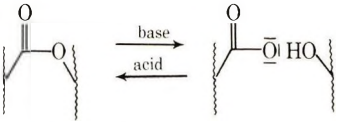

The fact that the photochemically oxidized film could have its gel content reduced from 44 to 25% by reaction with $NaOCH_3$ and the thermally oxidized film from 95 to 81% is indicative of a base sensitive crosslinking unit. Since these materials also have absorption at ca. 1730 cm^{-1}, we believe that the most likely unit is an ester group.

EXPERIMENTAL

Melting points are uncorrected. All infrared spectra were obtained on a Perkin-Elmer Model 337 instrument. NMR spectra were obtained on a Varian A-60 spectrometer. A preparative thin-layer chromatography (TLC) plate used in this research was made from silica gel, was activated at 110°C for at least 1 hr, and had the dimensions 8 in. × 8 in. × 1 mm. The high-resolution mass spectrum of compound VI was obtained at Battelle Memorial Institute, and the remaining spectra were obtained on a General Electric Monopole 600 spectrometer and a Consolidated Electrodynamics Corp. 21104 spectrometer.

2,6-Dimethylphenyl Phenyl Ether (I)

I was prepared by the Ullman reaction between 2,6-dimethylphenol and bromobenzene in 45% yield, mp 55.5–56.7°C (lit.[8] mp 55–56.5°C).

Oxidation of 2,6-Dimethylphenyl Phenyl Ether

2,6-Dimethylphenyl phenyl ether (3.569 g, 0.018 mole) was placed in a three-necked, 50-ml flask fitted with a thermometer, air-cooled condenser, and a gas inlet tube. The flask was placed in a Wood's metal bath maintained at 290°C, and oxygen was bubbled through the molten ether. The vapor temperature was 260°C. After 11 hr the reaction was terminated by cooling, and the contents of the flask and the condenser were taken up in ether, the ether filtered to remove a brown-black solid and extracted with 5% sodium hydroxide solution to give a neutral and acidic fraction. Drying and removal of the ether gave 2.666 g of a neutral material. Gas chromatographic analysis indicated that this consisted of 84.8% of 2,6-dimethylphenyl phenyl ether and the remainder consisted of chiefly three more polar materials. The acidic material was isolated by acidification of the sodium hydroxide solution and extraction with ether. This was partitioned into a phenolic fraction (0.141 g) and a carboxyl fraction (0.020 g) by bicarbonate extraction.

The phenolic fraction consisted of eight materials by gas chromatographic analysis. However, two of them (85%) were 2,6-dimethylphenol, retention time 4.0 min, and 2,6-dimethylphenyl phenyl ether, retention time 6.8 min. Under the same conditions, authentic 2,6-dimethylphenol had 3.9 min retention time, phenol had 5.0 min retention, and authentic 2,6-dimethylphenyl phenyl ether had 6.8 min retention time.*

* F & M Model 720, 6 ft 5% XE-60 column, 100°C start, 7.5°C/min program, 95 ml/min He flow.

A 2.290 g portion of neutral fraction was placed on a chromatographic column made from Fluorosil (70 g) in 1:1 benzene:hexane. The following materials were eluted in 100 ml fractions.

I. Fractions 1 and 2, eluted with 1:1 benzene:hexane gave 1.720 g of 2,6-dimethylphenyl phenyl ether, 56% recovery.

II. Fractions 13–38, eluted with benzene, consisted of predominantly four materials by TLC analysis. All the fractions combined, 328 mg, were placed on five preparative TLC plates and developed in benzene. Five zones were detected by ultraviolet scanning and were cut out. The products were recovered by elution with acetone and are listed in decreasing R_f values: zone A, 8 mg, oil; zone B, 16 mg, yellow oil; zone C, 104 mg, yellow oil; zone D, 104 mg, yellow oil; zone E, 52 mg, tan solid.

III. Fractions 39–51, eluted with 9:1 benzene:ethyl acetate, 163 mg, consisted of chiefly two materials by TLC analysis. The fractions were combined and placed on three preparative TLC plates and developed in 49:1 benzene:ethyl acetate. Four zones were located by ultraviolet scanning, cut out, and the materials recovered by elution with acetone. They are listed in decreasing R_f values: zone F, 4 mg, yellow oil; zone G, 32 mg, yellow oil; zone H, 120 mg, tan solid; zone I, 11 mg, amber oil.

IV. Fractions 52–56, eluted with 9:1 benzene:ethyl acetate, 48 mg, were combined and placed on one preparative TLC plate. After the plate was developed in 19:1 benzene:ethyl acetate, four zones were detected by ultraviolet scanning: zone J, just behind solvent front; zone K, R_f 0.8, zone L, R_f 0.5, 7 mg; zone M, R_f 0.2, 9 mg;

V. Fractions 57–61, eluted with 1:1 benzene:ethyl acetate, 36 mg. All the fractions were combined, placed on one preparative TLC plate and developed in 9:1 benzene:ethyl acetate. Two zones were located by ultraviolet scanning, cut out, and eluted with acetone: zone N, just behind solvent front; zone O, R_f 0.8.

Zone E, 52 mg, was placed on one preparative TLC plate and developed in benzene and again in 49:1 benzene:ethyl acetate. Two zones were located by ultraviolet scanning, cut out, and the material isolated by acetone elution: zone P, 41 mg; tan solid; zone Q, 7 mg, yellow oil.

Zone H was placed on three preparative TLC plates and developed once in 19:1 benzene:ethyl acetate and twice in benzene. The major blue fluorescing zone was cut out and eluted as before: zone R, 108 mg, slightly yellow solid.

Identification of 4-Methylxanthone (II)

Zones P and R were the same material, exhibiting a strong carbonyl band at 1660 cm^{-1}, a weak C—O stretching vibration at 1210 cm^{-1} and a very intense band at ca. 750 cm^{-1}. In addition, when TLC sidebands of these materials were sprayed with 2,4-dinitrophenylhydrazine reagent, no hydrazone color developed. These zones were combined (149 mg) and placed on two preparative TLC plates. The plates were developed in 9:1 benzene:-ethyl acetate and the major blue fluorescing zone cut out and eluted with

acetone. The crystals obtained were recrystallized twice from hexane to give 59 mg of 4-methylxanthone, mp 124–124.2°C, whose infrared spectrum was essentially identical with that of authentic material. The yield based on 149 mg was 3.9%.

Identification of 2-Hydroxy-3-methylbenzophenone (III)

Zones C and G had the same R_f values and their infrared spectra indicated that they were the same material; the infrared spectra (neat) had bands at 1620 cm^{-1} and a broad hydroxyl band at 3200 cm^{-1}. These zones were combined and placed on three preparative TLC plates and developed in benzene. The major ultraviolet absorbing zone was eluted plus one other: zone S, 7 mg, amber oil; zone T, 114 mg, yellow oil.

Zone T was placed on two preparative TLC plates and developed once in benzene and once in 32:1 benzene:hexane to give 113 mg of material. The NMR spectrum (CCl_4) indicated only one methyl group relative to 8 aromatic hydrogens which appeared at 2.25 ppm. The material had a 10.6 min VPC retention time.* Silylation of a small amount of this compound with bistrimethylsilylacetamide gave the trimethylsilyl ether which had an 11.6 min retention time. This peak was trapped and its infrared spectrum indicated a carbonyl band at 1670 cm^{-1}. All of the crude material was again subjected to chromatography on three preparative TLC plates in benzene. After elution with acetone, 101 mg of a yellow oil was obtained. This was distilled at 0.25 mm in a short path apparatus to give a yellow liquid which solidified to a yellow solid mp 41–43°C, 2-hydroxy-3-methylbenzophenone. Its infrared spectrum was identical to that of authentic compound III. The yield based on 113 mg was 3.0%.

Zones K and O were combined (29 mg) and identified as compound III by infrared spectroscopy.

Identification of 2-Phenoxy-3-methylbenzaldehyde (IV)

Zone D, 104 mg, showed infrared bands at 1700 (C=O), 1230 (Ar—O), and 2750 cm^{-1} (—C(=O)—H); the NMR spectrum gave ($CDCl_3$) δ 2.17 (*S*, 3, CH_3), 6.7–7.9 (*m*, 8, ArH), 10.25 (*S*, 1, —CHO). Short-path distillation, bp 100–110°C/0.25 mm (bath temperature) gave a clear colorless oil, n_D^{25} 1.5856; mass spectra *m/e* 212 and 211 (base peak). The yield based on 104 mg was 2.7%.

ANAL. Calcd for $C_{14}H_{12}O_2$: C, 79.22%; H, 5.7%. Found: C, 79.5%; H, 5.9%.

A small amount of the aldehyde was dissolved in acetone and oxidized by the dropwise addition of a chromium trioxide–sulfuric acid solution at ambient temperature. After methyl alcohol was added, the reaction was diluted with water, and extracted with ether. The ether was dried over $MgSO_4$ and stripped to give an oily solid. This was placed on one prepara-

* F & M Model 700, 2-ft SE 30 column, program 10°C/min from 100°C.

tive TLC plate and developed in benzene. The zone moving irregularly up from the origin was cut out and the product obtained by acetone elution. The crude product obtained was recrystallized once from hexane to give 2-phenoxy-3-methylbenzoic acid (V), mp 121.3–122.3°C. The infrared spectrum was identical to that of authentic material.

Identification of 2-Phenoxy-3-methylbenzyl *o*-Cresotinate (VI)

Zones B and F had identical infrared spectra and had the same R_f values as zone S when placed on a qualitative TLC plate and developed in 1:1 benzene:hexane. These three zones were combined and placed on one preparative TLC plate and developed twice in 1:1 benzene:hexane. The major zone, located by short-wavelength ultraviolet scanning, R_f 0.6, was eluted with acetone to give 16 mg of an amber oil; Infrared bands (neat) were at 1670 cm^{-1}, 1285, 1250, 1215 and 3200 cm^{-1} (broad); NMR ($CDCl_3$) showed δ 2.15 (*S*, 3, $—CH_3$), 2.28 (*S*, 3, $—CH_3$), 5.33 (*S*, 2, $—CH_2—$), 10.9 (*S*, 1, —OH); mass spectrometry (high resolution) showed peaks at *m/e* 348.1368 ($C_{22}H_{20}O_4$), 214.0986 ($C_{14}H_{14}O_2$), 197.09715 ($C_{14}H_{13}O$), 196.0872 ($C_{14}H_{12}O$), 195.0799 ($C_{141}H_1O$).

The infrared spectrum was essentially identical to that of authentic VI. The yield based on 16 mg was 0.25%.

Identification of 2-Phenoxy-3-methylbenzyl Alcohol (VII)

Zone Q, 7 mg, was one component by VPC; retention time 11 min; an infrared band (neat) was observed at 3350 cm^{-1} (strong). The infrared spectrum was essentially identical to that of authentic compound VII. Zone I, 11 mg, contained a major VPC peak at 11 min. It was placed on one preparative TLC plate and developed in 19:1 benzene:ethyl acetate twice. The major ultraviolet plus zone was cut out and eluted with acetone to give 3.5 mg of compound I.

Identification of 2-Phenoxy-3-methylbenzoic Acid (V)

The carboxyl fraction, 0.020 g, from the original acid fraction isolated from the reaction, was placed on one preparative TLC plate and developed once in 1:1 benzene:ethyl acetate and three times in ethyl acetate. An ultraviolet-positive zone, R_f 0.45, was cut out and eluted with acetone to give 3 mg of material. VPC* of this indicated the major peak at 14.5 min which is the retention time for compound V. This peak was trapped and its infrared spectrum was essentially identical to that of authentic compound V.

Identification of 2-Phenoxy-3-methylbenzyl 2-Phenoxy-3-methylbenzoate (VIII)

Zone A, 8 mg, by VPC* had the following peaks: 12.5 min (×8 peak height), 13.5 min (×4), 19 min (×2), 22 min (×2), and 25.5 min (×16).

* F & M Model 700, 4-ft SE 30 column; 100°C start, 10°C/min program.

All of the 25.5 min material was trapped. The infrared spectrum (neat) showed absorption at 1730 (C=O), 1285, 1255, 1222, and 1130 cm^{-1}; mass spectrometry gave peaks with m/e 424, 229, 211 (base peak), 197, 196, and 195.

Other Compounds Not Identified

Zones J and N combined showed blue fluorescence under ultraviolet scanning. VPC indicated several materials, none of which could be isolated. Zones L and M could not be identified.

Preparation of Standards

4-Methylxanthone (II). 2-Phenoxy-3-methylbenzoic acid (0.500 g, 2.18 mmole) was dissolved in approximately 15 ml of polyphosphoric acid, and the flask containing the solution was heated in an oil bath at 130°C for 24 hr. The reaction was terminated by pouring onto ice and the precipitated solid isolated by filtration. The filter cake was washed with water and dried in a vacuum desiccator overnight. The dry grayish solid weighed 0.456 g. Its infrared spectrum was transparent at ~1690 cm^{-1}, where the starting acid has a carbonyl band but did exhibit a strong band at 1655 cm^{-1}, which is within the range for xanthone carbonyls. One recrystallization from hexane gave slightly yellow crystals, mp 125–126°C (lit.[14] mp 126°C), wt. = 0.395 g, yield = 86%. The infrared spectrum (KBr) contained a strong band at 1660 cm^{-1}, a medium band at 1235 cm^{-1}, and a very intense band at 750 cm^{-1}.

2-Hydroxy-3-methylbenzophenone (III). A mixture of cresotic acid (15.0 g, .099 mole), benzene (50 ml), thionyl chloride (20 ml), and about 0.5 ml of pyridine was stirred at ambient temperature until a clear solution was obtained (approximately 4 hours). The benzene and excess thionyl chloride were removed at the aspirator and benzene (100–150 ml) and aluminum chloride (20 g) added and the reaction mixture magnetically stirred while in a water bath at ambient temperature over a weekend. The reaction was acidified with dilute hydrochloric acid. The benzene layer was separated, extracted with sodium bicarbonate solution, and dried. The benzene was removed to leave an amber oil. The oil was vacuum distillled and a yellow liquid was collected in two fractions: fraction I, bp 130–134°C/1 mm, 5.823 g; fraction II, bp 134–135°C/1 mm, 8.100 g. Fraction I was one peak on VPC and fraction II had about 3% of a more polar impurity. The total weight was 13.923 g, yield = 65%.

The oxime prepared from this ketone gave mp 162–164°C (lit.[15] mp, 164–165°C). The infrared spectrum of the yellow oil had a carbonyl peak at 1625 cm^{-1}, bonded —OH at 3200 cm^{-1} and a strong C—O stretching vibration at 1265 cm^{-1}.

2-Phenoxy-3-methylbenzoic Acid (V). Phenyl 2,6-dimethylphenyl ether (2.0 g, 0.01 mole), pyridine (68 ml), potassium permanganate (24 g, 0.152 mole), and water (45 ml) were placed in a 250-ml round-bottomed flask

and the solution heated at reflux for 5 hr with stirring.* After 75 ml of a pyridine–water azeotrope was distilled out, the reaction mixture was cooled and diluted with 75 ml of water. The mixture was acidified with concentrated sulfuric acid and decolorized by the addition of solid sodium bisulfate. An orange precipitate was collected and dried, 1.2 g. The infrared spectrum had a band at 1700 cm^{-1}. This material was dissolved in ether and extracted with 10% NaOH solution. The basic solution acidified with hydrochloric acid and the resultant precipitate collected and dried. The infrared spectrum indicated peaks at 1730 and 1700 cm^{-2}.

The ether containing neutral material was dried and stripped to give 0.207 g of a straw colored oil. The infrared spectrum indicated that this was starting ether.

All of the solid acid was placed on a column made from 50 g of silica gel in benzene. Elution with 2% ethyl acetate–benzene gave 0.560 g of solid in seven 100 ml fractions. The infrared spectra of the second and seventh fractions were essentially identical. The solid was recrystallized from hexane, mp 119–121°C. Several recrystallizations from hexane gave slightly cream colored crystals, mp 120°C. The NMR spectrum ($CDCl_3$) showed δ 2.13 (*S*, 3, $-CH_3$), 6.7–7.5 (*M*, 7, aryl H), 7.9 (*M*, 1, H ortho to CO_2H), 10.3 (broad, CO_2H). The infrared spectrum showed bands (KBr) at 1695 and 1670 cm^{-1} (C=O); mass spectrometry showed peaks *m/e* 228, base peak *m/e* 135.

ANAL. Calcd for $C_{14}H_{12}O_3$: C, 73.67%; H, 5.30%. Found: C, 73.6%; H, 5.38%.

2-Phenoxy-3-methylbenzyl Alcohol (VII). A 1.10 g portion of 2-phenoxy-3-methylbenzoic acid (V) was dissolved in 100 ml of a 3% methanolic hydrochloric acid solution and kept at ambient temperature overnight. The crude methyl ester was obtained by removing the solvent at the aspirator to give an amber oil. The infrared spectrum contained no hydroxyl absorption and had strong bands at 1725 and 1150 cm^{-1}. The crude ester was dissolved in ether and slowly added to a slurry made from 0.5 g of lithium aluminum hydride and ether under nitrogen. After the addition, the slurry was heated under reflux for 1.5 hr and cooled. A saturated aqueous sodium sulfate was added dropwise to decompose the excess lithium aluminum hydride, followed by solid sodium sulfate. The dried ether was filtered from the drying agent and removed at the aspirator to give 0.964 g of crude 2-phenoxy-3-methylbenzyl alcohol. The infrared spectrum of this crude material exhibited a broad band at 3350 cm^{-1} and was transparent at 1725 and 1150 cm^{-1}. A 150-mg portion of this material was distilled in a bulb-to-bulb apparatus at 0.15 mm and a bath temperature of 90–120°C to give a colorless liquid. The NMR spectrum (CCl_4) showed δ 2.05 (*S*, 3, $-CH_3$), 2.67 (*S*, 1, OH), 4.30 (*S*, 2, $-CH_2-$), 6.50–7.35 (*M*, 8, aryl H); a mass spectrometry peak was at *m/e* 214.

ANAL. Calcd for $C_{14}H_{14}O_2$: C, 78.48%; H, 6.59%. Found: C, 78.21%; H, 6.5%.

* This method of oxidizing a methyl group in a diaryl ether was developed by Dr. G. D. Cooper, General Electric Company, Selkirk, New York.

2-Phenoxy-3-methylbenzyl *o*-Cresotinate (VI). A slurry was made from cresotic acid (380 mg, 0.0025 mole), 8 ml of benzene, 0.5 ml of thionyl chloride, and one drop of pyridine. This was stirred at ambient temperature until all the solid acid disappeared (3 hr). The crude acid chloride of cresotic acid was obtained by removing the solvent and excess thionyl chloride under vacuum. To this was added a benzene solution of 2-phenoxy-3-methylbenzyl alcohol VII (430 mg, 0.0020 mole). The solution turned an orange color and an oil separated out. The mixture was stirred at ambient temperature overnight and the crude product obtained by removing the solvent under vacuum. All the crude product was placed on three preparative TLC silica gel plates and developed in 9:1 benzene:ethyl acetate and the least polar band, R_f 0.8, was cut out and eluted with acetone to give 453 mg of an oil. VPC indicated that this consisted of starting alcohol, retention time 12 min, and the expected ester, retention time 21 min. All of the mixture was placed on two preparative TLC plates (8 × 16 in.) and developed in 3:1 benzene:hexane. A broad band, R_f 0.7, was cut out and eluted to give 330 mg of the title compound. The yield was 47.5%. All of this compound was distilled in a micro bulb-to-bulb apparatus at 0.1 mm and a bath temperature of 195–220°C to give a viscous slightly yellow oil. The infrared spectrum (neat) showed bands at 3175 (—OH), 1670 (C=O), and 1285, 1245, 1215 and 1145 cm^{-1} (all C—O); NMR (CCl_4) showed δ 2.08 and 2.17 (*S*, 6, $—CH_3$), 5.25 (*S*, 2, $—CH_2—$), 6.35–7.4 (*M*, 11, aryl H), 10.9 (*S*, 1, —OH).

ANAL. Calcd for $C_{22}H_{20}O_4$: C, 75.84%; H, 5.50%. Found: C, 75.86, 75.80%; H, 5.85, 5.94%.

2-Phenoxy-3-methylbenzyl 2-Phenoxy-3-methylbenzoate (VIII). 2-Phenoxy-3-methylbenzyl alcohol (44 mg, 0.000205 mole) and 2-phenoxy-3-methylbenzoic acid (47 mg, 0.000206 mole) were sealed in a heavy-walled Pyrex tube, and the tube was heated in a furnace for 5.75 hr at 285°C. All the crude reaction material was placed on two preparative TLC silica gel plates and developed in benzene. The main ultraviolet-positive zone was cut out and the product isolated by eluting with acetone to give 57 mg of yellow oil. Repeating the TLC in 7:3 benzene:hexane gave 51 mg title compound (58.5%), light yellow oil. The infrared spectrum (neat) gave bands at 1730 (C=O), 1287, 1255, 1225, and 1133 cm^{-1} (C—O). All attempts to recrystallize this material failed. An attempt at vacuum sublimation gave distillation instead. The distillate had an NMR ($CDCl_3$), δ 2.10 and 2.15 (*S*, 6, $—CH_3$), 5.10 (*S*, 2, $—CH_2—$), 6.5–7.6 (*m*, 16, Ar—H) and gave a satisfactory analysis.

ANAL. Calcd for $C_{28}H_{24}O_4$: C, 79.22%; H, 5.70%. Found: C, 79.1%; H, 6.04%.

Attempted Conversion of 2-Hydroxy-3-methylbenzophenone (III) to 4-Methylxanthone (II). Compound III (1.666 g, 0.008 mole) was heated in a flask contained in a Wood's metal bath at 280°C. The reaction was run for 5.5 hr with a slow stream of oxygen passing through the molten

III. The dark oil solidified on cooling and was slurried with several portions of ether which were filtered. A brown solid remained on the filter. The filtrate was extracted with Claisen's alkali, dried, and removed under vacuum (20 mm) to give 150 mg of a dark oil. An infrared spectrum showed this to be chiefly starting compound III, but it also contained a small peak at 1665 cm^{-1}. All this material was placed on two preparative TLC plates and developed in benzene. A blue fluorescing zone was cut out and eluted with acetone to give 16.4 mg. The infrared spectrum was not correct for compound II.

4-Methylxanthone (II) from 2-Phenoxy-3-methylbenzoic Acid (V). Compound V (31.3 mg, 0.00014 mole) was sealed in a Pyrex heavy-walled tube, and the tube placed in a furnace at 280°C for 5 hr. The tube was cooled, opened and the contents placed on two preparative TLC plates and developed in benzene. Three zones were located by ultraviolet, cut out, and eluted with acetone: zone I, R_f 0.65, 2.5 mg, yellow oil; zone II, R_f 0.3, 2.6 mg, yellow oily solid; zone III, R_f 0–0.2, 17.8 mg, solid.

Zone II was identified as 4-methylxanthone by its infrared spectrum, yield = 8.3%. Zone III was chiefly starting acid, V.

Photochemical Oxidation of 2,6-Dimethylphenyl Phenyl Ether (I). Compound I (2.094 g, 0.0106 mole) was placed in a Petri dish and the dish placed on a hot plate with a surface temperature of 75°. A GE sunlamp (275 W) was placed 3.5 in. from the surface. The molten material was stirred magnetically and the infrared spectrum was determined at 0, 3, and 25.5 hr. The curves are shown in Figure 1. At the end of the experiment (25.5 hr) only 0.148 g of yellow amber material remained, 7.07%. VPC of this indicated that the chief material was the ether I followed by several oxo product. The following compounds were trapped from the VPC and identified by their infrared spectra: compounds IV (0.9% yield), VII (0.95%), III (0.3%), II (0.3%), and VIII (trace). In addition, there were several other peaks which could not be identified. The yields were determined by integration of the VPC curve.

Photochemical Oxidation of Poly(2,6-dimethyl-1,4-phenylene Oxide). A polymer film was placed in a hood and a GE sunlamp (275 W) was placed 3.5 in. away from it. The surface temperature at the film was ca. 50°C. The infrared spectrum was recorded over the course of the reaction and is shown in Figure 5. A 46.8 mg portion of this film was broken into small pieces and placed in 200 ml of refluxing benzene 18 hr, at which time 20.6 mg remained, 44% gel. The photochemically oxidized film [21.5 mg] was treated with 90 mg of sodium methoxide, 1 ml of methyl alcohol, and 30 ml of benzene at reflux for 20 hr. The solution was diluted with benzene and water and filtered. The pieces of film on the filter were washed with dilute HCl, water, and dried to give 6.5 mg, 25.6% gel.

Thermal Oxidation of Poly(2,6-dimethyl-1,4-phenylene Oxide). The polymer film was suspended in a forced-air oven at 200°C. The film was removed after 22 and 45 hr and the infrared spectrum determined. This film (33.9 mg) was placed in 300 ml of refluxing benzene for 18 hr; 1.7 mg

was solubilized for 95% gel content. The benzene-insoluble material (27 mg) was placed in 50 ml of refluxing benzene containing 2 ml of methyl alcohol and 0.216 g of sodium methoxide for 18 hrs; of this 2.1 mg was solubilized, 7.8% reduction in gel content.

In another experiment, 12.3 mg of the original heat-aged film was broken up and suspended in 40 ml tetrahydrofuran containing 0.5 ml water and 0.5 ml of 50% NaOH solution and heated at reflux for 12 hr. The solution was made acidic by the addition of concentrated HCl, the film pieces isolated, washed with water and dried, yielding 10.0 mg, 81% gel. The infrared spectrum of the material in KBr appears in Figure 3. The pieces were placed in a stirred solution of concentrated HCl in tetrahydrofuran for 10 hr isolated, washed with water, and dried. The infrared spectrum appears in Figure 3.

References

1. P. G. Kelleher, L. B. Jassie, and B. D. Gesner, *J. Appl. Polym. Sci.*, 11, 137 (1967).
2. J. W. Eustance, E. M. Boldebuck, and J. Kwiatek, unpublished results.
3. F. E. Karasz and J. M. O'Reilly, *J. Polym. Sci. B*, **3**, 561 (1965).
4. J. C. Roberts, *Chem. Revs.*, **61**, 591 (1961).
5. N. Campbell, S. R. McCallum, and D. J. Mackenzie, *J. Chem. Soc.*, **1957**, 1922.
6. A. D. Cross, *Introduction to Practical Infrared Spectroscopy*, Buttersworths, London, 1960.
7. H. Budzikiewicz, C. Djerassi, and D. H. Williams, *Mass Spectrometry of Organic Compounds*, Holden-Day, San Francisco, 1967, (a) Chap. 3; (b) Chap. 4.
8. A. Factor, H. Finkbeiner, R. A. Jerussi, and D. M. White, *J. Org. Chem.*, **35**, 57 (1970).
9. D. M. White, paper presented at 157th National Meeting, American Chemical Society, Minneapolis, April 1969; *Abstracts*, Org. Chem., No. 33.
10. J. E. Atkinson and J. R. Lewis, *Chem. Commun.*, **1967**, 803.
11. R. C. Ellis, W. B. Whalley, and K. Ball, *Chem. Commun.*, **1967**, 803.
12. M. A. Tobias and W. W. Kaeding, *Ind. Eng. Chem., Prod. Res. Dev.*, **8**, 420 (1969).
13. W. J. Farrissey, *J. Amer. Chem. Soc.*, **84**, 1002 (1962).
14. F. Ullmann and M. Zlokasoff, *Ber.*, **38**, 2111 (1905).
15. D. A. Reich and D. V. Nightingale, *J. Org. Chem.*, **21**, 825 (1956).

JOURNAL OF POLYMER SCIENCE: PART A-1 VOL. 9, 2029–2038 (1971)

Telechelic Diene Prepolymers. I. Hydroxyl-Terminated Polydienes

SAMUEL F. REED, JR., *Rohm and Haas Company, Philadelphia, Pennsylvania 19137*

Synopsis

Telechelic prepolymers of butadiene, isoprene, and chloroprene with hydroxyl end-groups have been prepared by the solution polymerization of the dienes under free-radical initiation. 4,4′-Azobis(4-cyano-*n*-pentanol) was employed as the initiator. Liquid prepolymers were obtained with molecular weights of 2000 to 20,000 and with functionalities usually greater than 2. The preparative procedure and prepolymer characterization are described.

INTRODUCTION

Difunctional polymers possessing hydroxyl or carboxyl terminal groups have generally been synthesized by the anionic polymerization of suitable monomers to give "living polymers" capable of reacting with various electrophilic reagents for the introduction of functionality.[1–4] An alternate approach which has received attention is one involving the use of a free radical polymerization mechanism employing initiators containing the desired functionality. Bamford and co-workers[5] demonstrated this technique utilizing 4,4′-azobis(4-cyanovaleric acid) and 4,4′-azobis(4-cyano-*n*-pentanol) as the initiators for the polymerization of styrene, acrylonitrile, and methyl methacrylate. Later, Marvel[6] prepared α,ω-glycols of polybutadiene by the free-radical polymerization of butadiene initiated with diethyl 2,2′-azobis(isobutyrate) followed by reduction of the ester groups to hydroxyl groups. More recently, the synthesis of low molecular weight hydroxyl-terminated *cis*-1,4-polybutadiene was prepared[7] by an indirect method involving the ozonolysis of a high molecular weight *cis*-1,4-polybutadiene followed by reduction of the ozonides. A special report issued by workers at Minnesota Mining and Manufacturing Company[8] described the preparation of carboxy-terminated polybutadiene by use of glutaric acid peroxide and 4,4′-azobis(4-cyanovaleric acid). These investigations demonstrated that the free-radical polymerization method is suitable for the preparation of low molecular weight prepolymers containing functional groups

This work describes additional polymerization studies with the use of 4,4′-azobis(4-cyano-*n*-pentanol) as the initiator. 4,4′-Azobis(4-cyano-*n*-pentanol) was prepared by a modification of the method of Bamford,[5] sep-

arated into two isomeric forms, and each form, as well as the isomer mixture, was examined as the initiator for the preparation of telechelic polybutadienes. In further studies the effect of the reaction parameters of time, initiator concentration, and diene concentration on prepolymer properties were investigated for prepolymers of butadiene, isoprene, and chloroprene. These products were characterized by molecular weight, molecular weight distribution, functionality, and endgroup and elemental analysis. The properties of the prepolymers as controlled by these parameters are discussed.

EXPERIMENTAL

Diene monomers employed were butadiene, isoprene, and chloroprene. Butadiene (Matheson Chemical Company, Inc.) was research grade material (99.9%) used without further purification. Isoprene (Aldrich Chemical Company) was distilled prior to use while chloroprene (Columbia Organic Chemicals Company, Inc.) was purchased as a 50% solution in xylene and used without purification. All solvents were distilled prior to use in the polymerization.

4,4′-Azobis(4-cyano-*n*-pentanol) (ACP) was prepared by the following modification of a known procedure.[5] A solution of 10.8 g of sodium cyanide in 100 ml of water was added slowly to a mixture of 14.3 g of hydrazine sulfate, 22.5 g of 5-hydroxy-2-pentanone, and 150 ml of water. The resulting solution was allowed to stand overnight. The mixture was then cooled in an ice bath and 15% aqueous hydrochloric acid was added until the solution was acidic. Bromine, 32 g, was then added over a 5 hr period. Any bromine color remaining was removed with sodium bisulfite. If the mixture of isomers was to be utilized, the solution was extracted with methylene chloride–acetone (2:1). Removal of the organic solvents left a solid residue which was recrystallized from chloroform–hexane to give 13–14 g of the isomeric azo compounds, mp 82–96°C. If separation of the isomers was desired, the insoluble isomer, mp 94–96°C, precipitated from the chilled aqueous solution. The soluble isomer, mp 81–83°C, was extracted from the aqueous solution with a mixture of methylene chloride–acetone (2:1).

Initiator Studies

Butadiene was polymerized on a 0.2-mole scale in thick-walled glass tubes at 65°C for periods of 72 hr. Butadiene concentration of 6.66 mole/l. in toluene, dioxane, dimethylformamide (DMF), or acetonitrile were employed in reactions where the ACP concentrations was maintained constant at the 3 mole-% level (based on diene). The prepolymers were isolated by evaporation of the solvent. Purification was accomplished by solution in 25 ml of diethyl ether and separation of the prepolymer on the addition of 250–300 ml of methanol. This treatment succeeded in removing the extremely low molecular weight, soluble prepolymer. For most samples the loss was maintained below 5% of the total prepolymer sample. The pre-

polymer samples submitted for analysis contained approximately 0.25% *N*-phenyl-α-naphthylamine as an antioxidant and each was dried under vacuum (1 mm) at 70–75°C to near constant weight.

Polymerization Parameter Studies

Butadiene, isoprene, and chloroprene were polymerized on an 0.2-mole scale in thick-walled glass reactors. Polymerization times were varied from 24 to 120 hr, ACP concentrations were varied from 0.5 to 10 mole-% (based on diene), and the diene concentrations were varied from 5 to 20 mole/l. Prepolymer isolation and purification were carried out as described above.

Prepolymer Characterization

Molecular weight measurements were obtained on a Mechrolab vapor pressure osmometer, with benzil and polystyrene ($\bar{M}_n$ 10,000) used as calibration materials. A Waters Instrument, Model 200 was employed for the gel-permeation chromatography. Degassed tetrahydrofuran flowing at 1 ml/min was the eluting solvent. Commercial Styragel columns of 10^4, 10^3, 600, and 100 Å mean permeability were employed in the GPC work. Each column configuration was calibrated (average angstrom length) by using special polystyrenes of narrow molecular weight distribution supplied by Waters Associates, Inc.

Hydroxyl endgroup determinations were carried out by a near-infrared spectral analysis. The fundamental free hydroxyl stretching vibration near 2.75 μ was observed in dilute carbon tetrachloride. Standard reference curves for primary and secondary alcohols were prepared from solutions of 4-penten-1-ol and 4-penten-2-ol. Sample solutions were prepared by diluting approximately 50 mg of sample to 50 ml with carbon tetrachloride. The solution was placed in a 10-cm cell and with CCl_4 in the reference cell, the spectrum from 2.85 to 2.70 μ was obtained on a Beckmann DK-1 spectrophotometer. The height of the hydroxyl absorption band was referred to a curve prepared from the appropriate standard.

RESULTS AND DISCUSSION

4,4′-Azobis(4-cyano-*n*-pentanol) (ACP) exists in two isomeric forms which differ in melting point and solubility characteristics. The higher-melting isomer (94–96°C) possessed a very limited solubility in toluene at ambient temperature and represented the isomer obtained in the lower yield. The low-melting isomer (81–83°C) is readily soluble in toluene and other common polymerization solvents. The isomer mixture as obtained from the reaction was almost completely soluble in toluene at 65°C. Dioxane, DMF, and acetonitrile are excellent solvents for all forms of the initiator. Reactions were carried out by using ACP in the three available forms: soluble ACP, insoluble ACP, and the mixture where soluble and insoluble refer to the isomer's solubility in toluene at ambient temperature.

Initial reactions were conducted in toluene solution at 65°C where it was though that the insoluble isomer might dissolve. Only partial solution was observed over the 3-day reaction period. The prepolymer yields from the toluene reactions demonstrated (Table I) that ACP was a suitable initiator in its soluble form (44% yield) or as a mixture of isomers (41% yield); however, the insoluble form was found to be relatively inefficient (17% yield) in initiating butadiene polymerization in toluene.

TABLE I
Polybutadienes Prepared in Different Solvents
With 4,4′-Azobis(4-cyano-*n*-pentanol) as Initiator[a]

Initiator form	Solvent	Yield, %	$\bar{M}_n$	OH, wt-%	Equivalent weight	Functionality
Soluble ACP	Toluene	44	3200	1.40	1215	2.63
Insoluble ACP	Toluene	17	3400	1.59	1070	3.18
Mixture ACP	Toluene	41	3000	1.43	1190	2.52
Insoluble ACP	Dioxane	51	3300	1.44	1180	2.79
Mixture ACP	Dioxane	45	3000	1.41	1205	2.49
Insoluble ACP	DMF	22	2900	1.69	1005	2.88
Mixture ACP	DMF	35	2800	1.50	1135	2.47
Mixture ACP	Acetonitrile	25	2600	1.42	1195	2.17

[a] Polymerization conditions: 65°C, 72 hr, [B] = 6.66 mole/l., [ACP] = 3 mole-%

Similar reactions conducted in dioxane, which was a good solvent for the insoluble isomer, gave good yields of the polybutadiene for both the insoluble and the isomer mixture. In contrast, reactions conducted in DMF, which is also an excellent solvent for all forms of the initiator, gave moderate to poor yields of the polybutadiene when the insoluble isomer (22%) and the isomer mixture (35%) were employed. Likewise, the use of acetonitrile as solvent gave a poor yield (25%) of polybutadiene when the isomer mixture was employed as the initiator.

It was apparent from the results reported (Table I) that a non-polar solvent such as toluene is not a suitable polymerization medium for the insoluble isomer, although toluene appeared to be satisfactory when the isomer mixture was employed. Dioxane was found to be the most appropriate solvent with respect to both yields of prepolymer and prepolymer properties. The polar solvents such as DMF and acetonitrile, while excellent solvents for the initiator in any form, did not give yields of prepolymer comparable with reactions carried out in dioxane. Reasons for the lower yields in polar solvents remain obscure.

Characterization of the prepolymers demonstrated that each was similar to the others in $\bar{M}_n$ and functionality. It was significant that the prepolymers obtained from reactions where the insoluble form of ACP was used exhibited the highest functionality. These data indicated that the isomer mixture of ACP could be employed as the initiator for diene polymerization in toluene, dioxane, or more polar solvents.

The free-radical-initiated polymerization of the common dienes such as butadiene, isoprene, and chloroprene with 4,4′-azobis(4-cyano-*n*-pentanol) in toluene or dioxane solution has given liquid prepolymers suitable for use in the formation of more highly developed networks. This study was undertaken with the purpose of determining the effect of various experimental parameters on prepolymer yield and properties. Certain conclusions have been made from an analysis of the results obtained.

The solution polymerization of dienes by radical initiation is known to proceed at a very slow rate and form low molecular weight polymers. Although rate studies were not performed in this study, a general qualitative measure of the polymerization rate may be ascertained from yield data obtained for the various dienes when polymerized under similar conditions. Qualitatively, the rate of polymerization of the dienes decreases in the order: chloroprene $\gg$ butadiene $>$ isoprene. Undoubtedly, the rate of polymerization is controlled to a large extent by the nature of the growing radical chain end of the polymer, particularly the spatial arrangement of the terminal monomer unit.

One of the areas of interest in the reaction parameter study was the yield of the prepolymers obtained from free-radical solution polymerization of the diene monomers. Reactions conducted over time periods of 24, 48, 72, and 120 hr, using 3 mole-% ACP in toluene and dioxane demonstrated that an increase in the prepolymer yield may be realized with an increase in reaction time. Prepolymer yields also increased with initiator concentrations; however, increasing the diene concentration from 5.0 to 20.0 mole/l. had little effect on the yields. The maximum yields for the polybutadienes and the polyisoprenes appeared to be near 60%; polychloroprenes could be obtained in near quantitative yields under appropriate conditions. Polymerizations conducted in dioxane gave slightly higher yields than in toluene. Depending upon conditions and the diene, the yields ranged from 13 to 99% (see Tables II–IV).

The molecular weight of the polydiene prepolymers was affected slightly by reaction conditions. An increase in the molecular weight was observed with an increase in the time of the reaction. In general, the molecular weight of the prepolymers were highest at low initiator concentrations. Although not consistent within a given prepolymer series, there appeared to be a trend towards higher molecular weights with increasing diene concentration. The molecular weight ranges for the polydienes were: polybutadienes 2200–5700, polyisoprenes 2200–6600, and polychloroprenes 2500 to >20,000. Within these molecular weight limits the ACP concentration may be utilized to exert the most control over the molecular weight of the prepolymers.

While molecular weight of the prepolymers normally ran in the expected order within any given series of polymerization reactions, there were instances where the molecular weight values were obviously high or low and did not fit into the pattern. Errors in the $\bar{M}_n$ values obtained by vapor-phase osmometry may be attributed to (a) impurity in the sample, or (b)

TABLE II
Butadiene Prepolymers[a]

[B], mole/l.	[ACP], mole-%	Time, hr	Yield, %[b]	$\bar{M}_n$	OH, wt-%	Equivalent weight	Functionality (OH)	$[\eta]$, dl/g[c]	$\bar{M}_w/\bar{M}_n$
				Effect of Polymerization Time					
6.66	3.0	24	41(39)	2400(3000)	1.23(1.39)	1380(1070)	1.74(2.80)	0.184	1.24
6.66	3.0	48	55(48)	2300(3800)	1.21(1.34)	1405(1265)	1.63(3.00)	0.205	1.73
6.66	3.0	72	41(61)	3000(3300)	1.43(1.44)	1185(1180)	2.53(2.79)	0.286	1.82
6.66	3.0	120	57(63)	3500(2500)	1.03(1.39)	1650(1220)	2.12(2.05)	0.434	1.91
				Effect of ACP Concentration					
6.66	0.5	72	23(21)	5000(5000)	1.30(0.69)	1310(2465)	3.82(2.03)	0.395	2.97
6.66	1.0	72	27(31)	4200(5700)	0.90(0.97)	1890(1750)	2.22(3.26)	0.315	1.97
6.66	2.0	72	34(44)	3700(4600)	1.17(1.19)	1455(1425)	2.54(3.23)	0.198	1.72
6.66	3.0	72	36(50)	3500(3800)	1.20(1.25)	1415(1355)	2.47(2.80)	0.210	1.46
6.66	10.0	72	20(42)	2500(2200)	1.27(1.92)	1335(885)	1.87(2.68)	0.120	1.24
				Effect of Butadiene Concentration					
5.0	3.0	72	33(46)	2500(3100)	1.37(1.35)	1240(1260)	2.01(2.45)	0.200	1.59
6.66	3.0	72	36(50)	3500(3800)	1.20(1.25)	1465(1470)	2.39(2.58)	0.210	1.46
10.0	3.0	72	35(52)	3900(3000)	1.45(1.31)	1170(1300)	3.33(2.31)	0.285	1.81
20.0	3.0	72	32(52)	5000(3700)	1.19(1.33)	1425(1275)	3.50(2.90)	0.296	1.85

[a] Numbers in parentheses refer to prepolymers prepared in dioxane, others prepared in toluene.
[b] Yield values represent yields of purified prepolymers.
[c] Measured in toluene at 30°C in Cannon dilution viscometers

TABLE III
Isoprene Prepolymers[a]

[I], mole/l.	[ACP], mole-%	Time, hr	Yield, %[b]	$\bar{M}_n$	OH, wt-%	Equivalent weight	Functionality (OH)	$[\eta]$, dl/g[c]	$\bar{M}_w/\bar{M}_n$
				Effect of Polymerization Time					
6.66	3.0	24	20(25)	2700(3000)	1.21(1.50)	1405(1135)	1.92(2.64)	0.108	1.15
6.66	3.0	48	27(39)	2500(3300)	1.19(1.31)	1430(1300)	1.74(2.54)	0.140	1.32
6.66	3.0	72	30(45)	3700(2700)	1.03(1.55)	1650(1095)	2.24(2.46)	0.154	1.41
6.66	3.0	120	30(45)	3700(3300)	0.96(1.42)	1770(1195)	2.09(2.76)	0.181	1.62
				Effect of ACP Concentration					
6.66	0.5	72	13(13)	6600(6400)	0.67(0.72)	2590(2365)	2.55(2.71)		
6.66	1.0	72	23(21)	5700(6600)	0.85(0.90)	2000(1890)	2.85(3.49)		
6.66	2.0	72	21(29)	4400(4400)	1.18(1.12)	1440(1520)	3.06(2.89)		
6.66	3.0	72	29(34)	3800(3200)	1.14(1.36)	1490(1250)	2.55(2.56)		
6.66	10.0	72	32(45)	3600(2300)	1.21(1.90)	1405(895)	2.56(2.57)		
				Effect of Isoprene Concentration					
5.0	3.0	72	27(33)	3900(2400)	1.28(1.16)	1330(1465)	2.93(1.63)		
6.66	3.0	72	30(34)	3800(3200)	1.14(1.36)	1490(1225)	2.54(2.61)		
10.0	3.0	72	25(37)	4500(2800)	1.10(1.14)	1545(1530)	2.91(1.83)		
20.0	3.0	72	28(46)	2200(4300)	0.90(1.07)	1895(1590)	1.15(2.83)		

[a] Numbers in parentheses refer to prepolymers prepared in dioxane, others prepared in toluene.
[b] Yield values represent yields of purified prepolymers.
[c] Measured in toluene at 30°C in Cannon dilution viscometers.

TABLE IV
Chloroprene Prepolymers[a]

[C], mole/l.	[ACP], mole-%	Time, hr	Yield, %[b]	$\bar{M}_n$	OH, wt-%	Equivalent weight	Functionality (OH)
			Effect of Polymerization Time				
6.66	3.0	24	57(58)	5300(5400)	0.39(0.46)	4360(3700)	1.21(1.46)
6.66	3.0	48	53(57)	5000(6100)	0.41(0.59)	4150(2880)	1.18(2.11)
6.66	3.0	72	59(58)	5500(3900)	0.56(0.39)	3035(4360)	1.81(0.89)
6.66	3.0	120	58(97)	8600(2800)	0.35(0.48)	4860(3540)	1.76(0.79)
			Effect of ACP Concentration				
6.66	0.5	72	78(86)	12,400(13,000)	0.29(0.16)	5850(10,600)	2.12(1.22)
6.66	1.0	72	71(92)	12,400(9200)	0.34(0.23)	5000(7400)	2.48(1.4)
6.66	2.0	72	94(99)	20,000(9700)	0.35(0.35)	4750(4750)	— (2.04)
6.66	3.0	72	97(98)	11,600(6100)	0.86(0.59)	1880(2880)	— (2.12)
6.66	10.0	72	98(99)	5300(2500)	0.75(1.28)	2270(1330)	2.33(1.88)
			Effect of Chloroprene Concentration				
5.0	3.0	72	82(97)	7500(8400)	0.60(0.66)	2830(2575)	2.64(3.26)
6.66	3.0	72	97(82)	11,400(4500)	0.86(0.60)	1980(2830)	— (1.59)
10.0	3.0	72	82(82)	6300(9700)	0.69(0.59)	3470(2880)	1.81(3.36)
20.0	3.0	72	85(83)	7500(10,800)	0.42(0.52)	4050(3270)	1.85(3.30)

[a] Numbers in parentheses refer to prepolymers prepared in dioxane, others prepared in toluene.
[b] Yield values represent yields of purified prepolymers.

errors introduced in the experimental determination of $\bar{M}_n$.[5] It was extremely difficult to determine the purity of the prepolymer samples, since the presence of small quantities of solvents or other low molecular weight compounds, which affect the measured $\bar{M}_n$ values drastically, are not easily accounted for by conventional means. To insure a certain degree of reproducibility of sample purity, a standard isolation and purification procedure (previously described) was employed. Although considerable variation was observed in molecular weight values, the trends in molecular weight were definitely established and have been confirmed by intrinsic viscosity measurements and gel permeation chromatography analysis.

One of the most important properties of the liquid prepolymers was their functionality since this number is an indication of the amount of coupling or crosslinking that can be achieved in the chain-extension of such prepolymers. Functionality was expressed as $\bar{M}_n$/hydroxyl (endgroup) equivalent weight. It appeared that there was a trend for the functionality values in any series of prepolymers to increase as the $\bar{M}_n$ values increased. In general, the functionality values were greater than 2.0, and in those instances where low values were obtained, probable errors existed in the measured values for M_n and/or weight per cent hydroxyl endgroups.

Intrinsic viscosity values $[\eta]$ were measured in toluene solution at 30°C in Cannon dilution viscometers. These values indicated that the molecular weight of the prepolymers increased with time, with reduction in ACP concentration, and with an increase in diene concentration. Hence, they tended to substantiate the trends developed in the $\bar{M}_n$ (VPO) data.

The molecular weight distribution values ranged from 1.24 to 2.97 for the polybutadienes and 1.15 to 1.62 for the limited number of polyisoprenes. It was apparent that the molecular weight distribution was increasing with longer reaction time as would be expected from duplicate reactions where the quantity of initiator was added in one single portion at the start of the polymerization. In addition, the increase in [ACP] produced a decrease in the molecular weight distribution for the polybutadienes whereas the butadiene concentration exhibited little effect on their distribution. It was demonstrated that under suitable conditions the molecular weight distribution could be controlled to give relatively low values in the range of 1.2–1.3.

The analytical contributions of Dr. K. E. Johnson and Mr. R. D. Strahm are gratefully acknolwedged. The technical assistance of Mr. J. O. Woods is appreciated.

This work was sponsored by the U.S. Army Missile Command, Redstone Arsenal, Alabama, under contract DAAH01-68-C-0632.

References

1. M. Szwarc, *Nature*, **178**, 1168 (1956).
2. D. H. Richards, *J. Polym. Sci. B*, **6**, 417 (1968).
3. C. A. Uraneck, H. L. Hsieh, and O. G. Buck, *J. Polym. Sci.*, **46**, 535 (1960).
4. H. Brody, D. H. Richards, and M. Szwarc, *Chem. Ind. (London)*, **1958**, 1473.
5. C. H. Bamford, A. D. Jenkins, and R. P. Wayne, *Trans. Faraday Soc.*, **56**, 935 (1960).
6. W. H. Stubbs, C. R. Gore, and C. S. Marvel, *J. Polym. Sci., A-1*, **4**, 1898 (1966).

7. W. D. Stephens, C. R. McIntosh, and C. O. Taylor, *J. Polym. Sci. A-1*, **6**, 1037 (1968).

8. Minnesota Mining and Manufacturing Co., *Carboxyl Terminated Polyhydrocarbons*, Summary Report for Period of July 1, 1964–June 30, 1966, Naval Weapons Center, China Lake, California, NOTS TP 4307, June 1967.

Received June 30, 1970
Revised March 5, 1971

JOURNAL OF POLYMER SCIENCE: PART A-1 VOL. 9, 2039–2049 (1971)

Polymerization of Methyl Methacrylate under Ultrasonic Irradiation. Part V. Effect of Ultrasonic Irradiation on Stereoregularity of the Polymers and Oligomers Produced by Grignard Catalyst in Toluene–Dioxane Mixed Solvent

ZENJIRO OSAWA, TAKAO KIMURA,* YOSHITAKA OGIWARA, and NORIYUKI MATSUBAYASHI,† *Department of Polymer Chemistry, Faculty of Engineering, Gunma University, Kiryu City, Gunma, Japan*

Synopsis

Polymerization of methyl methacrylate with Grignard reagent in toluene–dioxane mixed solvent was carried out under ultrasonic irradiation. The effects of ultrasonic irradiation and the order of catalyst addition on Grignard reagent and the microstructure in the reacting sites were examined on the basis of the stereoregularity of polymers and oligomers produced. The formation of oligomers was also discussed on the basis of the consumption of initiator. The stereoregularity of the polymers in series A (no ripening of catalyst with solvent) is higher than that in series B (ripening of catalyst with solvent). The effect of ultrasonic irradiation on the stereoregularity was completely reversed in series A and B; it increased in the former and decreased in the latter with ultrasonic irradiation. Similar results were obtained for the stereoregularity of the oligomers, but the stereoregularity of the oligomers was lower than that of polymers.

INTRODUCTION

In a previous paper[1] of this series, we proposed that ultrasonic irradiation affected both the chemical equilibrium of Grignard reagents in solution and the reacting sites in anionic polymerization on the basis of the stereoregularity of the polymers produced in dioxane–tetrahydrofuran mixed solvent. This paper deals with our efforts to confirm the proposal by examining the effect of ultrasonic irradiation on the stereoregularity of polymers (methanol-insoluble) and oligomers (methanol-soluble, water-insoluble) produced by Grignard reagents in toluene–dioxane mixed solvent.

In anionic polymerization of methyl methacrylate, it is well known that various kinds of by-products are produced other than polymeric materials.

* Present address: Electrical Communication Laboratory, Nippon Telegraph and Telephone Public Corp., Tokai Ibaragi, Japan.

† Present address: Hitachi Ltd., Naka Work, Katsuta City, Ibaragi, Japan.

Kawabata and Tsuruta[2,3] reported that in polymerization of methyl methacrylate with *n*-butyllithium in tetrahydrofuran, *n*-butane, carbonyl addition compounds, and dimer were produced as by-products, and ca. 25% of initiator in tetrahydrofuran and ca. 50% in *n*-hexane participated for the production of polymers. In *n*-butylmagnesium bromide-initiated polymerization, *n*-butane was also produced.[4]

Glusker et al.[5,6] reported that in polymerization of methyl methacrylate with 9-fluorenyllithium in toluene, about 90 mole -% of polymeric materials has a molecular weight lower than 2000, and postulated termination with a ring-complex structure. Goode et al.[7] reported the formation of polymers with a broad molecular weight distribution and several reaction products of Grignard reagent and methyl methacrylate in the phenylmagnesium bromide catalyst system.

Furthermore, Minoura et al.[8] showed that the degree of polymerization of the methanol-insoluble MMA polymer is higher than 1000, and that of the methanol-soluble portion is lower than 50 in an optically active Grignard reagent catalyst system.

Although a number of works on the stereospecific polymerization of methyl methacrylate have been published, very few systematic studies on the stereoregularity of the oligomeric materials produced in anionic polymerization of methyl methacrylate, in connection with that of polymeric materials, are available. Therefore, the stereoregularity of the polymers and oligomers produced by the polymerization of methyl methacrylate with Grignard reagent in toluene–dioxane mixed solvent was determined by NMR analysis, and the effect of ultrasonic irradiation on Grignard catalyst and the microstructure in the reacting sites is discussed

EXPERIMENTAL

Preparation of Reagents

Purification of the monomer and solvents and synthesis of the initiator were described in previous papers.[1,9–11]

Polymerization

Polymerizations were divided into two series, namely, series A (no ripening of initiator system) and series B (ripening of initiator system).

Series A. A solution of 4 ml of methyl methacrylate and 16 ml of mixed solvent of toluene and dioxane was placed in a 100 ml flask which had been previously flushed with dry nitrogen, and the contents were kept at 20°C. Then 3 ml of phenylmagnesium bromide in toluene solution ($2.8 \times 10^{-3} M$) was introduced by means of a syringe.

Series B. The same amounts of solvent and initiator as in series A were added to a 100 ml flask and the contents were allowed to stand for 10 min. Then 4 ml of monomer was introduced by means of a syringe and polymerization was started.

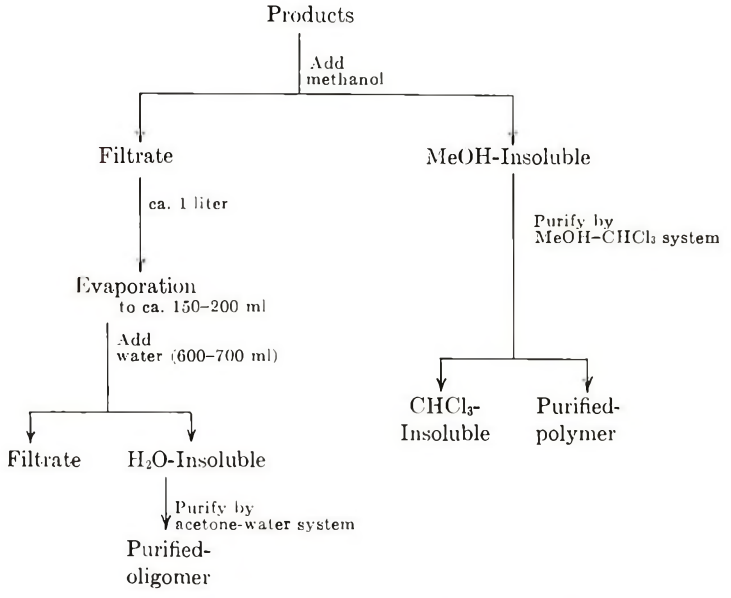

Fig. 1. Treatment of polymerization products.

Polymerization was carried out at 20°C for 30 min, and termination was obtained by addition of a large amount of methanol containing a small amount of hydrochloric acid. The methanol-insoluble and methanol-soluble, water-insoluble portions were separated and purified as shown in Figure 1.

Various mixed toluene–dioxane solvents, containing 0, 1, 5, 10, 20, 60, 80, 90, and 100 vol-% dioxane, were used. Parallel runs were carried out under ultrasonic irradiation at a frequency of 500 kcps and input power of 100 W.

Characterization of the Products

The molecular weights of the products were determined by viscometry, a vapor-pressure method, and osmometry. Determination of the structure of the polymers and oligomers were made by a NMR spectral analysis. The NMR instrument used was a Hitachi Model R-20 instrument.

RESULTS AND DISCUSSION

Polymerization conditions and yields of polymers and oligomers are listed in Table I. As shown in Table I, a distinct trend in yield of polymers and oligomers is not observable. However, the yield of polymers is almost 40–50% when 100 toluene is used as solvent, and a fairly large amount of oligomers is produced in each series.

The molecular weights of polymers and oligomers are shown in Table II. The number-average molecular weights of oligomers, as determined by the

TABLE I
Polymerization Conditions and Yields of Polymers and Oligomers

Toluene:dioxane (by volume)	Series A (no ripening)				Series B (ripened)			
	Polymer yield, %		Oligomer yield, %		Polymer, yield, %		Olligomer yield, %	
	Without US[a]	With US	Without US	With US	Without US	With US	Without US	With US
100:0	47.0[b]	47.0[b]	25.6[b]	29.4[b]	42.3[b]	48.2[b]	14.9[b]	6.7[b]
99:1	44.1	54.3	2.9	23.2	13.2	9.5	4.3	14.7
95:5	5.9	22.3	4.4	33.4	9.5	9.5	17.0	2.7
90:10	7.0[b]	9.6[b]	27.3[b]	23.4[b]	13.8[b]	13.6[b]	14.2[b]	16.6[b]
80:20	8.9	10.2	21.4	21.7	16.7	15.4	14.2	15.3
40:60	11.4	10.1	19.1[b]	13.8[b]	15.7	18.0	18.5[b]	Trace
20:80	11.4	13.3	14.1	12.7	18.0	15.0	5.7	1.1
10:90	13.5	14.2	13.4	10.9	16.1	19.0	18.7	7.8
0:100	14.2[b]	13.7[b]	11.6[b]	16.2[b]	14.1[b]	13.4[b]	14.9[b]	14.6[b]

[a] Ultrasonic irradiation.

[b] Data used for the calculation of consumption of initiator.

TABLE II
Molecular Weight of Polymers and Oligomers

Toluene: dioxane (by volume)	Series A (no ripening)				Series B (ripened)			
	Polymer MW × 10^{-5} [a]		Oligomer MW[b]		Polymer MW × 10^{-5}		Oligomer MW	
	Without US	With US	Without US	With US	Without US	With US	Without US	With US
100:0	10.38	4.11	640	734	7.75	4.06	842	1409
	(0.927)[c]	(0.362)[c]			(0.517)[c]	(0.457)[c]		
99:1	3.94	3.58			6.54	2.32		
95:5	2.40	4.89		1037	1.48	1.74		
90:10	2.45	4.26	691	754	1.86	1.86	1042	627
	(0.476)[c]	(1.06)[c]			(0.535)[c]	(0.514)[c]		
80:20	3.22	3.51	664		1.58	0.96		
40:60	2.73	2.86	726	647	0.86	0.81	819	
20:80	2.44	3.22			0.78	0.86		
10:90	1.59	2.76	826		0.70	0.69		
0:100	2.18	2.22	1183	887	0.71	0.63	1127	863
	(0.291)[c]	(0.381)[c]			(0.247)[c]	(0.283)[c]		

[a] Determined by a viscometric method.
[b] Determined by a vapor-pressure method.
[c] Determined by an osmotic-pressure method.

TABLE III
The Ratio $\bar{M}_v/\bar{M}_n$ for Polymers

Toluene:dioxane (by volume)	$\bar{M}_v/\bar{M}_n$			
	Series A (no ripening)		Series B (ripened)	
	Without US[a]	With US	Without US	With US
100:0	11.2	11.4	15.0	8.9
90:10	5.1	4.0	3.5	3.1
0:100	7.5	5.8	2.8	2.2

[a] Ultrasonic irradiation (100 W).

vapor pressure method, lie in the range 630–1410, which corresponds to a degree of polymerization of 6–13 if the chain-end phenyl group is excluded. On the other hand, the viscosity-average molecular weight of polymers ranges from 6300 to 1,038,000; in general, molecular weights of polymers from series A (no ripening) are higher than those of series B (ripening) and they decrease with increasing proportion of dioxane in the mixed solvent. However, a small effect of ultrasonic irradiation on the molecular weight of the products is observed.

It is well known that the viscosity-average molecular weight is close to the weight-average molecular weight, and the ratio $\bar{M}_w/\bar{M}_n$ is sometimes used as a measure of the breadth of the molecular weight distribution.[12] Therefore, the ratio, $\bar{M}_v/\bar{M}_n$, was calculated as a measure of the breadth of the molecular weight distribution. The $\bar{M}_v/\bar{M}_n$ ratios are shown in Table III.

It is reported that $\bar{M}_w/\bar{M}_n$ in a nonpolar solvent for PMMA is 7–18.[13] As shown in Table III, the ratio of $\bar{M}_v/\bar{M}_n$ in pure toluene solvent is 9–15 which is within the preceding range. However, it is much lower in pure dioxane or toluene–dioxane mixed solvent for both series. The ultrasonic irradiation lowers the ratio $\bar{M}_v/\bar{M}_n$ slightly.

As shown in Figure 1, the methanolic clear filtrate becomes cloudy on addition of a large amount of distilled water after removal of methanol-insoluble polymeric materials. On allowing the cloudy filtrate to stand for a day or more yielded white powder or yellowish paste precipitants. These products show almost identical infrared and NMR spectra as the polymeric materials. In the case of oligomers, a peak (τ = 2.85) in the lower magnetic field region was observed which was assigned to the end phenyl group in the oligomer. It is therefore possible to calculate the stereoregularity of the oligomers in the same way as that of the polymeric materials by analysis of NMR spectra. The number-average molecular weights of the oligomers determined by the vapor-pressure method are shown in Table II.

The stereoregularity of the polymers was determined by NMR spectral analysis, and plots of isotacticity and syndiotacticity against the concentration of dioxane in the mixed solvent are shown in Figures 2 and 3, respectively.

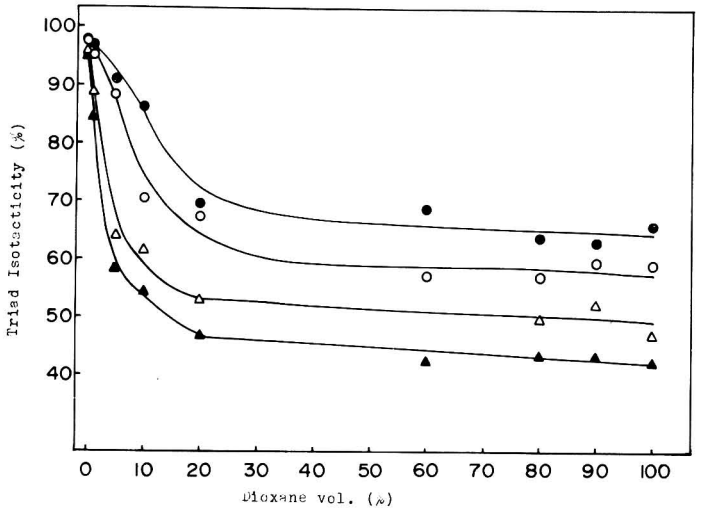

Fig. 2. Isotacticity of polymer: (O) series A (no ripening of initiator system), without ultrasonic irradiation; (●) series A (no ripening of initiator), with ultrasonic irradiation; (△) series B (ripening of initiator system), without ultrasonic irradiation; (▲) series B (with ripening of initiator), with ultrasonic irradiation.

The plots of isotacticity and syndiotacticity against the concentration of dioxane in mixed solvent gave four separate curves. The isotacticity decreases with increasing dioxane in mixed solvent up to a given level, after which it levels off at higher dioxane concentrations. The reverse tendency is observed in syndiotacticity (see Fig. 3). The stereoregularity of the polymers produced in the four series decreases in the order: no ripening, with ultrasonic irradiation > no ripening, without ultrasonic irradiation > ripening, without ultrasonic irradiation > ripening, with ultrasonic irradiation. The trend in isotacticity of polymers is consistent with that in dioxane–tetrahydrofuran mixed solvent.[1]

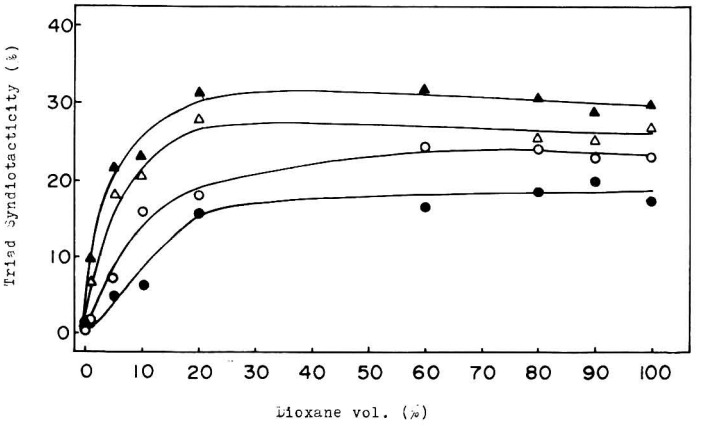

Fig. 3. Syndiotacticity of polymer. Symbols as in Fig. 2.

For the explanation of the results, we took into consideration two factors which may affect the stereoregularity of the polymers: namely, the chemical equilibrium of Grignard reagents and the effect of ultrasonic irradiation on reacting sites. The chemical equilibrium of Grignard reagents shown in eq. (1) and the relation between the stereoregularity of polymers and initiating species were discussed in some detail in the previous paper.[1]

$$2RMgX \rightleftarrows R_2Mg + MgX_2 \quad (1)$$

The results that isotacticity of series A (no ripening) is higher than that of series B (with ripening) might reflect the relative amounts of the active species, RMgX and R_2Mg, since in the ripening of Grignard reagent with toluene–dioxane mixed solvent, R_2Mg, which gives a polymer of low stereoregularity, might increase. In this connection, one should notice that reaction in pure toluene solvent, in all four series gives polymers with a extremely high isotactic content, and there is no difference in stereoregularity among four groups.

The opposite effect of ultrasonic irradiation on the stereoregularity of the polymers is also observed. In the case of series A (no ripening of catalyst system), the isotacticity of polymers produced with ultrasonic irradiation was higher than that without it, however, the converse is true in the case of series B (ripening of catalyst system). The preceding results are consistent with those reported in the previous paper.[1] Therefore, the conclusion that the ultrasonic irradiation affects the microstructure in the transition state of propagation, and increases R_2Mg if the catalyst system is aged seems to be valid.

As shown in Figure 4, the plots of isotacticity of oligomeric materials against the concentration of dioxane in mixed solvent give four separate

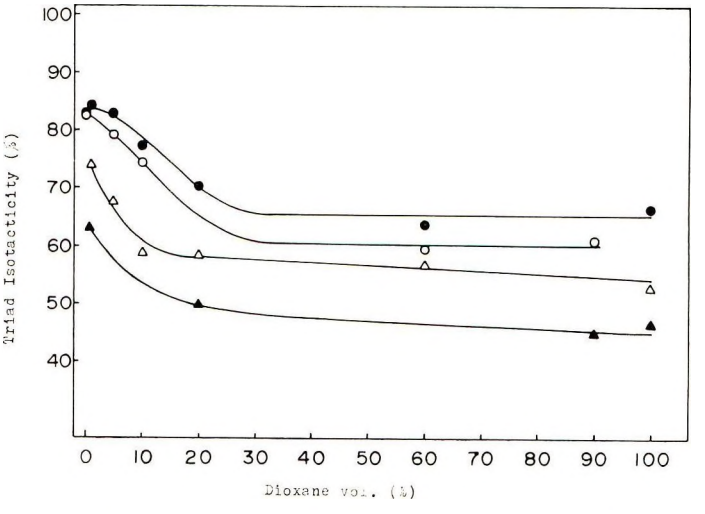

Fig. 4. Isotacticity of oligomer. Symbols as in Fig. 2.

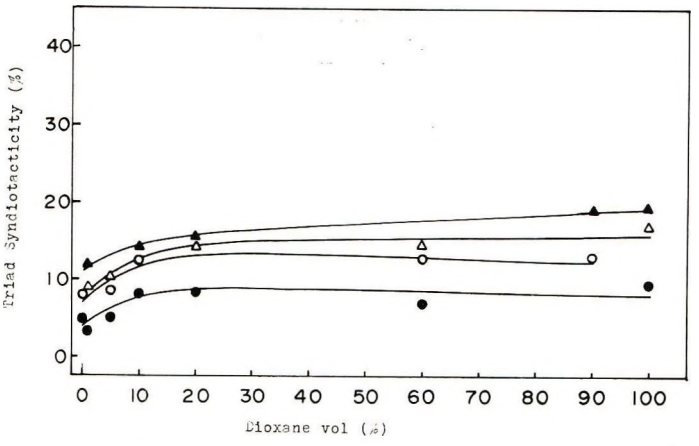

Fig. 5. Syndiotacticity of oligomer. Symbols as in Fig. 2.

curves which are similar to those for the polymers. The results might be explained in the same manner as for polymers. However, the isotacticity of oligomers is lower than that of polymers in the toluene-rich range. For examples, in pure toluene solvent the isotacticity is ca. 83% for oligomers, but ca. 95–98% for polymers. Glusker et al.[5,6] reported that beyond a limited monomer unit a helical structure of growing polymer is formed; in this helical structure the addition of monomer to growing polymer end with isotactic structure is favored. Therefore, the fact that the isotacticity of oligomers is lower than that of polymers is ascribed to the same reasons as Glusker proposed.

According to the Coleman's equation, it is possible to estimate the stereoregular sequence lengths by triad tacticity.[14] The results calculated were in good agreement with the stereoregularity; namely, the order of the mean lengths $\mu \{I\}$ of closed sequences o isotactic placements was consistent with the isotacticity.

See Figure 5 for information on triad syndiotacticity.

For the formation of oligomeric materials, various factors might be considered, for example, degradation of polymers by ultrasonic irradiation, termination by traces of impurities such as oxygen, moisture, or carbon dioxide, pseudo-termination association of growing polymers, and chain transfer to solvent. It is not likely that the formation of oligomer is due to degradation of polymers, since all four series give oligomeric materials.

The evaluation of the consumption of initiator would be very helpful in understanding the termination reaction by impurities. The consumption of initiator was therefore calculated for all series; results are shown in Table IV.

In anionic polymerization, small amounts of oxygen or moisture, can react instantly with initiator and growing polymers ends. Therefore, in series A (no ripening of catalyst), impurities might react with both initiator and growing polymer end; on the other hand, in series B (ripening of catalyst), the initiator may be consumed by the impurities during the

TABLE IV
Consumption of Initiator

	Series A (no ripening)		Series B (ripened)	
	Without US	With US	Without US	With US
Polymer, wt-%[a]	53.8	58.2	56.5	67.0
Oligomer, wt-%	46.2	41.8	43.5	33.0
Polymer, mole-%[a]	2.0	1.5	3.3	6.1
Oligomer, mole-%	98.0	98.5	96.7	93.9
Consumption of initiator, %				
Polymer	0.6	0.5	0.7	0.8
Oligomer	35.4	37.6	22.3	17.9
Others	64.0	61.9	77.0	81.3

[a] Chloroform-insoluble material excluded.

ripening of catalyst. If this kind of termination reaction occurs, the consumption of initiator by the formation of oligomers in series A must be higher than that in series B. As shown in Table IV the average initiator consumption by oligomer formation is 36.5% in series A and 20.1% in series B. The data seem to indicate that oligomer formation involves reaction between growing polymer and impurities. However, a large amount of oligomer is formed even in series A, in which almost all impurities should be reacted with initiator, and the formation of oligomers is not likely if the impurities were the only factor.

Glusker et al.[5,6] and Goode[7] assumed a pseudo-termination in polymerization of methyl methacrylate with 9-fluorenyllithium for the formation of oligomers. They assumed a change in mechanism at eight or nine monomer units which results in a large increase in the probability that each monomer addition will be isotactic. Therefore, one should take into consideration this pseudo-termination proposed for the formation of oligomers.

Although Makowski et al.[15] reported the association of low molecular weight species in the polymerization of butadiene, it is difficult to deduce the association of growing species with low molecular weight in our polymerization system.

Chain transfer to solvent is observed only rarely in anionic polymerization of methyl methacrylate in dimethyl sulfoxide;[16] in general chain transfer is less expected in anionic polymerization. It is, therefore, not probable to expect the chain transfer in our system. So far we have discussed the formation of oligomers; no adequate explanation is available at present.

Statistical treatment of the results showed that Bovey plots of stereoregularity of oligomers was different from that of an ideal Bernoulli process and was quite similar to that of polymers, and it did not fit Fueno's model[17] which is controlled by catalyst. Therefore, a penultimate effect must be

present in oligomer formation as well as polymer formation in anionic polymerization of methyl methacrylate.

References

1. Z. Osawa, T. Kimura, and T. Kasuga, *J. Polym. Sci. A-1*, **7**, 2007 (1969).
2. N. Kawabata and T. Tsuruta, *Makromol. Chem.*, **86**, 231 (1965).
3. N. Kawabata and T. Tsuruta, *Kogyo Kagaku Zasshi*, **68**, 239 (1965).
4. Y. Yasuda, N. Kawabata, A. Oda, and T. Tsuruta, *Kogyo Kagaku Zasshi*, **69**, 121 (1966).
5. D. L. Glusker, B. Yoncoskie, and E. Stiles, *J. Polym. Sci.*, **49**, 297 (1961).
6. D. L. Glusker, J. Lysloff, and E. Stiles, *J. Polym. Sci.*, **49**, 315 (1961).
7. W. E. Goode, F. H. Owens, and W. L. Myers, paper presented to the Division of Polymer Chemistry, American Chemical Society Meeting, 1960; *Polym. Preprints*, **1**, 79 (1960).
8. Y. Minoura and N. Kato, paper presented at 22nd Japanese Chemical Society Meeting, 1969; *Preprints*, **No. 4**, 2111 (1969).
9. Z. Osawa and N. Igarashi, *J. Appl. Polym. Sci.*, **9**, 3171 (1965).
10. Z. Osawa, *J. Appl. Polym. Sci.*, **10**, 1863 (1966).
11. Z. Osawa and M. Kusumoto, *Kogyo Kagaku Zasshi*, **71**, 168 (1968).
12. F. W. Billmeyer, *Textbook of Polymer Science*, Interscience, New York, 1962, p. 83.
13. Y. Yamashita, paper presented at 17th Polymer Summer Seminar, Japan, 1969; Preprint A2-7 (1969).
14. B. D. Coleman and T. G Fox, *J. Polym. Sci. A*, **1**, 3183 (1963).
15. H. S. Makowski and M. Lynn, *J. Macromol. Chem.*, **1**, 443 (1966).
16. A. G. Gosnell, J. A. Gervasi, and V. Stannett, *Makromol. Chem.*, **109**, 62 (1967).
17. R. A. Shelden, T. Fueno, T. Furukawa, and T. Tsuruta, *J. Polym. Sci.* **B, 3**, 23 (1964).

Received February 10, 1971.
Revised March 26, 1971.

JOURNAL OF POLYMER SCIENCE: PART A-1 VOL. 9, 2051-2061 (1971)

Determination of Chlorine Distribution in Chlorosulfonated Polyethylenes by High-Resolution NMR Spectroscopy

EDWARD G. BRAME, JR., *Elastomer Chemicals Department, Experimental Station, E. I. du Pont de Nemours and Company, Inc. Wilmington, Delaware 19898*

Synopsis

High-resolution proton magnetic resonance (NMR) spectroscopy was used to determine the sequence distribution of chlorines in elastomeric chlorosulfonated polyethylenes. The determination is based on measuring the relative amounts of methylene groups that are α, β, and γ (or greater) from chlorine containing groups (CHCl groups) in chlorosulfonated polyethylenes. The results obtained from the NMR examination at 220 MHz were compared with the theoretical predictions based on the statistics of substitution polymers. The comparison showed that polyethylenes chlorosulfonated by a solution reaction with gaseous chlorine and sulfur dioxide show a random chlorine distribution.

INTRODUCTION

High-resolution nuclear magnetic resonance spectroscopy has proved to be an effective tool for studying microstructure of chlorine-containing polymers.[1-13] Even though much of the work reported deals with studies on the stereochemical configuration of poly(vinyl chloride),[1-5] a number of workers have been involved with studies on sequence distributions of chlorine-containing copolymers.[6-13] Three of these studies[6-8] involved the microstructure investigation of vinylidene chloride–vinyl chloride copolymers. The NMR results reported from these studies showed that (1) even at high concentrations of vinylidene chloride some vinyl chloride sequences were observed and (2) two types of copolymers were found. One of the two types contained sequences of head-to-tail and head-to-head structure of vinylidene chloride and sequences of vinyl chloride and vinylidene chloride. The other type contained vinyl chloride sequences in addition to those mentioned in the first type.

Besides the NMR studies reported on vinylidene chloride-vinyl chloride copolymers sequence distribution measurements were reported on other kinds of chlorine-containing copolymers. Among them were vinylidene chloride–isobutylene copolymers,[10] vinylidene chloride–vinyl acetate copolymers,[11,12] and vinyl chloride–ethylene copolymers.[9,13] For the first

two kinds of copolymers, the sequence distribution measurements which were made in terms of diad or triad sequences showed that (1) for vinylidene chloride–isobutylene copolymers the NMR determination was as accurate as the chemical analysis and (2) for vinylidene chloride–vinyl acetate copolymer, a single NMR measurement could be used to specify the monomer sequence distribution. It was also found for the latter system that as the polymerization proceeds, the monomer sequence distribution becomes broader.

Of the different chlorine-containing copolymers studied by NMR, the one that comes closest to our NMR studies on chlorosulfonated polyethylene is the copolymer of ethylene and vinyl chloride. Schaefer[9] reported that vinyl chloride–ethylene copolymers prepared by free-radical polymerizations show a monomer distribution that is random or zeroth-order Markovian. However, Wilkes, et al.[13] showed that for vinyl chloride–ethylene copolymers prepared in bulk the copolymerization is not random and is first-order Markovian.

In our NMR investigation we studied the chlorine distribution of chlorosulfonated polyethylenes prepared by solution chlorosulfonation with gaseous sulfur dioxide and chlorine. In conjunction with the investigation, we developed an NMR method to determine the chlorine distribution by measuring the relative amounts of α, β, and γ (or greater) methylenes and then we compared the NMR measurements with the statistical predictions made for substitution polymers.[14]

EXPERIMENTAL

The five chlorosulfonated polyethylene samples used in the NMR studies had chlorine contents between 18 and 35 wt-%. The sulfur contents of each of these samples were about 1 wt-%. The one chlorinated polyethylene sample studied in this investigation contained 42 wt-% chlorine. All the samples were prepared by the gas-phase reaction[15] involving either chlorine and sulfur dioxide or chlorine alone in reaction with polyethylene dissolved in carbon tetrachloride.

Various chlorine containing model compounds were obtained for use in identifying lines in the NMR spectra. Samples of these compounds were obtained from Chem Service, Inc., Media, Pa.

The chlorosulfonated and chlorinated polyethylene samples were dissolved in either *p*-dichlorobenzene or Perclene at a concentration of about 20% (w/v) prior to their examination at elevated temperatures at 100 and 220 MHz. The 100 MHz spectra were obtained at approximately 150°C in *p*-dichlorobenzene solution with a Varian HA-100 spectrometer. The 220 MHz spectra obtained from *p*-dichlorobenzene solutions were examined at approximately 135°C with the Varian HR-220 spectrometer. Those 220 MHz spectra obtained from Perclene solutions were examined at about 115°C.

Interpretation of NMR Spectra

Figure 1 shows the NMR spectra obtained at 100 MHz and 220 MHz for the chlorosulfonated polyethylene sample containing 25 wt-% chlorine. This sample exhibits a pattern in the proton resonance spectrum that is typical of spectra obtained from chlorosulfonated polyethylenes whose chlorine contents are in the range from approximately 10 wt-% to approximately 40 wt-%. Based on a comparison of the two spectra in Figure 1, it is apparent that the spectrum obtained at 220 MHz is clearly superior to that obtained at 100 MHz. Not only are the different lines better resolved at 220 MHz but also the patterns obtained for the different lines clearly show multiplet splittings. Hence, it is readily seen that the data reported herein are based on work done at 220 MHz.

Table I lists the chemical shift values relative to hexamethyldisiloxane for chlorosulfonated polyethylenes, the structure assignments, and the

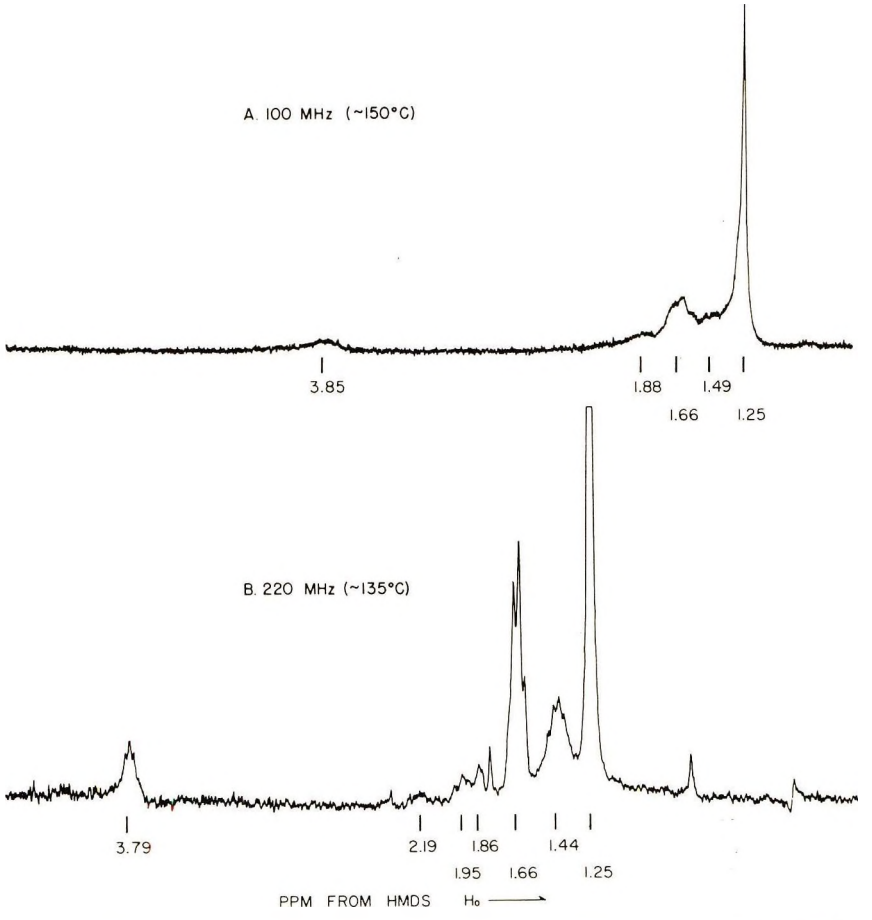

Fig. 1. NMR spectra of chlorosulfonated polyethylene containing 25 wt-% chlorine (*p*-dichlorobenzene solution).

TABLE I
Line Positions, Assignments, Methylene Sequences, and Literature Sources and Model Compounds Used for Line Assignments in NMR Spectra of Chlorosulfonated Polyethylenes

Chemical shifts, ppm from HMDS	Structure assignments	Methylene sequences	Literature sources and model compounds
1.25	—CH_2—CH_2—CH_2—	γ (or greater)	Refs. 9, 13
1.44	—CHCl—CH_2—CH_2—	β	Ref. 9 and 1-chloropentane
1.66	—CHCl—CH_2—CH_2—CH_2—CHCl—	α, β	Ref. 9 and 1-chloropentane
	—CHCl—CH_2—CH_2	α	
1.86	—CHCl—CH_2—CH_2—CHCl	α	Ref. 13 and 1,4-dichlorobutane
1.95	—CHCl—CH_2—CHCl—	α	Ref. 4, 9 (syndiotactic PVC)
2.19	—CHCl—CH_2—CHCl	α	Ref. 4, 9 (isotactic PVC)
3.79	—CH_2—CH_2—CHCl—CH_2—CH_2—	—	Ref. 9

literature sources and model compounds used in making the assignments. Even though the shift values are reported for the high frequency of 220 MHz, they were essentially consistent with those we obtained at 100 MHz and with most values reported by Schaefer[9] and Wilkes et al.[13] on similar sequences in copolymers of ethylene and vinyl chloride. The assignments made were based on a comparison of the shift values with those reported by Schaefer and Wilkes et al. as well as with the shift values obtained on identical groups in the indicated model compounds. However, because we are dealing with substitution polymers instead of vinyl copolymers and because we were able to obtain well resolved spectra at 220 MHz we decided to label the methylene sequences differently from the method described by Schaefer and Wilkes. We defined the sequences in terms of α, β, and γ (or greater) methylene groups as shown in Table I. This definition refers to methylene groups that are adjacent, two methylenes removed, and three or more methylenes removed, respectively, from CHCl groups. Even though there are several lines assigned to the different kinds of α-methylene groups, we lumped them together in our work for the sequence calculation of α-methylenes. The line at 1.66 ppm was included in the α-methylene sequence calculation although it contained one kind of β-methylenes.

Because some of the lines observed at 220 MHz clearly showed multiplet splitting patterns, we interpreted them in terms of their splitting patterns for comparison with the interpretations made from chemical shift measurements. The patterns associated with these various lines, the coupling constants measured, and the structures assigned are given in Table II.

The basis used for the structure assignments was twofold. First, we used the kind (singlet, quartet, etc.) of multiplet splitting pattern observed and second we used the value of the coupling constants determined for each of these lines. For the line at 1.25 ppm, a singlet is seen. Thus, it was assigned to polyethylenelike structure. For the line at 1.44 ppm, however, overlapping quintets are seen. The type of methylene group assigned to this line is seen to be surrounded by methylene groups with one of these methylene groups being adjacent to the chlorine-containing group. Hence, the reason for the quintet pattern. The appearance of overlapping quintets indicates that there is more than one kind of sequence for the β-methylenes. The line at 1.66 ppm shows a clearly defined quartet. This pattern can be assigned only to an α-methylene because it has to be the result of an interaction with three neighboring protons. One of the protons comes from the neighboring chlorine-containing carbon and the other two protons come from the neighboring β-methylene group. Following these assignments, we see that they compare very well with the same four chemically shifted lines in Table I except for the line at 1.66 ppm. One of the two sequence assignments in Table I is not indicated here. That sequence is the three methylene sequence between chlorine-containing groups. Since that sequence is not confirmed by the result of Table II, it is believed that it is very low in concentration at chlorine contents up to approximately 35 wt-%.

TABLE II
Multiplet Splittings, Coupling Constants, and Structure Assignments from 220 MHz NMR Spectra of Chlorosulfonated Polyethylenes

Chemical shifts, ppm from HMDS	Multiplet splittings	Coupling constants, Hz	Structure assignments
1.25	Singlet	—	—$\underset{\text{(d)}}{\underline{CH_2}}$—$\underset{\text{(d)}}{\underline{CH_2}}$—$\underset{\text{(d)}}{\underline{CH_2}}$
1.44	Overlapping quintets	$J_{bc} = J_{cd} = 7.0$	—$\underset{\text{(a)}}{CHCl}$—$\underset{\text{(b)}}{CH_2}$—$\underset{\text{(c)}}{\underline{CH_2}}$—$\underset{\text{(d)}}{CH_2}$
1.66	Quartet	$J_{ab} = J_{ab} = 7.0$	—$\underset{\text{(a)}}{CHCl}$—$\underset{\text{(b)}}{\underline{CH_2}}$—$CH_2$
3.79	Quintets	$J_{ab} = 7.0$	$\underset{\text{(b)}}{CH_2}$—$\underset{\text{(a)}}{\underline{CHCl}}$—$\underset{\text{(b)}}{CH_2}$

Method of Sequence Determination

The method developed to determine the chlorine distribution in chlorosulfonated polyethylenes is based on the measurement of relative areas of lines due to α, β, and γ (or greater) methylene groups in spectra of the polymers. In order for the determination to be valid and its results to be correlatable with the theoretical predictions that are based on statistics developed for substitution polymers[14] several assumptions were made. First,

the concentration of CCl_2 groups in chlorosulfonated polyethylenes in the concentration range from approximately 10 wt-% to approximately 35 wt-% chlorine was considered negligible. This assumption was verified upon correlating the results obtained from the area measurement of the line at 3.79 ppm (assigned to the CHCl group) with results of the elemental analysis for chlorine. Since it is known from literature data[7] that methylene groups adjacent to CCl_2 groups show their resonances in the 3–4 ppm region, a significant increase in the area measurement for this region over that predicted from the elemental analysis for chlorine would certainly indicate the presence of CCl_2 groups in the polymer. Based on this type of correlation, we found no indication for the presence of CCl_2 groups in chlorosulfonated polyethylenes up to about 35 wt-% chlorine. However, above about 35 wt-% chlorine some CCl_2 groups were indicated, and the content of these groups appeared to increase with increasing chlorine content. The second assumption was that sulfonyl chloride groups which are present in chlorosulfonated polyethylenes and which are seen to influence neighboring groups differently than chlorine groups (Table III shows that there is a difference of +0.27 ppm for a neighboring SO_2Cl group over a neighboring Cl group) were sufficiently low in concentration to make essentially negligible influence on the quantitative measurements for sequence determination. This assumption is based on the fact that the sulfur content of chlorosulfonated polyethylenes is the order of only about 1.0 wt-% and from this level of sulfur content and a 35 wt-% content of chlorine there would be only one $CHSO_2Cl$ group, on the average, for every 120 methylene groups and 30 CHCl groups. Finally, the third assumption made was that the content of the three intervening methylene sequence which is one of the two assignments made for the line at 1.66 ppm is very low and in fact is low enough to show little interference in our sequence determination for chlorosulfonated polyethylenes containing chlorine contents of 35 wt-% and below. This assumption is justified on the basis that at 35 wt-% chlorine there is on the average, as indicated above, only one chlorine for every five carbons so that at lower chlorine contents there would be significantly more carbons for each chlorine. Also, 220 MHz spectra (see Fig. 1) showed no evidence for this three-methylene sequence group. Thus, the line at 1.66 ppm was included with the α-methylenes for our sequence determination. After taking into account the three assumptions described above, we measured the integrated intensities in the following manner for determining the chlorine distribution of chlorosulfonated polyethylenes. The three regions are defined as: I, 0.74–1.26 ppm; II, 1.26–1.50 ppm; and III, 1.50–2.65 ppm:

$$k\mathrm{I} = 2[\gamma(\text{or greater})\text{—}CH_2 \text{ groups}]$$

$$k\mathrm{II} = 2[\beta\text{—}CH_2 \text{ groups}]$$

$$k\mathrm{III} = 2[\alpha\text{—}CH_2 \text{ groups}]$$

where k is a proportionality constant including the solution concentration and instrument variables, and the terms inside the brackets are the mole fractions of α, β, and γ (or greater) methylene groups. Therefore, by integrating these three regions, we can relate the integrated areas to the mole fractions of the three kinds of methylene groups. From this measurement, we can determine the degree of blockiness for methylene groups in chlorosulfonated polyethylenes and as a result determine the chlorine distribution.

TABLE III
Comparison of NMR Data from Model Compounds Containing Chlorine and Sulfonyl Chloride Groups

Model compounds	Chemical shifts, ppm	Assignments
$CH_2ClCH_2CH_2Cl$	2.18	—CCl—CH_2—CCl—
$CH_2ClCH_2CH_2SO_2Cl$	2.45	—CCl—CH_2—CSO_2Cl—

RESULTS AND DISCUSSION

In Table IV, we list the five different chlorosulfonated polyethylene samples and the one chlorinated polyethylene sample examined, their method of preparation, their chlorine contents, and the NMR results obtained on them. These NMR results are given in terms of the mole fractions of α, β, and γ (or greater) methylene groups. Plots of the mole fractions of α, β, and γ (or greater) methylene groups against chlorine content are shown in Figure 2. The experimental points are shown as triangles in the plots for the samples analyzed by NMR. The theoretical curves shown in Figure 2 were calculated by the following equations which are based on the statistical treatment of Frensdorff and Ekiner.[14]

$$\text{Mole fraction of } \alpha\text{-}CH_2 = 1\text{-}\Gamma_{00}^2$$

$$\text{Mole fraction of } \beta\text{-}CH_2 = \Gamma_{00}^2\,(1\text{-}\Gamma_{00}^2)$$

$$\text{Mole fraction of } \gamma\text{-}CH_2 = \Gamma_{00}^4$$

TABLE IV
Methylene Group Distributions of Chlorosulfonated Polyethylenes

Sample	Method of preparation	Cl, wt-%	Mole fractions of methylene groups: α	β	γ (or greater)
A	Gaseous $SO_2 + Cl_2$	18	0.22	0.11	0.67
B	Gaseous $SO_2 + Cl_2$	25	0.28	0.14	0.59
C	Gaseous $SO_2 + Cl_2$	26	0.29	0.14	0.57
D	Gaseous $SO_2 + Cl_2$	35	0.42	0.16	0.42
E	Gaseous $SO_2 + Cl_2$	35	0.43	0.16	0.41
F	Gaseous Cl_2	42	0.62	0.16	0.22

The values of Γ_{00} used in the calculation of these curves have been taken from their work (Table IV;[14] hindered. case 1; random, case 4). The amount of hindrance in their hindered case is based on isomer distributions obtained from chlorination studies of a model compound, 2-chlorohexane.[16] Thus, the hindered-distribution case states that the chlorine substitution is not equally likely on all sites, but is hindered from being substituted on adjacent carbons along the polyethylene chain.

In Figure 2 the two theoretical curves are shown for each of the three kinds of methylene groups. The chlorine concentration range over which these curves are drawn in each plot is from 0 to about 45 wt-% chlorine. Of the

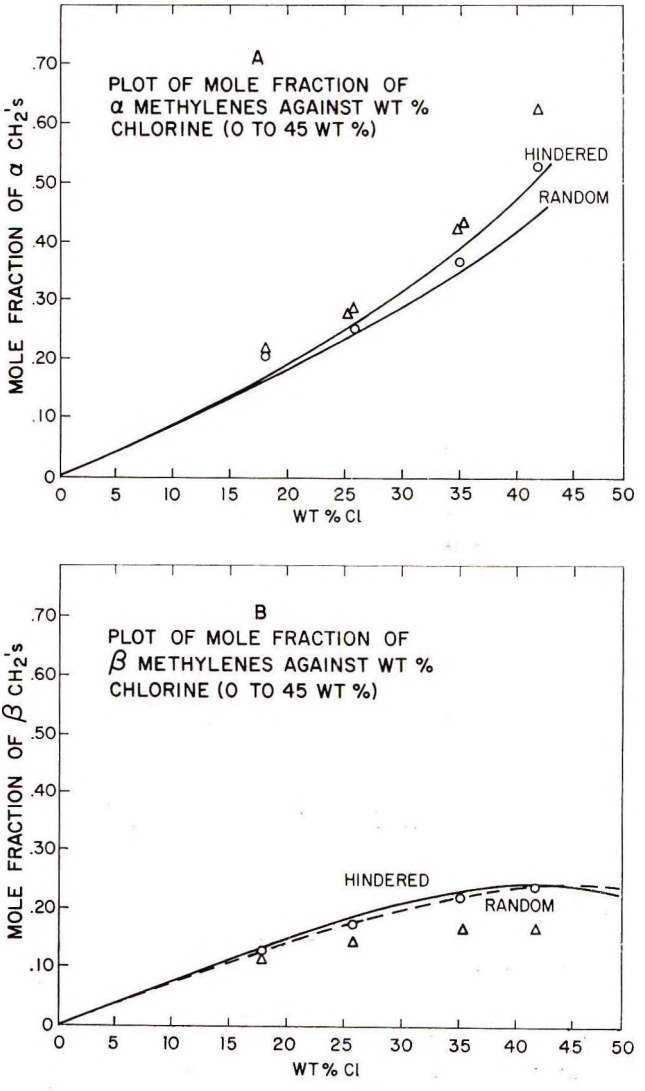

Fig. 2 (*continued*)

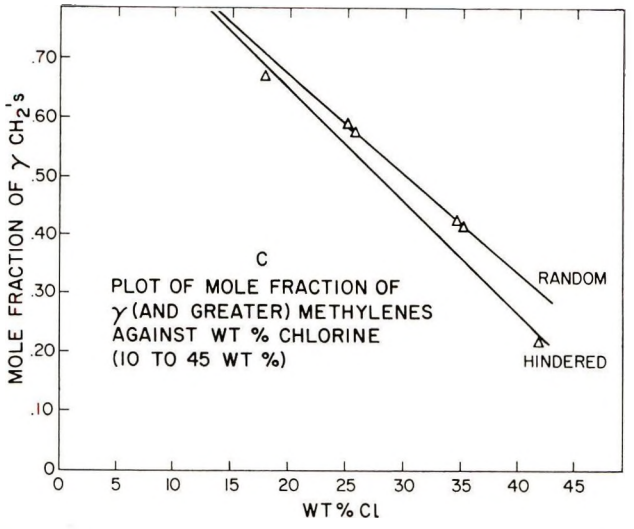

Fig. 2. The three plots of (*A*) α-methylenes, (*B*) β-methylenes, and (C) γ-methylenes show the theoretical curves for the cases of random and hindered chlorine distribution[14] as well as the NMR data experimentally obtained at 220 MHz on five chlorosulfonated polyethylenes and one chlorinated polyethylene prepared by the gaseous reaction: (△) experimental data; (○) corrected data.

three plots shown, the one that shows the largest difference between the random and hindered curves is the γ-methylene plot. At a chlorine concentration of 40 wt-% the difference is seen to be about 0.075 mole fraction of γ-methylenes. Meanwhile, at this same chlorine content the difference is seen to be about 0.05 mole fraction for α-methylenes and essentially zero for β-methylenes. At chlorine concentrations less than 40 wt-%, the difference between the two curves becomes smaller in all three plots. Even so, it is always seen to be larger in the γ-methylene plot than in the other two plots, while throughout this range of chlorine content from 0 to ~40-% the β-methylene plot shows very little difference between the two curves. Thus, based on these findings it is apparent that (1) the γ-methylene plot is the best one to use for determining the difference in chlorine distribution between the random and hindered cases and (2) the β-methylene plot is essentially useless for this determination.

Upon comparing the experimental data (triangles) obtained by NMR with the two theoretical curves in Figure 2, we find that the data fall off both curves in the plots of α- and β-methylenes but that the data fit the random curve more closely than the hindered curve in the plot of γ-methylenes. In fact the data show a good match for the random curve in the plot of γ-methylenes except for the chlorinated polyethylene sample containing 42 wt-% chlorine. Knowing from above that the γ-methylene plot is the best one to use in determining the chlorine distribution in chlorosulfonated polyethylenes we can then say that because of the good fit observed in Figure 2C between the experimental data and the random curve

the chlorine distribution in chlorosulfonated polyethylenes is random. The one sample of chlorinated polyethylene examined, however, showed its γ-methylene content to fit the hindered curve rather than the random curve. Now upon comparing the experimental data (triangles) for the six samples examined with both curves in the α-methylene and β-methylene plots (Figs. 2*A* and 2*B*) we see that the data do not fit either curve. In fact the data are higher than both curves in the α-methylene plot and are correspondingly lower than both curves in the β-methylene plot. This lack of fit between the experimental data and the theoretical curves for the α- and β-methylene plots is probably attributable to the NMR measurement rather than to the theoretical predictions because of the difference in the NMR measurement between the line due to the γ-methylene groups and the lines due to the α- and β-groups. The γ-methylene groups show only a relatively narrow line at 1.25 ppm, whereas the α-methylene groups show a set of both broad and complex lines in the range from 2.19 to 1.66 ppm, and the β-methylene groups show a very broad and complex line at 1.44 ppm. Thus, it appears possible that because of the greater complexity of the lines due to the α- and β-methylenes we are not as accurate in measuring their areas as we are in measuring the area of the relatively narrow line due to the γ-methylenes. In order to correct for this inaccuracy and to provide a better basis for comparing the experimental data with the two theoretical curves in Figure 2*A* for the α-methylenes we shifted the experimental data in the β-methylene plot to have these data fit the random curve. The data that have been shifted are represented as circles in Figure 2*B*. Because the difference between the two theoretical curves is essentially zero in the β-methylene plot over the chlorine concentration range of 0 to about 45 wt-% it is not critical which curve is actually used for fitting the experimental points. Then, following this correction we can proceed to make a correction in the α-methylene plot (Fig. 2*A*) for their experimentally determined points. However, the correction that we can make in the α-methylene plot is not arbitrary but is restricted to the amount made in the β-methylene plot as the total methylene count which includes α-, β-, and γ-methylene groups cannot exceed the mole fraction of unity. That correction is shown in Figure 2*A* with the corrected points given as circles. After making the corrections indicated we see that the fit in Figure 2*A* between the corrected points and the two theoretical curves is essentially the same as that shown in the γ-methylene plot. Both sets of data generally show a good fit with the random curve than with the hindered curve except for the 42 wt-% chlorine sample. It shows a better fit with the hindered curve in the α-methylene plot as it does in the γ-methylene plot.

From the NMR results obtained at 220 MHz and from their comparison with the theoretical curves in Figure 2, we see that chlorosulfonated polyethylenes prepared by the gaseous reaction process have a random chlorine distribution as opposed to a hindered chlorine distribution. For the chlorinated polyethylene sample containing 42 wt-% chlorine and prepared by the gaseous reaction with chlorine we see that the NMR data indicates

it to have a hindered chlorine distribution. The explanation for this difference between the chlorinated polyethylene and the chlorosulfonated polyethylenes is not apparent at this time. More studies need to be done to reveal the cause of this difference. Nevertheless, the NMR results show very clearly that 220 MHz NMR can be used effectively to determine the nature of the chlorine distribution in chlorosulfonated and chlorinated polyethylenes. Even a single NMR measurement when plotted on these graphs in Figure 2 following the above indicated correction can suggest the kind of distribution present in that sample of chlorosulfonated polyethylene. In the plot of Figure 2*C* it is seen that for a given chlorine content the higher the γ-methylene content the more blocky and the less regular is the chlorine distribution. On the other hand, the lower the γ-methylene content the less blocky but the more regular is the chlorine distribution. The reverse of this is the case for the α-methylene plot.

We wish to thank Dr. R. W. Keown for supplying the samples studied and Mr. V. A. Brown for prepairng them for the NMR examination and for running them at 100 MHz. We further wish to express our thanks for the help of H. K. Frensdorff in developing the theoretical relationships included in the text.

References

1. F. A. Bovey, E. W. Anderson, D. C. Douglas, and J. A. Mason, *J. Chem. Phys.*, **39**, 1199 (1963).
2. K. C. Ramey, *J. Phys. Chem.*, **70**, 2525 (1966).
3. F. A. Bovey, F. P. Hood, E. W. Anderson, and R. L. Kornegay, *J. Phys. Chem.*, **71**, 312 (1967).
4. F. Heatley and F. A. Bovey, *Macromolecules*, **2**, 241 (1969).
5. L. Cavalli, G. C. Borsini, G. Carraro, and G. Confalonieri, *J. Polym. Sci. A-1*, **8**, 801 (1970).
6. K. Okuda, *J. Polym. Sci. A*, **2**, 1749 (1964).
7. R. Chujo, S. Satoh, and E. Nagai, *J. Polym. Sci. A*, **2**, 895, (1964).
8. J. L. McClanahan and S. A. Previtera, *J. Polym. Sci. A*, **3**, 3919 (1965).
9. J. Schaefer, *J. Phys. Chem.*, **70**, 1975 (1966).
10. F. Fischer, J. B. Kinsinger, and C. W. Wilson, III. *J. Polym. Sci. B*, **4**, 379 (1966).
11. Y. Yamashita, K. Ito, S. Ikuma, and H. Koda, *J. Polym. Sci. B*, **6**, 219 (1968).
12. K. Ito and Y. Yamashita, *J. Polym. Sci. B*, **6**, 227 (1968).
13. C. E. Wilkes, J. C. Westfahl, and R. H. Backderf, *J. Polym. Sci. A-1*, **7**, 23 (1969).
14. H. K. Frensdorff and O. Ekiner, *J. Polym. Sci. A-1*, **5**, 1157 (1967).
15. J. J. Verbanc and R. G. Arnold, *Fatipec*, **1957**, 289.
16. N. Colebourne and E. S. Stern, *J. Chem. Soc.*, **1965**, 3599.

Received November 20, 1970
Revised February 15, 1971

JOURNAL OF POLYMER SCIENCE: PART A-1 VOL. 9, 2063–2070 (1971)

Oxidative Crosslinking in Poly(ethylene Terephthalate) at Elevated Temperatures*

D. L. NEALY and L. JANE ADAMS,
Research Laboratories, Tennessee Eastman Company, Division of Eastman Kodak Company, Kingsport, Tennessee 37662

Synopsis

Poly(ethylene terephthalate) oxidizes on being heated in air at elevated temperatures to form a crosslinked structure. The crosslinking occurs through a reaction which causes arylation of terephthalate rings to form a biphenyltricarboxylic acid derivative. This reaction is interpreted as a free-radical cleavage generating a substituted phenyl radical which selectively attaches to a terephthalate residue via substitution.

INTRODUCTION

Several papers have been published on the oxidative degradation of poly(ethylene terephthalate) (PET) at elevated temperatures.[1–4] Most of the work has been concerned with the increase in color and carboxyl content and the decrease in inherent viscosity when oxygen is present during thermal degradation.[1–3] Buxbaum exposed model compounds to oxidative degradation and determined the products formed,[1] and Kovarskaya et al. examined the volatile products of thermooxidative degradation.[4] Both proposed mechanisms for oxidation of the aliphatic portion of PET. The articles referred to above give no indication of oxidative crosslinking. Preliminary experiments with thermooxidatively degraded PET showed evidence of crosslinking (i.e., gels in hexafluoroisopropanol). Therefore, we undertook an experimental program to elucidate the chemistry of the crosslinking reaction. We oxidized the PET in air at high temperatures and analyzed the degraded polymer to determine possible crosslinking species. PET may be exposed to such conditions during extrusion of fibers, films, and molded articles in air.

EXPERIMENTAL

Oxidation of PET in Air at 300°C

The PET used had an inherent viscosity of 0.59 (60:40 phenol–tetrachloroethane) and a number-average molecular weight of 17,500. The polymer was made with a Zn (65 ppm)–Sb (230 ppm) catalyst system.

* Presented at the Southeastern Regional Meeting of the American Chemical Society, Richmond, Virginia, November 5–8, 1969.

PET granules were dried in a vacuum oven at ca. 100°C for 4 hr. Films (ca. 6 mil) of the dry polymer were pressed at 270°C for 15 sec on a Hannifan pneumatic press, then placed on Teflon resin sheeting in an aluminum weighing dish of 3 in. diameter. The films were heated in air in a muffle furnace for various times (1–15 hr) at 300°C, then removed, cooled in air, and characterized as follows.

Gel Formation

A sample (ca. 0.5 g) of the polymer was treated with hexafluoroisopropanol (ca. 5 ml) to determine if it dissolved or formed a gel. If the polymer formed a gel, it was considered crosslinked.

Methanolysis of PET

Samples of polymer (ca. 0.5 g) were placed in 7-oz beverage bottles. Then 50 ml of Eastman spectrograde methanol and approximately 3 drops of a 0.69% (w/v) alcoholic solution of titanium tetraisopropoxide were added to each bottle. The bottles and contents were weighed, purged with nitrogen, and sealed by a beverage bottle capper with crown caps lined with two layers of Teflon resin sheet. The bottles were then placed in an autoclave containing methanol (to equalize the pressure), heated at 200°C for 6 hr under autogenous pressure, then cooled to room temperature. The bottles and contents were then reweighed to ascertain if leakage had occurred. If so, the sample was discarded. Each sample was transferred to a 100-ml three-necked flask, and the methanol was removed under vacuum at a temperature below 50°C. The residue was then dissolved in chloroform (5–10 ml), and the solution was analyzed by gas chromatography.

Gas Chromatographic Analysis

The gas chromatographic analyses were done on an F & M Model 5750 gas chromatograph with thermal conductivity detector. The column used was 6 ft long × $^1/_4$ in. in ID and consisted of 10% Apiezon L oil on Chromosorb W(AW) solid support. The oven temperature was programmed at a rate of 10°C/min from 200 to 300°C, and the gas flow rate was 80 ml/min. The column was held at 300°C after programming until all components had been eluted. The peak areas were measured with a planimeter, and the percentages were calculated relative to the dimethyl terephthalate area. Untreated PET or PET heated in the absence of air showed only two major components, ethylene glycol and dimethyl terephthalate, in the gas chromatographic analysis of the methanolyzed products.

Identification of Unknown Compound From Methanolysis of Oxidized PET

The unknown component found by gas chromatography was identified by mass spectrometric, infrared, and NMR analyses and by synthesis. The mass spectrometric analyses were run on a Bell and Howell CEC Model

21-110B mass spectrometer, the infrared analyses were done on a Perkin-Elmer Model 421 spectrophotometer, and the NMR analyses were made on a Varian Model HA-100 NMR spectrometer.

The mass spectrum contained intense peaks at m/e values of 329 (15%), 328 (92%), 298 (19%), 297 (100%), and 253 (20%). The infrared spectrum contained the following prominent absorption bands: 1720, 1728, 1607, 1430, 1306, 1275, 1245, 1235, 1185, 1106, 1087, 1030, 755, 749 and 698 cm^{-1}. The NMR spectrum showed single peaks at 3.25 (3H), 3.53 (3H), and 3.56 (3H), ppm, an aromatic doublet containing two hydrogens at 7.12 ppm, a doublet at 7.68 (2H) ppm, and a complex region containing three aromatic protons centered at 7.96 ppm.

Preparation of 2,4′,5-Trimethylbiphenyl

The procedure used was similar to that described by Gomberg and Bachmann[5] for preparation of 4-bromobiphenyl. *p*-Toluidine (53.6 g, 0.5 mole) was weighed into a 1-l. Erlenmeyer flask and 40 ml of distilled water was added. Then 100 ml of concentrated hydrochloric acid was added slowly with mechanical stirring. The resulting solution of the *p*-toluidine hydrochloride was then placed in an ice bath and cooled to 0–5°C. Over a period of 1 hr, a solution of 36 g of sodium nitrite in 72 ml of water was poured slowly, with stirring, into a flask containing the *p*-toluidine hydrochloride while maintaining the temperature at 0–5°C. The solution was stirred for an additional 2 hr at this temperature. The diazotized solution was then poured into a 2-l., three-necked, round-bottomed flask in an ice bath. To this solution 650 ml of ice-cold *p*-xylene was added. Approximately 350 ml of pentane was added as a solvent for the *p*-xylene, which is a solid at this temperature. Then 116 g of 5*N* sodium hydroxide solution was added dropwise to the cold solution (0–5°C), which was stirred vigorously during the reaction. To ensure completion of the reaction, the solution was allowed to stir for 6 hr after addition of the sodium hydroxide solution. The mixture was allowed to warm to room temperature, and the organic phase was then separated from the aqueous phase. The organic phase was washed once with 500 ml of 5*N* hydrochloric acid solution and then distilled through a 1 × 7-in. Vigreux column. The fraction boiling from 80 to 140°C (2 mm) was further purified by preparative gas chromatography on a 10% Apiezon L oil on Chromosorb W(AW) column. Analyses of the collected material by mass spectrometry and NMR confirmed the structure as 2,4′,5-trimethylbiphenyl. The mass spectrum contained strong peaks at m/e values of 197 (17%), 196 (100%), 195 (17%), 181 (61%), 166 (20%), and 165 (34%). The NMR spectrum showed single peaks at 2.18 (3H), 2.27 (3H), and 2.32 (3H) ppm; four aromatic hydrogens at 7.14 ppm; and a multiplet containing three aromatic hydrogens centered at 7.0 ppm. The infrared spectrum showed the following absorption bands: 3010, 2920, 2860, 1606, 1510, 1490, 1445, 1373, 1175, 1130, 1100, 1032, 1015, 815, 805, 745, 579, and 535 cm^{-1}.

Preparation of 2,4′,5-Biphenyltricarboxylic Acid

The procedure followed was that of Friedman et al.[6] 2,4′,5-Trimethylbiphenyl (0.3 g) was placed in a thick-walled glass tube, and sodium dichromate dihydrate (2.32 g) and water (5 ml) were added. The tube was sealed under nitrogen, and the reaction mixture was heated in an autoclave at 270°C for 4 hr. The mixture was then cooled and filtered. The filtrate was then made slightly acidic with 5*N* hydrochloric acid to precipitate the biphenyltricarboxylic acid. The product was collected on a filter, rinsed with water, and air dried. The yield was 0.27 g (60%); the mp was above 313°C (poorly defined). The structure was confirmed by infrared and mass spectrometry. The mass spectrum contained strong peaks at *m/e* values of 286 (100%), 285 (26%), 269 (46%), 268 (19%) 242 (17%), and 152 (15%). The infrared spectrum showed absorption bands as follows: 1690, 1608, 1405 1285, 1237, 780, and 745 cm^{-1} and a broad band from 3100 to 2800 cm^{-1}.

Preparation of Trimethyl 2,4′,5-Biphenyltricarboxylate

An ethereal solution of diazomethane was prepared by the method of Moore and Reed.[7] 2,4′,5-Biphenyltricarboxylic acid (0.23 g) was placed in a beaker containing 20 ml of anhydrous ether. The diazomethane-ether solution (40 ml) was added and the mixture was allowed to stand until most of the solid had dissolved. Evaporation of the filtered ether solution yielded 0.21 g (79%) of crystals of trimethyl 2,4′,5-biphenyltricarboxylate, mp 105–108°C.

ANAL. Calcd for $C_{18}H_{16}O_6$: C, 65.85%; H, 4.88%. Found C, 65.98%; H, 4.96%.

The infrared, NMR, and mass spectra of this compound were identical to those of the unknown component isolated from the methanaolyzed products from thermal oxidation of PET.

DISCUSSION

PET films heated in air at 300°C showed considerable crosslinking, as evidenced by gels in hexafluoroisopropanol. These crosslinked polymer samples were depolymerized in excess methanol at 200°C and then analyzed by

TABLE I
Area Percentages of Unknown Present in PET Heated in Air at 300°C for Various Times

Heating time, hr	Unknown, area %[a]
1.0	1.18
3.0	3.98
5.0	4.90
7.25	5.23
15.0	7.81

[a] Relative to dimethyl terephthalate.

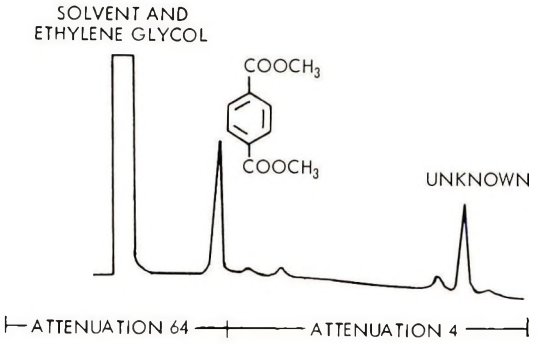

Fig. 1. Gas chromatogram of methanolyzed and degraded PET.

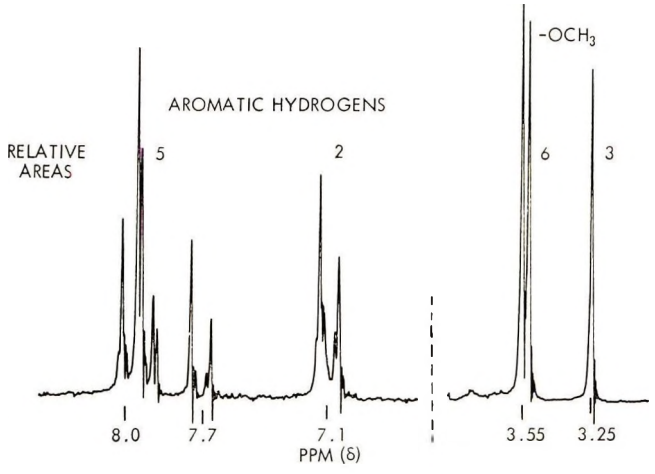

Fig. 2. HA-100 NMR spectrum of unknown.

gas chromatography. A gas chromatogram of methanolized PET showed one major component other than the expected dimethyl terephthalate and ethylene glycol, as shown in Figure 1. This component was present in various amounts relative to the original dimethyl terephthalate, depending on time of heating. The results listed in Table I indicate the relative amounts of unknown material generated upon heating for different times. A sample of the unknown component was isolated by gas chromatography and analyzed by mass spectrometry and infrared spectroscopy. The mass spectrogram showed the presence of OCH_3 groups, gave a molecular ion peak at 328 mass units, and indicated a probable molecular formula of $C_{18}H_{16}O_6$. The infrared spectrum showed characteristic ester carbonyl and C—O stretch absorptions at 1735 cm^{-1} (5.75μ) and 1275 cm^{-1} (7.85μ), respectively. An NMR spectrum of the unknown component is shown in Figure 2. The spectrum indicates two types of hydrogens (aromatic and OCH_3) in a 7:9 ratio, with two of the aromatic hydrogens and one of the methoxyl groups at higher magnetic fields. The mass spectrometric, in-

frared, and NMR data indicated that the unknown component had the structure I.

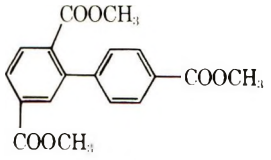

I

The NMR signal of the methyl ester group *ortho* to the biphenyl linkage would be expected to occur at a higher magnetic field because of the shielding of the second aromatic ring in the expected nonplanar conformation of this hindered biphenyl system.

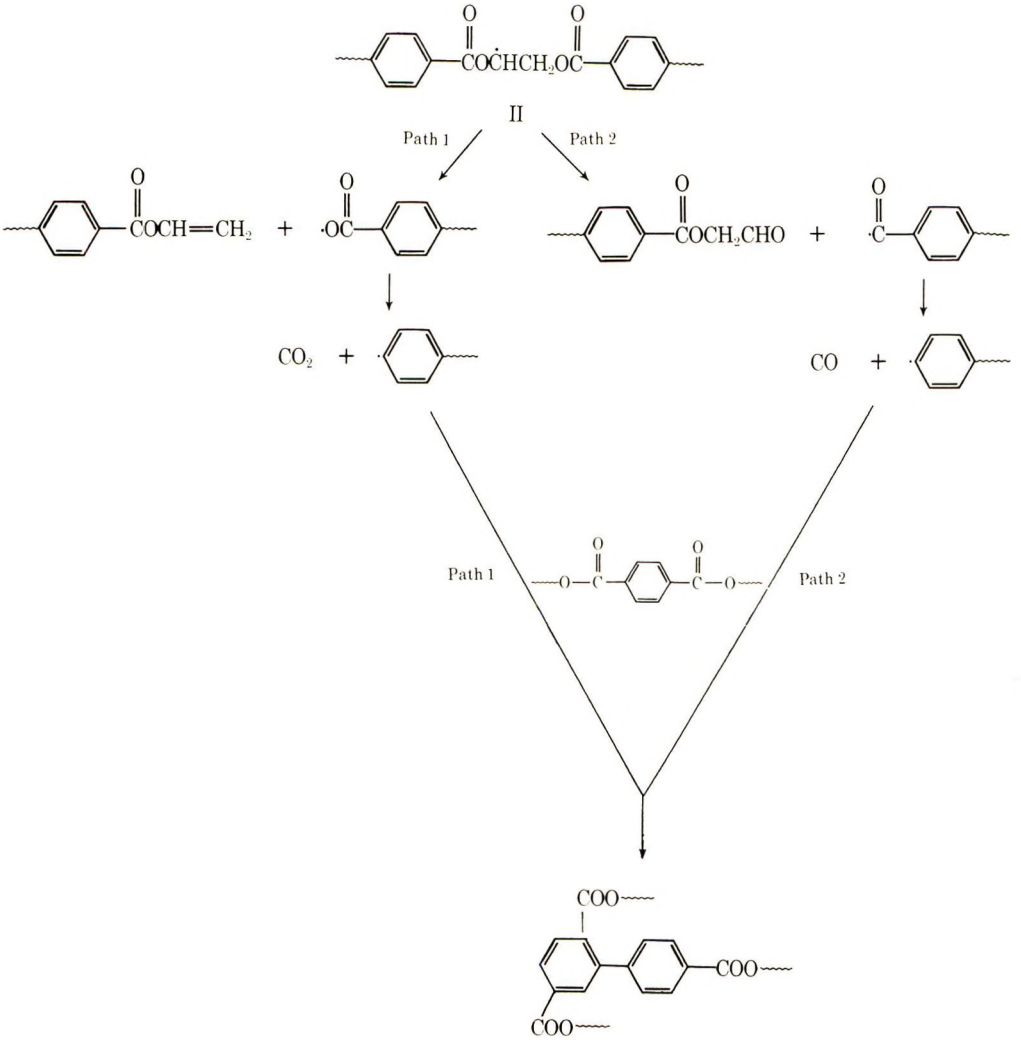

This triester was synthesized for confirmation of structure. The steps in the synthesis are outlined in the Experimental Section. *p*-Toluidine was diazotized and coupled with *p*-xylene to form 2,4′,5-trimethylbiphenyl. The trimethylbiphenyl was then oxidized to the corresponding acid by heating in a sodium dichromate dihydrate-water solution at 270°C. The methyl ester was prepared by treating the triacid with diazomethane. Gas chromatographic, mass spectrometric, and NMR analyses of the synthesized compound confirmed that it was indeed identical to the unknown product from oxidation of PET. We concluded that this arylation product is responsible for oxidative crosslinking in poly(ethylene terephthalate) at elevated temperatures.*

The following two possible mechanisms by which the biaryl derivative may be formed. Initially there is oxidative hydrogen abstraction from the methylene groups to generate the radical II, which then may react by two paths. Both mechanisms involve the generation of an alkyl radical which then cleaves by one of two pathways to produce a *p*-substituted phenyl radical. The phenyl radical can then attack a terephthalate ring to form a biphenyl derivative. These two mechanisms for the formation of phenyl radicals are similar to those suggested by Marcotte et al.[9] in connection with work on the irradiation of PET. A preference for path 2 is supported by the work of Kovarskaya et al.,[4] who showed that much more carbon monoxide than carbon dioxide is generated in oxidative degradation of PET. One might expect that, if these mechanisms or any mechanism involving a phenyl radical were operative, benzoate derivatives would be generated by hydrogen abstraction by the substituted phenyl radical. However, no methyl benzoate was detected in the methanolyzed samples. Also, the volatile products were trapped when PET was heated in air at 300°C, but mass spectrometric and gas chromatographic analyses of the condensate revealed none of the expected benzoate derivatives. Apparently, the phenyl radical attacks the aromatic ring with high selectivity. This result is consistent with work of Inukai et al.[10] in the phenylation of anisole with aromatic diazo compounds. Their results showed that only 15.4% of the phenyl radicals abstracted hydrogen from anisole, even though a large excess of the OCH_3 hydrogens was available for extraction.

The authors thank J. C. Gilland, Jr., and J. T. Dougherty, who contributed significantly to this research through their analysis and interpretation of the mass spectrometric and NMR data.

References

1. L. H. Buxbaum, paper presented to American Chemical Society, Division of Polymer Chemistry, 1967; *Polym. Preprints*, **8**, p. 552 (1967).

2. L. H. Buxbaum, *Angew. Chem., Int. Ed.*, **7**, 182 (1968).

3. N. H. Mikhailov, L. G. Tokareva, K. K. Buravchenko, G. M. Terekhova, and P. A. Kirpchnikov, *Vysokomol. Soedin.*, **4**, 1186 (1962); *Chem. Abstr.*, **59**, 813c (1963).

* Since submission of our paper, Yoda and co-workers[8] have proposed an alternative mechanism for crosslinking through a 1,2,4-butanetriol species.

4. B. M. Kovarskaya, I. I. Levantovskaya, A. B. Blyumenfel'd, and G. V. Dralyuk, *Sov. Plast.*, **1968**, 34 (May 1968).

5. M. Gomberg and W. E. Bachmann, in Organic Syntheses, Coll. Vol. I, H. Gilman, Ed., Wiley, New York, 1941, p. 113.

6. L. Friedman, D. C. Fishel, and H. Shechter, paper presented to American Chemical Society, Division of Petroleum Chemistry, 1964; *Preprints*, **9**, No. 4, D87–D93 (1964).

7. J. A. Moore and D. E. Reed, *Org. Syn.*, **41**, 16 (1961).

8. K. Yoda, A. Tsuboi, M. Wada, and R. Yamadera, *J. Appl. Polym. Sci.*, **14**, 2357 (1970).

9. F. B. Marcotte, D. Campbell, J. A. Cleveland, and D. T. Turner, *J. Polym. Sci. A-1*, **5**, 481 (1967).

10. T. Inukai, K. Kobayashi, and O. Simamura, *Bull. Chem. Soc. Japan*, **35**, 1576 (1962).

Received July 7, 1970
Revised March 1, 1971

NOTES

Photopolymerization of Tetrafluoroethylene to a Fusible Polymer

The gas phase polymerization of C_2F_4 (TFE) has been photosensitized by mercury at 2537 Å although c-C_3F_6 appeared to be the main product.[1] Polymerization of gaseous TFE has also been photochemically initiated in the presence of mercury bromide[2] and by Cl atoms produced by the photolysis of phosgene at 2537 Å.[3] Cohen and Heicklen reported c-C_3F_6 as the only product of the Hg-sensitized photolysis of TFE at pressures less than 60 torr.[4] Mercury-photosensitized oxidation of TFE in the presence of O_2 produced CF_2O and C_2F_4O as well as c-C_3F_6.[5] Some polymer was reported when TFE reacted with oxygen atoms produced by the Hg-photosensitized decomposition of N_2O.[6] Vogh has claimed that a white solid PTFE polymer is formed when TFE is photolyzed at 2537 Å in the presence of admixed N_2O.[7] Addition of O_2 in amounts up to 20 ppm appears to favor formation of PTFE during the photolysis of (TFE + O_2) mixtures at 1849 Å and 2537 Å,[8] although addition of larger amounts yielded primarily oxides and a solid whose infrared spectrum differed from that of PTFE by an adsorption band at 1040 cm^{-1}.[9] In a patent mainly concerned with production of CF_2 radicals in the singlet state, and their subsequent reaction with olefinic compounds to yield fluorinated three-membered rings, Mastrengelo has claimed that a polymer is produced during the direct photolysis (over the 2000–3000 Å region) of TFE at pressures about 380 torr.[10] It has also been reported that PTFE is one of the products produced from the Xe-photosensitized reaction of perfluorocyclobutane at 1470 Å,[11] and may be produced in the similar process with CF_4.[12]

The surface-photopolymerization of TFE in a vacuum system has been shown to yield continuous, adherent polymeric films on various substrates at monomer pressures less than 3 torr.[13] We wish to report now on the powdery, white polymer ("floc)" formed in the gas phase during the direct photolysis of TFE vapor at pressures ranging from about 10 torr to 760 torr. The polymer is subject to fusion at 330°C in air to a continuous, transparent deposit.

Tetrafluoroethylene from a cylinder (Peninsular Chemical Research Inc., Gainesville, Florida) was purified from inhibitor by bulb-to-bulb distillations. It was introduced at various pressures through metal valves to a deposition system pre-evacuated to a few

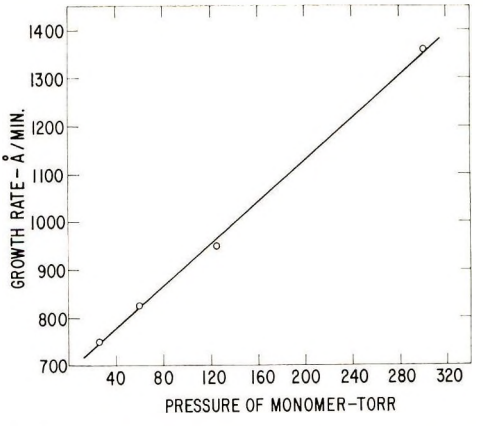

Fig. 1. "Floc" growth from TFE vs. monomer pressure.

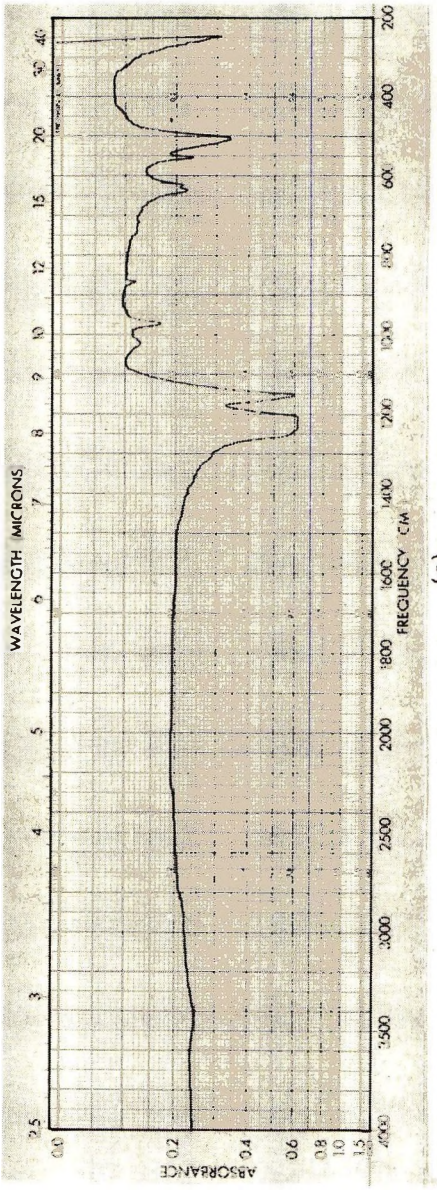
WAVELENGTH MICRONS
ABSORBANCE
FREQUENCY CM
(a)

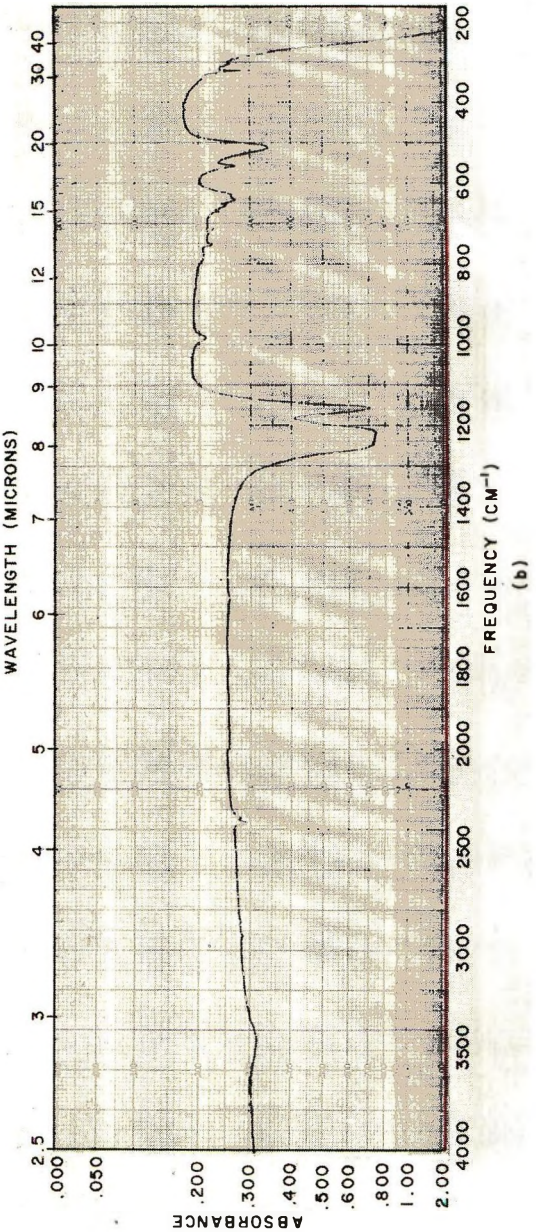
WAVELENGTH (MICRONS)
ABSORBANCE
FREQUENCY (CM⁻¹)
(b)

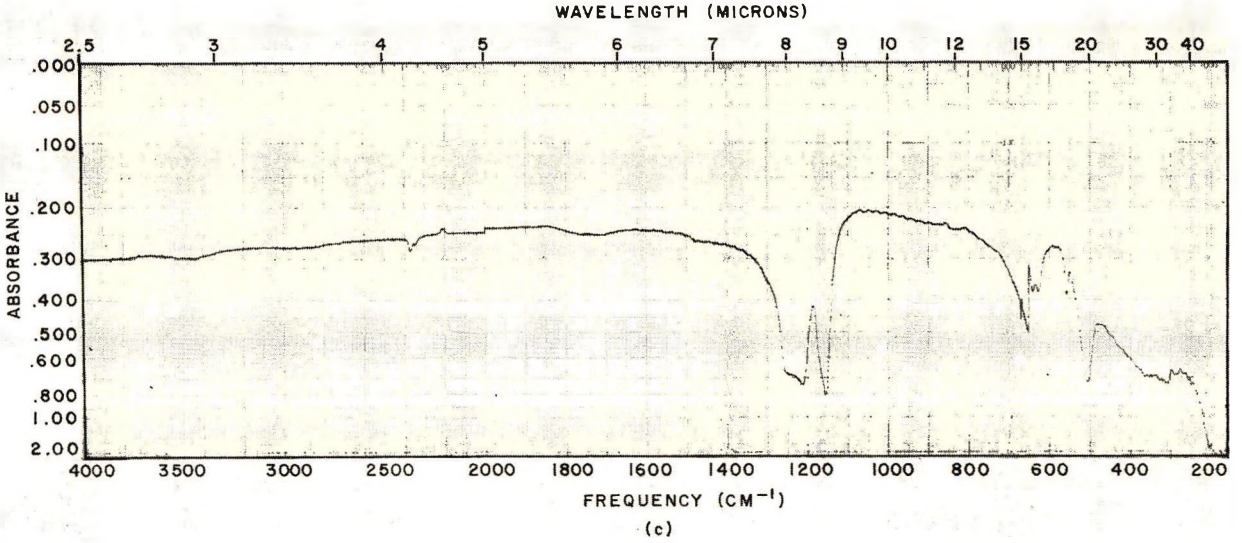

Fig. 2. (a) IR absorption spectra of TFE "floc" formed at 300 torr, 7.07 mg/g KBr. (b) IR absorption spectra of commercial Teflon (FEP) TL-120 powder in KBr. (*c*) IR absorption spectra of commercial Teflon (PTFE) #6 powder in KBr.

microns. Substrates such as evaporated aluminum on 1 × 3-in. microscope slides or aluminum coupons of similar dimensions were irradiated in the presence of monomer gas with the full output of a 700 watt Hanovia lamp (model No. 674A), which emitted about 17 watts over the wavelength region 1849 to 2400 Å. The lamp was positioned 5 cm above a 8 × 20 cm quartz (GE 151) window which permitted passage of low wavelength UV light into the reactor. The total distance between lamp and substrate surfaces was about 8 cm. Unlike the surface-photopolymerization process wherein film deposition is restricted to irradiated surfaces,[13] the polymer "floc" was deposited on all internal surfaces of the reactor. Mass deposition rates on the substrates were determined by before and after weighings on a Satorius balance. The thickness of the fused "floc" material was also measured by capacitance techniques with a mercury drop counterelectrode.

The dependence of "floc" growth rate on TFE monomer pressure is shown in Figure 1. Even at the lowest pressure essentially all the actinic radiation was absorbed in the gas

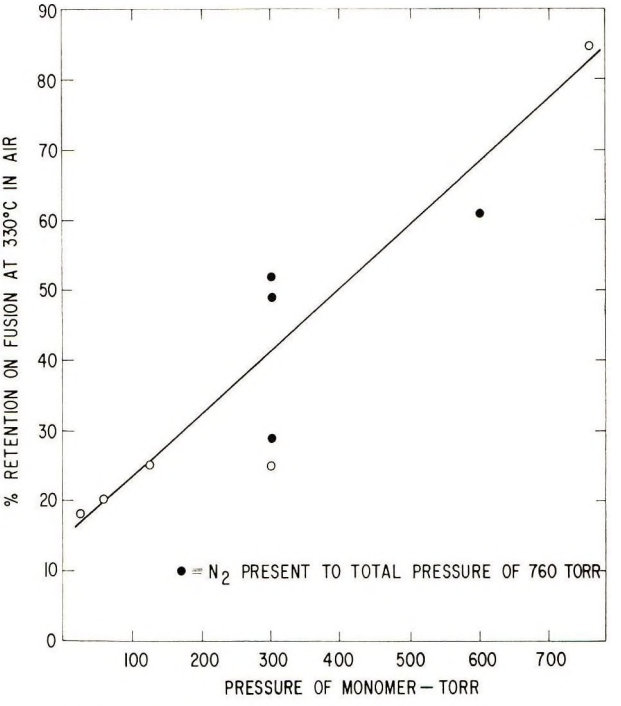

Fig. 3. Fusion of TFE "floc" as function of monomer pressure.

phase under the described experimental conditions. Thickness of the polymeric deposits was inferred from a constant value for the density. Irradiations were of 35 to 135 min duration. The reaction was "flushed" by evacuation every 10 min to ~1 torr and then refilled to the required monomer pressure. Although most depositions were at substrate temperatures near 25°C, variations in temperature from 0 to 200°C did not seem to have pronounced effects on the growth rate. With the experimental geometry outlined above, "floc" deposition was measurable at monomer pressure as low as 8 torr with no contribution from the continuous film-forming surface process which dominates[13] at lower pressures. Addition of gaseous nitrogen to a total reactor pressure of 760 torr had no significant effect on the "floc" growth rate at monomer pressures of 300 torr. No "floc" could be detected after 30 min irradiation through a 0.312-cm thick Corning filter No. CS7-54-(9863) which passed UV light with at least 27% transmission down to wavelengths about

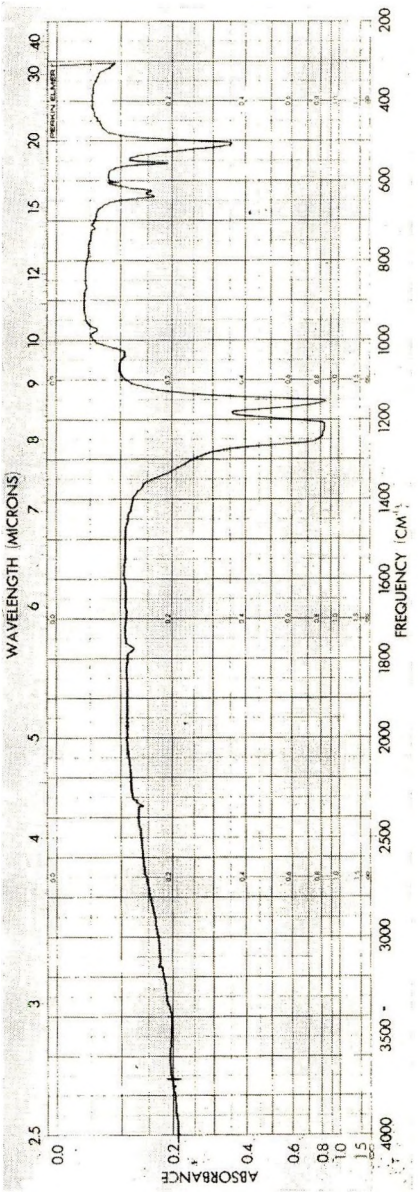

Fig. 4. IR absorption spectra of TFE "floc" formed at (200 torr TFE + 480 torr air), 4.58 mg/g KBr.

2400 Å. The direct photolysis requires then absorption of light at or very near the nonbonded continuum[14] associated with dissociation of TFE at 2150 Å.

As illustrated in Figure 2, the "floc" formed from gas phase photolysis of TFE showed considerable infrared absorption at 980 cm^{-1}. In this respect, it differs from the PTFE form of Teflon (Fig. 2) but resembles the films surface-photopolymerized directly from TFE at lower pressures.[13] This absorption is found in the FEP form of Teflon (Fig. 2) and may be associated with the presence of either CF_3 groups, or of cyclic fluorocarbons.[15] For "floc" produced at TFE pressures $\leq$300 torr both KBr pellet and multiple reflection infrared studies indicated that this absorption peak tended to disappear on fusion in air at 330°C.

The percentage retention of the "floc" on fusion at 330°C in air is a strong function of the monomer pressure during deposition as illustrated in Figure 3. Again, the presence of added nitrogen to a total deposition pressure of 760 torr had no appreciable effect on the process.

Unlike the surface-photopolymerized films,[13] the "floc" showed evidence for first-order transitions at 20–30°C on DSC. X-ray analyses gave *d*-values of 4.954 to 4.965. These were slightly decreased (4.929–4.939) for deposition in the presence of nitrogen, but still appeared to be between the values measured for PTFE-Teflon #6 and FEP Teflon, 4.904 and 4.983, respectively. Thermal gravimetric analyses indicated that the fused "floc" closely resembled PTFE in thermal stability, e.g., no rapid weight loss in air until about 500°C.

Although the fusion process to a clear coating of high temperature stability is not understood, it may be a consequence of the particle size and molecular weight (thermal stability) of the polymer formed in the photopolymerization process, which is in turn controllable by the monomer pressure during deposition of the "floc." The fusion is also accompanied by adhesive as well as cohesive forces. For example, glass microscope slides coated (300 torr TFE + 440 torr N_2) with about 5μ of "floc," placed together with the polymer layers intermediate to form a lap joint with one square inch of overlap, and then heated for 100 min to 330°C under a load of 7 oz./in.^{2} showed Instron shear strengths somewhat greater than 50 lbs./in.^{2}.[16]

The presence of even air did not seem to appreciably affect the "floc" deposition process, e.g., the deposition rate from a mixture of (200 torr TFE + 480 torr air) was comparable to that from 200 torr TFE alone, and the infrared absorption spectra (Fig. 4), per cent retention on fusion, and thermal properties of the "floc" were not greatly changed.

Mechanistic studies on this photopolymerization process will be reported. It may be noted that Dacey and Littler have recently indicated that, in addition to C_2F_6, C_2F_2, c-C_4F_8, c-C_3F_6, C_3F_6, and C_3F_8, some "high molecular weight product" is produced during photolysis of C_2F_4 at 1849 Å.[17] The quantum yield of all products depended on the TFE pressure, with the polymeric material showing a relative *decrease* in yield as the pressure was increased to about 1 torr.

We thank W. R. Burgess, C. O. Kunz, and D. H. Maylotte for assistance during this work.

References

1. B. Atkinson, *Nature*, **163**, 291 (1949); *J. Chem. Soc.*, 2684 (1952).
2. B. Atkinson, *Experimentia*, **14**, 272(1958).
3. D. G. Marsh and J. Heicklen, *J. Am. Chem. Soc.*, **88**, 269 (1966).
4. N. Cohen and J. Heicklen, *J. Chem. Phys.*, **43**, 871 (1965).
5. J. Heicklen and V. Knight, *J. Phys. Chem.*, **70**, 3901 (1966).
6. D. Saunders and J. Heicklen, *J. Phys. Chem.*, **70**, 1950 (1966); J. Heicklen and V. Knight, *J. Phys. Chem.*, **70**, 3893 (1966).
7. J. W. Vogh, U.S. Patent 3,228,865, Jan. 11, 1966.
8. F. Gozzo and G. Camaggi, *Tetrahedron*, **22**, 2181 (1966).

9. F. Gozzo and G. Carraro, U.S. Patent 3,392,097, July 9, 1968.
10. S. V. R. Mastrengelo, U.S. Patent 3,228,864, Jan. 11, 1966.
11. J. E. Davenport and G. H. Miller, *J. Phys. Chem.*, **73,** 809 (1969).
12. J. R. Dacey and J. W. Hodgins, *Can. J. Res.*, **B28,** 173 (1950).
13. A. N. Wright, *Nature*, **215,** 953 (1967).
14. J. R. Lacker, L. E. Hammel, E. F. Bohnfalk, and J. D. Park, *J. Am. Chem. Soc.*, **72,** 5486 (1950).
15. D. G. Weiblin, in *Fluorine Chemistry*, (J. H. Simons, Ed.), Academic Press, N.Y., 1954, p.449.
16. V. J. Mimeault and A. N. Wright, unpublished results.
17. J. R. Dacey and J. G. F. Littler, *Can. J. Chem.*, **47,** 3871 (1969).

E. V. Wilkus

General Electric Company
Wire & Cable Department
Bridgeport, Connecticut

A. N. Wright

General Electric Company
Research & Development Center
Schenectady, New York

Received September 1, 1970
Revised November 5, 1970

Polymerization of the N-*Carboxy Anhydrides of Alloisoleucine**

We have been investigating some unusual kinetic features of *N*-carboxyamino acid anhydride (4-substituted 2,5-oxazolidinedione, NCA) polymerizations. The polymerization of γ-benzylglutamate NCA, for example, exhibited unusual rate curves which produced two straight lines when plots of the log of the fractional conversion versus time were made.[1,2] This indicated to the investigators that a two-stage first-order reaction had occurred. In addition, because α-amino acid NCAs contain an asymmetric carbon atom (with the exception of glycine NCA), the copolymerization of enantiomers was possible. It was found that the rate constants decreased when a D-monomer was added to an L-monomer, and reached a minimum at the racemic composition.

These results were rationalized on the basis of a conformational transition from random coil to α-helix with the assumption that a growing random coil will add NCA at a rate different from that of an α-helix. The occurrence of the second stage of a two-stage propagation was believed concomitant with the polyamino acid reaching a sufficient length to stabilize an α-helix. Furthermore, since the rate constants were determined as a function of the D/L ratio for γ-benzylglutamate and were found to decrease to a minimum at the racemic composition, it was assumed that inclusion of optical "impurities" into the polymer chain decreased the possibility of the formation of α-helices and thereby the rate.

We have recently reinvestigated the polymerization of γ-benzylglutamate NCA but our results could not be rationalized on the basis of coil–helix transitions.[3] Our evidence indicated that a solubility phenomenon and not a conformational transition was responsible for the two-stage rate curve.

The present study was undertaken to reinvestigate both the unusual kinetic behavior of NCA polymerizations and the copolymerization of optical isomers. Isoleucine NCA was chosen as monomer for two reasons: it has two asymmetric carbon atoms which permit the copolymerization of diastereomers as well as enantiomers, and polyisoleucine is a β-substituted polyamino acid which for steric reasons cannot form α-helices.[4,5]

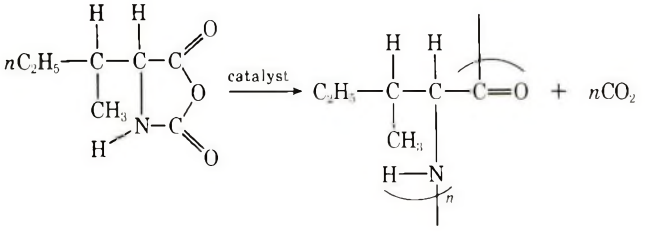

EXPERIMENTAL

Preparation of Materials

Monomers. The NCAs of alloisoleucine were prepared by the established procedure of bubbling phosgene through a dioxane suspension of the amino acid.[6] The NCAs were recrystallized from ethyl acetate–hexane. The recrystallized monomer was sublimed to remove any traces of chloride, stored at 10°C, and then resublimed immediately before use.

Solvents. Dioxane was refluxed with 10% 1*M* HCl for 12 hr prior to the addition of KOH. The dioxane was separated from the two layers which formed and more KOH was added. After 12 hr the dioxane was decanted onto sodium from which it was distilled immediately before use.

* Presented to the International Symposium on Macromolecular Chemistry, Budapest, Hungary, 1969.

Ethyl acetate and hexane were stored over calcium hydride and filtered before use.

Catalyst. Sodium methoxide catalyst was prepared by the method of Fritz and Lisicki[7] and was standardized by titrating benzoic acid to a thymol blue endpoint. It was stored in the dark to prevent decomposition.

Polymerization Procedure

Polymerizations were conducted in dioxane at an NCA concentration of 0.064 mole/l. and at a ratio of monomer to initiator concentration of 40. The rates of polymerization were measured by a conductometric method utilizing the fact that a mole of CO_2 is generated for each mole of NCA reacted.[8] CO_2 was swept from the reaction vessel with dioxane-saturated nitrogen (to minimize loss of solvent by evaporation) and into a conductance cell containing $Ba(OH)_2$. The decrease in conductance as a result of $BaCO_3$ precipitation was related to the amount of NCA reacted.

RESULTS

Typical rate curves expressed as fraction of NCA reacted with time are shown in Figure 1. These curves are similar to those required previously for the polymerization of the NCAs of γ-benzylglutamate.

Since the rates of polymerization of NCAs are first-order in both NCA and initiator, the rate equation in terms of the fraction f of monomer reacted may be expressed as

$$\ln [1/(1 - f)] = kIt$$

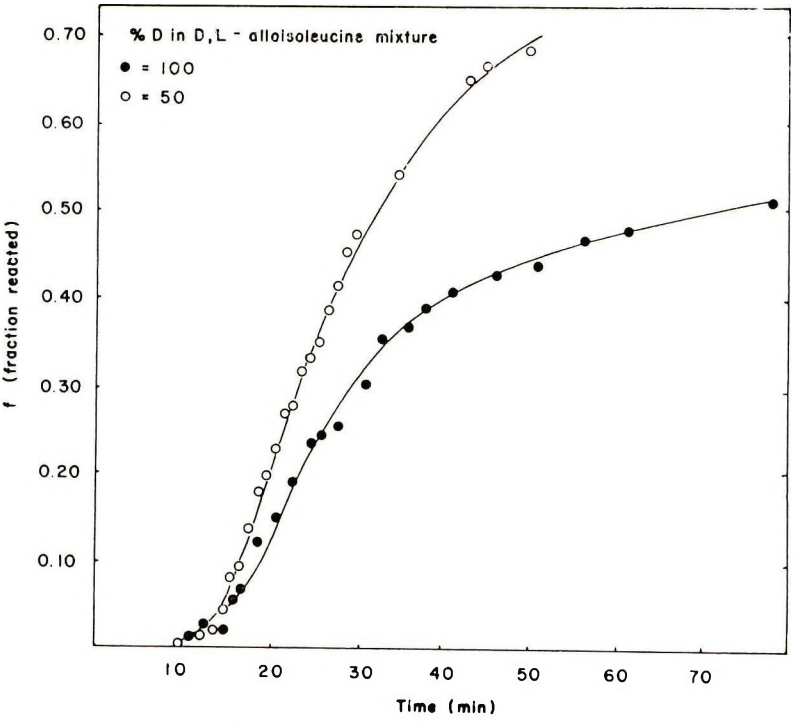

Fig. 1. Rate Curves. Fractional conversion vs. time for (●) D-alloisoleucine NCA and (○) racemic mixture of alloisoleucine NCA. [NCA] = 0.064 mole/l., [NCA]/[I] = 40.

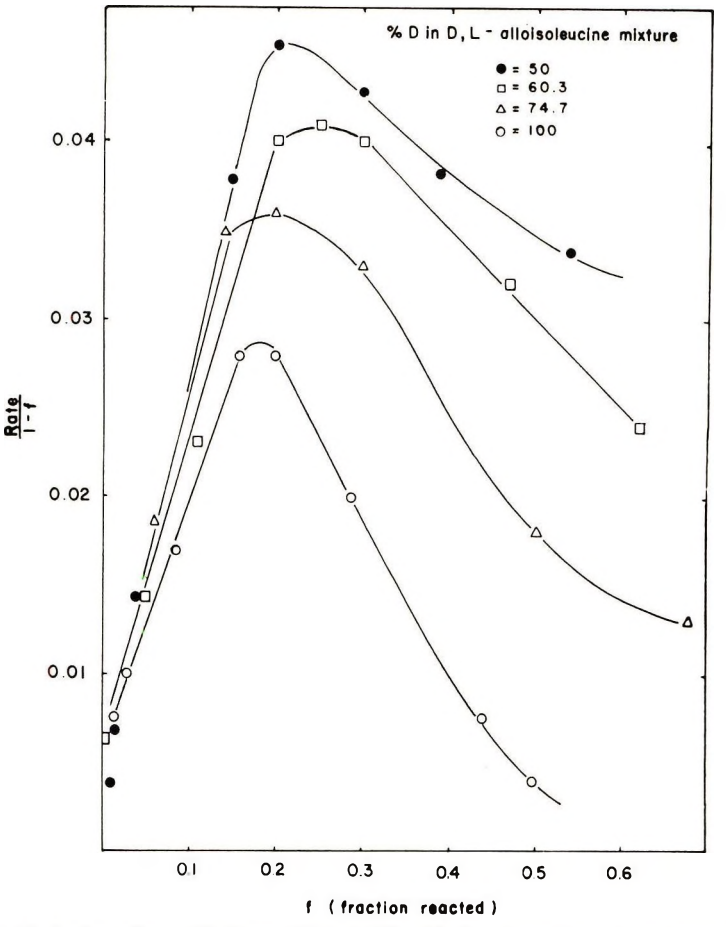

Fig. 2. Variation of rate/(1-f) or $\phi(f)$ or $\phi(k)$ with fraction of monomer reacted for D-alloisoleucine NCA–L-alloisoleucine NCA mixtures: (○) 100% D-alloisoleucine NCA; (△) 74.7% D-alloisoleucine NCA; (□) 60.3% D-alloisoleucine NCA; (●) 50% D-alloisoleucine NCA.

Plots of $\ln[1/(1-f)]$ versus t did not show the clear relationships which were evident during the γ-benzylglutamate NCA polymerizations.

If growing polymer in some way influenced the rate, then the rate law previously expressed is incomplete and should include a factor for the effect of polymer. Therefore we may write

$$-d[\text{NCA}]/dt = k[\text{I}][\text{NCA}]\phi[\text{polymer}]$$

where ϕ[polymer] is some function of the polymer concentration expressed as moles of monomer reacted/liter. Rewriting this equation in terms of the fraction of monomer reacted, we obtained

$$-ad(1-f)/dt = kIa(1-f)\phi(f)$$

$$df/dt = k'(1-f)\phi(f)$$

where $k' = kI$ and a is the initial concentration of monomer in moles/liter. The variation of $\phi(f)$ with f was obtained by plotting $(df/dt)/(1-f)$ versus f and is shown in Figure 2.

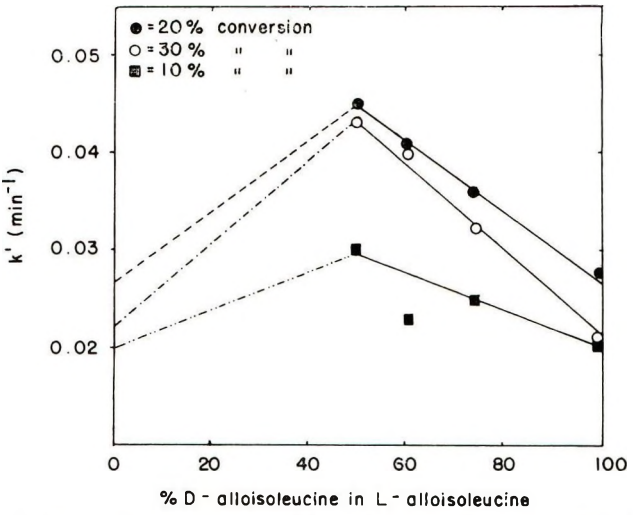

Fig. 3. Pseudo-first-order rate constants k' as a function of D- and L-alloisoleucine NCA at (□) 10%, (●) 20%, and (○) 30% conversions.

Plots of the pseudo-first-order rate constants at 10, 20, and 30% conversion versus monomer composition for the copolymerization of the alloisoleucine enantiomers is shown in Figure 3.

DISCUSSION

The shape of the rate curves (Fig. 1) and the two-stage first-order plots are in cursory way similar to those obtained for the polymerization of γ-benzyl glutamate NCA. In this latter case, however, the results were rationalized on the basis of conformational transitions and differences in reactivity between random coils and α-helices. These explanations cannot be applied to the present system of alloisoleucine, since for steric reasons, polyisoleucines are unable to form helices.[4,5]

Other results similar to our data and to those previously ascribed to conformational variations have been obtained by Ballard and Bamford[9,10] and by Iwakura et al.[11] In the latter investigation, rate changes were related to the heterogeneity of the reactions. Indeed, recent work in our laboratories repeated the polymerization of γ-benzyl glutmate NCAs; the results indicated that a solubility phenomenon and not a conformational transition produced the results obtained.[3] Such an effect may be more pronounced in the present system because of the high insolubility of polyisoleucines. Nevertheless, it is likely that the systematic variation of rate constants and the relatively high yields in the present research are attributable to several factors including heterogeneity.

The rate curves may be explained qualitatively on the basis of an auto-acceleration resulting from adsorption of monomer onto growing polymer. Initially, when the chains are small, relatively little monomer is adsorbed. As the chain grows, more sites

TABLE I
Molecular Weight of Alloisoleucine NCAs

	Molecular weight		Dimerization, %
	Actual	Observed	
D-Alloisoleucine NCA	157	150	0
DL-Alloisoleucine NCA	157	180	26

[a] Determined on a Hewlett-Packard Vapor Pressure Osmometer in dioxane at 25°C.

become available for adsorption by hydrogen bonding, and the local concentration of monomer increases, thereby increasing the rate. When polymer becomes sufficiently long, monomer adsorbed on the unreactive end is essentially removed from solution and the reaction is self-inhibited.

Values of rate$(1 - f)$ would all be equal to kI for uncomplicated pseudo-first-order reactions. Figure 2 indicates, however, that plots of rate$(1 - f)$ versus f rose to a maximum at $f = 0.2$ and thereafter rapidly decreased. This curve may be interpreted as indicating the variation of the pseudo-first-order rate constants with per cent conversion.

It should be noted that in all cases k' maximized at approximately $f = 0.2$. Since the monomer/initiator ratio was 40, this was equivalent to an average degree of polymerization of eight. These results agree well with independent experiments aimed directly at the influence of initiator size on initial rates.[9,10,12]

The effect of copolymerizing enantiomers of alloisoleucine NCA is demonstrated in Figures 1, 2, and 3. Figure 1 shows that both the rate and maximum conversion are higher for DL-alloisoleucine NCA than for the pure optical isomer. Figures 2 and 3 clearly indicate that the rate constants increase steadily from optically pure monomer to the racemic composition. This result is in sharp contrast to the decrease in rate obtained when D- and L-γ-benzyl glutamate NCAs are copolymerized.[1,3] A rate constant for the polymerization of the racemic monomer which is higher than for the pure optical isomer led to the immediate assumption that the end unit of polyisoleucine added preferably to monomer of opposite configuration. Although this may be partially true, subsequent experiments which measured the apparent molecular weight of D- and DL-alloisoleucine NCA in dioxane solution indicated that dimers formed. Table I gives these results. The conclusion that dimers of DL-alloisoleucine form is substantiated by melting point data, which indicated the existence of a congruently melting compound at the racemic composition. The DL-alloisoleucine dimers may increase the rate of reaction by being more reactive than monomer or by having different solubility properties. Work on this system is continuing to distinguish between these possibilities.

References

1. R. D. Lundberg and P. Doty, *J. Amer. Chem. Soc.*, **79**, 3961 (1957).
2. T. Tsuruta, S. Inoue, and K. Matsura, *Chem. Eng. News*, **44**, 40 (Dec. 19, 1966).
3. F. D. Williams, M. Eshaque, and R. Brown, *Biopolymers*, **10**, 753 (1971).
4. E. R. Blout, in *Polyamino Acids, Polypeptides, and Proteins*, M. A. Stahmann, Ed., Univ. Wisconsin Press, Madison, Wisc., 1965, p. 275.
5. A. M. Liquori, in *Perspectives in Polymer Science* (*J. Polym. Sci. C*, **12**), E. S. Proskauer, E. H. Immergut, and C. G. Overberger, Eds., Interscience, New York, 1966, p. 235.
6. W. E. Hanley, S. G. Waley, and S. D. Watson, *J. Chem. Soc.*, **1950**, 3009.
7. J. Fritz and N. Lesicki, *Anal. Chem.*, **25**, 1554 (1953).
8. J. W. Brietenbach and K. Allinger, *Monatsh. Chem.*, **84**, 1103 (1953).
9. D. G. H. Ballard and C. H. Bamford, *J. Chem. Soc.*, **1959**, 1039.
10. D. G. H. Ballard and C. H. Bamford, *Proc. Roy. Soc.* (London), **A236**, 384 (1956).
11. Y. Iwakura, K. Uno, and M. Oya, *J. Polym. Sci. A-1*, **6**, 2165 (1968).
12. M. Sisido, Y. Imanishi, and S. Okamura, *Biopolymers*, **7**, 937 (1969).

FRED D. WILLIAMS
RONALD D. BROWN

Department of Chemistry and Chemical Engineering
Michigan Technological University
Houghton, Michigan 49931

Received June 8, 1970
Revised January 25, 1971

Polymerization Studies of Isopropenylferrocene

Interest in polymers containing the ferrocene group has centered around their electrical and magentic[1] and their electron-exchange properties.[2] Polymerization studies on vinylferrocene have been reported by various investigators,[3,4] including a comprehensive study by Baldwin and Johnson.[5] The polymerization studies on other alkenylferrocenes have been very limited;* however, studies have now been extended to include isopropenylferrocene. This paper describes the attempted homopolymerization of isopropenylferrocene and its copolymerization with methyl methacrylate and styrene by free-radical initiation.

EXPERIMENTAL

Materials

Isopropenylferrocene (IPF) was prepared from acetylferrocene by first reacting with methyl Grignard reagent followed by dehydration of the resulting 2-hydroxy-2-ferrocenylpropane.

2-Hydroxy-2-ferrocenylpropane. Acetylferrocene (0.44 mole) was placed in a predried glass reactor, 750 ml of THF added, and methyl Grignard reagent (0.75 mole) added under a nitrogen atmosphere at 0–5°C over a period of 1.15 hr. The mixture was stirred for approximately 16 hr. After adding 200 ml of ether, the mixture was treated with an ammonium hydroxide solution saturated with ammonium chloride until reflux stopped. Upon filtration the filtrate was washed twice with water, dried over anhydrous magnesium sulfate, and the solvents removed by evaporation. A red oil which crystallized on standing was obtained in 95% yield. Its infrared and ^{1}H NMR spectra were indicative of the 2-hydroxy-2-ferrocenylpropane.

Isopropenylferrocene. 2-Hydroxy-2-ferrocenylpropane (0.41 mole) was dissolved in 2.5 liters of dry methylene chloride containing 21 meq of *p*-toluenesulfonic acid and 9.1 meq of *N*-phenyl-2-naphthylamine. The mixture was heated to reflux under nitrogen for 2.5 hr with the water eliminated as the azetrope. Upon completion, 10 ml of triethylamine was added to neutralize the acid and the solvent was totally removed by evaporation at below ambient temperature (0–10°C). The oily residue was extracted several times with pentane, the extracts combined, methylene chloride added to give a 30:1 pentane–methylene chloride mixture, and this solution passed through a silica gel column (2 in. ID, 12 in. high). One liter of the 30:1 solvent mixture was used to elute the column. Removal of the solvents gave a yellow solid (64.3%) which was recrystallized from methanol–water, mp 66.5–67°C. The infrared and ^{1}H NMR spectra were similar to those previously reported.[7–9]

ANAL. Calcd for $C_{13}H_{14}Fe$: C, 69.04%; H, 6.24%. Found: C, 68.40%; H, 6.44%.

Other monomers were fractionally distilled prior to use. All solvents were reagent-grade, distilled materials. 2,2′-Azobis-isobutyronitrile (AIBN) were recrystallized from methanol, mp 102–103°C with decomposition.

Polymerization

Homopolymerization reactions of IPF were carried out with the use of 2.0 g monomer in 20 ml of toluene in a small (50-ml capacity) glass flask. 2,2′-Azobisisobutyronitrile or benzoyl peroxide was added at the 0.1, 0.5, and 1.0 mole-% levels and the flasks heated at 65, 80, and 100°C for periods of 24 hr. The solvent was removed by evaporation and the solid reside examined by infrared spectroscopy. In all instances the solid isolated was almost identical with IPF by comparison of their infrared spectra.

*Pittman *et al.*[6] have studied the polymerization of ferrocenyl acrylate and methacrylate.

Techniques

Dilatometric polymerization rate measurements have been described elsewhere.[10]

Solution viscosities were determined in Cannon dilution viscometers at 30°C. Toluene were used as solvent.

Iron analyses were carried out on a Perkin-Elmer atomic absorption spectrophotometer, Model 303.

A Waters Associates analytical instrument was employed for GPC analyses. Degassed tetrahydrofuran flowing at the rate of 1 ml/min was the eluting solvent. Styragel columns (10^4, 10^3, 600, and 100 Å mean permeability) in series were used to fractionate the polymers. Each column configuration was calibrated in terms of average length by using narrow molecular weight distribution polystyrenes supplied by Waters Associates, Inc.

RESULTS AND DISCUSSION

Copolymerization reactions were carried out at three different concentrations of isopropenylferrocene (IPF) with both MMA and styrene to determine the concentration effects of IPF. Major emphasis was directed to the effect of low concentration of IPF on the rate of polymerization and properties of the copolymers. Experimental data for these reactions are presented in Table I. The R_{p_0} and $[\eta]_0$ values refer to the rate of polymerization of MMA and styrene and the intrinsic viscosity of the appropriate homopolymer, respectively.

Several interesting observations were made from the MMA copolymerizations. The rate of the copolymerization was reduced drastically by the addition of IPF at even very low concentrations as evidenced by the low values (0.05–0.13) of R_p/R_{p_0}. In a similar manner, the intrinsic viscosities of the copolymers were severely reduced at low IPF concentrations and continued to decrease as the low IPF concentration increased. This fact was established by the low $[\eta]/[\eta]_0$ values of 0.12–0.06. Iron analysis of the copolymers showed that IPF was entering the copolymers in a ratio considerably less than was present in the comonomer charge, particularly at the higher IPF concentrations.

A similar effect of IPF on the copolymerization reactions with sytrene was noted except the reduction in rate of polymerization and in the intrinsic viscosity of the copolymers was not as severe. Both rates were reduced by approximately 40% at the highest IPF concentration. Iron contents of the styrene copolymers were slightly higher for the MMA copolymers, and they approached a composition equivalent to that of the comonomer charge for the lower IPF concentration.

No quantitative description of the free radical polymerization behavior of IPF has been reported, although vinylferrocene has been studied in some detail.[3–5] Our attempts to homopolymerize IPF with either azobisisobutyronitrile or benzoyl peroxide in toluene solution at temperature up to 100°C were all unsuccessful, and no polymerization was observed. In this way, IPF appears to exhibit free-radical polymerization characteristics typical of α-methyl-styrene.[11,12]

Since α-methylstyrene readily enters into copolymerization with vinyl monomers in reactions involving free-radical initiation, it was expected that the structural related IPF would also behave in the same manner. The copolymerization reactions of IPF with MMA and styrene demonstrated that this expectation was essentially correct. Although IPF was an active monomer in the copolymerizations, its basic effect was to lower the rate of reaction and the intrinsic viscosity of the copolymers. These effects were notably severe for the MMA copolymers.

These results depict the copolymerization behavior of IPF as a monomer which is capable of interacting with radical intermediates in copolymerization reactions, but one that produces a chain-end radical which is either of very low reactivity or readily undergoes chain transfer with monomer as has been described for certain allylic monomers. The most likely reason for the behavior of IPF is that the chain-end radical is of low

TABLE I
Experimental Data for Copolymerizations

No.	[MMA], mole/l.[a]	[Styrene], mole/l.[b]	[IPF], mole/l.	Mole ratio comonomers	R_p, %/min	R_p/R_{p0}	$[\eta]$, dl/g	$[\eta]/[\eta]_0$	Fe, % Calcd	Fe, % Found
1	5.00	—	—	—	2.3×10^{-3}	1.000	1.580	1.000	—	—
2	4.75	—	0.11	43.2	3.0×10^{-4}	0.130	0.190	0.120	1.25	1.65
3	4.25	—	0.33	12.9	2.0×10^{-4}	0.086	0.155	0.098	3.69	3.18
4	3.75	—	0.55	6.8	1.5×10^{-4}	0.065	0.090	0.057	6.18	4.08
5	—	4.84	—	—	7.0×10^{-4}	1.000	0.260	1.000	—	—
6	—	4.56	0.11	41.5	4.0×10^{-4}	0.571	0.275	1.057	1.23	1.42
7	—	4.09	0.33	12.4	4.0×10^{-4}	0.511	0.225	0.865	3.69	3.87
8	—	3.60	0.55	6.5	4.3×10^{-4}	0.614	0.170	0.654	6.21	5.12

[a] [AIBN] = 0.025 mole/l.
[b] [AIBN] = 0.05 mole/l.

reactivity because of resonance interaction possibilities with the ferrocene group, and thus, it fails to propogate chain growth to the usual extent. In this picture the intermediate radical may have a propensity to terminate via combination with other radical intermediates as has been observed for dimer formation in certain allylic radical systems.

The analytical contributions of Dr. K. E. Johnson and Mr. R. D. Strahm are gratefully acknowledged. The technical assistance of Mr. J. O. Woods is appreciated.

This work was sponsored by the U. S. Army Missile Command, Redstone Arsenal, Alabama, under Contract DAAH01-69-C-0772.

References

1. A. A. Dublov, A. A. Slinken, and T. M. Rubenshtein, *Vysokomol. Soedin.*, **5**, 1441 (1963).
2. D. A. Seanor, *Fortsch. Hochpolym. Forsch.*, **4**, 317 (1965).
3. F. S. Arimoto and A. C. Haven, Jr., *J. Amer. Chem. Soc.*, **77**, 6295 (1955).
4. Y.-H. Chen, M. Fernandez-Refojo, and H. G. Cassidy, *J. Polym. Sci.*, **40**, 433 (1959).
5. M. G. Baldwin and K. E. Johnson, *J. Polym. Sci. A-1*, **5**, 2091 (1967).
6. C. U. Pittman, J. C. Lai, and D. P. Vanderpool, *Macromolecules*, **3**, 105 (1970).
7. C. R. Hauser, R. L. Pruett, and T. A. Mashburn, *J. Org. Chem.*, **26**, 1800 (1961).
8. W. M. Horspool and R. G. Sutherland, *Can. J. Chem.*, **46**, 3453 (1968).
9. W. P. Fitzgerald, Ph.D. Thesis, Purdue University, 1963.
10. M. G. Baldwin and S. F. Reed, Jr., *J. Polym. Sci., A1*, 1919 (1963).
11. H. M. Stanley, *Chem. Ind.* (London), **58**, 1080 (1939).
12. A. B. Hersberger, J. C. Reid, and R. H. Heiligmann, *Ind. Eng. Chem.*, **37**, 1073 (1945).

Morris Howard
Samuel F. Reed, Jr.

Rohm and Haas Company
Philadelphia, Pennsylvania 19137

Received June 30, 1970
Revised March 2, 1971

Particle Morphology in Emulsion Polymerization

Grancio and Williams[1] have recently proposed a heterogeneous model (hereafter termed model I) for the monomer–polymer particles participating in styrene emulsion polymerizations. This is contrary to the normally assumed homogeneity in the Smith-Ewart theory of emulsion polymerization.[2] Model I postulates that each particle is composed of an expanding polymer-rich core that is surrounded by a monomer-rich shell. The outer shells serve as monomer reservoirs for propagation; they are presumed to be the major loci of polymerization within the particles, and in them Smith-Ewart case 2 kinetics are considered to prevail.

Although both kinetic and morphological evidence was adduced to support model I, no physical explanation for the phenomenon of monomer heterogeneity was advanced. Moreover, model I appears suspect on another score: if, as assumed by Grancio and Williams, polymerization occurs primarily in the peripheral zones of the particles, any simple diffusion approach predicts that these outer regions would, if anything, be monomer-deficient in any dynamic situation because of the consumption of monomer therein. The inner regions would thus function as monomer reservoirs, the chemical potential of the monomer decreasing in the outwards direction. Model I adopts just the reverse phenomenology, no explanation being given as to why the ordinary laws of diffusion do not prevail; it requires that the presence of a single free radical can dramatically reduce the chemical potential of the monomer over large distances in the outer shells.

Because of these physical discrepancies, an alternative model (II) is proposed. This predicts[3] the observed heterogeneity in the distribution of newly formed polymer in seeded growth studies and is consistent with the kinetic observations of Grancio and Williams. An added attraction is that it does not violate the ordinary notions of diffusion. Model II is a minor adaptation of a theory that has successfully explained the heterogeneous polymerization of vinyl acetate.[4]

Model II initially recognizes that sulfate anion (or hydroxyl) free radicals, formed by peroxydisulfate decomposition, are unlikely *per se* to leave the highly polar aqueous environment and enter into the less polar polymer particles, even if swollen with monomer. Monomer must therefore initially add on to these primary free radicals in the aqueous phase. Propagation produces amphipathic free radical oligomers, which resemble conventional surfactant molecules.[5–7] These oligomeric species adsorb onto the surface of the polymer particles. It seems unlikely that the entire oligomers penetrate into the swollen particles, partly because of the high internal viscosity of the particles.[8] Further, the polar sulfate anions seem likely to remain at the particle–water interface, providing interface anchoring groups.[3,9]

Further propagation of the oligomeric free radicals adsorbed on the particles proceeds by monomer addition, the direction of propagation being, on the average, towards the direction of maximum monomer flux. Simple diffusion considerations imply that the direction of maximum monomer flux will be outwards from the center of each particle and so, on average, propagation will be directed towards the centre of the particle. Each monomer addition moves the propagating free radical site one monomer unit further into the particle away from the particle surface. A pictorial analogy is the growth of a stalagmite towards its feed source. In the absence of free radical transfer, the major locus of polymerization will thus be inside the particle but, at any instant, in the immediate subsurface regions. It is here that new polymer is formed if chain transfer is small.

According to model II, the cores of the seed particles will not contain significant new polymer, in the absence of chain transfer, primarily because this region is relatively inaccessible to free radicals; the monomer present in the cores is therefore not polymerized locally but diffuses to, and polymerizes in, the peripheral zones. In contradistinction, model I postulates that the absence of new polymer in the cores is due to an unexplained paucity of monomer in these regions. The two models can be distinguished experimentally by adding a chain transfer agent that is incorporated into the swollen particles.

Model I still predicts morphological heterogeneity whereas model II demands a more homogeneous distribution of new polymer in the seed particles when chain transfer is frequent. The polymerization of a monomer, e.g., vinyl acetate, that undergoes significant chain transfer might also discriminate between the two models.

Grancio and Williams[1] provided suggestive electron microscopic evidence that when butadiene was copolymerized with styrene in seeded systems, the copolymer was formed in the peripheral regions of the particles. Assuming that the observed heterogeneity was not an artifact arising from the electron microscopic method of observation, it is clear that model II is able to account for this heterogeneity in terms of the subsurface polymerization concept.

The kinetic evidence in favor of model I is also equivocal. Because the average dynamic monomer concentration in the polymer particles was found to decrease by a factor of 2 during polymerization, a decrease in the rate of polymerization would be anticipated if the average number of free radicals per particle ($\bar{n}$) was constant and equal to $^1/_2$. Grancio and Williams[1] interpreted their kinetic results as showing that the rate of polymerization was constant. They concluded that the monomer concentration in the particles must therefore be constant in the propagation zones. This led to the idea of a monomer-deficient core surrounded by a monomer-rich zone.

Some doubt necessarily attends any determination of dynamic monomer concentrations, first because of the difficulty of stopping propagation in latex particles instantaneously and second because equilibration is likely to occur in the time required to separate out the latex particles. Moreover, inspection of the kinetic curves of Grancio and Williams[1] shows that almost all curves are convex to the time axis, i.e., the instantaneous rate of polymerization actually increases as polymerization proceeds. Autoacceleration of this type is characteristic of an increase in $\bar{n}$.[10] This is to be expected with oligomeric free radicals as the chain carriers from the aqueous phase; their mutual termination is hindered by restricted diffusional mobility, i.e., a Trommsdorff effect occurs. If $\bar{n}$ increases as polymerization proceeds, the need to postulate a monomer-rich outer polymer shell that violates simple diffusion considerations vanishes. It merely requires that any increase in $\bar{n}$ counterbalances any decrease in the monomer concentration at the propagation sites, as, e.g., has been found for the heterogeneous polymerization of vinyl acetate.[10]

Perhaps the only evidence cited by Grancio and Williams that seemingly contradicts model II are the initiation perturbation studies. These suggest that $\bar{n}$ is rigorously equal to $^1/_2$. The results of these studies are at odds with their other kinetic results discussed above, which imply an increase in the rate of polymerization as polymerization proceeds. Their data also disagree with the results of the initiator perturbation studies of Gerrens,[11,12] who detected a small increase in rate with increasing initiator concentration as expected if $\bar{n}$ is somewhat greater than $^1/_2$. However, Grancio and Williams perturbed their initiator concentration by only a factor of 3, and their electron microscopic method of studying the kinetics was probably too insensitive to detect any changes in rate.

The observed morphological heterogeneity in styrene-butadiene copolymerization should not be taken as support for the Medvedev theory that emulsion polymerization occurs primarily on the surfaces of the particles.[8] For a propagating free radical to remain at the particle–water interface, the most probable direction of propagation would have to be at least tangental to the surface, if not directed away from it into the dispersion medium. This, too, seems unlikely because it is not the direction of maximum monomer flux.

References

1. M. R. Grancio and D. J. Williams, *J. Polym. Sci. A-1*, **8**, 2617 (1970).
2. W. V. Smith and R. H. Ewart, *J. Chem. Phys.*, **16**, 592 (1948).
3. A. E. Alexander and D. H. Napper, *Progr. Polym. Sci.*, **4**, 181 (1970).
4. A. Netschey, D. H. Napper, and A. E. Alexander, *J. Polym. Sci., B*, **7**, 829 (1969).
5. D. H. Napper and A. E. Alexander, *J. Polym. Sci.*, **61**, 127 (1962).

6. R. M. Fitch, *Off. Dig. J. Paint Technol. Eng.*, **37,** 32 (1965).
7. R. M. Fitch and C. H. Tsai, *J. Polym. Sci. B*, **8,** 703 (1970).
8. S. S. Medvedev, *Coll. Czech. Chem. Commun.*, **22,** 174 (1957).
9. J. W. Vanderhoff, H. J. Van Den Hul, R. J. M. Tausk, and J. Th. G. Overbeek, in *Clean Surfaces*, G. Goldfinger, Ed., Dekker, New York, 1970, p. 17.
10. D. H. Napper and A. G. Parts, *J. Polym. Sci.*, **61,** 113 (1962).
11. H. Gerrens, *Angew. Chem.*, **71,** 608 (1959).
12. H. Gerrens and E. Kohnlein, *Z. Elektrochem.*, **64,** 1199 (1960).

D. H. Napper

Department of Physical Chemistry
University of Sydney
N.S.W. 2006, Australia

Received December 29, 1970
Revised March 2, 1971

Apparatus for Measurement of Viscosity of Molten Polymers Sensitive to Moisture and Oxygen

A complication frequently encountered in the determination of the viscosity of molten polymers is instability caused by chemical reactions of the melt with water vapor or oxygen. This note describes a simple apparatus which has been found to be successful in making it possible to obtain measurements on such sensitive polymers as poly(hexamethylene adipamide) (nylon 66) and poly(ethylene terephthalate) with a conventional capillary flow rheometer. The apparatus as described is specifically suitable for the Sieglaff-McKelvey rheometer,[1] but with minor modification the principle should be applicable to other instruments.

The only modification required for the rheometer itself is that the retaining nut that holds the rheometer barrel in the heating furnace is replaced by the one shown in Figure 1. The new retaining nut has provision for blanketing the polymer melt with an inert gas. A circular disk of silicone rubber about 0.015 in. thick (Ronthor 6060; Ronthor Reiss Corporation, Little Falls, N. J.), held in place by the retaining ring, seals the top of the barrel. Two slits, 0.3 in. long and perpendicular to each other are cut in center of the rubber disk by means of a punch to permit the passage of the rheometer plunger. The flaps formed by the slits serve as a seal against the atmosphere, and present negligible friction as measured by the rheometer load cell to the motion of the plunger.

The material to be tested, most conveniently in the form of small pellets, is put into the sample tube (Fig. 2) and attached to a vacuum line capable of attaining pressures below 5×10^{-6} torr. After the desired conditioning, for example, drying and/or adding known amounts of water, the sample manifold and tube are filled with Research Grade

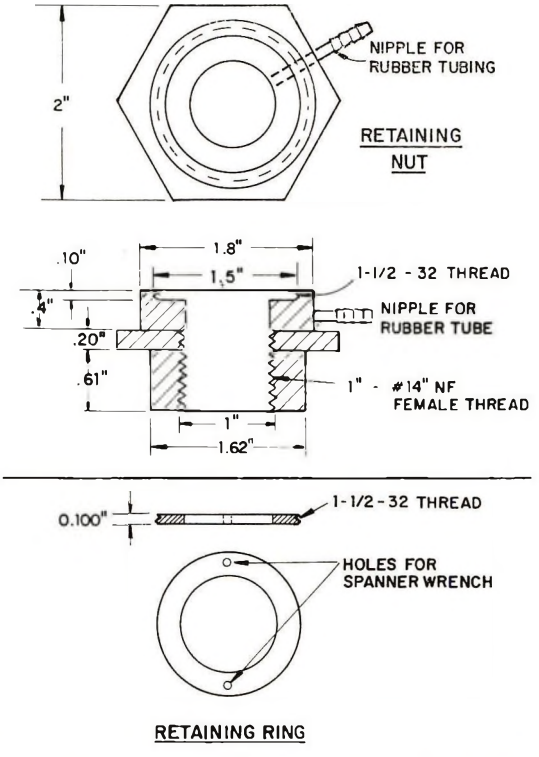

Fig. 1. Modified barrel retaining nut and retaining ring for rubber disk.

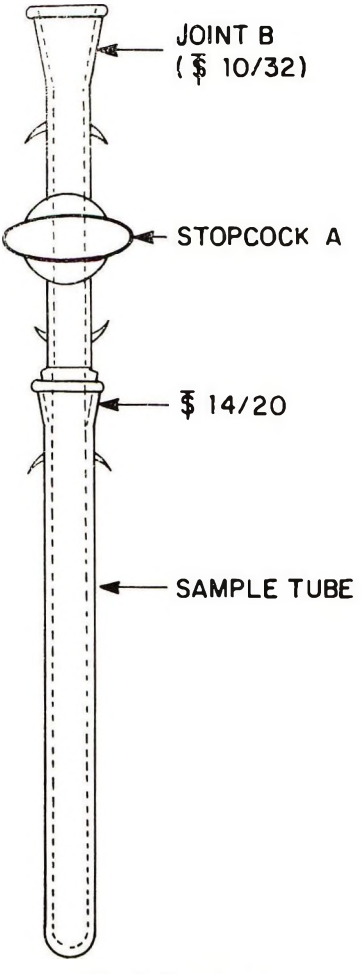

Fig. 2. Sample tube.

Argon (Matheson) at about 750 torr, stopcock A is closed, and the sample tube is removed from the line at joint B.

To transfer the polymer from the sample tube to the barrel of the rheometer with minimum exposure to the atmosphere, the sample addition fixture shown in Figure 3 is placed over the retaining nut. The inner tube of this fixture protrudes so as to pass through the slit in the silicone rubber diaphragm and to rest on top of the rheometer barrel. The capillary die at the bottom of the barrel is protected from the atmosphere during loading by another removable fixture, shown in Figure 4, which is flushed with a flow of nitrogen during loading. With the bottom of the barrel sealed this way, and the top of the addition tube sealed by the tamper and O-ring, the only place for the nitrogen being flushed through the bottom and through the retaining nut to escape is by way of the side tube of Figure 3.

After several minutes of nitrogen flushing, the sample tube is brought next to the side arm of the addition fixture, the stopcock is removed from the sample tube, and the tube is slipped onto the ground joint of the side arm. This transfer step is the only time at which the sample is exposed to the atmosphere, and the exposure is minimized by the nitrogen stream from the side arm. Tapping and rotating the sample tube causes the

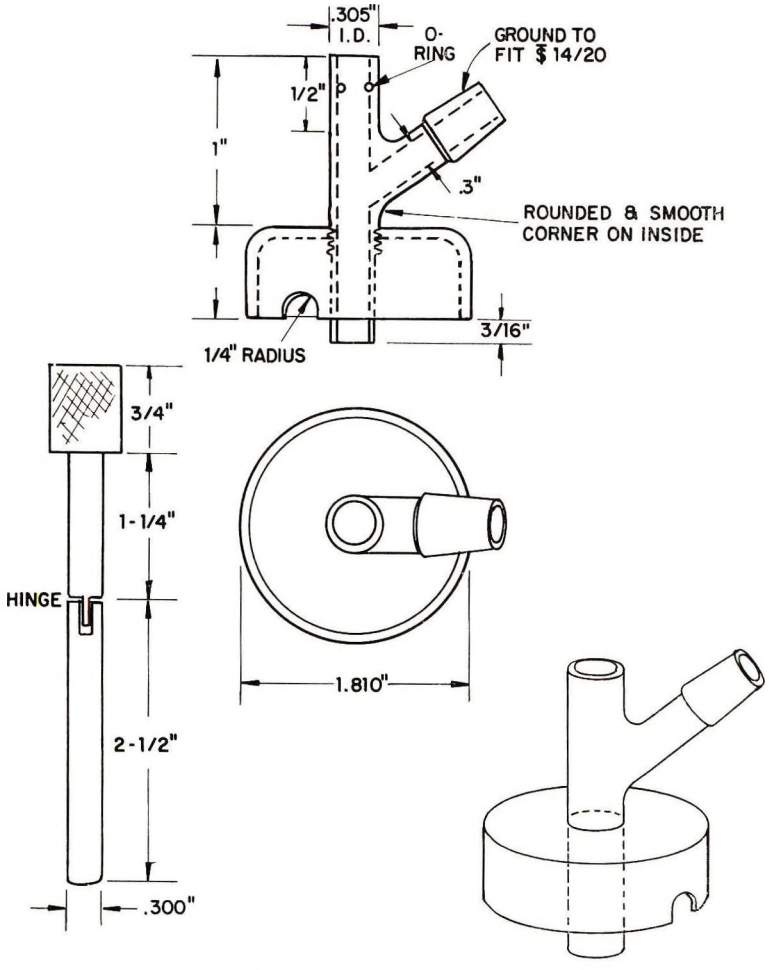

Fig. 3. Sample addition fixture and tamper.

polymer to fall into the barrel, and occasional tamping compacts the melt. During the sample transfer the flow of nitrogen to the bottom of the barrel is stopped and that to the top reduced in order to not build up enough pressure to impede the transfer. When the transfer is complete the addition tube and bottom fixture are removed, the rheometer plunger is inserted, and measurements are made in the normal manner. During measurement the nitrogen flow is controlled by a flow meter in order to maintain a light positive pressure of nitrogen, just enough to bulge the rubber disc.

The results obtained with this apparatus have been quite satisfactory and are illustrated in Figures 5 and 6. The data of Figure 5 were obtained on a sample of poly(ethylene terephthalate) dried 5 hr *in vacuo* at 150°C. Data were taken over a range of shear rates, and after a pause of several minutes this procedure was repeated twice. The total residence time in the rheometer was about 20 min. The data points shown as squares were obtained by the loading procedure described above. The circles represent data taken on a duplicate sample, dried in the same way and measured under nitrogen, but loaded in the conventional way in the presence of air. Loading took about 5 min. The viscosity measured this way was appreciably lower even initially than measured in the first trial, and had dropped by a factor of two after 20 min. Figure 6 shows the viscosity,

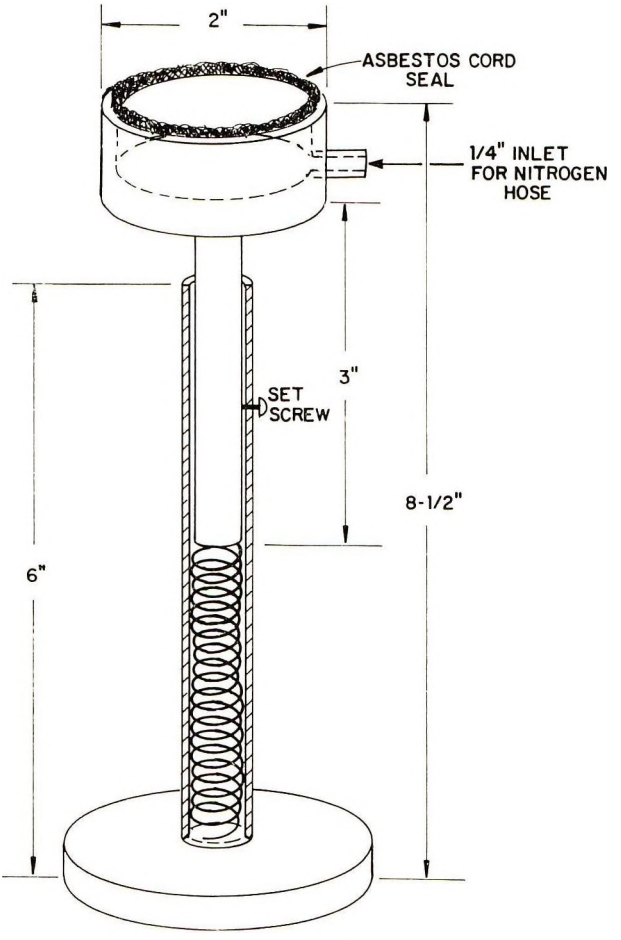

Fig. 4. Bottom flushing fixture.

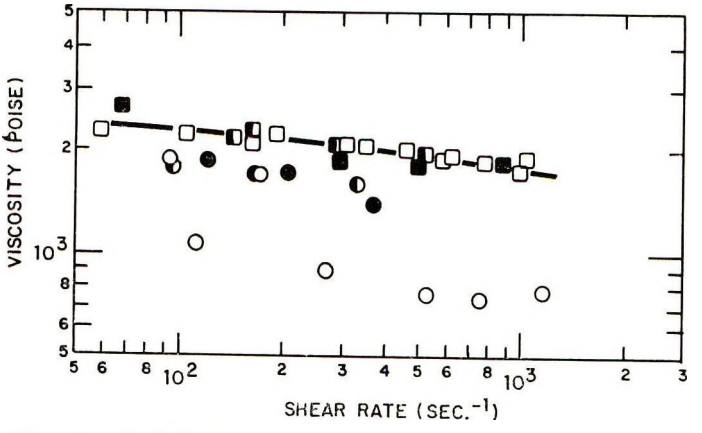

Fig. 5. Viscosity of poly(ethylene terephthalate) vs. shear rate and residence time in barrel at 275°C (□,◧,■) in an inert atmosphere and (○,◐,●) when exposed to air during loading: (■,●) residence time = 5–7 min; (◧,◐) residence time = 10–12 min; (⊡,⊙) residence time = 17–20 min.

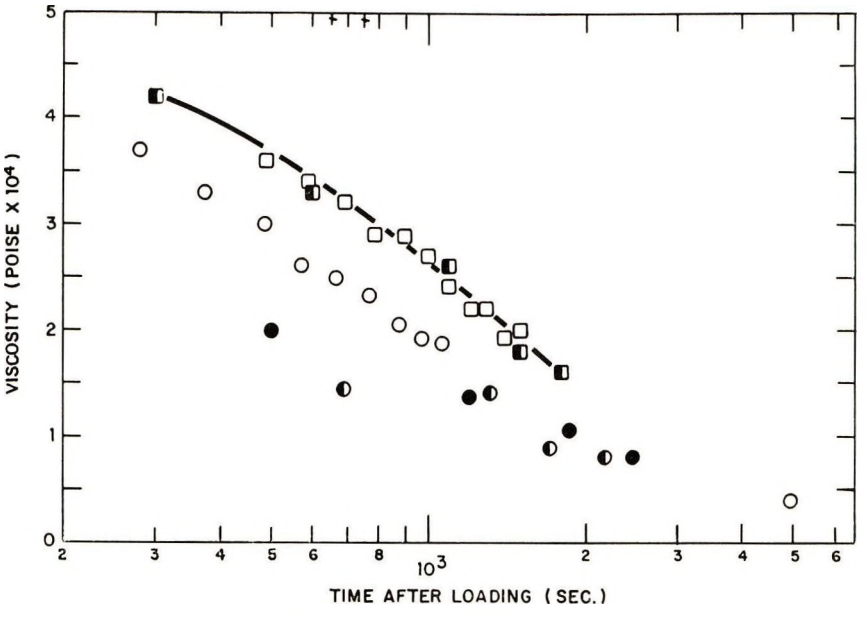

Fig. 6. Viscosity vs. time at 285°C of undried nylon 66. Replicate measurements made (⊡,◧) in inert atmosphere and (⊙,◐,●) in air.

measured at constant stress, of a sample of high molecular weight nylon 66 containing excess water and therefore hydrolyzed in the rheometer.[2] The data obtained by the apparatus and technique described are quite reproducible, whereas those measured conventionally are lower and more erratic. Also, the extrudates from the inert atmosphere measurements were white and uniform, whereas those from air were dark brown and bubbly, indicating the occurrence of oxidative degradation.

The reproducibility of the results, the stability of the viscosity with time of dried samples, and the absence of visible degradation indicate that the apparatus as described is adequate to make reliable measurements of the melt viscosity of polymers subject to degradation by constituents of the atmosphere.

The authors wish to thank Messrs. A. Gerken and W. W. Chadwick for their assistance in the design and construction of the apparatus.

References

1. C. L. Sieglaff, *SPE Trans.*, **4**, 1 (1964).
2. G. Pezzin and G. B. Gechele, *J. Appl. Polym. Sci.*, **8**, 2195 (1964).

K. F. Wissbrun
A. C. Zahorchak

Celanese Research Company
Summit, New Jersey 07901

Received December 4, 1970
Revised March 18, 1971

Viscometric Constants for Molecular Weight Determination of Cellulose Trinitrate in Tetrahydrofuran

Introduction

Tetrahydrofuran (THF) is a widely used solvent in the field of gel-permeation chromatography (GPC).[1] Solutions of cellulose trinitrate in THF are employed in the GPC method developed at this laboratory for obtaining molecular chain-length distributions in cellulose.[2] Intrinsic viscosities $[\eta]$ of the fractionated solutions eluted from the GPC columns are involved in the pertinent calculations, but further application of the solvent in classical procedures for determination of average molecular weight has been restricted because little has been reported in the literature concerning this solute-solvent system.

In recent publications[3–5] and theses,[6,7] two sets of values have been reported for the viscometric constants of the Mark-Houwink equation

$$[\eta] = KM^a$$

relating intrinsic viscosity of cellulose trinitrate solutions in THF to molecular weight M of the polymer. When these values were used with this laboratory's data from viscometric measurements of THF solutions of cellulose trinitrate samples, the molecular weights did not agree with those obtained from the ethyl acetate solutions of the same samples. (Ethyl acetate is one of the solvents normally used in viscometric studies of cellulose trinitrate. Viscometric constants for ethyl acetate solutions have been published for a wide range of molecular weights.)

Because of the observed lack of agreement, the THF and ethyl acetate data were studied to resolve the problem. This paper presents the results of this study.

Experimental

Twenty cellulose samples were used here; these included cotton fabrics, cotton linters, wood pulps and their α-cellulose fractions, and formaldehyde-crosslinked cotton fabrics. The molecular weights ranged from 1.44×10^5 to 2.02×10^6, corresponding to degrees of polymerization (DP) from 500 to 7000. The samples were nitrated, stored, and handled as described in earlier work.[1,2] Nitrogen contents determined by a semimicro Kjeldahl method[1] varied from 13.5 to 13.9%.

For viscosity determinations the nitrated samples were dissolved in ethyl acetate and in tetrahydrofuran at initial concentrations not greater than 0.05 g/dl. Dust particles and extraneous fibers were removed by pressure filtration with nitrogen; this technique avoided evaporation of solvent and change in concentration. Viscometric measurements were carried out with calibrated, Cannon-Ubbelohde, four-bulb, shear dilution viscometers.[8] Size 50 viscometers gave flow times greater than 100 sec for ethyl acetate and THF so that kinetic energy corrections were unnecessary; all viscosities were run at 25.0°C. Nitrogen pressure was also used during the filling operation[2] to force the solutions into the capillary and bulbs of the viscometer to prevent solvent evaporation.

Viscosities of unnitrated cellulose samples were determined in cadoxen (Size 100 cometers) in the manner previously reported.[9]

In calculating intrinsic viscosity for each sample, first shear corrections were made by plotting relative viscosity versus mean shear gradient $\bar{G}$ in order to extrapolate to obtain the relative viscosities at shear rates of 0, 500, or 1200 sec^{-1}. Reduced viscosities calculated from these relative viscosities were then plotted versus concentration to obtain the intrinsic viscosity (in dl/g) at zero concentration for each shear rate.[9,10] All calculations and extrapolations were carried out by computer.

Molecular weight or DP was calculated for each sample in ethyl acetate by means of the Mark-Houwink equation and the constants given by Marx-Figini and Schulz[11] and by Huque et al.[12] Marx-Figini and Schulz present one set of constants for DP $\geq$ 1000 and another for DP $<$ 1000 with reduced viscosities taken at $\bar{G} = 1200\ sec^{-1}$. The con-

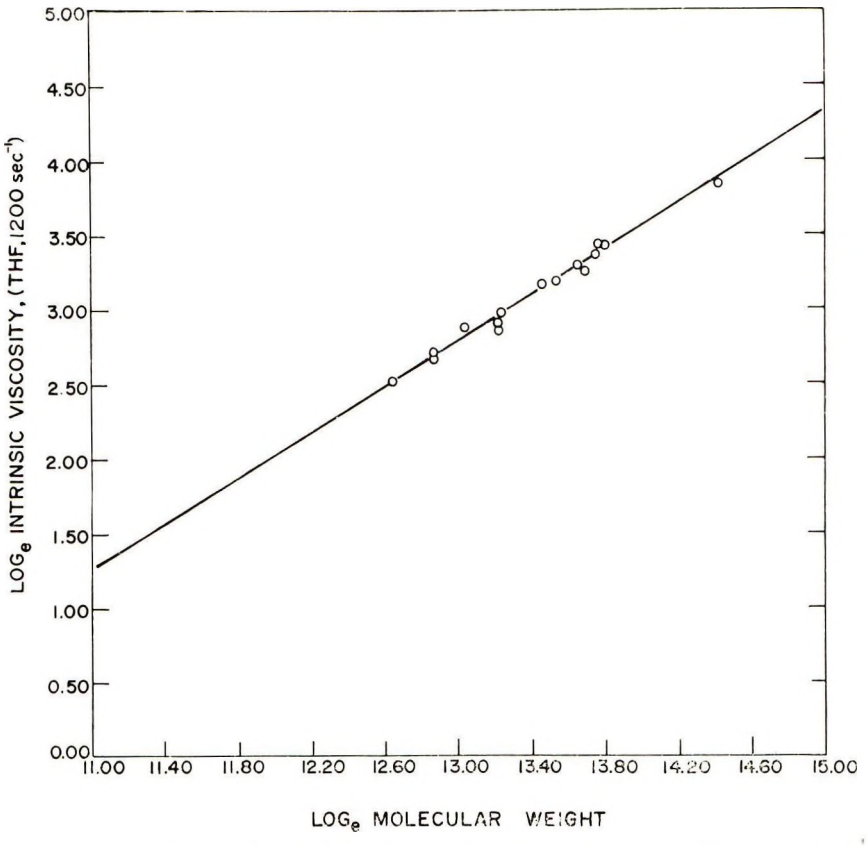

Fig. 1. Plot of ln [η] THF vs. ln M EtAc, both at $\bar{G} = 1200\,\text{sec}^{-1}$. Molecular weight M calculated from ethyl acetate viscosity by using constants of Marx-Figini and Schulz[11] for DP ≤ 1000, $\bar{G} = 1200\,\text{sec}^{-1}$.

stants published by Huque et al, apply to high molecular weight cellulose trinitrate only (DP > 2350) at the more conventional mean shear gradients of 0 and 500 sec^{-1}.

Intrinsic viscosities of the nitrated samples were uncorrected for nitrogen content. The majority of these samples had nitrogen contents of 13.6% which corresponds to a weight of 288.0 for the nitrated anhydroglucose unit.[13] To obtain DP, then, M is divided by 288.0.

For each sample in the series, the molecular weight determined in ethyl acetate according to the specifications given by Marx-Figini and Schulz and by Huque et al. was related to its respective intrinsic viscosity in THF. The logarithm of molecular weight for the sample was plotted against the logarithm of intrinsic viscosity of the THF solutions. The constant a for the THF solution is obtained from the slope of the plot, while the constant K is obtained from the intercept. Plotting of data and calculation of the slopes and intercepts were handled by computer in a least squares linear regression. In all cases an excellent straight-line fit was achieved, as illustrated by Figure 1.

Results and Discussion

Table I summarizes the results of this study. The constants K and a for cellulose trinitrate in THF are indicated with the appropriate shear corrections and DP ranges. The restrictions are those given by the previous workers for the ethyl acetate–cellulose

TABLE I
Values for the Viscometric Constants K and a for Cellulose Trinitrate in Tetrahydrofuran

Constants for tetrahydrofuran				Constants for ethyl acetate[a]		
$K \times 10^4$	a	DP range	Mean shear gradient, sec^{-1}	$K \times 10^4$	a	Reference
2.33	0.84	≥ 2350	0	1.66	0.86	12
3.67	0.81	≥ 2350	500	2.60	0.83	12
0.0747	1.14	≤ 1000	1200	$\overline{DP}_w = 0.95[\eta]^b$		11
8.26	0.76	≥ 1000	1200	$\log \overline{DP}_w = 1.32 \log [\eta] - 1000^b$		11
3.21	0.83	60–6000	0	3.85[c]	0.76[c]	14

[a] Constants used in obtaining DP's which were related to THF solutions.
[b] $[\eta]$ in ml/g.
[c] These constants for cadoxen solutions of cellulose (unnitrated).

trinitrate system and therefore are those which apply to the present results with THF Comparison of the a values in THF and ethyl acetate show that they are very similar for the same conditions; K values, too, are similar in order of magnitude. However, the constant a does seem to vary with the DP range as it does in the Marx-Figini and Schulz relationships. It should be pointed out also that the ratios $[\eta]$THF/$[\eta]$EtAc range from 0.98 to 1.2.

As mentioned, no correction for nitrogen content was made. Huque et al. derived their constants without nitrogen content corrections, while Marx-Figini and Schulz normalized all viscosities to a 13.6% nitrogen content.

For cellulose (unnitrated) in cadoxen, Brown and Wikstrom[14] provide constants for the Mark-Houwink equation which apply over a wide DP range, 60–6000. Results for THF based on cadoxen DP data are also included in Table I. Interestingly enough, K and a obtained in this manner are similar to values based on the equation of Huque et al.

Merle[4,6] published the equation

$$[\eta]_{\mathrm{THF}} = 1.50 \times 10^{-3}\bar{M}_w^{1.01}$$

where $[\eta]$ is given in milliliters per gram. With these constants and the intrinsic viscosities of the present solutions, values for DP were obtained which were consistently much higher (25–150%) than the DP values obtained with ethyl acetate. In other publications of this equation,[3,5] there are mistakes which are apparently typographical errors. The derivation of these constants[6] from only three samples of DP 350, 4000, and 9000 (by light scattering) is not straightforward. For example, no corrections for shear effects in the solutions of the two high DP samples are mentioned.

Jenkins[7] has also given an equation

$$[\eta]_{\mathrm{THF}^{25^\circ\mathrm{C}}} = 10.55 \times 10^{-3}(\overline{\mathrm{DP}}_w)^{1.014}$$

where $[\eta]$ is in deciliters per gram. According to Jenkins' work, the equation applies over the DP range of 60–1500. Jenkins derived the constants by relating the intrinsic viscosities of samples dissolved in THF with the DP's of the same samples dissolved in acetone. Viscometric data from the acetone solutions were handled by the Marx-Figini and Schulz equation for the appropriate DP range. Again, when Jenkins' constants were utilized with current intrinsic viscosity data, the DP's obtained did not agree with those from the ethyl acetate solutions. In this case they were approximately 25% lower.

When the constants listed in Table I for THF with the specific DP ranges and with the appropriate shear gradient corrections are applied to samples not included in this study, DP data are obtained which relate very favorably with those from the ethyl acetate solutions. Whereas acetone is considered a "poor" solvent for cellulose nitrate, ethyl acetate is considered a "good" one. The values of the ratio $[\eta]$THF/$[\eta]$EtAc stated above show that THF is at least as "good" a solvent for cellulose nitrate as is ethyl acetate. On this basis, then, studies of the configuration of the molecule in THF and solvation of the polymer should show similar behaviors with respect to coil size and related parameters.

The authors thank Mr. J. I. Wadsworth for his cooperation with the conputer programs. They are indebted to Dr. J. P. Merle for a copy of his dissertation, and to Dr. R. Y. M. Huang for the copy of Mr. Jenkins' thesis.

References

1. L. Segal, *J. Polym. Sci. B*, **4**, 1011 (1966).

2. L. Segal, J. D. Timpa, and J. I. Wadsworth, paper presented at the 158th National Meeting, American Chemical Society, New York, N. Y., Sept. 7–12, 1969; *J. Polym. Sci. A-1*, **8**, 25 (1970).

3. M. Rinaudo and J. P. Merle, *C. R. (Paris), Ser. C*, **268**, 593 (1969).

4. M. Rinaudo, F. Barnoud, and J. P. Merle, in *Proceedings of the Sixth Cellulose Conference* (*J. Polym. Sci. C*, **28**), R. H. Marchessault, Ed., Interscience, New York, 1969, p. 197.

5. M. Rinaudo and J. P. Merle, *Europ. Polym. J.*, **6**, 41 (1970).

6. J. P. Merle, Dissertation, Doctorat de Specialite, Universite de Grenoble, France, 1968.

7. R. G. Jenkins, Thesis, University of Waterloo, Canada, 1968.

8. J. Schurz and E. H. Immergut, *J. Polym. Sci.*, **9**, 279 (1952).

9. L. Segal and J. D. Timpa, *Svensk Papperstidn.*, **72**, 656 (1969).

10. H. A. Swenson, in *Methods of Carbohydrate Chemistry*, Vol. III, R. L. Whistler, Ed., Academic Press, New York, 1963, p. 84.

11. M. Marx-Figini and G. V. Schulz, *Makromol. Chem.*, **54**, 102 (1962).

12. M. J. Huque, D. A. I. Goring, and S. G. Mason, *Can. J. Chem.*, **36**, 952 (1958).

13. M. L. Hunt, S. Newman, H. A. Scheraga, and P. J. Flory, *J. Phys. Chem.*, **60**, 1278 (1956).

14. W. Brown and R. Wikstrom, *Europ. Polym. J.*, **1**, 1 (1965).

Judy D. Timpa
Leon Segal

Southern Regional Research Laboratory
Southern Utilization Research and Development Division
Agricultural Research Service
U. S. Department of Agriculture
New Orleans, Louisiana 70179

Received January 20, 1971

Diffusion and Permeation of Gases Through Nitroso Rubber

Nitroso rubber is of considerable interest for air space applications because of its resistance to strong oxidants and its good low-temperature flexibility.[1] A limited study of transport of gases through this rubber has been carried out, since such information is of importance for its potential use.

Experimental

Two nitroso rubber samples were studied. One sample membrane had been manufactured by Thiokol Chemical Corp. (CTVR-CTA cured); its thickness was 35.0 ± 0.5 mil. The second sample was prepared in our laboratory from materials procured by Mr. D. Lawson from Jet Propulsion Laboratory, Pasadena. Nitroso terpolymer CF_3NO–CF_2=CF_2–$ON(CF_2)_3COOH$ (100 parts), Cab-O-Sil silica (20 parts), and chromium trifluoroacetate (5 parts) were blended by standard procedures and cured at 150°C for 45 minutes; the resulting membrane had a thickness of 20 ± 3 mil. Both membranes were very soft and elastic.

High purity (99%+) O_2, N_2, CO_2, CH_4, C_2H_6, and C_3H_8 from cylinders were used without drying.

The instrument and the methods for measuring diffusion and permeation coefficients have been described elsewhere.[2,3] Determinations were made at about 60, 70, 80, and 90°C; for these thick membranes, the transmission rates became too small at lower temperatures to permit reliable measurements.

Results and Discussion

In Table I the permeation and diffusion coefficients P and D at 60°C, and the heats of permeation and diffusion E_P and E_D are tabulated. Since at most four experimental points were available for each Arrhenius plot (and only three for the thicker Thiokol membrane), the uncertainties in the heats, which are proportional to the slopes, are quite large, possibly 0.5 kcal/mole. The solubilities k, which are included in the table, are derived from the permeation and diffusion data in the usual way, $k = P/D$. The data obtained for the two membranes agree quite closely, if one takes into account the rather large uncertainties in the measurements.

The transport parameters follow a systematic pattern. The diffusion coefficients decrease and the solubilities increase with increasing boiling point (or molecular diameter) of the gases; the inverse holds for the heats of diffusion and solution. Similar correlations have been found for polyethylene[4] and FEP Teflon.[5]

The transport properties of N_2, O_2, CO_2, and CH_4 in nitroso rubber (extrapolated to 25°C) and in natural rubber,[6,7] are compared in Table II. The diffusion coefficients and the activation energies of diffusion of the gases (except of CO_2) are about the same in the two rubbers, but the solubilities are two to four times larger in the nitroso rubber, which is therefore more permeable. The somewhat different pattern for CO_2 may indicate strong specific interactions between CO_2 and the nitroso rubber.

The authors are indebted to Mr. David D. Lawson for suggesting this research and for furnishing the materials. The work was supported by the Jet Propulsion Laboratory, California Institute of Technology, Pasadena, California, sponsored by the National Aeronautics and Space Administration under Contract NAS 7-698.

TABLE I
Transport Data for Nitroso Rubber

Membrane	Gas	$P_{60} \times 10^8$, cc(STP)-cm / cm²-sec-cm Hg	E_P, kcal/mole	$D_{60} \times 10^6$, cm²/sec	E_D, kcal/mole	$k_{60} \times 10^2$, cc (STP) / cc-cm Hg	ΔH_S, kcal/mole
SRI membrane	N_2	1.05	7.1	3.2	6.9	0.33	0.2
	O_2	2.1	5.3	4.3	6.3	0.49	−0.1
	CO_2	4.8	5.2	1.2	8.8	4.0	−3.5
	CH_4	1.15	6.7	2.6	7.5	0.44	−0.8
	C_2H_6	1.30	6.5	1.0	8.3	1.3	−1.8
	C_3H_8	1.35	5.9	0.56	8.7	2.4	−2.8
Thiokol membrane	O_2	2.0	5.6	5.4	5.7		
	CO_2	4.6	4.9	1.6	8.2		
	C_2H_6	1.3	6.3	1.3	7.9		

TABLE II
Comparison between Nitroso (Ni) and Natural (Na) Rubber

	$D_{25} \times 10^6$, cm²/sec		E_D, kcal/mole		K_{25}, cc (STP)/cc-atm		$P_{25} \times 10^7$, cc (STP)-cm/cm²-sec-atm	
Gas	Ni	Na	Ni	Na	Ni	Na	Ni	Na
N_2	0.92	1.1	6.9	8.7	0.23	0.055	2.1	0.6
O_2	1.35	1.6	6.3	8.3	0.46	0.112	6.2	1.8
CO_2	0.25	1.1	8.8	8.9	5.8	0.90	14.5	9.9
CH_4	0.66	0.9	7.5	8.7	0.43	0.25	2.8	2.2

References

1. N. B. Levine, in *New Polymeric Materials* (*Appl. Polym. Sym.* **11**), P. F. Bruins, Ed., Interscience, New York, 1969, p. 135.

2. R. A. Pasternak, J. F. Schimscheimer, and J. Heller, *J. Polym. Sci. A-2*, **8**, 467 (1970).

3. R. A. Pasternak and J. McNulty, *Modern Packaging*, **43**, 89 (1970).

4. A. S. Michaels and H. J. Bixler, *J. Polym. Sci.*, **50**, 373,413 (1961).

5. R. A. Pasternak, M. V. Christensen, and J. Heller, *Macromolecules*, **3**, 366 (1970).

6. G. J. van Amerongen, *Rubber Chem. Technol.*, **37**, 1101 (1964).

7. J. Crank and G. S. Park, Eds., *Diffusion in Polymers*, Academic Press, New York–London, 1968, p. 50.

R. A. Pasternak*
M. V. Christensen

Stanford Research Institute
Menlo Park, California 94025

Received February 22, 1971

* Present address: Pharmetrics, Palo Alto, Calif. 94304.

Contents (continued)

The *Journal of Polymer Science* publishes results of fundamental research in all areas of high polymer chemistry and physics. The *Journal* is selective in accepting contributions on the basis of merit and originality. It is not intended as a repository for unevaluated data. Preference is given to contributions that offer new or more comprehensive concepts, interpretations, experimental approaches, and results. Part A-1 *Polymer Chemistry* is devoted to studies in general polymer chemistry and physical organic chemistry. Contributions in physics and physical chemistry appear in Part A-2 *Polymer Physics*. Contributions may be submitted as full-length papers or as "Notes." Notes are ordinarily to be considered as complete publications of limited scope.

Three copies of every manuscript are required. They may be submitted directly to the editor: For Part A-1, to C. G. Overberger, Department of Chemistry, University of Michigan, Ann Arbor, Michigan 48104; and for Part A-2, to T. G Fox, Mellon Institute, Pittsburgh, Pennsylvania 15213. Three copies of a short but comprehensive synopsis are required with every paper; no synopsis is needed for notes. Books for review may also be sent to the appropriate editor. Alternatively, manuscripts may be submitted through the Editorial Office, c/o H. Mark, Polytechnic Institute of Brooklyn, 333 Jay Street, Brooklyn, New York 11201. All other correspondence is to be addressed to Periodicals Division, Interscience Publishers, a Division of John Wiley & Sons, Inc., 605 Third Avenue, New York, New York 10016.

Detailed instructions in preparation of manuscripts are given frequently in Parts A-1 and A-2 and may also be obtained from the publisher.